



University of  
**Nottingham**

UK | CHINA | MALAYSIA

# **The Functionalisation of Terpenes for Sustainable Polymerisations Towards Biomedical Applications**

Dara M. O'Brien, B.A.

Thesis submitted to the University of Nottingham for the  
degree of Doctor of Philosophy

December 2020



Biomaterials  
Discovery

*"There is no science without fancy and no art without facts."*

*Vladimir Nabokov*

## Abstract

This thesis details a variety of methods in which monoterpenes can be employed in different stages of sustainable polymerisation mechanisms, with a view to using the polymeric materials in biomaterials applications such as anti-microbial formulations.

In the first experimental chapter, it is demonstrated that a variety of terpenoids with either primary or secondary alcohols can be employed as initiators in a ring opening polymerisation of racemic lactide. This synthesis enables a fully green and sustainable polymerisation, employing a naturally-derived organocatalyst and the bio-renewable solvent 2-methyl tetrahydrofuran. Lactide was selected as a monomer, as not only is it derived from biomass, but its resultant polymers are both biocompatible and biodegradable. Each of the synthesised oligomers were found to retain at least one alkene functional group in the oligomer, facilitating potential post-polymerisation modifications. However, even in the absence of additional functionalities, each of the terpenoid-initiated oligomers were found to self-assemble in water to produce well-defined nanoparticles, without the use of additional stabilisers. This has introduced a promising approach toward the synthesis of fully green surfactants for biomaterials applications.

In the second chapter, the terpenoid (*R*)-carvone is employed in the synthesis of a terpene-derived, aliphatic, bis-epoxide monomer. The synthesis of this monomer was achieved using green methodologies, avoiding the use of toxic or chlorinated solvents. This was then employed in two simple epoxy/amine polymerisation reactions with diamine co-monomers to produce low molecular weight oligomers. This was achieved in the absence of solvent, catalyst or additional reacting components. The linear oligomers formed with a di-secondary diamine were found to be water-soluble, and as such were investigated for antifungal activity in combination with two commercially available anti-fungals. The data showed a synergistic, antifungal relationship against two fungal strains, *Trichoderma virens* and the human pathogen *Candida albicans*. This relationship enables lesser amounts of each component to be used in formulations, as each one is provided below the minimum

inhibitory concentrations that would be required if they were used on their own. This is beneficial from a cost perspective but also can be considered superior as a treatment, as it is usually more difficult for pathogenic strains to develop resistance to two components rather than a single one.

Finally, in the last chapter the synthesis of a number of terpene-based poly-ols is described. Each of the poly-ols feature two nucleophilic alcohol groups, enabling their use as monomers in the synthesis of bio-based polyesters through polycondensation with di-carboxylic acid co-monomers. Furthermore, four of these poly-ols were then converted to their corresponding di-acrylate compounds, employing a green synthetic methodology. These di-acrylate compounds were found to have much potential for use in the aza-Michael polymerisation, forming poly-( $\beta$ -amino ester)s up to  $4900 \text{ g}\cdot\text{mol}^{-1}$ , with good dispersities ( $\mathcal{D} < 2$ ). While much of the research relating to this project remains to be investigated, nonetheless this demonstrates the first time that terpene renewable feedstocks have been used in this polymerisation type.

Overall, this thesis highlights the synthetic versatility of a number of monoterpenes as feedstocks in both small molecule and polymer reactions. It is demonstrated that terpenes present a wealth of opportunity in the field of polymer therapeutics, not least in terms of increasing the sustainability and circularity of the field.



## **Acknowledgements**

I would like to begin by thanking my three supervisors, Professors Rob Stockman, Steve Howdle and Cameron Alexander, for giving me the opportunity to come to Nottingham and complete this PhD in their research groups. Thanks to each for their support and advice over the four years and for the opportunities along the way: the many conferences attended and the hosting of one of our own. I would also like to thank everyone involved in the Next Generation Biomaterials Discovery programme grant, past and present, for their helpful advice both scientific and otherwise, particularly to Elizabeth Hufton and Sian Rankin-Turner, as well as everyone involved in the RC2 division. Thank you to Mr. Arsalan Latif and Dr. Robert Cavanagh for the cell culture studies, and to Professor Simon Avery and Dr. Cindy Vallières for their work (and patience) in introducing me to the world of fungal microbiology.

This research would not have been possible without the hands-on help of a number of postdocs and group members over the years. First of all, thank you to Dr. Benoit Couturaud for introducing me to the community that is polymer chemistry. From Nottingham, members of the Stockman, Howdle and Alexander groups past and present are thanked, who have helped and supported me along the way. In particular, thank you to Dr. Vincenzo Taresco for the advice and counsel over the years. Thank you for sharing your wisdom and expertise along the way, which should hopefully be weaved into each of the chapters of this thesis. Thank you as well for your friendship since the beginning, and of course the trips to Abruzzo.

Thank you to all of my friends at home and abroad, and the many 'from home; abroad', without whom this work would never have been finished. Thank you to the McGlone family for all the support and friendship over the years and the very good job you all do at pretending to be interested in polymers. Thank you to the girls from Flat 16 (plus Safa) who helped me to adjust and settle in Nottingham when I first moved here. Thank you to Larissa, Orla and Kathryn for always being the other end of a phone call and for all the times you've reassured me and laughed with me along the way. Thank you to Gruppo Quarantena for getting me through Lockdown 1.0 with daily phone calls, and to the 'Group', who've

been my original support and WhatsApp group since the Leaving Cert. Thank you to James, for occasionally taking out the bins a couple of times when it was *really* hard for me, and for putting up with a few washing-machine related break downs over the years.

Thank you to Valentina, your continuous support and encouragement has helped my science and has helped me; keeping me motivated and ultimately bringing this thesis to completion. But thank you most of all for your friendship, the teas and treats, manicures and gossiping.

Thank you to Rob, for teaching me about cells and how they can be neat. Thank you for all the meals and movies at your apartment and for patiently listening to my many monologues and rants. I couldn't have asked for a better support bubble.

Finally, thank you to my family: my Mum and Dad and Simon. Thank you for always being in my corner and believing in me, especially during the more turbulent times. Thank you for all the calls, the last-minute flights, the Barry's tea and everything that has made this journey possible. Your continued love, guidance and support has empowered me not only to become a better scientist, but a better human.

## Abbreviations

9-BBN	9-borabicyclo(3.3.1)nonane
AFP	Antifungal Peptide
AMP	Antimicrobial Peptide
aq	Aqueous
ATR	Attenuated Total Reflectance
ATRP	Atom Transfer Radical Polymerisation
BHT	Butylated Hydroxy Toluene
CHO	cyclohexene oxide
CMR	carcinogenic, mutagenic and reprotoxic
COSY	Correlation Spectroscopy
Đ	Dispersity index
d	Doublet
Da	Daltons
DBU	1,8-Diazabicyclo [5.4.0]undec-7-ene
DCM	Dichloromethane
DEPT	Distortionless Enhancement by Polarization Transfer
DGEBA	Diglycidyl ether of bisphenol-A
DLS	Dynamic Light Scattering
DMA	Dynamic Mechanical Analysis
DMC	Dimethyl carbonate
DMDO	Dimethyl dioxirane
DMF	Dimethyl formamide
DP	Degree of Polymerisation
DSC	Differential Scanning Calorimetry
ESI	Electrospray Ionisation
FICI	Fractional Inhibitory Concentration Index
FRP	Free Radical Polymerisation
FTIR	Fourier Transform Infrared Spectroscopy
GPC	Gel Permeation Chromatography
HMBC	Heteronuclear Multiple Bond Correlation
HRMS	High Resolution Mass Spectrometry
HSQC	Heteronuclear Single Quantum Coherence
LDH	Lactate Dehydrogenase

m	Multiplet
m.p.	Melting point
mCPBA	<i>meta</i> -Chloroperbenzoic acid
Mg	Megagram/ metric tonne
MIC	Minimum Inhibitory Concentrations
M <sub>n</sub>	Number-average molecular weight
MS	Mass Spectrometry
M <sub>w</sub>	Weight-average molecular weight
NIPU	Non-Isocyanate Polyurethane
NMR	Nuclear Magnetic Resonance
NOESY	Nuclear Overhauser Effect Spectroscopy
PBS	Phosphate Buffer Saline
PCL	Polycaprolactone
PDB	Potato Dextrose Broth
PDI	(Poly)Dispersity Index
PDLA	Poly(D-lactide) or poly(D-lactic acid)
PDLLA	Poly(D,L-lactide) or poly(D,L-lactic acid)
PEG	Polyethylene glycol
PGA	Polyglycolide
PLA	Poly(lactide) or poly(lactic acid)
PLGA	Poly(lactic-co-glycolic acid) or poly(lactide-co-glycolide)
PLLA	Poly(L-lactide) or poly(L-lactic acid)
PMMA	Poly-methyl methacrylate
r.t.	Room temperature
RAFT	Reversible Addition-Fragmentation chain Transfer polymerisation
ROCOP	Ring Opening Co-Polymerisation
ROP	Ring Opening Polymerisation
SEC	Size Exclusion Chromatography
t	Triplet
T <sub>g</sub>	Glass transition temperature
TLC	Thin Layer Chromatography
TMC	Trimethylcarbonate
YPD	Yeast Extract Peptone Dextrose
Θ <sub>w</sub>	Water Contact Angle

## Table of Contents

<b>Abstract</b> .....	iii
<b>Acknowledgements</b> .....	v
<b>Abbreviations</b> .....	vii
<b>1 Chapter One: Introduction</b> .....	<b>1</b>
1.1 A call for renewable polymer systems .....	1
1.2 Current polymers from biomass .....	7
1.3 Terpenes as a renewable feedstock from biomass.....	14
1.4 A history of the direct polymerisation of terpenes .....	17
1.5 The functionalisation of terpenes towards useful monomers ..	22
1.5.1 Terpene-based polycarbonates and polyurethanes from epoxides .....	23
1.5.2 Other syntheses of terpene- polycarbonates and polyurethanes.....	26
1.5.3 Terpene-based polyesters by condensation mechanisms....	27
1.5.4 Terpene-based polyesters by Ring Opening Polymerisation	29
1.5.5 Terpene-based polyamides by Ring Opening Polymerisation	31
1.5.6 Radical-type mechanisms of terpene polymerisation .....	33
1.5.7 Summary .....	35
1.6 Epoxy-amine resins and polymer systems .....	36
1.7 Polymers for biomedical and antimicrobial applications.....	43
1.7.1 Poly(lactide): A biocompatible biopolymer .....	47
1.7.2 Amphiphilic polymers and surfactants .....	52
1.7.3 Fungal pathogens and the need for novel treatments .....	58
<b>2 Chapter Two: Terpenes as initiators for 'green' ring opening polymerisations</b> .....	<b>64</b>
2.1 Introduction: Surfactants for biomaterials .....	64
2.2 Aims and Objectives.....	66
2.3 Results and Discussion .....	70
2.3.1 Synthesis of trans-sobrerol ( <b>12</b> ) .....	70

2.3.2	Synthesis of geraniol-initiated PDLLA oligomers.....	74
2.3.3	Synthesis of PDLLA oligomers using green synthetic methods. .....	80
2.3.4	Surface Activity Investigations .....	85
2.3.5	Chain length investigations in <b>12</b> -PDLLA oligomers. ....	88
2.3.6	Cytocompatibility Evaluation .....	95
2.3.7	Alkene functionalisation .....	97
2.3.8	Green ROP of Trimethylcarbonate (TMC) .....	101
2.4	Conclusions.....	104
2.5	Experimental.....	107
2.5.1	General Materials and Methods .....	107
2.5.2	Synthesis of trans-sobrerol ( <b>12</b> ) .....	109
2.5.3	Synthesis of <b>10</b> -PDLLA using 'conventional' (DCM) method.... .....	110
2.5.4	'Fully Green' ROP syntheses.....	111
2.5.5	Nanoparticle Preparation and Stability Assay.....	117
2.5.6	Critical Aggregation Concentration (CAC) calculation.....	117
2.5.7	Cell Culture .....	117
2.5.8	Cytocompatibility Evaluation .....	118
<b>3</b>	<b>Chapter Three: Epoxy-amine oligomers for synergistic antifungal applications .....</b>	<b>119</b>
3.1	Introduction: Epoxy-amine resins for antifungal applications	119
3.2	Aims and Objectives.....	123
3.3	Results and Discussion .....	128
3.3.1	Synthesis of carvone-based bis-epoxide monomer using mCPBA .....	128
3.3.2	Synthesis of terpene-based bis-epoxide monomer using Oxone® .....	133
3.3.3	Synthesis One of $\beta$ -amino alcohol oligomers .....	142
3.3.3.1	<i>Temperature screen</i> .....	142
3.3.3.2	<i>Time Screen</i> .....	155
3.3.4	Synthesis Two of $\beta$ -amino alcohol oligomers .....	157
3.3.4.1	<i>Temperature screen</i> .....	158

3.3.4.2	<i>Reaction Time Screen</i> .....	171
3.3.4.3	<i>Solvent screen</i> .....	174
3.3.5	<i>Synergistic Antifungal Investigations</i> .....	177
3.3.5.1	<i>Synergistic investigations of iodopropynyl butylcarbamate (IPBC) and oligomer <b>44</b> against <i>Trichoderma virens</i> ...</i>	178
3.3.5.2	<i>Synergistic investigations of Amphotericin B and oligomer <b>44</b> against <i>Candida albicans</i></i> .....	185
3.3.5.3	<i>Cytocompatibility test</i> .....	191
3.3.5.4	<i>Mechanism Discussions</i> .....	195
3.4	<i>Conclusions</i> .....	198
3.5	<i>Experimental</i> .....	201
3.5.1	<i>General Materials and Methods</i> .....	201
3.5.2	<i>Experimental procedures for monomer syntheses</i> .....	202
3.5.3	<i>Experimental Procedures for polymer syntheses</i> .....	206
3.5.4	<i>Experimental Procedures for antifungal studies</i> .....	208
<b>4</b>	<b>Chapter Four: A brief insight into polymerisations using oxidised terpenes</b> .....	<b>211</b>
4.1	<i>Introduction: alcohol-based terpene monomers</i> .....	211
4.2	<i>Aims and Objectives</i> .....	216
4.3	<i>Results and Discussion</i> .....	222
4.3.1	<i>Synthesis of terpene-based diols</i> .....	222
4.3.2	<i>Attempted polycondensation of terpene-based poly-ols with camphoric acid</i> .....	231
4.3.3	<i>Synthesis of terpene-derived diacrylate monomers</i> .....	236
4.3.4	<i>Synthesis of terpene-derived poly <math>\beta</math>-(amino ester)s via the aza-Michael polymerisation</i> .....	239
4.3.4.1	<i>Initial investigations</i> .....	239
4.3.4.2	<i>Solvent Screen</i> .....	244
4.3.4.3	<i>Full terpene-diacrylate aza-Michael polymerisations</i> ....	247
4.4	<i>Missing Data Caveat</i> .....	249
4.5	<i>Conclusions</i> .....	250
4.6	<i>Experimental</i> .....	254

4.6.1	General Materials and Methods .....	254
4.6.2	Synthesis of terpene-derived poly-ols .....	255
4.6.3	Synthesis of polyester <b>50</b> and <b>51</b> .....	261
4.6.4	Syntheses of terpene-derived di-acrylates .....	262
4.6.5	Synthesis of terpene-based $\beta$ -(amino ester)s via the aza- Michael polymerisation.....	266
<b>5</b>	<b>Conclusions and future outlook.....</b>	<b>271</b>
<b>6</b>	<b>Appendix .....</b>	<b>278</b>
<b>7</b>	<b>References.....</b>	<b>283</b>



# 1 Chapter One: Introduction

## 1.1 A call for renewable polymer systems

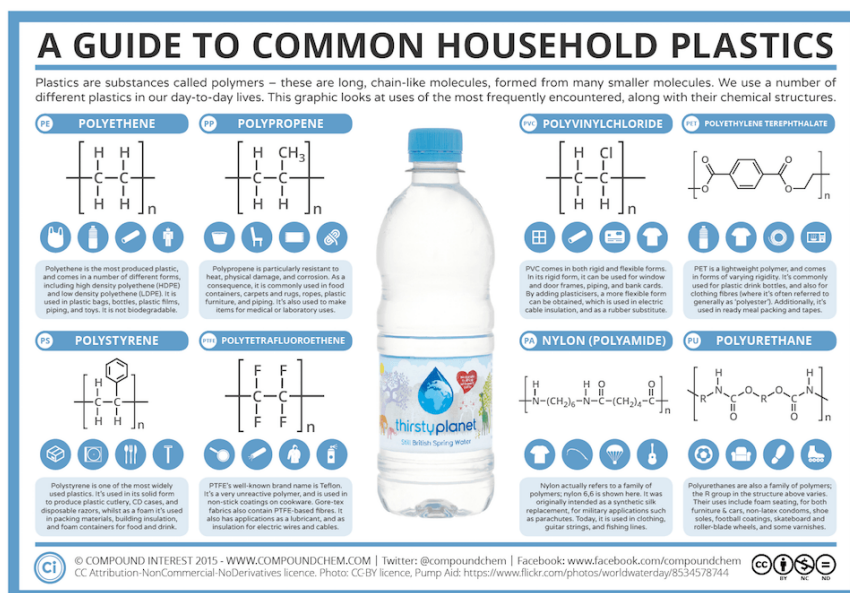


**Figure 1.** Details of the structures and applications of the most common polymers in household plastics. Image: Compound Interest 2015 ©.

It was Hermann Staudinger who first proposed the idea that polymers were chains of identical small molecules linked by strong chemical bonds.<sup>1</sup> Although his hypothesis was met with resistance, with most academics at the time preferring the idea that they were instead looser aggregations of small molecules,<sup>2</sup> Staudinger's idea proved true, and he received the Nobel Prize for Chemistry in 1951 for his work in the field.

Since then, polymers have become ubiquitous (**Figure 1**). The 20<sup>th</sup> century saw the reliance of the global population on polymer-based materials increase twenty-fold.<sup>3</sup> Since the turn of the 21<sup>st</sup> century, polymer manufacturing and use has continued to grow: in 2015, synthetic polymer production worldwide hit 300 million tonnes;<sup>2</sup> this compares to approximately 150 million tonnes twenty years ago,<sup>4</sup> and it is expected to double again within the next twenty years.<sup>3</sup> These figures alone speak of the unrivalled functionality of polymers in the modern age. They are used in everyday items such as clothing, paints, and goods packaging, to more sophisticated 3-D printing systems, medical devices, and the aeronautical

industry makes use of them in constructing aeroplanes.<sup>2</sup> It is easy to understand why they are so popular: their versatile nature allows polymers to couple low-cost manufacturing with a wide range of functions.<sup>3</sup>

With a wealth of aforementioned applications, polymers have undoubtedly led to an improved quality of life,<sup>4,5</sup> and it is expected that the uses of synthetic polymer systems is set to continue to expand.<sup>2</sup> New monomers which can lead to systems and materials with novel properties is at the forefront of polymer research,<sup>6</sup> work which is becoming increasingly interdisciplinary as researchers pool their knowledge to better predict polymer properties, and develop novel systems.<sup>2</sup>

Most of the polymers in current use are derived from petrochemicals.<sup>5</sup> There is a drive to find new polymer feedstocks due to the environmental, and subsequent economic, impact of using these fossil fuel-derived systems.<sup>3,7</sup> Economies of scale reveal that while polymers used for plastics can initially appear to be cheap to produce, the costs associated with retrieving plastic that has escaped collection systems (which account for a massive 32%), push costs on the economy far beyond the profit pool of the plastic packaging industry.<sup>3</sup> These expenses are significant, especially considering that, in the United States for example, plastic for packaging accounts for one-third of all plastic use.<sup>7</sup> Economics to one side, the growing concern surrounding plastics that have escaped collection results primarily in environmental burdens. A report in 2016 by the Ellen McArthur Foundation revealed that by 2050, there could be more plastic than fish in our oceans by weight (**Figure 2**).<sup>3</sup> This highlights the need for new polymers to address the environmental concerns not only in their production, but also at their end of life.<sup>5</sup>

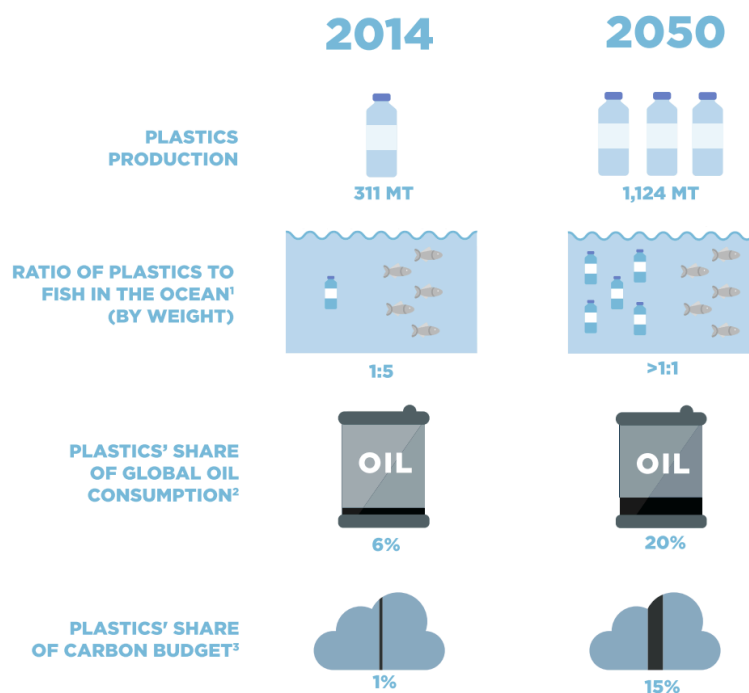


**Figure 2.** Cartoon depiction from the Ellen McArthur Foundation, indicating the global crude oil and plastics consumption in 2014 and the predicted situation in 2050, by which time it is expected there will be more plastic than fish in the world's oceans.<sup>3</sup>

Of the plastic that does not end up as litter and is instead collected, only 14% of plastic packaging is sent for recycling and only 5% is retained for future use.<sup>3</sup> The majority of plastics end up in landfill waste and present a plethora of environmental problems, namely due to their durability which prevents their easy biodegradation.<sup>8-10</sup> These environmental issues must be addressed if the polymer industry is to be expanded, or even maintained. It is vital therefore that new polymer systems are introduced which can be easily recycled and/or degraded to harmless by-products over reasonable time frames (**Figure 3**).<sup>11</sup>

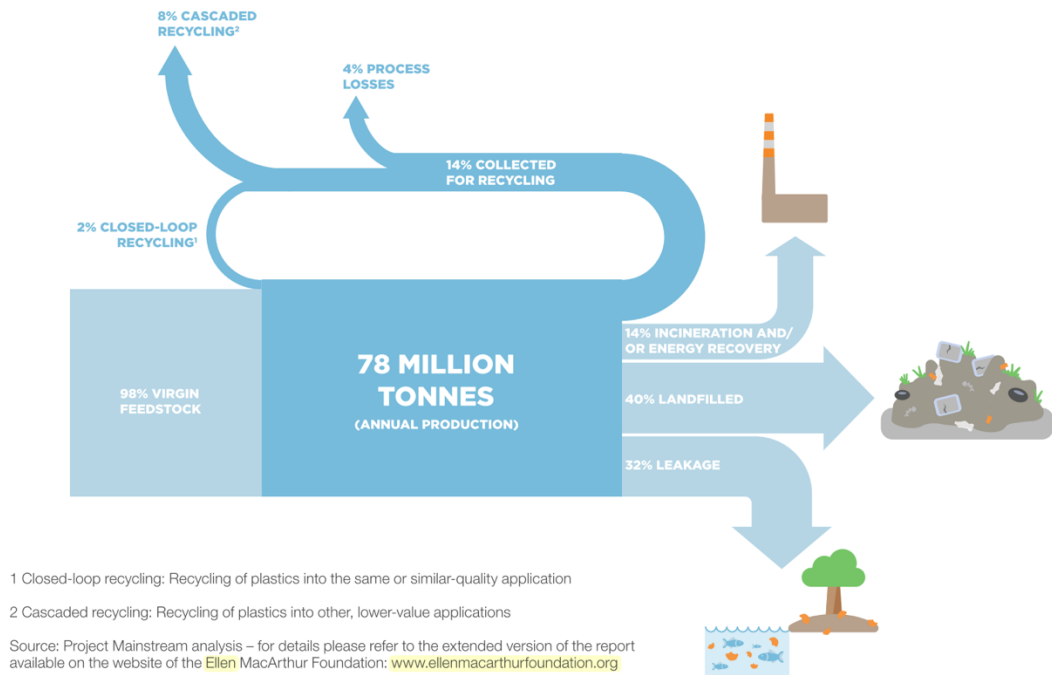


**Figure 3.** Image depicting the life cycle of global plastic production and consumption. Up to 32% of plastic escapes collection and ends up as ocean plastic and litter. Only 14% is collected for recycling.<sup>3</sup>

Another issue concerning the continued production of polymer systems (especially those which are not degradable) is that of carbon-resources. There are expected to be more people seeking to reap the benefits of polymer technologies in the coming century: at the beginning of the twenty first century there was a global population of approximately six billion people and by 2050, this figure is estimated to pass ten billion.<sup>4</sup> With this increase in population comes a variety of problems in relation to our reliance on polymer systems,<sup>4</sup> primarily to do with the fact that the majority of our polymer materials are derived from fossil-fuel petrochemicals.<sup>5</sup> Although polymer production accounts for only approximately 7% of the total oil produced worldwide,<sup>5,8</sup> the global oil production is expected to peak within the upcoming decades, and crude oil and gas feedstocks are expected to be entirely depleted within the next century.<sup>8</sup> This alone demands that polymer production find new, renewable feedstocks.

The Earth has only a finite amount of carbon-based feedstocks that are being rapidly depleted by an increasing energy demand.<sup>11</sup> The majority of plastic packaging (an estimated 86%) is used only once before it is discarded, usually to landfill, where its carbon is not recoverable.<sup>2</sup> In looking to replace crude oil as a feedstock, only biomass can provide enough renewable carbon in sufficient quantities, when considering the vast array of organic polymer structures that exist, and that continue to be developed.<sup>6</sup>

As a result, bio-based raw materials are now considered the preferred alternative to fossil-fuel carbon sources in polymer and monomer research.<sup>12</sup> However, there is no cure-all for the complexity of environmental problems associated with our reliance on polymer materials.<sup>5</sup> The polymer's life cycle (from 'cradle-to-grave') should adhere, as much as possible, with the twelve principles of green chemistry.<sup>6,13</sup> This necessitates that in designing new monomer and polymer materials, an effort should be made to employ nontoxic or environmentally benign reagents, in addition to sustainable chemical modifications and polymerisation methods.<sup>6</sup> Ideally, the polymers should also undergo a method of biodegradation at their end-of-life which would allow for the carbon in their structures to be recovered. Classifying a polymer (or indeed any chemical) as 'sustainable' is thus the subject of considerable debate, with many parameters to be considered.<sup>14</sup>

Demand for renewable polymers is undoubtedly growing; production capacities for bio-plastics passed 2 million tonnes in 2018.<sup>12</sup> Despite this, sustainable polymers still constitute less than 1% of the total commercial plastics market.<sup>5</sup> One of the reasons for this is that polymers from renewable sources are usually more expensive to make than their petroleum counterparts.<sup>2,8,15</sup> It is expected that the development of biorefinery processes will increase production and reduce costs of renewable polymeric materials,<sup>8</sup> in the same way that the petrochemical refinery process did for plastics from crude oil.<sup>8,12</sup> It is worth remembering that petroleum-based plastic has benefited from decades of commercial-scale optimisation and research, while the use of sustainable polymers is still relatively new.<sup>9</sup>

Another barrier facing renewable polymer production (particularly on a large, commercial scale) is the requirement of agricultural land (often of high-quality) on which to grow the required bio-based feedstocks. This problem introduces ethical issues in terms of the use of land for 'food verses fuel', and has slowed the progress and production of bio-based plastics.<sup>12</sup> Still, even if bio-based plastic production saw a 50-fold increase to approximately  $100 \times 10^6$  tonnes per annum, this would account for only 1% of the world's agricultural land use.<sup>12</sup>

Evidently, this is an area in which there is plenty of room for growth; polymers from renewable feedstocks is a field of research with ever-increasing importance, with much untapped potential.

## 1.2 Current polymers from biomass

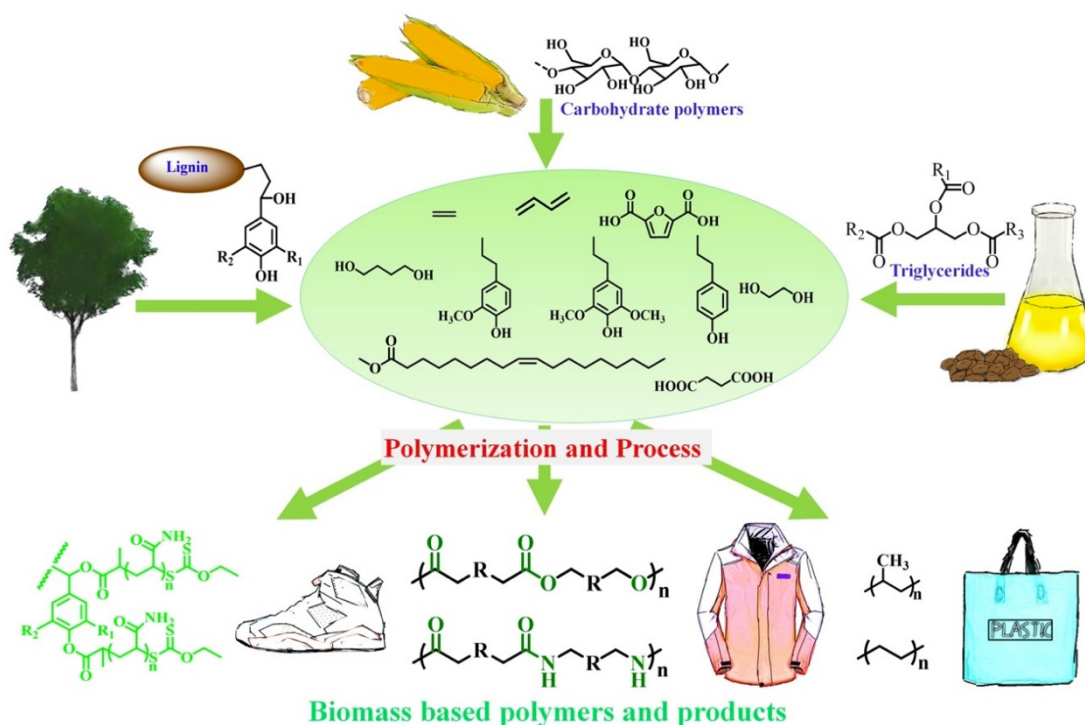


**Figure 4.** A selection of feedstocks (lignin, carbohydrates and vegetable oils) and their corresponding polymer structures and applications.<sup>16</sup>

Biomass can be considered as any renewable, environmental-derived, organic material used to produce energy or fuel. It is increasingly being investigated as a lone source of sustainable, renewable carbon, in quantities great enough to maintain and grow our polymer material needs.<sup>6</sup> Of the molecular biomass that is available, it can be categorised based on its composition of hydrogen, carbon and oxygen.<sup>9,15</sup> These categories are as follows (**Figure 5**):

1. Oxygen-Rich molecular biomass: with the molar ratio of C:O less than 5.0 (an arbitrarily assigned number). This class includes carboxylic acids, polyols, dianhydroalditols and furans.<sup>15</sup>
2. Hydrocarbon-rich molecular biomass: with the molar ratio of C:O larger than 5.0. This class includes vegetable oils, fatty acids, terpenes and terpenoids.<sup>15</sup>

3. Hydrocarbon molecular biomass: Not incorporating oxygen. This class includes bioethene, biopropene, and bioisoprene.<sup>15</sup>
4. Non-Hydrocarbon molecular biomass: including carbon dioxide.<sup>15</sup>

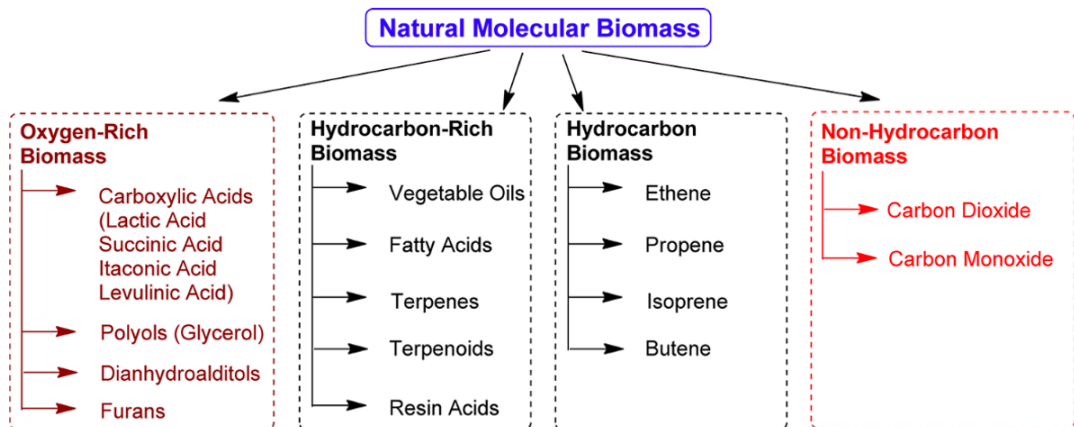


**Figure 5.** The four categories of molecular biomass.<sup>15</sup>

The incorporation of oxygen and other heteroatoms is a hurdle to overcome for many renewable polymers, because it can affect the polymer's properties, stiffening the material compared to the flexible alternatives such as polyethylene or polypropylene.<sup>2</sup> Renewable starting materials tend to contain more of these groups than petrochemical-based plastics do. For sustainable polymer systems to be successful, they must offer competitive performance properties to their crude oil alternatives, and it is this which remains the key barrier in shifting to renewable, bio-derived plastics.<sup>11</sup> However, there are a great many examples of bio-derived polymers which have had success in replacing crude-oil derived polymers, even in spite of a high oxygen content. Possibly the best-known example of this is the use of poly(lactic acid) (**Figure 6**), also known as poly(lactide) (PLA), as a replacement for polystyrene.<sup>17</sup>



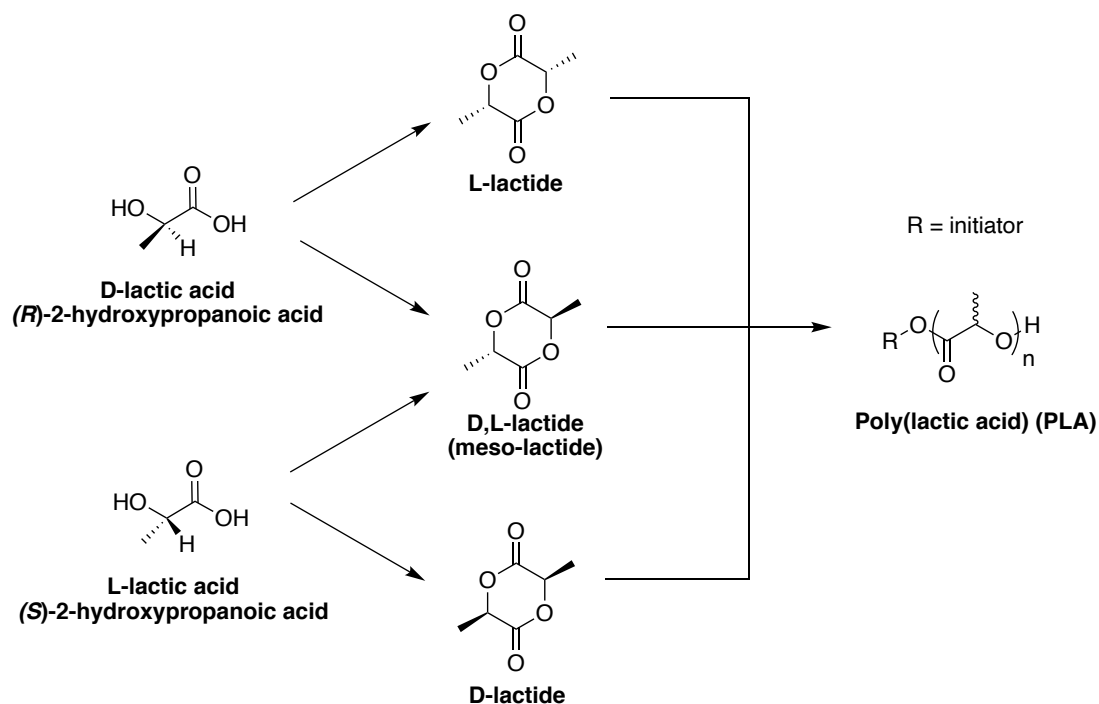
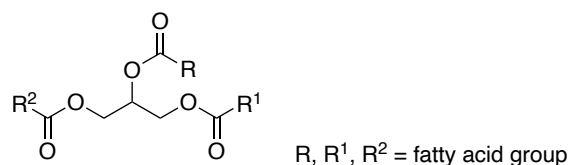


**Figure 6.** The structures of L- and D-lactic acid and their corresponding lactide dimers. Both functional groups can lead to the formation of poly(lactic acid) (PLA).<sup>18</sup>

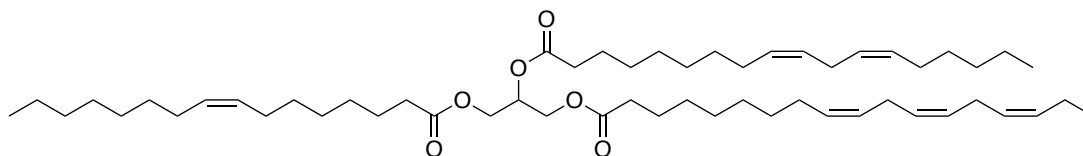
In 2014, PLA accounted for one of the three main products by volume of the renewable polymer industry.<sup>5</sup> It has received significant commercial attention due to its potential to replace polyolefins such as polystyrene, amongst other petrochemical derived polymers such as polyethylene and polypropylene.<sup>9,19</sup> It is produced from either lactic acid or lactide monomers,<sup>20</sup> which are producible on a mass scale through fermentation of a carbohydrate (usually glucose), after which polymerisation techniques are applied.<sup>18</sup> The fermentation process currently produces about 350,000 tonnes per year of lactic acid and growth in this industry is expected over the coming decades.<sup>15</sup> PLA is a particularly successful renewable polymer because not only is it derived from biomass, but it is also biocompatible and will break down in the body to form lactic acid.<sup>21</sup> This makes it particularly attractive for biomedical applications such as drug or vaccine delivery, as lactic acid is simply converted to glucose by the body as in the process of anaerobic respiration. PLA therefore offers an example of a useful polymer that can be considered safe and devoid of any major

toxicity.<sup>21</sup> Current biomedical applications include its use in screws, pins and plates which are intended to biodegrade within six to twelve months.<sup>22</sup> These are discussed in further detail towards the end of this introduction (section 1.7.1, *vide supra*).

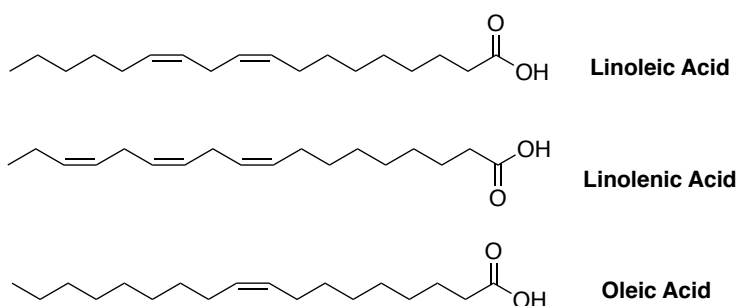
Another source of biomass which has seen a burst of research interest into its potential as a feedstock for renewable polymers, is that of vegetable oils. This family of compounds is considered hydrocarbon-rich molecular biomass, and the most commonly used oils for polymer synthesis include palm, soybean, linseed, castor, olive and sunflower oils.<sup>15</sup> The main component of these are triglycerides (**Figure 7**), formed from the esterification of glycerol with three fatty acids.<sup>23</sup> Following the hydrolysis of glycerol, these fatty acid components are polymerisable either directly *via* the functional groups on these fatty acid backbones, or after chemical modification of these groups to more useful monomer functionalities.<sup>15</sup>



**General Triglyceride Structure**



**Typical Triglyceride Oil Molecule**



**Common Fatty Acid Chemical Structures**

**Figure 7.** *The general chemical structure of triglycerides, the main component of vegetable oils of interest to polymer chemistry (top). A typical triglyceride (middle) and the fatty acid substituents available from it following the hydrolysis of glycerol (bottom).*<sup>8,15</sup>

Direct polymerisation of triglycerides has led to the formation of ink resins through the cross-linking of the alkene moieties, though these often have to undergo a post-curing step of oxidative coupling.<sup>8</sup> More progress has been made by olefin metathesis of a wide variety of fatty acid monomers in straightforward syntheses.<sup>23</sup> Chemical modification of the functional groups of fatty acids has led to a wealth of monomers, with a variety of versatile polymers and materials available as a result.<sup>8,24</sup> This, combined with their world-wide availability, low cost and facile routes to

functionalisation, makes vegetable oils a very attractive resource for polymer science.<sup>23</sup>

Lignin (the name of which is derived from the Latin for wood), is the second most rich renewable resource of carbon, next to cellulose.<sup>25</sup> As such, this biopolymer has been extensively studied as a feedstock for renewable polymer systems. Lignin is considered an aromatic, highly branched, amorphous biomacromolecule.<sup>26</sup> It consists of phenyl propane units originating primarily from three hydroxycinnamyl alcohols ('monolignols') (**Figure 8**).<sup>26</sup> These monolignols bond together without well-defined repeating units, through a series of characteristic linkages formed in dehydration reactions, to arrive at the analogous guaiacyl (G), syringyl (S), and p-hydroxyphenyl (H) polymer units (**Figure 8**).<sup>25,27</sup>

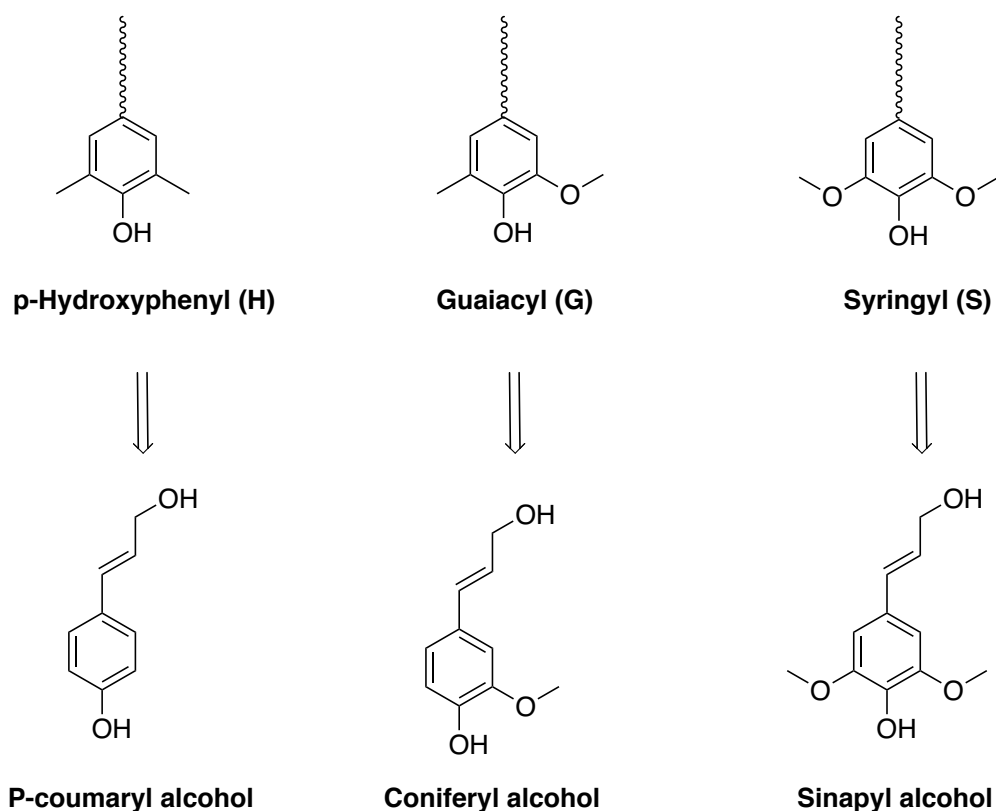


**Figure 8.** The structures of p-hydroxyphenyl (H), guaiacyl (G) and syringyl (S), and their corresponding monolignol precursors.<sup>26,27</sup>

In plants, the function of lignin is to provide strength and structure to cell walls and offer a natural hydrophobicity, which likely is why it helps control

fluid flow.<sup>27</sup> In polymer science, the aromaticity of lignin renders it a useful adhesive and rubber intensifier.<sup>25</sup> Additionally, it is used in lubricants, surfactants and fire retardants, amongst many other composite applications.<sup>27</sup>

The use of waste CO<sub>2</sub> is very attractive as a source of sustainable carbon which would adhere well with the concept of the circular economy, considering it is a waste stream of many processes.<sup>28,29</sup> Similarly, another option includes the use of 'furanics' such as furfural, furfuryl alcohol, 5-methylfurfural and 5-hydroxymethylfurfural (HMF) (**Figure 9**), which are well-developed monomers available from waste biomass.<sup>9,29</sup>

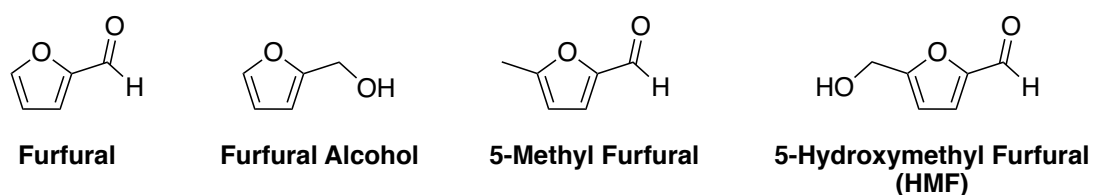


**Figure 9.** A selection of furan-based monomers.<sup>9</sup>

These monomers have another advantage over other bio-based monomers such as PLA, in that their production can avoid the fermentation process entirely, which, even in a perfectly quantitative efficiency, loses one third of the available carbon to carbon dioxide.<sup>29</sup> While research into furan-based monomers and polymers has been slow, the area shows a lot of promise and room for expansion.<sup>30</sup>

These bio-based polymer resources offer insight into only a handful of examples of the wide range biomass feedstocks being investigated for polymer science. Another source of carbon-based biomass are terpenes and terpenoids, which fall into the hydrocarbon-rich category of molecular biomass.<sup>15</sup> These are of increasing interest to polymer science due to the vast range of molecules available which give rise to a variety of desirable properties.<sup>9,31</sup>

### 1.3 Terpenes as a renewable feedstock from biomass

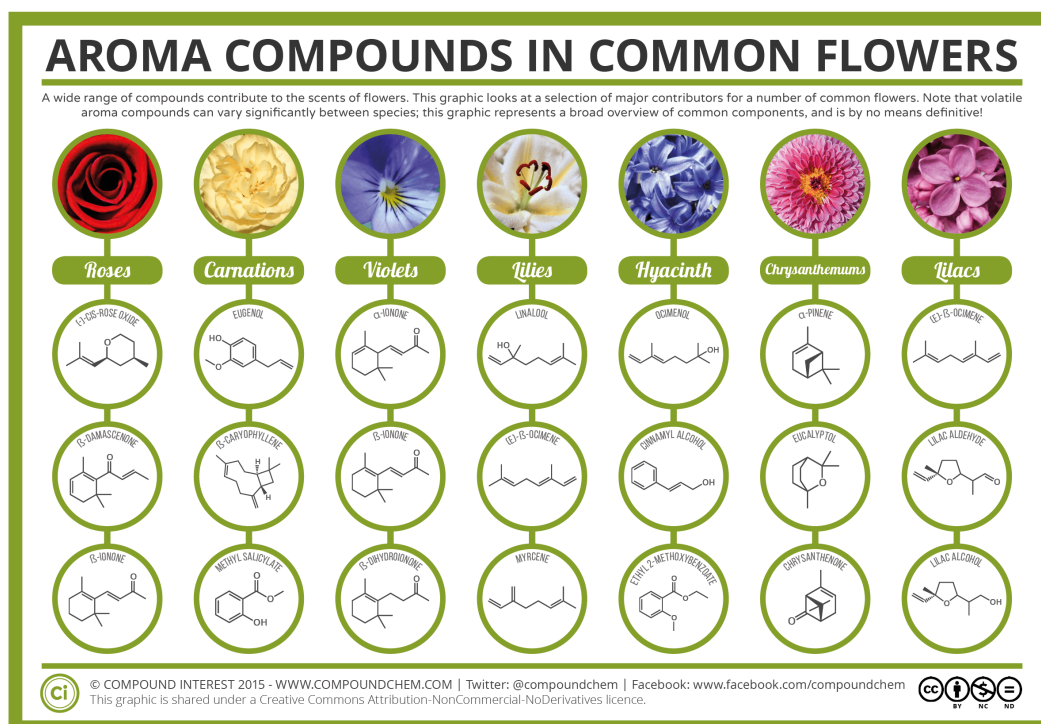


**Figure 10.** Some terpene and terpenoid feedstock compounds which are responsible for the aroma of flowers. Image: Compound Interest 2015 ©.

The term 'Terpene' refers to one of the most diverse families of naturally occurring, organic compounds.<sup>31</sup> These compounds are found in abundance in nature in a variety of plants and fungi (**Figure 10**).<sup>6</sup> They are formed in a common biosynthetic pathway, resulting in a variety of structures made up of units of isoprene (**1**), with enormous structural diversity.<sup>9,31</sup> This diversity is seen in both the number of carbon atoms in the compounds (which varies by 5; isoprene contains 5 carbon atoms), in addition to the stereochemical configurations, and the arrangement of the atoms in the carbon skeleton, resulting in a wide variety of biosynthetic isomers.<sup>31</sup>

'Terpenoids' are similar isoprene-based structures which have incorporated at least one oxygen atom, differentiating them from terpenes which can be traditionally considered to be hydrocarbons. However, the term terpene is increasingly being used to incorporate terpenoid structures. This added diversity allows for the classification of terpenes as hydrocarbon-rich molecular biomass.<sup>15,32</sup> 'Monoterpenes' are the most

common type of terpenes, comprising two isoprene units, with the general formula  $C_{10}H_{16}$  (**Figure 11**).<sup>9</sup>

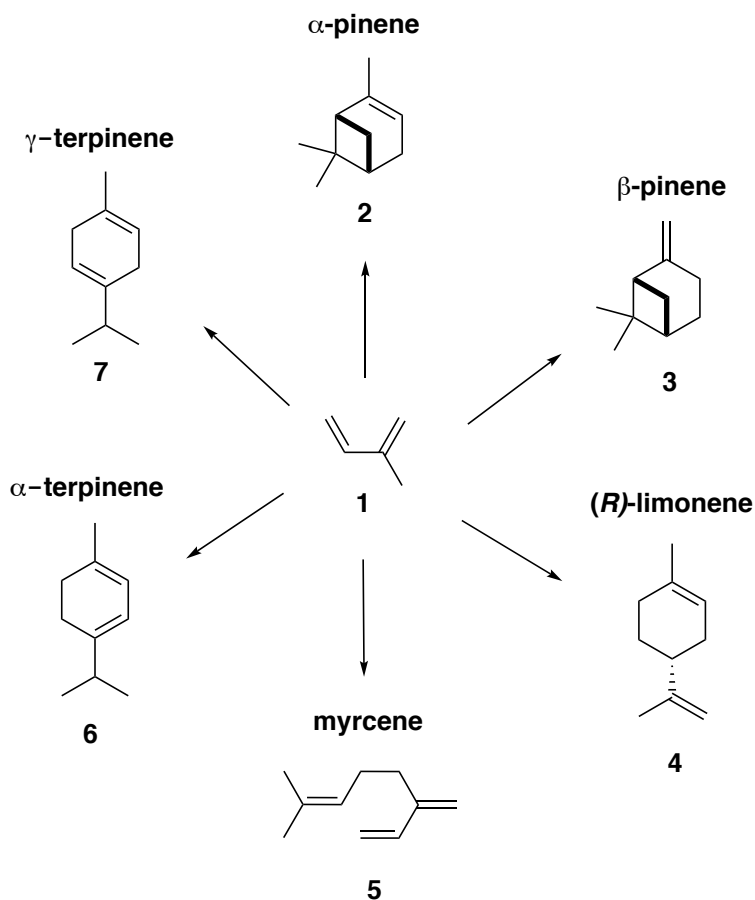


**Figure 11.** Common monoterpenes, which are characteristic of comprising two units of isoprene (**1**).<sup>9</sup>

Terpenes were originally thought to be waste products of plant metabolism with no specific biological role. However, it has since been found that the secondary metabolites offer some functions in ecological roles such as insect repellents, and some terpenes have even been found to act as intermediate species in biosynthetic processes.<sup>31</sup>

Most terpenes are obtained for commercial purposes from natural sources,<sup>33</sup> the most common of which is turpentine, the volatile fraction isolated from pine resin on a scale of about 350,000 tonnes per year.<sup>31,32</sup> Its composition is dependent on the age and species of the tree, amongst other factors, but its major components are  $\alpha$ -pinene (**2**) and  $\beta$ -pinene (**3**)

amongst other small amounts of other monoterpenes.<sup>5,32</sup> Turpentine can also be used to access a variety of other monoterpenes: their basic skeletons can readily interconvert to give rise to any monoterpene from another abundant precursor.<sup>9</sup> As such, oxygenated derivatives including menthol (**9**), carvone (**8**) and others including cyclic terpene alcohols can also be derived from turpentine (**Figure 12**).<sup>34</sup>

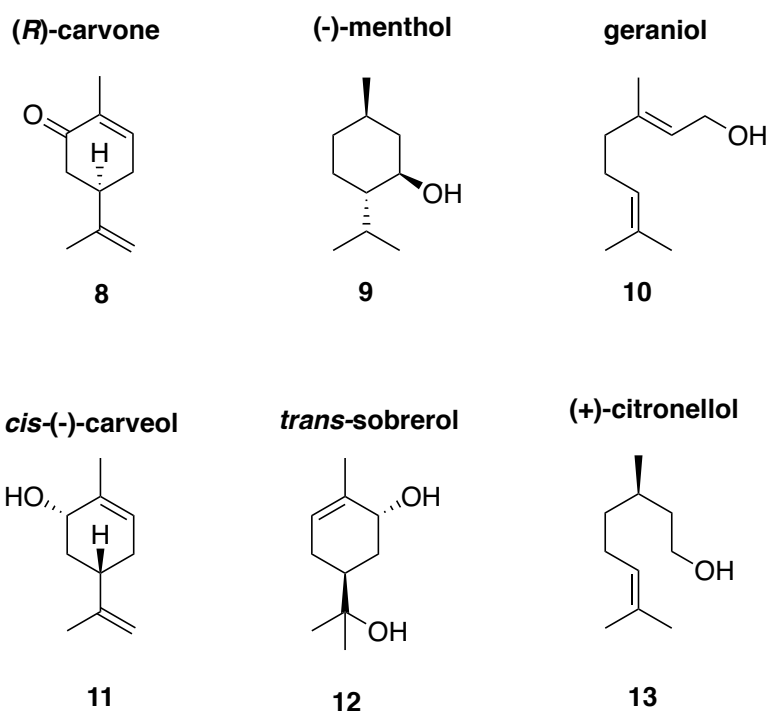


**Figure 12.** Some common monoterpenoids.

Limonene (**4**) is the third most abundant terpene found in turpentine, though it is more commonly found in citrus peel, in concentrations of over 90% (in addition to being present in over 300 plants).<sup>15,34</sup> Indirectly, limonene is also formed as a by-product of the citrus fruit industry,<sup>33</sup> the (*R*)- enantiomer in particular is a prominent waste stream, produced on a scale of approximately 70,000 tonnes per year.<sup>35</sup> The terpenoid carvone (**8**) is naturally derived from spearmint and caraway oils, in concentrations of up to 80%.<sup>34</sup> However, carvone is usually prepared synthetically by the oxidation of limonene, meaning large quantities could be derived in ethical and resourceful methods from the juicing industries.<sup>36</sup> Similarly, the terpenoid menthol (**9**) can be made from  $\beta$ -pinene as a precursor, which



in turn can be obtained as a waste product of the paper industry's Kraft process.<sup>36,37</sup>

Many terpenes, such as  $\alpha$ -terpineol and camphor, are made through cost-effective, catalytic industrial processes. Terpenes are well-known and important structures in many industrial processes, having had a long history of use in flavouring and fragrances,<sup>34</sup> as solvents,<sup>15,31</sup> and even ancient medicines.<sup>31</sup> Their use as monomers or monomer precursors has become a major focus in recent years.<sup>6</sup>

#### 1.4 A history of the direct polymerisation of terpenes

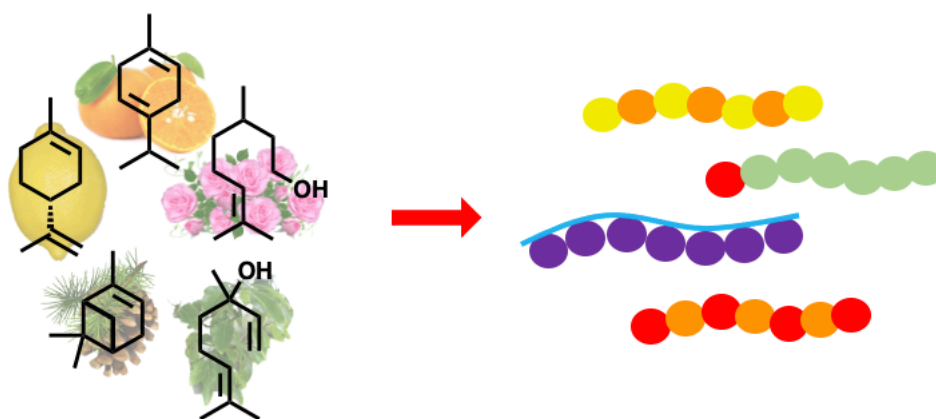
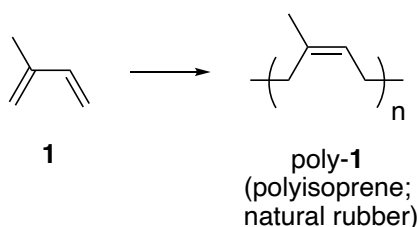


**Figure 13.** *Cartoon representation of the polymerisation of terpenes.*

Possibly the best-known and most successful example of a polyterpene is natural rubber (**Scheme 1**).<sup>5</sup> It is harvested from the Brazilian rubber tree (*Hevea brasiliensis*), and composed of units of isoprene arranged in *cis*-1,4 linkages. Natural rubber has a number of favourable properties as a result of its naturally high molecular weight ( $>1 \text{ Mg.mol}^{-1}$ ), including efficient heat dispersal, elasticity, and malleability at low temperatures, amongst others.<sup>38</sup> More than 10 megatonnes of natural rubber are produced per year, though this accounts for only 40% of rubber demand, the remaining 60% coming from synthetic rubber. However, the natural form offers superior properties to that of synthetic rubber. This is thought to arise from the incorporation of certain secondary components such as proteins,

carbohydrates and lipids into its structure during its biosynthesis. This cannot be duplicated in synthetic rubber alternatives, and as such, its synthesis is reaching a plateau, while the production of natural rubber is increasing, particularly in south-east Asia.<sup>5,38</sup>



**Scheme 1.** The structure of isoprene and its polymer, natural rubber, which is arranged in cis-1,4 linkages.<sup>39</sup>

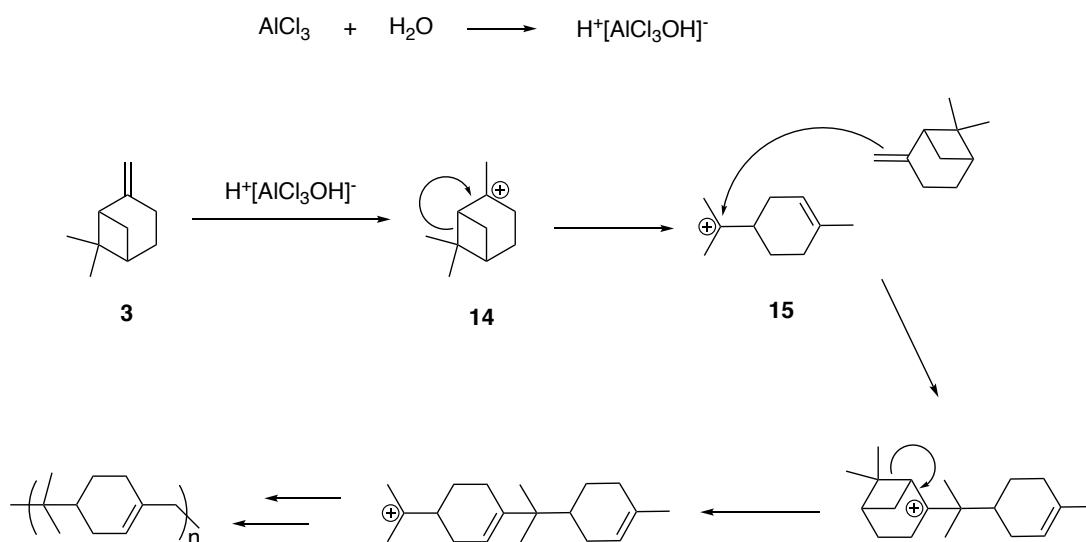
Other than synthetic rubber, research into the use of terpenes for polymerisation has largely focused on the use of  $\alpha$ -pinene (**2**) and  $\beta$ -pinene (**3**), as well as limonene (**4**) and myrcene (**5**).<sup>40</sup> These are some of the most abundant forms of monoterpenes, and they are relatively easy and inexpensive to isolate.<sup>9</sup>

The most accessible and straightforward means of polymerising these monoterpenes is to do so by making use of their alkene functionalities. Given that for a majority of terpenes and their isomers, these alkene groups are flanked by an electron-donating methyl group, it follows that the earliest known examples of polymerisation is *via* cationic polymerisations.<sup>6,40</sup> Of these,  $\beta$ -pinene has been the most widely studied, due to its accessible exocyclic alkene unit, which aids in polymerisations. Comparatively, only oligomers are achievable with  $\alpha$ -pinene, due to the alkene functionality being endocyclic, trisubstituted and thereby less accessible in polymerisations.<sup>15</sup>

The mechanism for the cationic homopolymerisation of  $\beta$ -pinene was first proposed by Roberts and Day,<sup>41</sup> and involves the use of a Lewis Acid which induces a thermally fast and very vigorous reaction even at catalyst loadings of <1%.<sup>42</sup> A direct method, in which the monomer is added gradually to a suspension of solvent and catalyst, is favourable over the indirect method which involves adding the catalyst to a suspension of

monomer and solvent, because the former allows for more efficient control of the heat generated.<sup>42</sup>

According to the proposed mechanism (**Scheme 2**), a strong proton donor is formed in a reaction between the Lewis acid and water (a co-catalyst). This is followed by the protonation of  $\beta$ -pinene, forming a carbocation (**14**).<sup>31</sup> This cation is very short lived, as the molecule isomerises to break the highly strained cyclobutane ring, forming the comparatively more stable para-menthane carbocation species (**15**). This ion is stabilised from the electron-donating effects of its three alkyl groups, allowing it to be long lived enough to electrophilically attack another monomer, and thus this is the species responsible for the propagation of the reaction to form oligomers and polymers.<sup>9,31,42</sup>



**Scheme 2.** Proposed mechanism for the cationic polymerisation of  $\beta$ -pinene (**3**).<sup>9,31,42</sup>

The use of Lewis acids such as  $\text{AlCl}_3$  leads to polymers of  $M_n \leq 4000$  g/mol.<sup>15</sup> Despite this polymerisation having been known for a long time, its use in the formation of polymers with high molecular weights, under mild conditions, has remained a challenge.<sup>6</sup> Higher molecular weights would require temperatures in the region of  $-40$  °C, which is difficult to achieve given the high exothermic nature of the reaction.<sup>31</sup> Despite this, notable progress has been made, specifically through the use

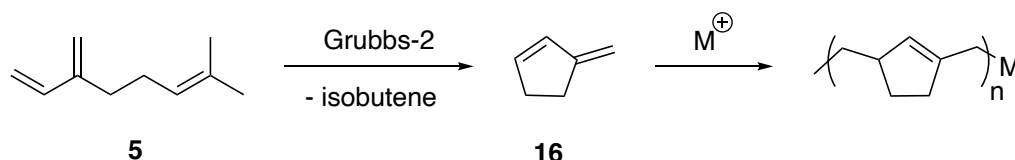
of co-catalysts based on  $\text{H}_2\text{O}/\text{EtAlCl}_2$ , which allow lower temperatures to be reached.<sup>15,31</sup> Using this co-catalytic system, polymers up to  $M_n = 40,000 \text{ g}\cdot\text{mol}^{-1}$  were made when cryogenic temperatures were applied, reaching  $-80 \text{ }^\circ\text{C}$ .<sup>40</sup>

As mentioned, a cationic polymerisation mechanism of this type for  $\alpha$ -pinene (**2**) is not as successful because although the formation of the para-menthane carbocation **15** is possible, polymerisation would require attack of an *endocyclic* alkene to the cationic site. This is limited by steric hindrance and as such, propagation is not as favoured.<sup>31</sup> The fact remains, however, that **2** is the most abundant component of turpentine, and so much research has been conducted into its cationic polymerisation.<sup>31</sup> While some success has been reached through the use of a  $\text{SbCl}_3$  co-catalytic system, in general  $\alpha$ -pinene is not thought to have the appropriate properties to be used as a renewable polymer for homopolymerisation.<sup>9</sup> Research has instead turned its attention to synthetic modifications of **2**, to generate useful monomers for other polymerisation types (*vide supra*).

Cationic polymerisations of limonene (**4**) have also seen only limited success, with low conversions and molecular weights.<sup>9</sup> Similar results have been observed when **4** is subjected to radical-mediated homopolymerisations, due in part to termination reactions of the primary radical.<sup>43</sup> Limonene has shown more successful polymerisation results when co-polymerised, which is largely achieved through radical polymerisation, as in the case of its co-polymerisation with methyl methacrylate (MMA) and acrylonitrile.<sup>15,31</sup> A common problem with polymerising limonene in this way is that it tends to act as a chain transfer agent, thus producing very low molecular weight polymers, with this occurring increasingly as the molar ratio of limonene is increased.<sup>9,15</sup> Though methods of homopolymerising limonene have shown little success, its abundance, especially as a waste material, means that continued and fresh research into monomeric potential is both valid and required.<sup>9</sup> As with  $\alpha$ -pinene, much success has been found through the functionalisation of the alkene moieties of limonene, to produce compounds which more readily undergo polymerisation (*vide supra*).

Myrcene (**5**) is an acyclic monoterpene with three double bonds meaning that it is also theoretically available for both cationic and radical

polymerisation.<sup>9</sup> The Hillmyer group demonstrated that **5** could be homopolymerised by ring-opening techniques, by first employing ring-closing metathesis of the terpene using Grubbs second generation catalyst, followed by cationic polymerisation of the 3-methylenecyclopentene (**16**) product (**Scheme 3**).<sup>44</sup> This method led to the production of polymers of **16** with  $M_n = 22,000 \text{ g}\cdot\text{mol}^{-1}$ , when the initiation system *i*-BuOCH(Cl)Me/ ZnCl<sub>2</sub>/Et<sub>2</sub>O was used.<sup>40</sup>



**Scheme 3.** Ring-closing metathesis of myrcene (**5**), which evolves isobutene, the principal starting material for rubber, as a by-product.<sup>44</sup> This is followed by the cationic Ring Opening Polymerisation of 3-methylenecyclopentene (**16**).  $M^+$  refers to the initiation system *i*-BuOCH(Cl)Me/ ZnCl<sub>2</sub>/ Et<sub>2</sub>O.<sup>40,44</sup>

Myrcene has also been shown to polymerise *via* Reverse Addition Fragmentation chain-Transfer (RAFT) polymerisation, in solvent free conditions, resulting in polymers of low dispersity and a predominantly 1,4-polymyrcene structure.<sup>6</sup> Its three alkene units are also available for functionalisation, opening up the possibility of a wide range of polymers with a variety of applications.<sup>9</sup>

Despite these examples representing some of the significant efforts (and progress) in the synthesis of polymers directly from terpenes, results show that the materials generally lack the desired properties to compete with commercial alternatives.<sup>35,45</sup> However, the functionalisation of terpenes has shown the feedstock has huge potential for polymerisation.<sup>46</sup> Synthetic methods have been developed which over the past 20 years have seen terpenes undergo facile and robust (as well as bespoke) chemical modifications, to arrive at a wealth of monomeric compounds with potential for polymer materials. These will now be discussed in the following section.

## 1.5 The functionalisation of terpenes towards useful monomers

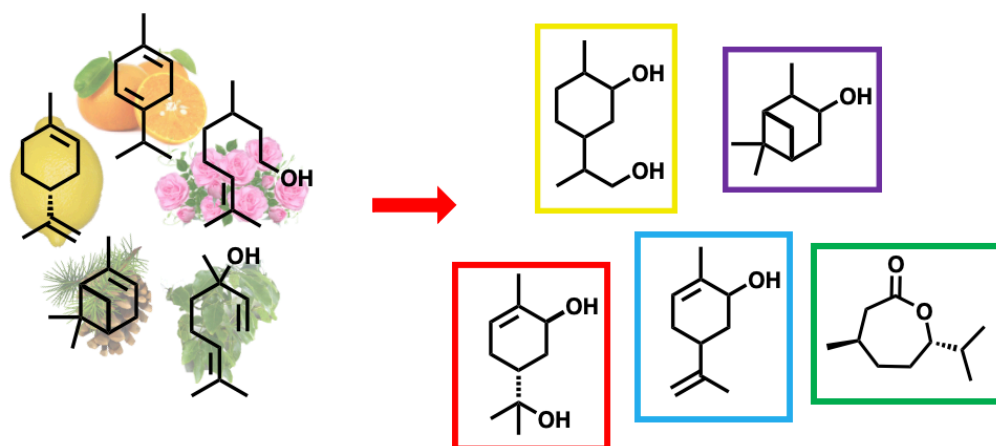


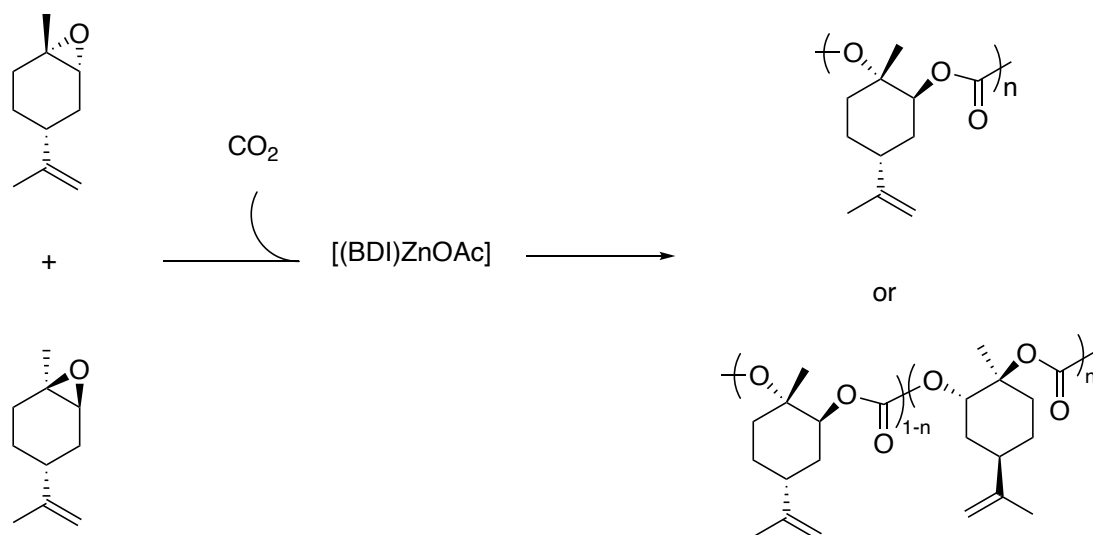
**Figure 14.** Representation of some of the monomers available from terpenes-based biomass.

While much progress has been made over the past decades in the direct polymerisation of terpenes, it has been generally recognised that these polymers still lack the desired properties to compete with the low-cost and versatile nature of the commercial alternatives derived from crude oil.<sup>35</sup> However, the chemical modifications of terpenes to create useful monomeric products has, on the other hand, proved remarkably successful, indicating that there remains huge potential for polymerisation for the renewable feedstock.<sup>46</sup> To begin to tap into the full potential of terpene-based polymers, research has focused on the functionalisation of terpenes to produce monomers that can be used in well-established, robust polymerisation methods.<sup>35,45</sup> As such, sustainable and controlled methods of functionalising terpenes as compounds that can be easily “dropped in” to these existing polymerisation synthetic methods is at the forefront of terpene-based polymer research. In fact, research of this nature has often focused methods of accessing these monomers independent to the investigations into their polymerisations.<sup>47,48</sup> Some examples are discussed in the sub-sections that follow, categorised based on either the monomer or polymer functional groups.

### 1.5.1 Terpene-based polycarbonates and polyurethanes from epoxides

The epoxidation of terpenes has proved a popular and successful method of modifying terpenes to generate monomers and monomeric precursors for a wide variety of polymer types. To name only a handful of examples, bio-based polycarbonates,<sup>28,49–51</sup> polyurethanes<sup>52,53</sup> and polyethers<sup>54,55</sup> have all been synthesised following the epoxidation of terpenes, often limonene in particular. These compounds also have applications as bio-based crosslinkers in epoxy-resin chemistry.<sup>56,57</sup> Recently, a sustainable, catalytic protocol was described for epoxidation of a wealth of terpenes, using H<sub>2</sub>O<sub>2</sub> as an oxidant.<sup>58</sup>

A green and sustainable synthesis of bio-based epoxides is particularly attractive for the synthesis of polycarbonates, as the other reactive component is CO<sub>2</sub>, an abundant waste-stream. In 2004, Byrne *et al.* described for the first time the alternating synthesis of polycarbonates from limonene oxide and CO<sub>2</sub> with the use of β-diiminate zinc catalysts (**Scheme 4**).<sup>28</sup> This system allowed for high stereocontrol of the polymer, with 98.3% repeating units in the *trans*-orientation. Later, the Kleij group synthesised similar polymers using the nucleophilic, binary catalyst Al<sup>Me</sup>/PPNCl.<sup>59</sup> This allowed for better incorporation of *cis*- repeating units (up to 33%), suggesting that the change in catalyst resulted in better conversion of the *cis*-limonene oxide monomer (in addition to the *trans*-one). This same group went on to prepare a number of terpolymers the following year, of limonene oxide and cyclohexane oxide (CHO) with CO<sub>2</sub>.<sup>50</sup>



**Scheme 4.** *Byrne et al. synthesis of polycarbonates based on limonene oxide and carbon dioxide. BDI =  $\beta$ -diiminato.*<sup>28</sup>

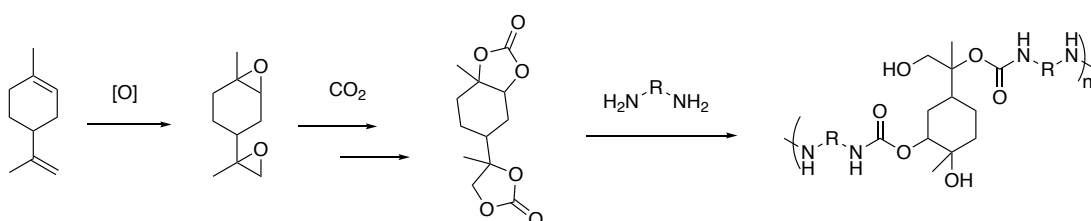
Generally, this method of forming polycarbonates through the ring-opening co-polymerisation (ROCOP) of epoxide groups is most successful with cyclic epoxides such as CHO.<sup>60</sup> Much progress has been made in recent years in the synthesis of novel heterodinuclear catalysts for the co-polymerisation of such epoxides and CO<sub>2</sub>.<sup>61,62</sup> The use of terpenes for this synthesis is therefore a versatile area of polymer chemistry with much room for exploration,<sup>51</sup> particularly considering the structural similarities between CHO and cyclic terpene epoxides such as limonene oxide. In this context, the epoxidation of  $\alpha$ -pinene (**2**) in the formation of  $\alpha$ -pinene oxide (usually achieved in quantitative yields using *m*CPBA) has also proved successful in the synthesis of polycarbonates. In this case, a Cr(III) (salen) complex with [PPN]Cl was employed as a catalyst. As with limonene-oxide, the polycarbonate is then synthesised in a ROCOP mechanism with CO<sub>2</sub>.<sup>63</sup>

Importantly, polycarbonates (including those made from terpenes such as limonene) are biodegradable,<sup>64</sup> rendering them of particular interest as it may allow for the carbon in their backbone to be recoverable at their end-of-life. Aliphatic polycarbonates are also commonly bio-compatible, rendering them an attractive substitute to bisphenol-A based aromatic alternatives, in a variety of applications.<sup>60</sup>



The synthesis of non-isocyanate polyurethanes (NIPUs) has recently emerged as an area of interest to green polymer chemistry; a field for which epoxidised terpenes may prove of great value. Unlike isocyanate-based polyurethanes, NIPUs usually exhibit improved thermal stability, higher stiffness and tensile strength.<sup>52</sup> Similar to polycarbonates, these polymers can be accessed using CO<sub>2</sub>, which is promising in the field of renewable polymer chemistry because not only does it mean their synthesis avails of a renewable terpene biomass for the epoxide component, but also gives rise to the opportunity of upcycling waste CO<sub>2</sub> in the following step; conversion to a carbonate monomer.

Bähr *et al.* showed that polymers and oligomers of this nature could be prepared through the bis-epoxidation of limonene, followed by the conversion of this compound with CO<sub>2</sub> to the corresponding limonene di-carbonate.<sup>52</sup> The synthesis of this monomer was conducted on a large scale of 1 kg, and their best results employed a quaternary alkyl ammonium catalyst in 3 mol% loadings, with 30 bar CO<sub>2</sub> at 140 °C (**Scheme 5**). This monomer was then polymerised with amine co-monomers, in a step growth mechanism, controlling the end-groups with the stoichiometry of the two monomers. This led to the production of linear NIPUs and functional prepolymers. Polyamines were then employed to generate non-linear, branched composites, which formed attractive new additives and curing agents for epoxy resins and the production of segmented polyurethanes.

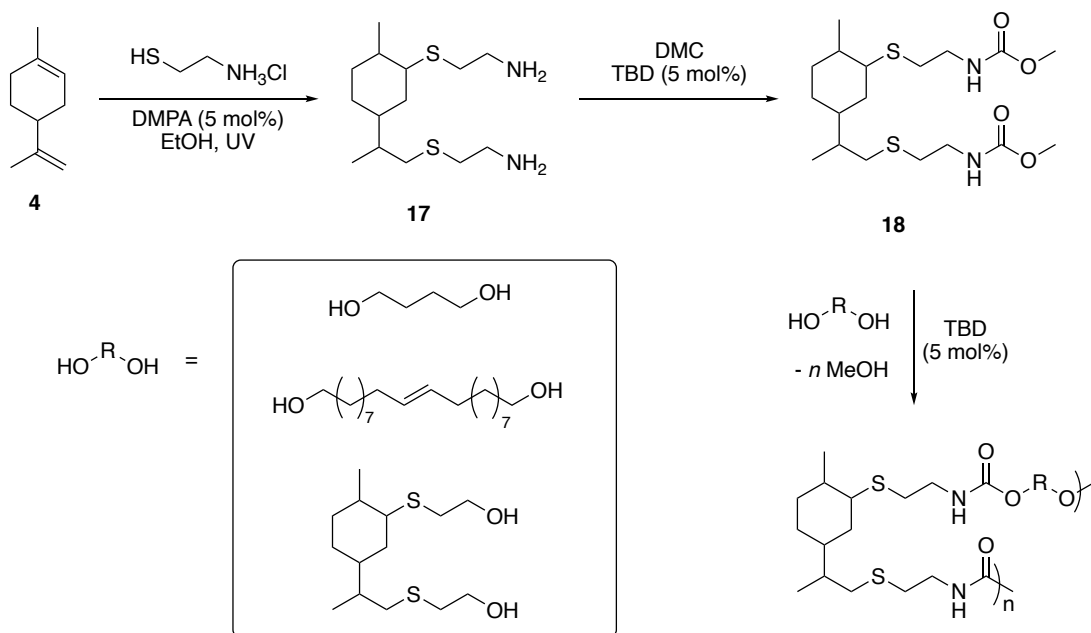


**Scheme 5.** The synthesis of a limonene-derived di-carbonate monomer by Byrne *et al.*, followed by its curing with di- and poly-amines to produce non-isocyanate polyurethanes (NIPUs).<sup>52</sup>

The Mülhaupt group later expanded on this work, in the preparation of a number of linear and cross-linked NIPUs with a variety of di- and polyamines.<sup>53</sup> In this further work the authors demonstrated the improved performance of the oligomeric material in terms of the glass transition temperature and stiffness, when the limonene dicarbonate monomer was recrystallised to a high degree of purity. The resulting NIPUs have potential to be explored for coating applications.

### 1.5.2 Other syntheses of terpene- polycarbonates and polyurethanes

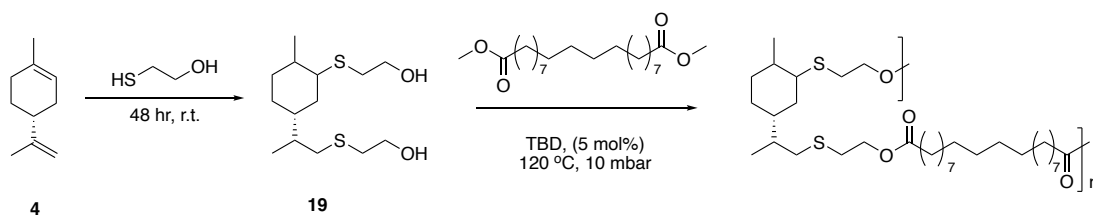
NIPUs can alternatively be synthesised without the use of epoxides, through a polycondensation mechanism using diols and carbamates.<sup>60</sup> In 2013, the Meier group reported the synthesis of a di-carbamate monomer from limonene, synthesised in two steps (**Scheme 6**).<sup>65</sup> First, *via* a thiol-click reaction exploiting the alkene moieties of **4** with cysteamine hydrochloride. This diamine product (**17**) was then further converted to the di-carbamate **18** by a TBD-catalysed reaction with dimethyl carbonate (DMC). TBD was again employed as a catalyst in the polycondensation of this monomer with a selection of diol co-monomers, generating polymers of up to 12,600 g·mol<sup>-1</sup>, with polydispersities ranging from 1.8 to 2.2.<sup>65</sup>



**Scheme 6.** The synthesis of a di-carbamate monomer from limonene by Firdaus et al., followed by its condensation polymerisation with a selection of diols.<sup>65</sup>

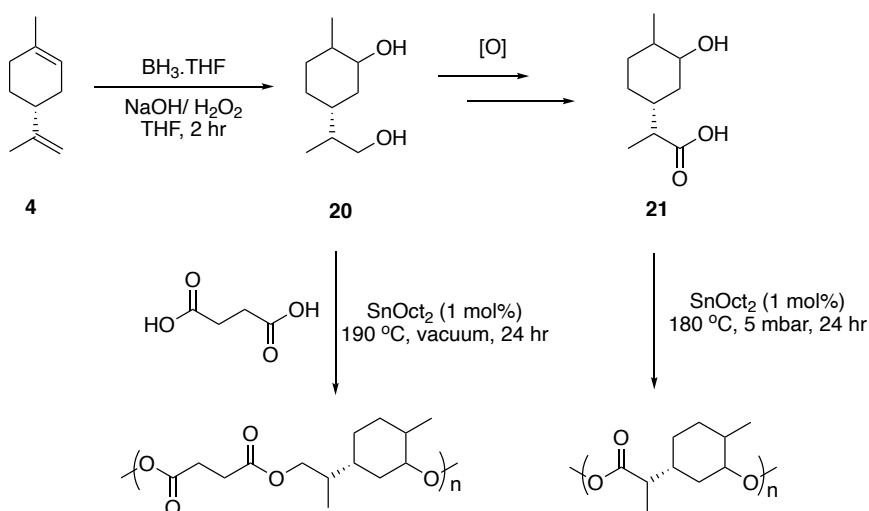
### 1.5.3 Terpene-based polyesters by condensation mechanisms

This strategy of using thiol-click chemistry has proved a popular way in which to modify terpenes with handles for step-growth polymerisations. In previous work, the Meier group had employed this synthetic strategy in the synthesis of a number of alcohol and carbonate monomers from limonene and  $\beta$ -pinene.<sup>66</sup> A variety of these compounds were then used in the synthesis of polyesters with a limonene/ fatty acid backbone, by condensation polyesterification, employing TBD as a catalyst. An example of one of the many such monomers and polymers from the library of compounds synthesised in this work is shown in **Scheme 7**.<sup>66</sup>



**Scheme 7.** The Meier group's synthesis of a limonene-based diol **19** via thiol-click chemistry, followed by its use in the synthesis of polyesters in a condensation mechanism with a di-carbonate co-monomer.<sup>66</sup>

An alternative diol monomer (**20**) from limonene was synthesised by Thomsett *et al.* in 2019, through the use of Brown's hydroboration/oxidation mechanism.<sup>35</sup> This was used in combination with the bio-based di-acid co-monomer succinic acid in the synthesis of polyester materials up to  $30,000 \text{ g}\cdot\text{mol}^{-1}$ . Three routes towards the oxidation of **20** to a hydroxy-acid monomer (**21**) were then screened according to a green chemistry metrics evaluation. This monomer had the necessary functional groups to allow for the formation of a homopolymer by polycondensation, and was found to produce oligomers with a high terpene content and molecular weights up to  $2,600 \text{ g}\cdot\text{mol}^{-1}$  (**Scheme 8**).<sup>35</sup>

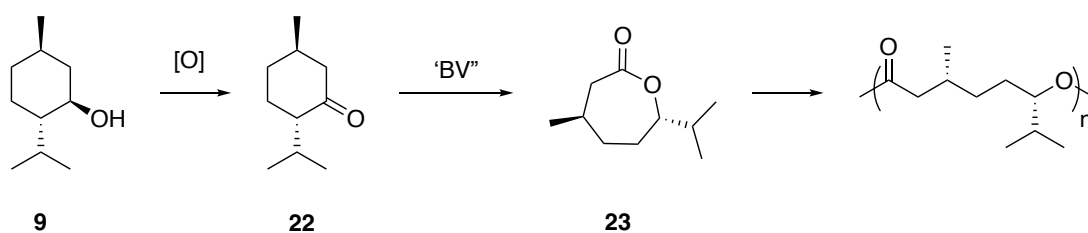


**Scheme 8.** The synthesis of limonene-diol **20** followed by its oxidation to the hydroxy-acid **21**. **20** was polymerised using a di-acid co-monomer to produce high molecular weight polymers while **21** was homo-polymerised, resulting in the synthesis of low molecular weight oligomers.<sup>35</sup>

### 1.5.4 Terpene-based polyesters by Ring Opening Polymerisation

The synthesis of aliphatic polyesters has proved one of the most promising classes of sustainable polymers, owing to their general biocompatibility as well as relatively facile methods of degradation at their end of life.<sup>60</sup> Terpenes offer a diverse and plentiful feedstock for such polymers. Other than polycondensation mechanisms, Ring Opening Polymerisation (ROP) has proved a facile method in which to form polyesters from lactones.

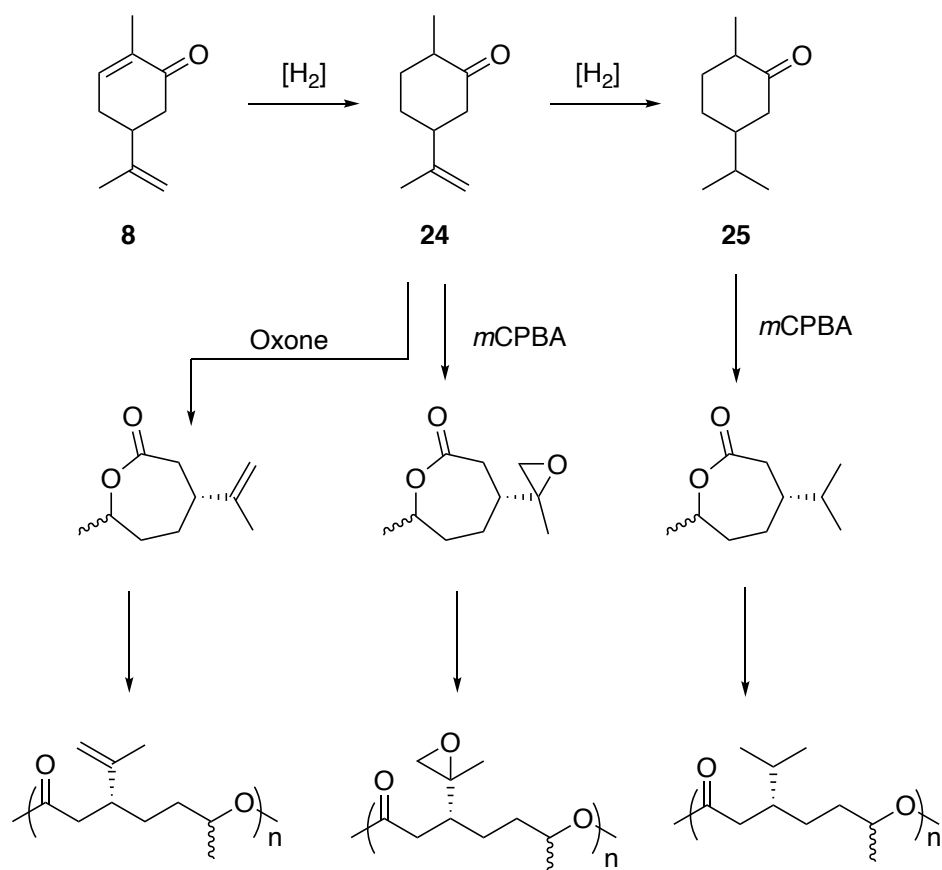
The Baeyer-Villiger oxidation has been employed by the Hillmyer group in numerous examples over the past 15 years, to arrive at a number of terpene-based lactones, derived from carvone (**8**) and menthone (**22**).<sup>11,43,67-69</sup> The strain of the seven membered rings enable the molecules to undergo ROP in a controlled mechanism (with use of a catalyst). In the first such example, **22** was converted to menthide (**23**), and a phenoxy-amine-Zn complex was employed as a catalyst to synthesise aliphatic polyesters in an analogous method to that used to synthesise polycaprolactone (PCL) polyesters (**Scheme 9**).<sup>67</sup> The control of the monomer/ catalyst ratio led to the controlled synthesis of polymers ranging from 3,000 to 91,000 g·mol<sup>-1</sup>. This method of ROP also proved successful in the formation of block co-polymers.<sup>60</sup>



**Scheme 9.** The synthesis of aliphatic polyesters from 'menthide' lactone **23**, synthesised via the Baeyer-Villiger oxidation of **22**, a derivative of menthol (**9**). (BV = Baeyer Villiger oxidation).

Carvone (**8**) is more highly functionalised than menthone, featuring two alkene groups in addition to a ketone. When the Hillmyer group applied this ROP methodology to lactones derived from **8**, it allowed for the synthesis of a wider variety of monomers and polymers, featuring a greater

range of functionality in the polymer backbones (**Scheme 10**). Under normal conditions however, when carvone is treated with *m*CPBA it does not form a lactone, but instead the peroxy-acid will epoxidise the exocyclic, electron rich alkene, leaving the ene-one moiety intact.<sup>70</sup> To circumvent this problem, the group first reduced the endocyclic ene-one of **8**, to synthesise dihydrocarvone (**24**), which renders it susceptible to the ring-expansion/oxidation mechanism of the Baeyer-Villiger reaction when *m*CPBA is applied. In two separate pieces of work, the authors then conducted this Baeyer-Villiger oxidation on **24** using either Oxone<sup>®</sup> or, as usual, *m*CPBA. When Oxone<sup>®</sup> was employed, it selectively formed the 7-membered lactone from the cyclic ketone, leaving the exocyclic alkene intact.<sup>69</sup> Alternatively, when *m*CPBA was used, the molecule underwent a global oxidation, resulting in the 7-membered lactone ring, with an exocyclic epoxide group.<sup>68</sup> In a third comparison, the group also reduced **24** further to the saturated species (save for the ketone group), carvomenthone (**25**).<sup>69</sup> This was then treated with *m*CPBA to form the monomer lactone species carvomenthide (analogous to **23**).



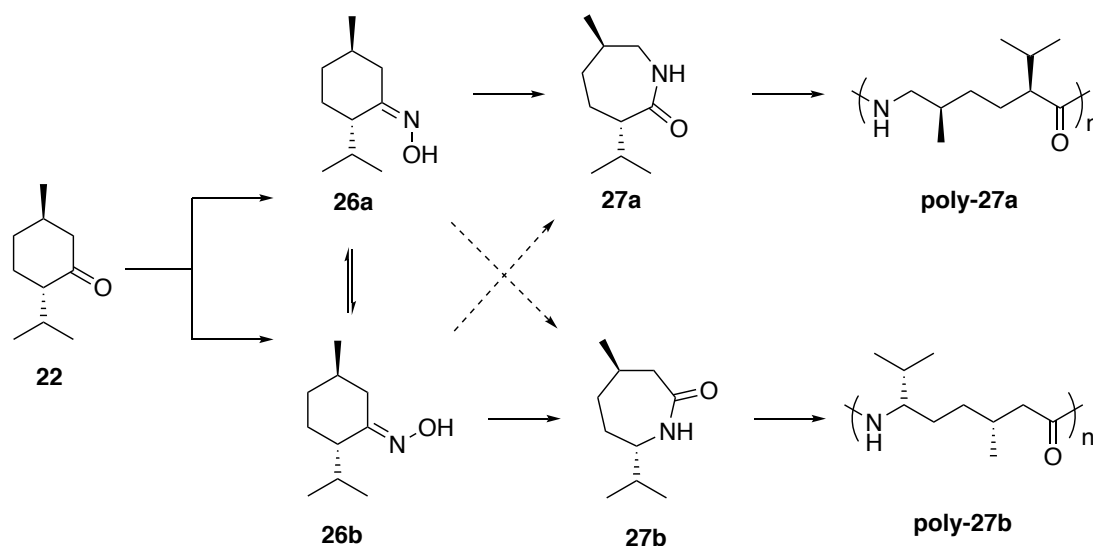
**Scheme 10.** Three examples of the lactone monomers that are accessible from **8**, and the corresponding polyesters which were formed by ROP.<sup>60</sup>

### 1.5.5 Terpene-based polyamides by Ring Opening Polymerisation

Analogous to the terpene-based lactones prepared by the Hillmyer group; terpenoids with a ketone functionality can be readily converted to oximes, which can in turn undergo the Beckmann rearrangement, resulting in the corresponding lactams. These can then undergo ROP to produce polyamides.<sup>43,71–73</sup>

In 2014 Winnacker *et al.* extensively studied this methodology with menthone (**22**), in what may be considered the first such example,<sup>73</sup> though technically this monomer synthesis and a similar lactam polymerisation method had been known since 1992 and 1961, respectively.<sup>74,75</sup> From **22**, Winnacker and co-workers synthesised the two oxime regioisomers **26a** and **26b** using hydroxylamine. These were found

to interconvert with one another, rendering the synthesis of a single isomer very difficult. Additionally, the Beckmann rearrangement to yield the corresponding lactams resulted in a mixture of the isomers of **27**, even when a single isomer of **26** was used. The authors were however able to isolate separate samples of the monomers **27a** and **27b** by column chromatography. This enabled the preparation of oligomers using anionic polymerisation, employing potassium as an initiator with benzoyl chloride as a co-initiator (**Scheme 11**). An acid catalysed mechanism with HCl at 230 °C was also investigated, but it was found to only be successful for **27a**. The oligomers formed in this study were all of  $M_n < 2,800 \text{ g}\cdot\text{mol}^{-1}$ .<sup>60</sup>



**Scheme 11.** The synthesis of oligo-amides from terpene-derived lactams **27**, made via the Beckmann rearrangement on terpene-derived oximes.<sup>73</sup>

Later, a direct, stereoselective route from **22** to the lactam **27b** was described by the same group, employing hydroxylamine-*O*-sulfonic acid as a catalyst.<sup>76</sup> This allowed for the more facile preparation of oligomers of **27b**, which featured a melting temperature of approximately 300 °C.

More recently, this method of polyamide formation has been achieved by Stockmann *et al.*, who described the scalable and stereoselective synthesis of 3-carene based lactams.<sup>71</sup> These polymers were found to retain the three-membered ring and the methyl group featured in the terpene, which bestowed intriguing properties in terms of



the crystallinity, transparency and thermal properties of the polymer material. The synthesis of the monomer is cumbersome, requiring four synthetic steps from the terpene biomass. However, the authors demonstrated that the reactions were scalable to molar amounts, and could be achieved in an at-least partially sustainable one-vessel process.<sup>60,71</sup>

#### 1.5.6 Radical-type mechanisms of terpene polymerisation

While much success has been made, and is yet to be explored, in relation to above kinds of ROP, ROCOP and polycondensation polymerisation types with terpenes, there has also been a good deal of research into the use of terpenes in radical-type polymerisations. A variety of examples exist of terpenes, and frequently, their (meth)acrylate derivatives, used in free radical and RAFT polymerisations.<sup>77,78</sup>

The Howdle, Stockman and Irvine groups at the University of Nottingham have made progress over the last decade in generating (and capitalising upon naturally occurring) alcohol-functionalised terpenes for these polymerisation types. In 2016, Sainz *et al.* demonstrated that a number of terpene-alcohols could be accessed from a selection of abundant terpene feedstocks. These were in turn easily converted to (meth)acrylate monomers (**Figure 15**).<sup>45</sup> Initially, investigations formed these (meth)acrylates through a non-sustainable route involving (meth)acryloyl chloride but later a one-pot, catalytic approach was employed. These monomers were shown to readily polymerise by conventional free radical polymerisation, leading to the production of polymers with a range of properties, including an application as a powdered acrylic coating.<sup>45</sup>

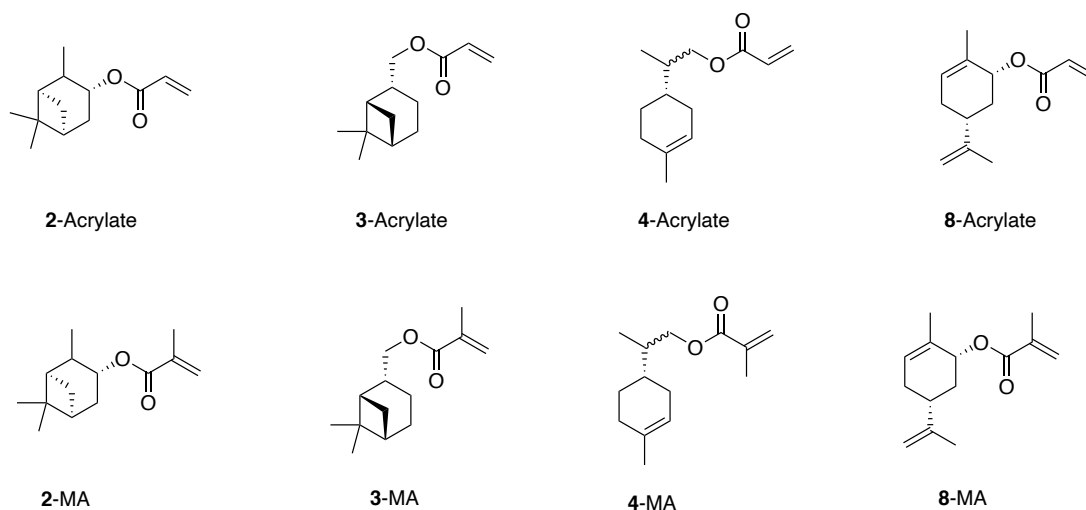
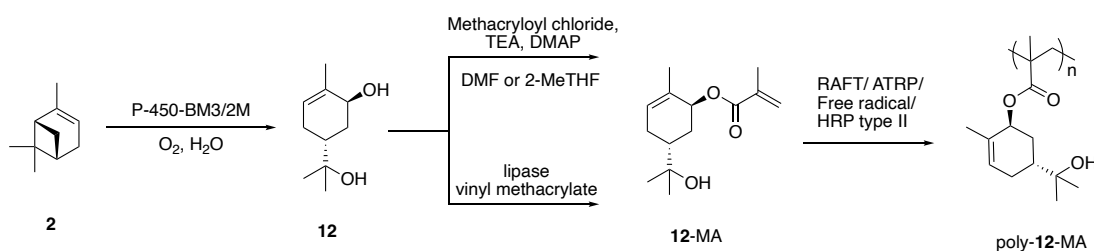


**Figure 15.** The structures of terpene-derived acrylate and meth-acrylate (denoted 'MA' in the figure) monomers used for free radical polymerisations by Sainz et al.<sup>45</sup>

More recently, *trans*-sobrerol methacrylate was synthesised by Stamm *et al.*, and polymerised by a variety of radical means including free radical, RAFT and Atom Transfer Radical Polymerisation (ATRP).<sup>78</sup> *Trans*-sobrerol (**12**) is most commonly and commercially made *via* oxidation of  $\alpha$ -pinene, the most abundant terpene in turpentine, making it an attractive starting point for polymer feedstocks.<sup>78</sup> Additionally, it is known to have many desirable properties which could be interesting to exploit for biomaterials and medical devices, including anti-mycotic properties,<sup>79</sup> as well as being known to prevent breast cancer development<sup>80</sup> and pulmonary hypertension.<sup>81</sup> Its cyclic structure suggests that it could be used to produce polymers with high glass transition temperatures ( $T_g$ ) and, interestingly, it is hydrophilic and poorly soluble in a variety of organic solvents, likely due to the presence not only of the secondary  $\alpha,\beta$ -unsaturated alcohol, but also the additional exocyclic alcohol group.<sup>78</sup>

In this work, the authors demonstrated the chemo-enzymatic synthesis of *trans*-sobrerol directly from  $\alpha$ -pinene with cytochrome P450 in one pot, without having to first synthesise the intermediate  $\alpha$ -pinene oxide. While this is currently still only available on a small scale, nonetheless it shows the potential to use biocatalysts in place of harsh

chemicals or cumbersome synthetic methodologies in the preparation of the useful monomeric precursor. In the methacrylation step using methacryloyl chloride, the authors reported the synthesis of the monomer in dimethyl formamide (DMF), but given its toxicity, they reported that 2-MeTHF would be a preferred alternative, though the yield is compromised slightly from 65% to 57%. Alternatively, to avoid this type of chemical synthesis entirely, the methacrylation can be conducted using the enzyme Amano lipase, resulting in a 96% yield without the need for further purification when conducted on a small scale. The monomer can therefore be fully synthesised using enzymatic routes. Furthermore, in addition to the conventional radical polymerisation methods mentioned above, the monomer was also polymerised using enzyme catalysis at room temperature in water, showing superior activity (**Scheme 12**). Results showed that the polymers had a  $T_g$  of up to 150 °C, which could be tailored by co-polymerisation with other polymers such as poly-methyl methacrylate (PMMA).



**Scheme 12.** The chemo-enzymatic synthesis of trans-sobrerol (**12**), followed by its methacrylation (**12-MA**) and polymerisation (poly-**12-MA**) using either conventional or enzymatic means.<sup>78</sup>

### 1.5.7 Summary

It is evident that the nature of terpenes being made up of a variety of double bonds, chiral centres and isomeric forms (as well as the extra diversity bestowed by heteroatoms of the terpenoid classes), means that there is a wealth of organic chemistry transformations available to the natural molecules. This in turn means a vast variety of monomer structures are available, and as such, terpenes constitute a useful feedstock to a

variety of applications in polymer chemistry. With plenty of different monomers easily accessible through green and sustainable chemistry, it follows that a plethora of potential polymer systems with diverse applications are attainable from the bio-based feedstocks.

### 1.6 Epoxy-amine resins and polymer systems

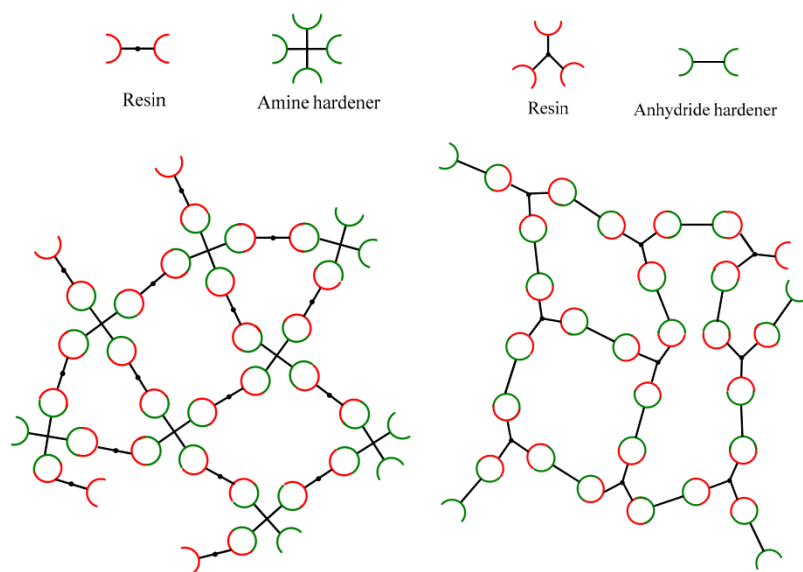


**Figure16.** Representation of the reaction of two kinds of epoxy resins with two curing agents, one amine- and one anhydride-based.<sup>82</sup>

Other than categorising polymers by their feedstock or monomers, it is also possible to categorise them by polymerisation type. One such example is that of epoxy-resin chemistry.

Since their commercialisation in the 1940s,<sup>83</sup> epoxy-resin materials have become a particularly well-developed area of polymer science. In 2014, the production of epoxy resins in the U.S. alone was more than 250,000 metric tonnes,<sup>84</sup> while in 2015, their global market size was found to be almost \$8 Billion.<sup>85</sup> The materials evidently account for a sizable share of the polymer industry, a fact that is becoming increasingly problematic as almost all epoxy polymers are petroleum-derived.<sup>86</sup>

Strictly, 'epoxy resin' refers to unreacted monomers or oligomers featuring epoxide groups, which can undergo curing to form polymers and

networks of crosslinked chains. However, in practise, the term has come to colloquially refer to the already-cured systems.<sup>83,87</sup> Epoxy resins are known for their excellent mechanical strength, electrical insulation and thermal resistance,<sup>88</sup> rendering the materials among the most versatile thermosetting polymers in the world.<sup>86</sup> But their applications are diverse and versatile, depending on the structure of both the epoxy-monomer and the curing agent, as well as the curing reaction conditions;<sup>83,88</sup> there is also evidence to suggest that these kinds of materials have suitable properties to be used in the biomaterials industry.<sup>89,90</sup>

The reaction of bis-epoxides with diamines can lead to the formation of either linear polymers or networks,<sup>91</sup> and has been described as one of the most usual reactions in curing in polymer chemistry.<sup>92</sup> Epoxy-amine networks are the most widespread of epoxy-resin systems<sup>93</sup> and curing is most usual with di- or poly-amines,<sup>92</sup> which may be aliphatic, cycloaliphatic or aromatic, and either primary or secondary.<sup>88</sup> Curing happens in a simple addition reaction, whereby the nucleophilic amine ring-opens the epoxide, forming a  $\beta$ -amino alcohol (**Figure 17**).<sup>92</sup> Where more than one epoxide is present, or, more usually, more than one reactive amine-hydrogen bond, the reaction occurs over and over to form polymers. While linear polymers are possible, it is more usual for branching to occur, generating networks of epoxy-resin polymers (**Figure 17**). This is particularly true where primary amines are used; a single addition of the amine to the epoxide results in a secondary amine with extra nucleophilicity, which thus will react with the remaining epoxides, inducing branching.<sup>93</sup> Networks such as these can also be formed by varying the epoxide/ amine stoichiometric ratio (**Figure 17**).<sup>92</sup>

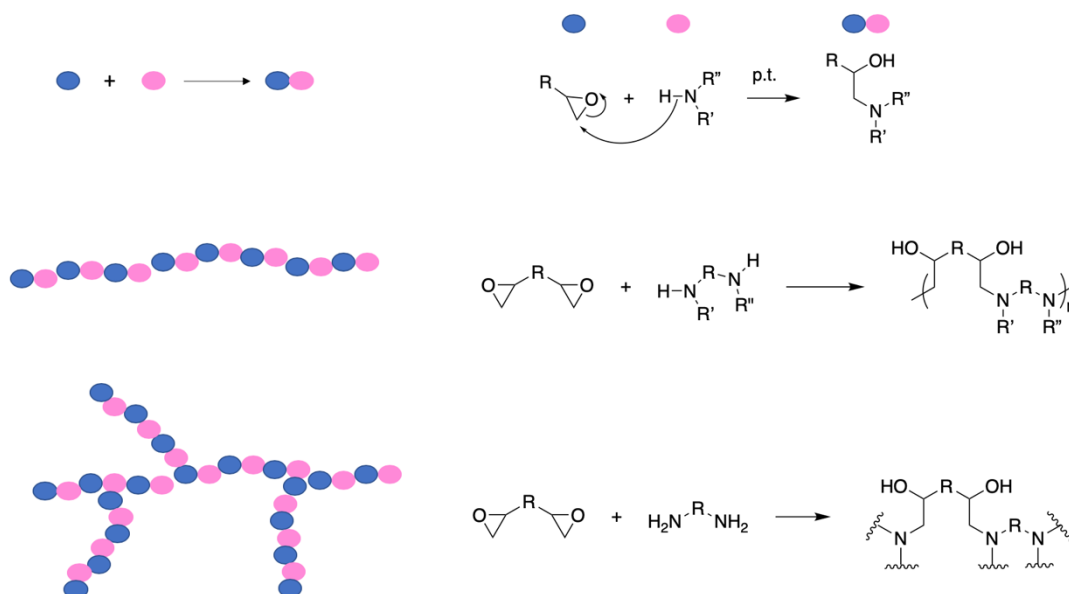
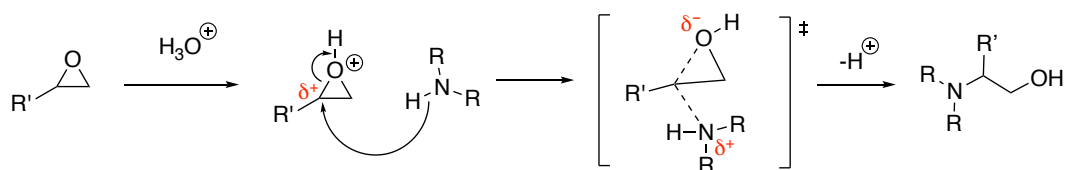


**Figure 17.** Cartoon representing the reaction of epoxides with amines to form linear polymers (middle) and networks (bottom).

The addition can occur *via* either an acid or base-catalysed reaction.<sup>94</sup> The two pathways feature different mechanisms and as such this can lead to the formation of different products: regioisomers. Where acid is present in the reaction, the epoxide will first become protonated, producing an oxonium cation. A pseudo-cation then begins to form on the most favourable adjacent carbon centre, *i.e.* the more sterically hindered one, as the molecule attempts to better redistribute its electron density. This 'activates' the epoxide towards nucleophilic attack, and as such the amine will then approach the epoxide at this sterically hindered centre, and the electron density is shifted formally to the oxonium ion (**Figure 18**).<sup>94</sup> As a result, the product will structurally reflect this minimum-energy transition state. Alternatively, should the reaction occur in basic conditions, there are no available protons in solution and so the oxonium ion does not form. As a result, the mechanism is governed entirely on sterics rather than electronics. The amine will thus add nucleophilically to the least-hindered position of the epoxide, generating an alkoxide anion.<sup>94</sup> A proton transfer will then occur, producing the corresponding  $\beta$ -amino alcohol product (**Figure 18**).

### Acid Catalysed Mechanism



### Base Catalysed Mechanism

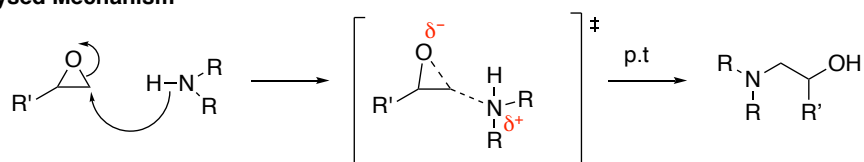


**Figure 18.** The acid and base mediated ring opening of epoxides by a generic amine, producing two different  $\beta$ -amino esters, which are regioisomers of one another.

Of the current epoxy-resin materials in use, composites based on diglycidyl ether of bisphenol-A (DGEBA) (**Figure 19**) are the most widely researched and commercially employed.<sup>86</sup> DGEBA represents more than 90% of the epoxy-precursors for the world's supply of epoxy-based thermosets, and as with most of the commercially available epoxy networks, it is of petroleum origin.<sup>86</sup> It is made from bisphenol A (**Figure 19**), a common phenol derivative for epoxy resin monomers, but which has been recently found to be an endocrine-disrupting chemical which has led to health damages, and a water contaminant, resulting in widespread human exposure.<sup>95,96</sup> The other component is epichlorohydrin (**Figure 19**), a well-known carcinogenic, mutagenic and reprotoxic (CMR) substance.

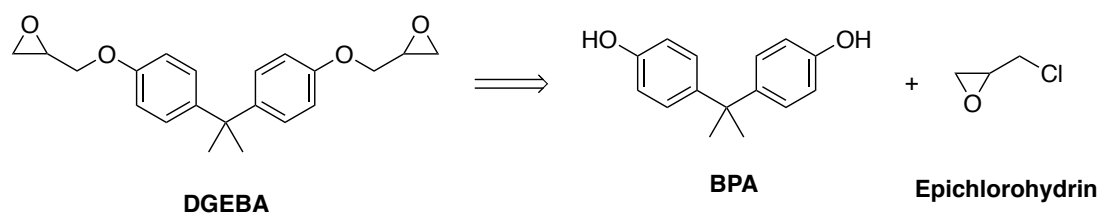


**Figure 19.** The structure of the commonly employed epoxy resin diglycidyl ether of bisphenol-A (DGEBA) and its precursors, bisphenol A (BPA) and epichlorohydrin.

The use of these toxic components results in limiting the use of DGEBA to a variety of applications,<sup>86</sup> with a growing effort thus being made to develop new, nontoxic, partially or fully bio-based epoxy thermosets.<sup>84,86,97,98</sup> Similarly, sustainability issues surrounding the use of crude oil is also driving the development of renewable feedstocks for alternative epoxy resin systems.<sup>99</sup> It is generally acknowledged that only biomass can supply the required renewable carbon, in sufficient quantities, to provide for the vast array of organic polymer structures that exist, and continue to be developed.<sup>6</sup>

Research into renewable epoxy resin materials have examined both the epoxide monomers as well as their curing agents from bio-based sources.<sup>84</sup> Due to the toxicity associated with BPA and epichlorohydrin, much of the research has tended to focus on the replacement of DGEBA in epoxy resins with new, non-toxic, eco-friendly monomers.<sup>95,100</sup> Investigations into replacement monomers have therefore looked to synthesising bis-epoxides with rigid, aromatic rings to infer similar properties to the polymers.<sup>95</sup> Xu *et al.* showed that certain cured resins of de-polymerised Kraft and organosolv lignin showed promise as a substitute of petroleum-based epoxy resins.<sup>100</sup> Similarly, Caillol *et al.* developed a novel epoxy-monomer from eugenol, a monolignol primarily found in cloves. When cured with aliphatic and aromatic amines, the resins were found to form thermosets with high glass transition temperatures and good thermomechanical properties.<sup>86</sup> These are only two examples of the considerable research that has been conducted in the synthesis of



renewable epoxy resins from bio-based sources such as lignin, rosin, tannins and sugars.<sup>98</sup>

Similarly, research has also focused on the synthesis of bio-based curing agents for epoxy resins.<sup>84</sup> While renewable amides, phenols, polyphenols, hydroxyls and acid anhydrides have been researched as curing agents,<sup>84,101</sup> amines have again proved a popular choice in the renewable curing agent market. Often a challenge is met in ensuring the amination uses mild, non-toxic chemistry.<sup>84</sup> However, in an extensive review on the synthesis and use of biobased amines, Froidevaux *et al.* describe a variety of methods in which natural products can be used as starting materials for the synthesis of amines.<sup>102</sup> In one example, the aliphatic di-primary diamine 1,6-hexanediamine can be synthesised from adipic acid, by first of all accessing adipodinitrile using nitrogen gas, before dehydration.<sup>103</sup> Alternatively, an array of poly- and di-amines can be accessed *via* the decarboxylation of amino acids,<sup>102</sup> a biochemical transformation already exploited by a variety of plants and animals.<sup>104</sup> The most well-known example is that of lysine, a low-cost amino acid which can be easily converted to 1,5-pentanediamine (also known as cadaverine).<sup>102</sup> Spermine, spermidine and putrescine are further examples of naturally occurring, aliphatic (poly)amines which have been identified as having potential as monomers in epoxy-resin (and other) chemistry.<sup>104</sup>

As mentioned, the polymers formed from the curing of DGEBA (and similar bisphenol-A derivatives) with diamines traditionally form hard, rigid materials, with excellent mechanical strength, electrical and thermal stability.<sup>84,95,105</sup> This is thought to be, at least in part, due to the rigid aromatic rings in the structures which impart toughness, rigidity and elevated temperature performance, while the ether linkages are thought responsible for giving chemical resistance to the material.<sup>83</sup> This does not necessarily mean that the materials' applications lie outside the remit of biomaterials: DGEBA represents the most widely used organic matrix for preparing reinforced materials for orthopaedic and dental applications.<sup>89,96</sup> Analogous epoxy resins are also thought to be suitable for these applications; their physical properties rendering them useful as biomedical cements and adhesives.<sup>90</sup>

It is hypothesised that replacing DGEBA with an aliphatic or cycloaliphatic bis-epoxide could significantly alter the polymer properties, moving away from the toughness and rigidity to potentially render more supple materials that may be useful in other medical or biomaterials applications, particularly if coupled with aliphatic diamines. Hamid *et al.* showed that hydrogels could be formed from epoxy/amine polymer networks based on aliphatic monomers, with potential applications in tissue engineering supports and drug delivery systems.<sup>106</sup> Negrell *et al.* also demonstrated that the use of epoxidised algal oil provided a bio-based, aliphatic monomer that formed foams when coupled with amines derived from vegetable oils. A subsection of these foams were suitable for use in lightweight materials, with the most flexible considered applicable in medical applications.<sup>97</sup>

It is clear that epoxy resin chemistry is broad and versatile, lending itself to a variety of different monomers and a plethora of potential polymer systems, with diverse applications. While epoxy-resins evidently already account for a sizeable share of the polymer industry,<sup>107</sup> undoubtedly their full potential in the future of our polymeric systems is far from complete, particularly in regards to systems made from renewable sources of biomass.

## 1.7 Polymers for biomedical and antimicrobial applications

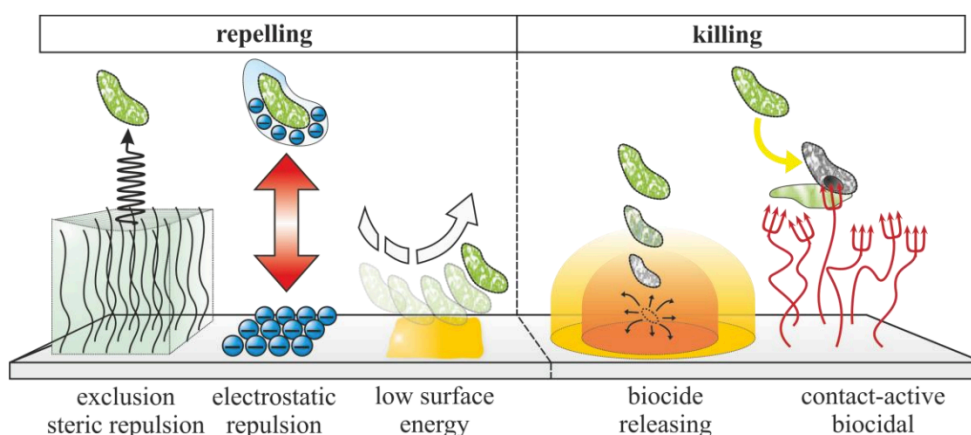


**Figure 20.** *Some interactions of different types of antimicrobial polymer surfaces with microbes.*<sup>108</sup>

The versatile nature of polymeric materials, which results in a wide range of chemical, physical and mechanical properties, makes them suitable for many purposes in medicine.<sup>109</sup> Since the development of synthetic polymer systems in recent decades, biomaterials of this nature are reaching broad new applications in modern medicine.<sup>2,110</sup> Polymer systems and technologies have revolutionised the biomaterials-based health care industry,<sup>111</sup> and are currently employed in pacemakers, synthetic blood vessels, breast and knee implants, amongst a variety of other applications.<sup>112</sup> These technological advancements have led to an improved quality of life, driven by a variety of factors, including the medical needs of a growing and ageing population.<sup>111</sup>

There still remain many shortcomings in our therapeutic care and medical devices, some of which polymer technology has the ability to improve. For instance, some diseases, such as diabetes, require that drugs be delivered at specific time intervals, while some therapies are limited in the dosage of drugs that can be administered, to avoid toxic or ineffective results.<sup>113</sup> 'Smart' polymeric systems, i.e. ones which can give a non-linear response to an external stimulus,<sup>114</sup> are being investigated as a solution to some of these problems. Systems such as these usually fall under the remit of 'nanomedicine', i.e. the design of diagnostics and/ or therapeutics on

the nanoscale.<sup>115</sup> Synthetic polymer nanoparticles are among the most studied strategies for nanomedicine, owing to the flexibility in their design based on functionalisation, macromolecular synthesis methods and polymer diversity.<sup>116</sup>

In particular, a wealth of research has been conducted into nanomedicines for cancer immunotherapies and drug delivery systems, capitalising upon the ability of these 'smart' systems to deliver controlled, targeted drug release.<sup>117-120</sup> Systems such as these are often designed to respond to cellular signals, while others will instead direct specific cell behaviours.<sup>110</sup> Either way, an understanding of the nano-bio interface on a cellular level is of paramount importance for the successful design of the system.<sup>116</sup> Physio-chemical, macro- and supra-molecular features of nanoparticles such as their size, shape, geometry, elasticity, porosity and surface characteristics (amongst others) greatly influences this, in addition to other properties such as their solubility, stability and degradation leading to clearance *in vivo*.<sup>121</sup> Synthetic polymer nanoparticles in particular are desirable, as they offer an opportunity in the field of nanomedicine to customise many of these features, such as molecular weight, geometry, biodegradability and hydrophobicity.<sup>121</sup>

A variety of polymer nanoparticles have been investigated at an increasing rate over the past 20 years, with many now approved for clinical use.<sup>121</sup> Initially, polymers used for these nanoparticles were based on non-biodegradable systems derived from crude oil, such as poly(methyl methacrylate), polyacrylamide and polyacrylates.<sup>116</sup> The use of these systems in drug delivery requires that the nanoparticle be of suitable dimensions and properties to enable clearance from the body, so as to avoid accumulation or distribution into tissues at toxic levels. Nonetheless, these types of polymer particles have various applications in wound healing and antimicrobial materials.<sup>116</sup> For drug delivery, biodegradable nanoparticles are considered the preferred alternative.<sup>122</sup> Typically, biodegradable nanoparticles feature hydrolysable bonds in the polymer backbone, which can undergo gradual, diffusion-limited degradation *in vivo*.<sup>122,123</sup> Aliphatic polyesters such as PLA, PCL, polyglycolide (PGA) and poly-lactide-co-glycolide (PGLA) (**Figure 21**) fit this remit, and have proved very popular for a wide range of biomedical applications, owing to

the polymer material properties, in addition to biocompatible and biodegradable properties.<sup>123</sup>

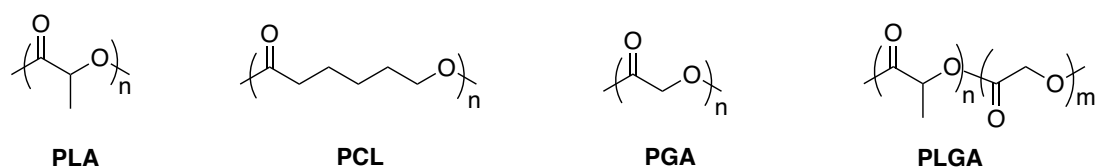


**Figure 21.** The repeating units of polylactide (PLA), polycaprolactone (PCL), polyglycolide (PGA) and poly-lactide-co-glycolide (PLGA), common degradable, aliphatic polyesters used for drug delivery and biomaterial applications.

Other than drug delivery particles for nanomedicine, synthetic polymers are also being investigated for applications in broad and versatile areas of biomedical applications, such as medical devices,<sup>124</sup> vaccine development<sup>125</sup> and antimicrobials.<sup>10</sup>

Multidrug resistance to a variety of antimicrobials, such as bacteria and fungi, is rapidly becoming a major worldwide health concern, and antimicrobial or antibiotic polymers are thought to have a significant role in the global efforts to combat this.<sup>126</sup> Generally speaking, a polymer can be antimicrobial either passively or actively. Where the polymer is passively antimicrobial, it infers that the adhesion of the microbe to the surface of the polymer material is prevented; repelling it without actively interacting with it, and preventing colonisation on the surface of the material.<sup>126</sup> The design of polymer systems that are passively antimicrobial therefore offer a pragmatic method in which to develop medical devices (and other materials) that prevent biofilm formation, amongst numerous other problems caused by the attachment of microbes to surfaces.<sup>124</sup> Research is now being conducted to find ways in which to both fast-track the discovery of polymers of this nature,<sup>127</sup> and formulate them to have the desired groups at the surface of the material.<sup>128</sup>

Actively antimicrobial polymers will, on the other hand, interact with the microbes and kill them. This can be achieved through the functionalisation of the material surface with agents such as cationic

biocides, antibiotics and/or antimicrobial peptides, which are known to kill microbes.<sup>126</sup> Synthetic polymers are also useful in this category because they may be specifically tailored to incorporate these features on the surface of materials.

The design of the polymer system is evidently of paramount importance in terms of addressing both the shortcomings of current biomedical polymers, and their potential uses in the future. Their design is dictated primarily by their function and application, and successful structures must find a balance between being biodegradable and biostable, with respect to their biomedical purpose.<sup>129</sup> But even when given the correct physical and mechanical properties, not all polymers are suitable for biomedical applications; once in the body, side effects can occur from a variety of factors, including leftover components of the polymerisation conditions such as monomers and catalysts.<sup>109</sup> This renders clinical approval of new biomaterials difficult and expensive, and a more integrated approach to the polymer's design is required, which considers from the start all components that may render the material toxic or bio-incompatible.<sup>109</sup> To this end, syntheses that are designed from beginning-to-end to employ non-toxic and/or non-hazardous components at each step are critical for the generation of new materials that will have real potential in healthcare and biomedicine. In a similar respect, owing to the current global environmental crisis, there is an onus to find green and sustainable chemical methodologies for the syntheses of these materials, which can meet the requirements of a circular economy. This is of paramount importance in relation to the end of life of the polymer chains, in order to avoid the accumulation of polymer materials in the oceans and landfills. But before reaching that stage, any and all efforts to move towards more green and sustainable, non-toxic and non-hazardous polymer synthesis for biomaterials is a welcome step forward.

The following sub-chapters discuss in more detail a number of topics in relation to biomedical polymers, relevant to the experimental chapters of this thesis.

### 1.7.1 Poly(lactide): A biocompatible biopolymer



**Figure 22.** Some of the biomedical applications of PLA-based polymers.<sup>130</sup>

PLA was first discovered by Carothers in 1932, when he heated lactic acid under vacuum while removing the condensed water; the result was PLA oligomers.<sup>131</sup> This method of polycondensation is still used to generate PLA, though it is not an easy way in which to generate high molecular weight polyesters with good mechanical properties. Instead, this is usually accomplished in industry through the ring opening of lactide.<sup>19</sup> For the synthesis of PLA for biomedical applications, ROP is also usually employed, and often lactide is co-polymerised with other lactone monomers such as glycolide or caprolactone.<sup>132</sup>

As discussed in the Introduction (section 1.2), lactide is the ring-formed dimer of lactic acid, the chiral nature of which results in three different forms of lactide: L-lactide, D-lactide and D,L-lactide (**Figure 23**).

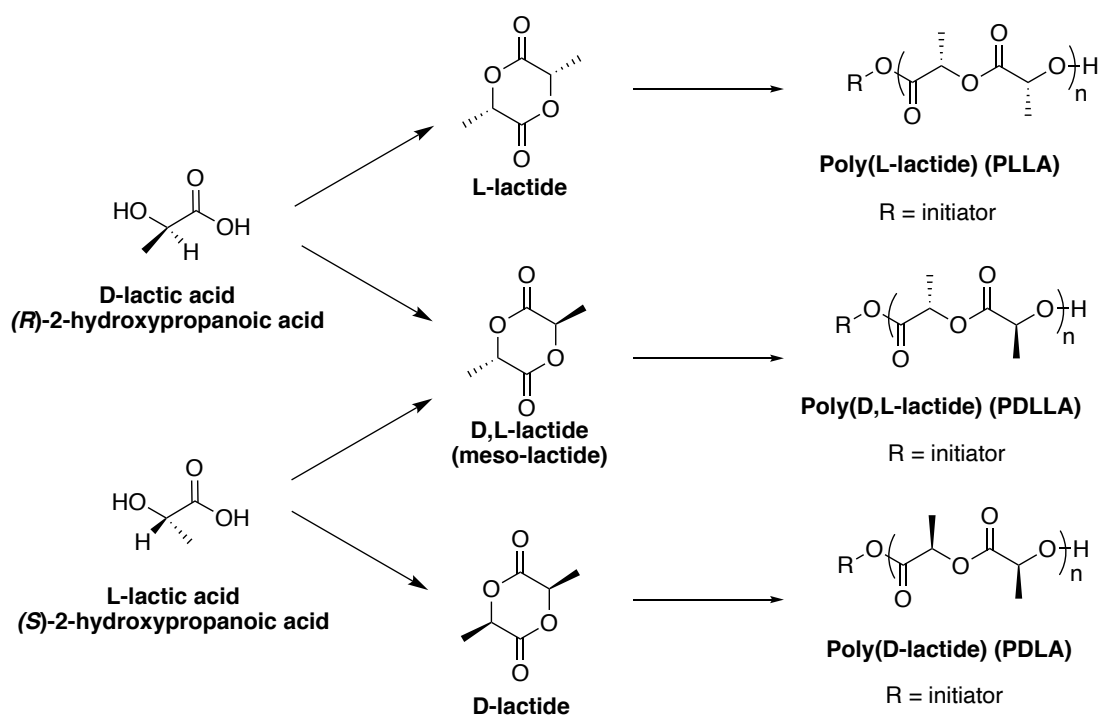


**Figure 23.** The structures of D- and L- lactic acid which dimerise to form D-lactide, L-lactide and D,L-lactide. These monomers can then undergo ROP with a nucleophilic initiator to form either PLLA, PDLA or PDLLA.<sup>18,133</sup>

As a result of there being three optical isomers of lactide, with the help of stereoselective catalysts, there are also three stereoisomers of PLA: poly(L-lactide) (PLLA), poly(D-lactide) (PDLA) and poly(D,L-lactide) (PDLLA) (**Figure 23**). Physically, these are crystalline, but the notation 'PDLLA' can also be used to describe the amorphous, random polymer made from racemic mixtures of L- and D-lactide. PLLA is the most popular for biomaterials, because it is considered to be the most biocompatible.<sup>123</sup> However, for certain nanomedical applications such as drug delivery, the amorphous PDLLA is preferred over the crystalline polymers. Stereoisomeric mixtures of PLLA and PDLA result in stereocomplexes, through physical association of the polymer chains. This gives rise to polymers with distinctive physical and chemical stability and enhanced mechanical strength.<sup>132</sup> In this thesis, 'PLA' is used as an acronym to describe polylactide without being specific as to which stereoisomer is involved. When specificity is required, 'PDLLA', 'PDLA' or 'PLLA' will be



used. The term 'PDLLA' will be used to refer to the amorphous polymer made from racemic lactide, rather than that made from meso-lactide.

The conversion of lactic acid to lactide is usually achieved through a depolymerisation process of PLA oligomers formed by polycondensation, and as a consequence the purity of the lactic acid is imperative in generating optically pure lactide and PLA.<sup>19</sup> On a mass scale, lactic acid can be produced through the bacterial fermentation of a carbohydrate, which is usually glucose.<sup>18</sup> In terms of atom economy, one molecule of glucose is converted to two molecules of lactic acid, resulting in a very efficient monomer product, with practical yields of 85-95%.<sup>12</sup>

After dimerisation, the ROP of lactide can be conducted either using melt conditions, or in solvent *via* an anionic, cationic or co-ordination mechanism, depending on the initiator used.<sup>131</sup> Factors such as the polymerisation temperature, initiator and catalyst concentrations and types, amongst others, have a significant effect on the resulting polymer properties such as molecular weight and degree of crystallinity. In turn, these properties will then affect the physio-mechanical properties of the polymer material.<sup>131</sup> The most common industrially applied catalyst is tin(II)octanoate ( $\text{SnOct}_2$ ). This highly active compound is commercially available, soluble in common organic solvents and usually used at 140-180 °C with reaction times of only minutes to hours.<sup>134</sup> The mechanism for how this occurs is generally acknowledged to be *via* a co-ordination-insertion.<sup>134</sup> The initiation of this process is still, however, the subject of some debate, with the addition of protic agents such as methanol (or other protic solvents) and impurities believed to be involved.<sup>134</sup> While  $\text{SnOct}_2$  has received FDA approval, there are still concerns relating to 'leftover' traces of the metal catalyst, which are potentially toxic, and so this catalyst is considered undesirable for biomedical or biological applications of PLA.<sup>123</sup> Zinc and aluminium based catalysts are commonly employed as alternatives,<sup>123,134</sup> although these reactions traditionally require up to several days at 140 °C.<sup>134</sup> However, there has been much research into the use of bespoke catalysts for the ROP of lactide and similar lactones, with a variety of metal and organobase catalysts available for use at ambient conditions.<sup>135,136</sup>

PLA for biomedical applications is usually synthesised *via* anionic polymerisation, which makes use of a nucleophilic initiator, often an alcohol or amine group.<sup>22</sup> Catalysts for these polymerisations historically have been metal-based, but a variety of non-metal, organic catalysts have been shown to be effective, including tertiary amines, phosphines and *N*-heterocyclic carbenes.<sup>136,137</sup> Recently it has been demonstrated that organobase catalysts such as 1,8-diazabicyclo[5.4.0]undec-5-ene (DBU) can be used.<sup>138,139</sup>

PLA has proved a particularly successful renewable polymer because not only is it derived from biomass, but it is also biocompatible (with FDA approval for many of its formulations)<sup>132</sup> and biodegradable, both in the body and environmentally in the ecosystem, through hydrolysis of the polyester backbone.<sup>131</sup> This gives PLA a distinct advantage in terms of sustainability, which focuses on the entire life cycle of a material from cradle-to-grave. It also has been shown to have net-negative greenhouse gas emissions when its lifecycle is monitored from cradle-to-factory, due to the absorption of CO<sub>2</sub> from the atmosphere when corn (for lactic acid fermentation) is grown.<sup>131</sup> Its biocompatibility is also particularly attractive for biomedical applications such as drug or vaccine delivery, as lactic acid (the degradation product following hydrolysis) is simply converted to glucose; well tolerated by the body. This is particularly applicable to PDLLA, which, being amorphous, has a faster degradation rate than that of PLLA,<sup>140</sup> the latter of which is more commonly used for long-term tissue engineering biomaterial applications. The biodegradable nature of PDLLA therefore offers an example of a useful polymer for nanomedicine, that can be considered safe and devoid of any major toxicity.<sup>21</sup>

Current biomedical applications for PLA (in particular, PLLA) include its use in biomedical screws, pins and plates which are intended to biodegrade within six to twelve months.<sup>22</sup> Its low immunogenicity and good mechanical properties also make it a useful polymer for drug delivery systems when PDLLA is used.<sup>132</sup> However, the amorphous polyester is hydrophobic, so it must be coupled with a hydrophilic moiety to enable self-assembly *in vivo* for these applications to be successful. As a result, as with most aliphatic polyesters, PLA used for biomaterials such as drug delivery is usually synthesised as an amphiphilic co-polymer. The self-

assembly of the co-polymer molecules result in a hydrophilic corona that not only ensures water solubility, but also can improve circulation times *in vivo*.<sup>132</sup>

Extensive research has looked into synthetic methods of generating these amphiphilic polymers, and the different architectures available.<sup>132,138,139</sup> PLA poses a major challenge in that the backbone of the polyester does not have many available handles for functionalisation, however, a number of synthetic strategies are being investigated to overcome this.<sup>132,139</sup> Of particular interest in this regard is the exploitation of an initiating species; using it as a docking point for post-polymerisation functionalisations. In a recent review, Phan *et al.* describe how a broad range of properties can be accessed when a variety of 'active' initiating species are used to bring about ROP reactions of aliphatic polyesters.<sup>140</sup> This can not only provide the resulting polymers with interesting properties themselves, but can also render the macromolecules useful for other polymerisation techniques.

In the field of nanomedicine, focus is shifting to 'smart' polymer materials, i.e. those which can respond to multiple signals, such as change in pH, the redox environment, or light.<sup>123</sup> As such, there remains an unmet challenge in methods of modifying PLA, or adapting it with functional handles, so as to expand the scope of applications for this biocompatible and sustainable polymer.

### 1.7.2 Amphiphilic polymers and surfactants

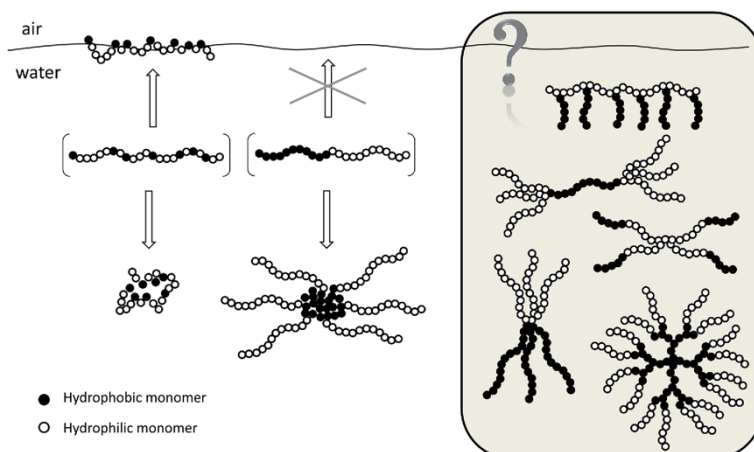


**Figure 24.** *Cartoon representation of the behaviour of both random- and block-co-polymer surfactants at an air/water interface, and how architecture of the structures influences their self-assembly properties.*

Amphiphilic molecules are those which contain two distinct, covalently bonded components within the same molecule, with different affinity for solvents.<sup>141</sup> Amphiphiles, particularly those that act as surfactants, have been employed in soaps and as cleansers for centuries.<sup>142</sup> Today, these compounds are ubiquitous, with diverse applications beyond cleaning: they are found in food, medicines, paints, coatings and automotive fluids, amongst others.<sup>141-143</sup>

**Surface Active Agents**, abbreviated to **surfactants**, are molecules that, as implied in their name, are active at surfaces between phases; they adsorb and adhere at interfaces, lowering the surface energy of the bulk material at those phases.<sup>143,144</sup> This is due to the molecular structure of the surfactant molecules being amphiphiles and consisting of both a hydrophobic and hydrophilic unit, thus displaying amphiphilic (i.e. amphipathic) behaviour (**Figure 25A**).<sup>145</sup>

Due to this amphiphilic nature, when surfactant molecules are added to a two-phase system, the molecules will gather at the interface or surface, so as to minimise the undesirable interactions, for example, of a hydrophobic moiety (such as a long carbon chain in a triglyceride) and a hydrophilic solvent such as water. As a result, the interfacial tension (i.e.

surface energy) will decrease, up to the point where the surface is saturated with surfactant molecules (**Figure 25B**).<sup>144</sup> The interfacial tension for a liquid-gas is referred to as surface tension, thus, surfactants can lower the surface tension of water, and other (commonly hydrophilic) liquids.<sup>144</sup>

After saturation of the surfactant at the surface, the molecules will then begin to aggregate together to form self-assembled molecular clusters known as micelles (**Figure 25C**). The Critical Micelle Concentration (CMC) is defined as the concentration at which surfactants form micelles.<sup>142</sup>

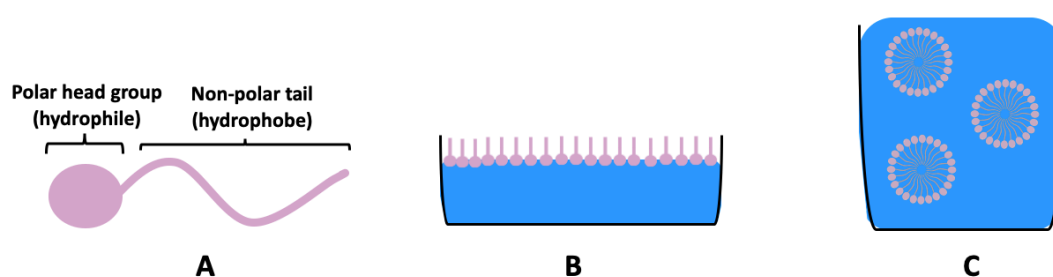


**Figure 25.** A cartoon representation of a surfactant molecule featuring a polar, hydrophilic head group and non-polar, hydrophobic tail (**A**). When surfactants are added to a two-phase system (such as water/air) they will accumulate at the surface (**B**), before reaching the critical micelle concentration (CMC), at which point the molecules self-assemble into (usually spherical) micelles (**C**).

Broadly speaking, surfactants can be categorised into four groups: anionic, cationic, amphoteric and non-ionic.<sup>143</sup> These refer to the charge at the polar head group of the molecule, so anionic surfactants are those which give rise to a negatively charged surfactant ion upon dissolution in water, while cationic will be positive.<sup>143</sup> Amphoteric (or zwitterionic) surfactants are those which possess both a positive and negative charge, while non-ionic surfactants are species that are not charged. (**Figure 26**).

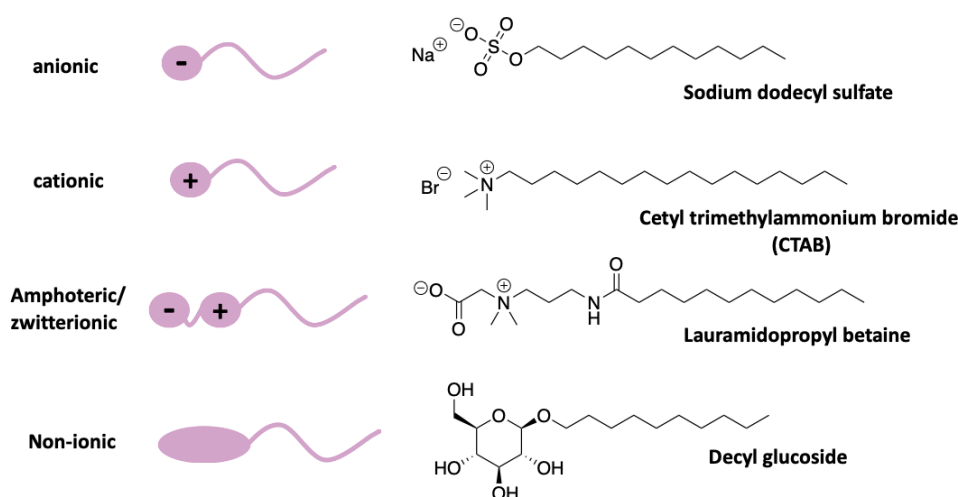


**Figure 26.** *The four main categories of surfactants: anionic, cationic, amphoteric and non-ionic, and examples of each.*<sup>142,143</sup>

Anionic surfactants usually have excellent cleaning properties, and are the most widely used for laundering, washing up liquid and shampoos.<sup>143</sup> They are also usually relatively non-toxic, which adds to their utility and renders them the largest class of surfactant. The most common anionic surfactants feature a saturated or unsaturated aliphatic alkyl chain (usually about 12 to 18 carbon units), with commonly a carboxylate, sulfate or sulfonate ion head group.<sup>143</sup> In contrast to these, cationic surfactants do not make good cleaning products, but instead are known to be good emulsifying agents, increasing the kinetic stability of the mixtures. Often the cationic charge is a result of a quaternary ammonium head group, which can bestow antimicrobial properties to the molecule.<sup>146</sup> As such, these kinds of surfactants are known for their germicidal properties and are often found to be good bactericides and topical antiseptics.<sup>143</sup>

Amphoteric or zwitterionic surfactants are considered very mild in that they are less toxic and irritant to humans than their charged alternatives.<sup>147</sup> This makes them particularly suitable for use in personal care items such as baby shampoos and other household cleaning products.<sup>146</sup> Additionally, these kinds of surfactants are known for their high foaming properties, and as such are often present in shampoos and cosmetic products. However, they are not as common as their cationic or anion alternatives.<sup>146</sup>

Non-ionic surfactants are excellent grease removers, and are the kind of surfactant compounds most frequently studied for use in biomaterials applications such as drug delivery.<sup>143</sup> While all surfactants by definition are amphiphilic, the nature of the solubility of the 'head group' and the 'tail' of the molecule will render it more suitable for use in either for oil-in-water or water-in-oil applications. Ionic surfactants are usually more 'hydrophilic', in the sense that they are better for oil-in-water applications. On the other hand, non-ionic surfactants can be either 'hydrophilic' or 'lipophilic' (hydrophobic) in this way, and vary depending on the hydrophobic-hydrophilic balance of the molecule.<sup>142</sup> As such, these kinds of surfactants can enable dissolution in *either* water-in-oil (when more hydrophobic), or oil-in-water (when more hydrophilic). These properties will also determine the nature of the surface activity of the compound, in particular in relation to micelle formation, and even the shapes and geometries of the aggregates formed.<sup>144</sup> For example, generally speaking it is observed that non-ionic surfactants make larger micelles than ionic ones. The size in this case can usually be explained by a larger aggregation number,  $N_{agg}$ , i.e. the number of surfactant molecules associated with a micelle.<sup>143</sup>  $N_{agg}$  for a micelle will vary depending on the chemical nature and structure of the surfactant molecules (amongst other parameters).

As mentioned, surfactants are those kinds of amphiphilic molecules that can 'spontaneously aggregate' (i.e. self-assemble) as a result of solvophobic interactions, when the concentration of amphiphiles is above the CMC.<sup>141</sup> However, a spherical micelle is not the only morphology which can form after reaching saturation of the molecule at a surface. A wide variety of nanostructures are feasible, including cylindrical micelles,

lamellae and vesicles, in addition to a number of aggregates without well-defined structures.<sup>141</sup> Therefore, to describe these structures more generally, the critical aggregation concentration (CAC) is often used to refer to the point at which surfactant molecules begin self-assembling.<sup>147</sup>

Predicting the nature of the particles that may form is very challenging, and often amounts to educated guess-work based upon a variety of factors including molecular structure, temperature, solvent and concentration.<sup>142</sup> In this regard, nanoparticles made from synthetic amphiphilic polymers (rather than small-molecule amphiphiles) are of particular interest, as the synthesis of these macro-amphiphiles can allow for precise control of the polymer structure and chemistry, and their sizes can allow for the formation of suitable nanoparticle dimensions for these applications. This in turn has the potential to enable the physiochemical properties to be readily tuned, tailoring the nanoparticles to meet the requirements of the specific application.<sup>138</sup> As a result, nanoparticles are increasingly being investigated for use in biomedicine, biomaterials and pharmaceuticals, in particular as carriers in drug delivery applications.<sup>110,114</sup>

The design of amphiphilic polymers for these applications has been facilitated by the development and advances of polymerisation techniques including RAFT, ATRP and ROP.<sup>141</sup> Amongst the various architectures available through these techniques, linear block-co-polymers have been particularly successful in terms of synthesising polymeric surfactants.<sup>132,148</sup> For drug delivery applications for example, these types of co-polymers have been particularly relevant, as they can allow for the formation (through self-assembly) of 'stealthy' nanoparticles that can circulate *in vivo* with the encapsulation of 'cargo' within a core region of the particle.<sup>111,148</sup> As such, these block-co-polymers commonly feature a hydrophilic segment to act as the biocompatible corona, conjugated to a hydrophobic segment (which is also biocompatible), that can facilitate encapsulation of hydrophobic drugs.<sup>138</sup> Systems based upon poly ethylene glycol (PEG) moieties have been a popular selection for such hydrophilic segments, as have poly(meth)acrylates and polypeptides.<sup>132</sup> These are commonly conjugated to aliphatic polyesters such as PLA, PCL and PGA (see **Figure 21**, section 1.7), which have proved successful as the hydrophobic



blocks for these kinds of amphiphilic, self-assembling biomaterials in extensive studies.<sup>132,148,149</sup>

Many clinically relevant nanomedicines are beginning to incorporate these amphiphilic polymer and surfactant designs, with some technologies now in clinical trials.<sup>138</sup> The use of polymeric surfactants for drug delivery systems (and other biomaterials) has become an important field of both clinical and academic research, and as polymer chemistry advances, it is likely that these systems will become of ever-increasing relevance in healthcare.<sup>111,150</sup> As such, given the urgent need for polymer chemistry to move towards green and sustainable processes,<sup>2,3,8,13</sup> there is now a parallel need to seek green and sustainable methods of synthesising these polymeric surfactants employed in biomaterial applications and beyond.

### 1.7.3 Fungal pathogens and the need for novel treatments

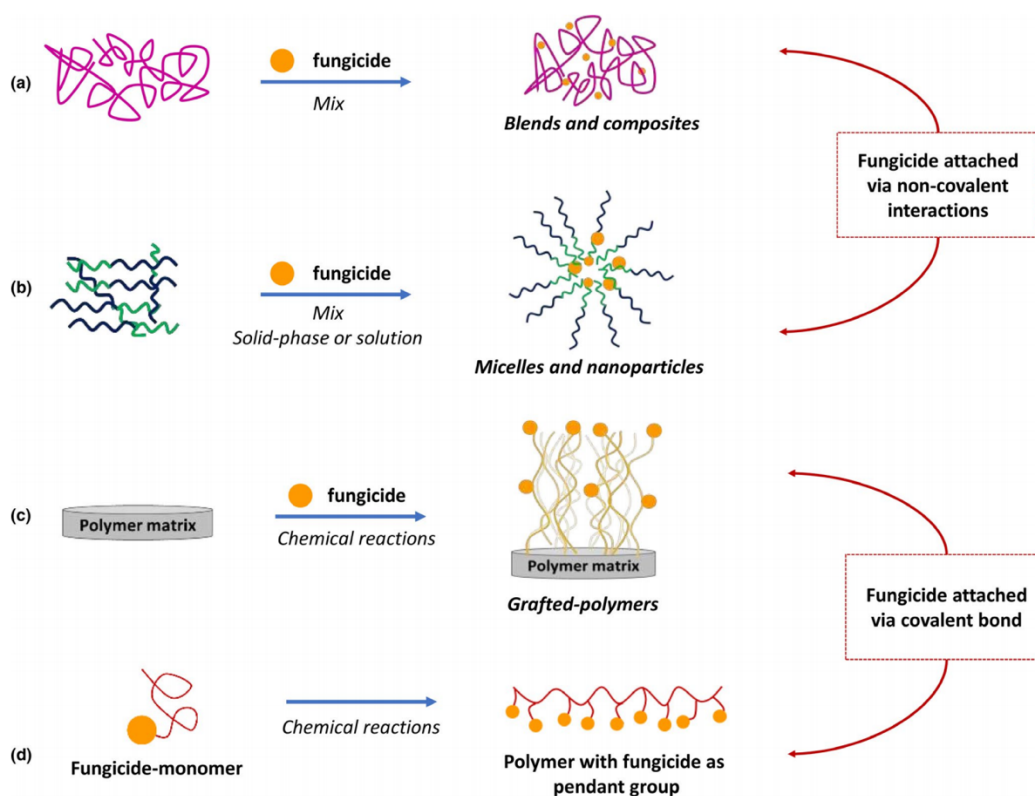


**Figure 27.** A variety of methods in which fungicides may be incorporated into different polymer types.<sup>151</sup>

One of the biggest emerging threats to worldwide healthcare is the emergence of multi-drug resistant pathogens. The World Health Organisation estimates that failure to develop adequate solutions to this problem could result in as many as 10 million deaths per year, as a result of microbial infection, by 2050.<sup>126</sup> More and more patients are presenting with infections that resist multiple last-line antibiotics, while at the same time very few new antimicrobial drugs are coming on to the market, with the result being that we are quickly entering a post-antibiotic era, and novel, pragmatic solutions are required to begin to address these issues.<sup>127</sup> This is a significant barrier to overcome for the biomaterials-based healthcare industry, with many healthcare-associated infections arising as a result of medical-device related infections.<sup>152</sup> The micro-organisms which are most responsible for causing these infections include gram-positive

bacteria and yeasts, particularly *Candida* strains. Specifically, it is the irreversible growth of these micro-organisms into biofilms (communities attached to a surface and bounded into a 'slime' matrix) which cause the most harm and are most difficult to combat.<sup>127,152</sup>

Compared with antibacterial treatments, finding fungal-specific agents is considered more challenging. This is (at least in part) a result of fungi being eukaryotic, as are their human hosts, and so finding therapies which can effectively treat the fungus but not damage host cells can be difficult.<sup>153</sup> The eukaryotic cells of the pathogen will be similar to those of the host in terms of their biochemistry, metabolism, genetic composition and cell architecture. Therefore, drugs which target eukaryotic micro-organisms should focus on the differences from the eukaryotic norm, and/or specialisms of the particular pathogen group.<sup>154</sup> As bacteria are prokaryotic, it is not usually necessary to specifically target a feature of a specific pathogen, and drugs can generally target the general physiology of the micro-organism without causing excessive harm to the host.<sup>153,154</sup>

As a result of the rarity of effective fungal treatments, the global antifungal and fungicide industry now has a combined net worth of more than \$30 billion, and that is before considering other undesirable fungi.<sup>124</sup> In fact, there is a wealth of other reasons outside of healthcare for which a diversity of fungi are undesirable, be it in terms of food spoilage, or the deterioration of materials.<sup>155</sup>

"Lock" therapy is the current most popular method of guarding against fungal infection amongst biomaterials and medical devices. It involves treating the device with high concentrations of antifungal drugs before use, or by coating or impregnating them with inhibitory agents.<sup>124</sup> The problem with this is that it does not amount to a long-term fungal control strategy, as these bioactive agents are becoming increasingly ineffective towards resistant fungal strains: Microbial cells replicate more rapidly than mammalian ones, and as such, resistance can be selected in a relatively short timescale in a treated host population.<sup>154</sup> The current arsenal of approved agents for anti-fungal or fungicidal use is quickly being eroded by this (and general societal) fungal resistance.<sup>124</sup> The development of new antifungal therapeutics has been met with many challenges in

recent decades, and there is now an urgent need for effective new treatments, particularly those with novel mechanisms of action.<sup>153,156</sup>

Of the approaches being researched to overcome fungal infections and biodeterioration, limiting the attachment of the cells to surfaces, and/or methods of preventing the growth of the micro-organism before biofilm formation has a chance to take hold, are among the promising current areas of research.<sup>124,127</sup>

In this remit, research has recently turned to the use of biocidal polymers as an active mode of action against fungal growth and colonization.<sup>126</sup> Biocidal polymers are those which kill or inhibit micro-organisms (usually bacteria) and prevent biofilm formation.<sup>146</sup> There are numerous advantages to using polymers for this strategy over small-molecules, not least because polymer materials can offer physical and chemical stability and usually a longer shelf-life, which results in long-lasting resistance against micro-organisms.<sup>146</sup> Additionally, the cost of biocidal polymers is generally much lower than advanced antibiotics. The versatile nature of polymers, including their facile synthesis methods, can enable the specific design of a high concentration of active components in the synthetic polymer materials.<sup>146</sup> Furthermore, these can often be designed to mimic the structural features of host defence peptides and/or other antimicrobials that reduce residual toxicity, and as such this gives the polymers potential for therapeutic use.<sup>157,158</sup>

The mechanisms in which polymers can be biocidal are underpinned by a number of structural features including (but not limited to) the polymer's molecular weight, amphiphilic balance, structure of ammonium groups and alkyl side chains, and the composition of non-antibiotic co-monomers.<sup>146</sup> These features are biocidal because they interact with (and usually damage or destroy) cell membranes or walls (where applicable), or they interfere with key intracellular processes.<sup>126</sup> Most of this research has been conducted on bacteria, though biocidal mechanisms which involve an interaction with the cell membrane are also applicable to fungi.<sup>146,156</sup> Arguably the most significant feature which makes a polymer biocidal is its composition of a cationic charge. Cations are well known to be biocidal because they damage the microbial cytoplasmic membrane, leading to the leakage of intracellular components.<sup>126</sup> This mechanism has

been known since 1935, and quaternary ammonium salts have been a particularly well developed example since then, popular for a variety of formulations used in disinfectants (**Figure 28**).<sup>158</sup>

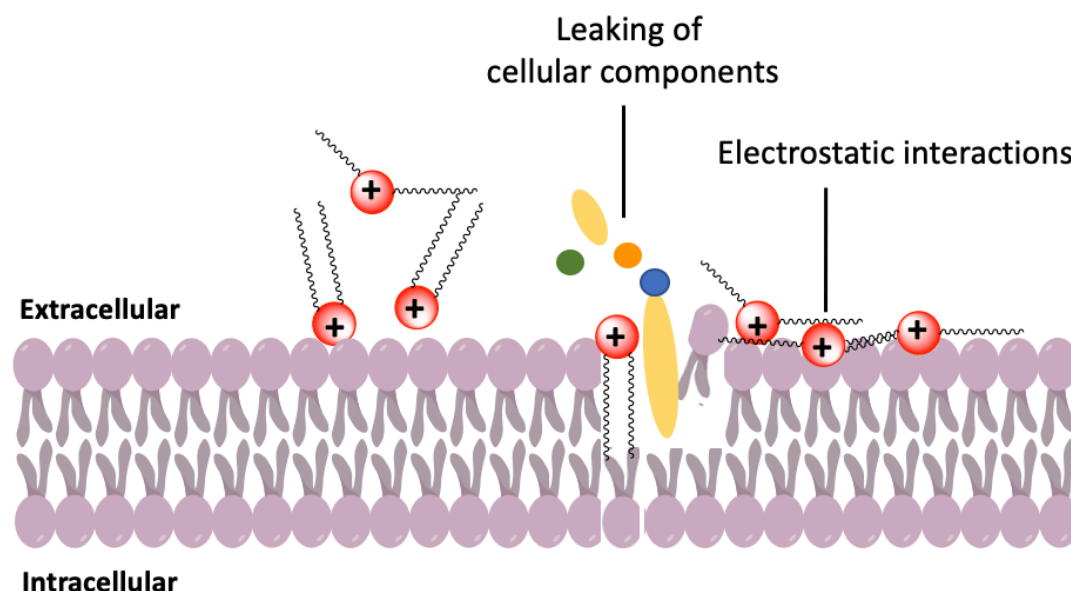


**Figure 28.** *The mechanism described by Jennings et al. in which quaternary ammonium salts and other cations interact with cytoplasmic membrane via electrostatic interactions. This leads to the leaking of cellular components, membrane destruction and thinning, a disruption of essential gradients and ultimately, the death of the cell and micro-organism.*<sup>158,159</sup>

Over recent decades, a range of cationic polymer architectures have been studied for their ability to kill or inhibit micro-organisms.<sup>160</sup> Amine groups have been a popular choice for introducing cations to polymers, as under certain pH ranges and physiological conditions, these groups will become protonated, generating the biocidal quaternary cationic species.<sup>146</sup>

Along with their inherent biocidal properties, the presence of cationic groups have further implications on the overall amphiphilic balance of the polymer, which is significant in terms of its interaction with the microbial membrane and overall biocidal activity.<sup>146</sup> The molar fraction of cationic charge will largely influence the hydrophilicity of the polymer, which then must be balanced by a degree of hydrophobicity to achieve amphiphilicity,

usually bestowed to the polymer by an alkyl group, either in the backbone or as a side chain.<sup>146</sup> The composition of these hydrophobic groups, though often non-antibiotic themselves, in turn help to determine the overall hydrophobicity of the polymer, which further modulates the permeabilization of the membrane.<sup>146</sup> For bacteria, the combination of cations and hydrophobic moieties work together in the antimicrobial polymer, with the former binding to the negatively charged phospholipid membrane, and the latter inserting and disrupting the membrane, leading to cell leakage and ultimately death (**Figure 29**).<sup>146</sup> While the entirety of the mechanisms of antifungal activity remain unresolved, there is evidence that the fungi cell walls and membranes are susceptible to binding and permeabilization respectively, and a degree of amphiphilicity in the active agent is hypothesised to be essential for this.<sup>161</sup>

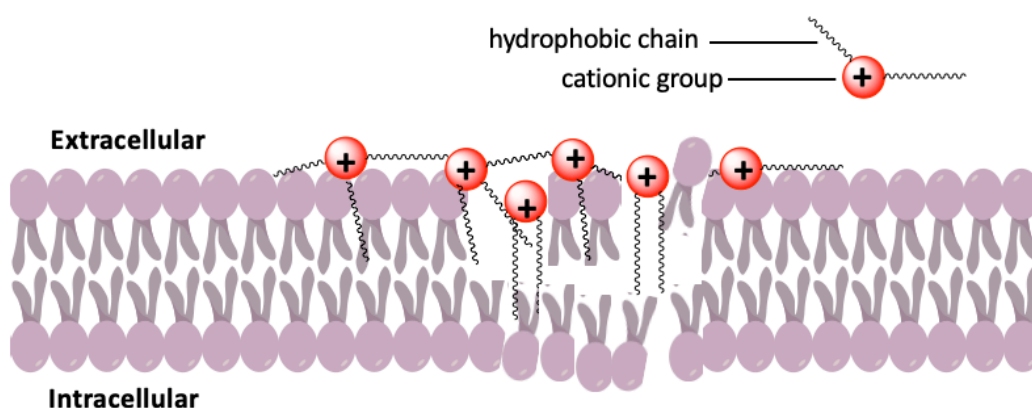


**Figure 29.** *The mechanism by which cations and hydrophobic moieties work together in antimicrobial polymers to disrupt microbial membranes and cause cell death.*<sup>162,163</sup>

In addition to the use of biocidal polymers as a novel method of protecting against antimicrobial infections, synergistic and combination therapies may also offer a pragmatic approach to the problem, and is particularly attractive in terms of guarding against antimicrobial resistance.<sup>155</sup> This is particularly true of antifungals and fungicides: these therapies allow for the development of potent new formulations without the need for specific new agents (the development of which has been particularly slow for

antifungals). This means that new therapies can potentially be facilitated by repurposing known antifungals, which is beneficial in terms of the timescale of approval and the cost.<sup>107,153</sup> Arguably the most attractive feature that synergistic therapies offer, however, is a lower likelihood of the fungi developing resistance to the therapy. This is because the evolution of resistance to more than one agent is much slower than with a single one.<sup>155</sup> Vallières *et al.* recently showed that novel combinations of non-antifungal drugs (all of which are approved for use in other clinical applications) were effective against azole-resistant clinical isolates.<sup>164</sup> Furthermore, synergistic combinations enable lower amounts of active agents to be used, lessening potential concerns surrounding non-specific toxicity, or cost.<sup>107,155</sup>

The discovery of novel synergistic combinations is not a straightforward process however, and strong interactions between potential antifungals is not very common.<sup>153</sup> More research is required into the mechanism of antifungal activities in order to begin pairing combinations to induce potential synergy. This has been facilitated by using model systems such as those based on the yeast *Saccharomyces cerevisiae*, considered a eukaryotic cell model,<sup>153</sup> as well as screening methods for the detection of synergy.<sup>164,165</sup> The biggest challenge for these novel combination therapies now is thought to be the discovery of fungal-specific agents which can target the new antifungal mechanisms being discovered.<sup>165</sup>

The discovery of novel synergistic combinations could help to alleviate the pressing need to find strategies to combat microbial resistance. Combination therapies are already in use to treat many infectious diseases such as HIV, tuberculosis and malaria, and as such the area has garnered a lot of interest in the treatment of fungal pathogens.<sup>165</sup> While there has been research into synergistic combinations of known antifungal and fungicidal small molecules,<sup>153,166</sup> the use of biocidal polymers as one of the synergistic components has the potential to develop versatile and cost-effective antifungal formulations.

## 2 Chapter Two: Terpenes as initiators for 'green' ring opening polymerisations

### 2.1 Introduction: Surfactants for biomaterials

As mentioned in the Introduction (section 1.7.2), **Surface Active Agents**, abbreviated to **surfactants**, are amphiphilic molecules that, as implied in their name, are active at surfaces; they adsorb and adhere at interfaces, lowering the surface energy of the bulk material at those phases.<sup>143,144</sup> When surfactant molecules are added to a two-phase system, the molecules will gather at the interface or surface, so as to minimise the undesirable interactions, for example, of a hydrophobic moiety (such as a long carbon chain in a triglyceride) and a hydrophilic solvent such as water. After saturation of the surfactant at the surface, the molecules will then begin to aggregate together to form self-assembled molecular clusters known as micelles (**Figure 30C**). The Critical Micelle Concentration (CMC) is defined as the concentration at which surfactants form micelles.<sup>142</sup>

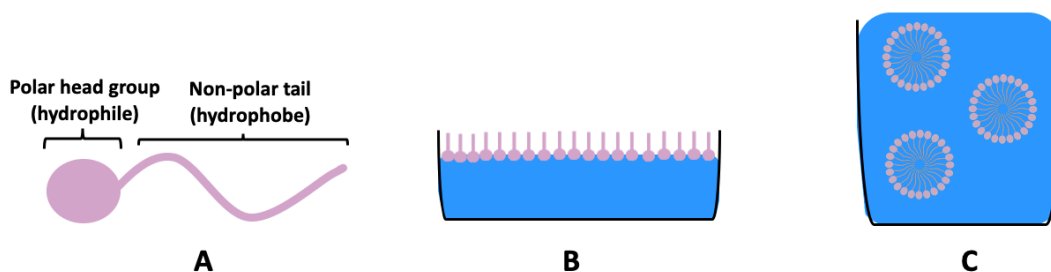


**Figure 30.** A cartoon representation of a surfactant molecule featuring a polar, hydrophilic head group and non-polar, hydrophobic tail (**A**). When surfactants are added to a two-phase system (such as water/air) they will accumulate at the surface (**B**), before reaching the critical micelle concentration (CMC), at which point the molecules self-assemble into (usually spherical) micelles (**C**).

As a result of this amphiphilicity, surfactant molecules can 'spontaneously aggregate' (i.e. self-assemble) as a result of solvophobic interactions, when the concentration of amphiphiles is above the CMC.<sup>141</sup> A spherical



micelle is not the only morphology which can form after reaching saturation of the molecule at a surface. A wide variety of nanostructures are feasible, including cylindrical micelles, lamellae and vesicles, in addition to a number of aggregates without well-defined structures.<sup>141</sup> Therefore, to describe these structures more generally, the critical aggregation concentration (CAC) is often used to refer to the point at which surfactant molecules begin self-assembling.<sup>147</sup> Predicting the nature of the particles that may form is very challenging, and often amounts to educated guess-work based upon a variety of factors including molecular structure, temperature, solvent and concentration.<sup>142</sup>

In this regard, nanoparticles made from synthetic amphiphilic polymers (rather than small-molecule amphiphiles) are of particular interest, as the synthesis of these macro-amphiphiles can allow for precise control of the polymer structure and chemistry, and their sizes can allow for the formation of suitable nanoparticle dimensions for these applications. This in turn has the potential to enable the physiochemical properties to be readily tuned, tailoring the nanoparticles to meet the requirements of the specific application.<sup>138</sup>

Amongst the various architectures available, linear block-co-polymers have been particularly successful in terms of synthesising polymeric surfactants.<sup>132,148</sup> For drug delivery applications for example, these types of co-polymers have been particularly relevant, as they can allow for the formation (through self-assembly) of 'stealthy' nanoparticles that can circulate *in vivo* with the encapsulation of 'cargo' within a core region of the particle.<sup>111,148</sup> As such, these block-co-polymers commonly feature a hydrophilic segment to act as the biocompatible corona, conjugated to a hydrophobic segment, that can facilitate encapsulation of hydrophobic drugs.<sup>138</sup> Systems based upon poly ethylene glycol (PEG) moieties have been a popular selection for such hydrophilic segments, as have poly(meth)acrylates and polypeptides.<sup>132</sup> These are commonly conjugated to aliphatic polyesters such as PLA, PCL and PGA, which have proved successful as the hydrophobic blocks for these kinds of amphiphilic, self-assembling biomaterials in extensive studies.<sup>132,148,149</sup>

Of these, PLA has proved particularly successful because not only is it derived from biomass, but it is also biocompatible (with FDA approval for

many of its formulations)<sup>132</sup> and biodegradable, both in the body and environmentally in the ecosystem, through hydrolysis of the polyester backbone.<sup>131</sup> This gives PLA a distinct advantage in terms of sustainability. Current biomedical applications for PLA (in particular, PLLA) include its use in biomedical screws, pins and plates which are intended to biodegrade within six to twelve months.<sup>22</sup> Its low immunogenicity and good mechanical properties also make it a useful polymer for drug delivery systems when the amorphous PDLLA is used.<sup>132</sup>

Extensive research has looked into synthetic methods of generating these amphiphilic polymers, and the different architectures available.<sup>132,138,139</sup> Despite the aforementioned advantages, PLA also poses a major challenge in that the backbone of the polyester does not have many available handles for functionalisation. As such, there remains an unmet challenge in methods of modifying PLA, or adapting it with functional handles, so as to expand the scope of applications for this biocompatible and sustainable polymer.

Given the urgent need for polymer chemistry to move towards green and sustainable processes,<sup>2,3,8,13</sup> there is now a parallel need to seek green and sustainable methods of synthesising these polymeric surfactants employed in biomaterial applications and beyond. This chapter discusses the synthesis of oligomers of PDLLA, employing terpenes as the initiator species and DBU as a catalyst, aiming to achieve a 'fully-green' synthesis of biobased surfactants with built-in handles for post-polymerisation modification.

## 2.2 Aims and Objectives

PLA has proved a versatile polymer for a variety of applications ranging from commodity plastics to biomaterials. In particular, the amorphous PDLLA made from racemic lactide has proven itself as a useful amorphous polyester for applications in nanomedicine such as drug delivery.<sup>123,147</sup> However, the backbone of the polymer does not offer much opportunity for post-polymerisation modifications, or functionalisation for specific requirements. On the other hand, terpenes are a feedstock that are highly

functionalised, usually with a variety of double bonds and often oxygen heteroatoms. The aim of this project is to couple the high utility and versatile, amorphous nature of PDLLA, with the high functionality of terpenes, to generate polymers of PDLLA that offer enhanced opportunity for post-polymerisation modifications.

Four terpenoids were identified as suitable candidates for these reactions: geraniol (**10**), carveol (**11**), limonene-alcohol (**28**) and *trans*-sobrerol (**12**) (**Figure 31**). **10** and **11** are both commercially available natural products, found in rose and spearmint oils, respectively. **28** can be accessed directly from limonene *via* hydroboration/ oxidation of the exocyclic alkene using 9-BBN, or *via* a sustainable catalytic method.<sup>45</sup> Similarly, **12** is accessed through the aqueous oxidation of  $\alpha$ -pinene, and a recent study by Stamm *et al.* showed that this could be achieved enzymatically in one step.<sup>78</sup>

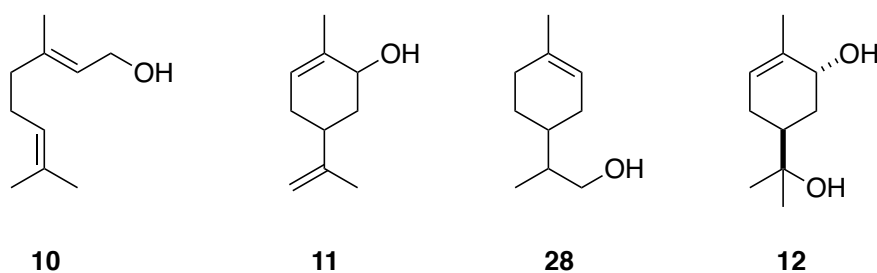


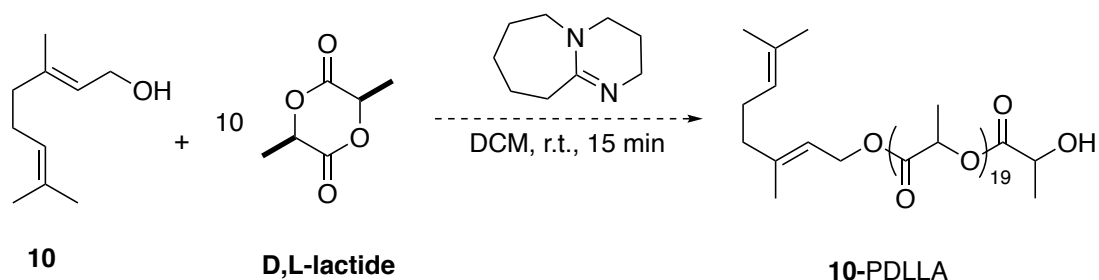
**Figure 31.** Structures of the four proposed terpenoid initiators.

These four terpenoids were each identified as suitable candidates to use as they are all readily available, either commercially or *via* green synthetic routes, and act as good examples of the diversity of terpenoids: this selection features both cyclic and acyclic terpenoids, each with one or two alkene groups. Additionally, **11** is employed as a mixture of *cis/trans* isomers, while **12** is employed as the single *trans*-isomer and **10** does not feature a stereocentre. Unlike the others, **12** is unusually hydrophilic; soluble in water and poorly soluble in a range of organic solvents. Importantly, each of the terpenoids features a reactive (primary or secondary) alcohol. This is in addition to at least one alkene, which has the potential to act as a handle for post-polymerisation modifications.<sup>167</sup> As

such, the retainment of these groups during the polymerisation is of paramount importance in each case.

The target was to employ the primary or secondary alcohol groups of the terpenoids as initiators in the ROP of racemic lactide. The ROP process has proved a facile method in which to form high molecular weight polymers of PLA, forming materials often used in commodity plastics.<sup>131</sup> In the first instance, the aim was to use the ROP process to generate oligomers of PDLLA with geraniol (**10**), in order to determine whether or not the reaction would proceed, and gain an insight into the material

properties of the oligomers formed (**Scheme 13**). The reaction was designed as described by Pearce *et al.*<sup>168</sup> This involves conditions that are similar to conventional ROP methodology, but use ambient conditions and the organocatalyst 1,8-Diazabicyclo [5.4.0]undec-7-ene (DBU), thus avoiding the need for high temperatures, long reaction times, extensive purification and tin or other potentially toxic, metal-based catalysts.<sup>138,139</sup>

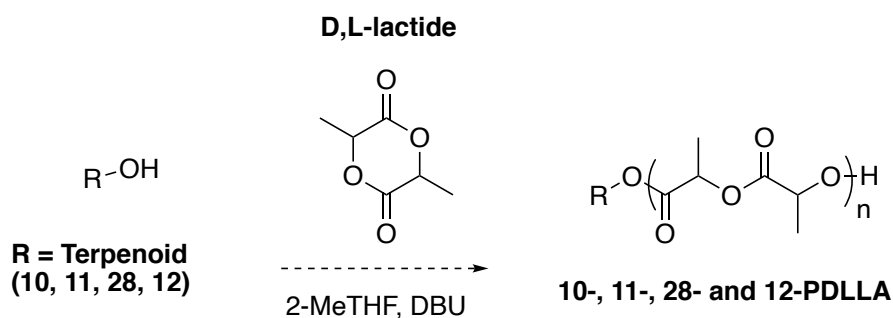


**Scheme 13.** The predicted synthesis of PLA oligomers employing racemic lactide and the terpene initiator geraniol, using conditions described by Pearce *et al.*<sup>168</sup>

Following the successful synthesis of PDLLA oligomers using these methods, it would then be intended to introduce a fully sustainable method in which to synthesise the same polymers. The catalyst DBU is naturally occurring, but the use of DCM is not sustainable, and so its replacement with a more sustainable alternative, such as 2-Methyl THF (2-MeTHF), is highly favourable. By comparing the properties of the oligomers made with **10** in DCM, to analogous oligomers made in the green solvent, it was endeavoured to show that this method could prove a facile and green way

in which to synthesise versatile, functionalisable poly- or oligomers of PDLLA, without compromise to their material properties.

Should this prove successful, and the oligomers from both the DCM and 2-MeTHF methods prove indistinguishable with **10** as the initiating species, the aim would be to employ the remaining 3 terpenoid initiators using the same reaction conditions in the green solvent (**Scheme 14**).

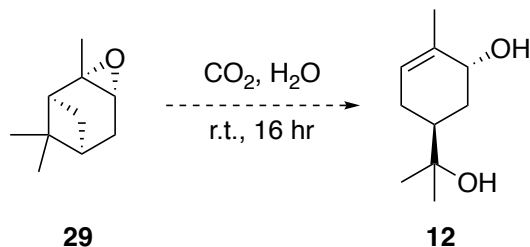


**Scheme 14.** *The predicted ROP of racemic lactide in a fully green ROP process: employing terpenoid initiators and an organobase catalyst with the sustainable solvent 2-MeTHF.*

Upon reaching this point, four PDLLA oligomers with different terpene head groups would be synthesised. It would at this point be intended to test and compare the chemical and material properties of the oligomers, in order to determine what contribution these head groups have on the overall macroscopic properties of the materials. This may give insight into a specific functional use of the individual oligomers. Finally, it was aimed to demonstrate that the 'newly introduced' alkene moiety of the PDLLA head group could be retained and used for post-polymerisation functionalisation.

## 2.3 Results and Discussion

### 2.3.1 Synthesis of *trans*-sobrerol (**12**)



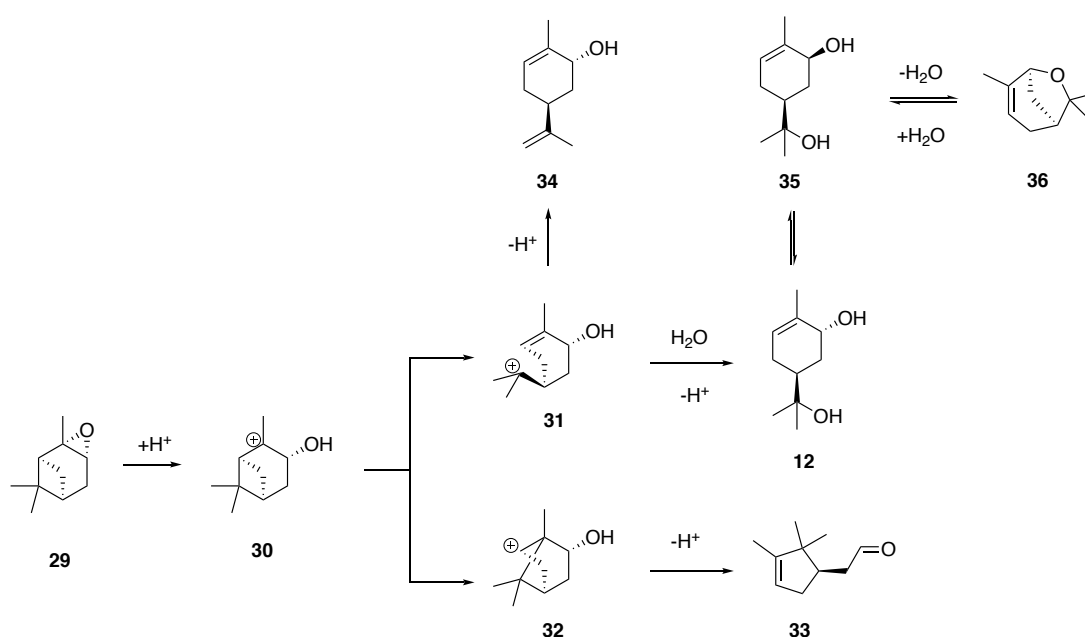
**Scheme 15.** The proposed ring opening of (+)- $\alpha$ -pinene oxide (**29**), to yield *trans*-sobrerol (**12**).

The synthesis of *trans*-sobrerol (**12**) was designed *via* the ring-opening of (+)- $\alpha$ -pinene oxide (**29**), the epoxidised product of  $\alpha$ -pinene, which is produced efficiently on an industrial scale due to its use in the synthesis of many chemicals for fragrances.<sup>169</sup> The ring opening of **29** can be achieved with a variety of catalysts and results in numerous terpenoid products.<sup>169,170</sup> When treated with acidified water (easily achieved using a flow of CO<sub>2</sub>), the result is **12**.<sup>171</sup>

As such, CO<sub>2</sub> was bubbled through water until acidic conditions of pH 4 were reached. **29** was then added resulting in a 0.5 M solution of the terpenoid in water, and the mixture was vigorously stirred for 16 hours. After this time a white solid was visible having crashed out of solution. The water was evaporated, and the white solid collected and purified by vacuum filtration, washing with cold ethyl acetate (EtOAc), resulting in **12** as a white solid, in a 47% yield isolated as the single *trans*-isomer.

A number of different reaction conditions have been previously thoroughly investigated in the Stockman research group and it has proved very difficult to synthesise pure samples of **12** in high yields.<sup>171</sup> The 47% yield in this case was considered in good agreement with standard yields for this reaction, and as such these conditions and yield was considered sufficient, especially given that the reaction is relatively 'green', making use of CO<sub>2</sub>, an abundant waste stream.

As mentioned, the ring-opening of **29** results in a number of terpene-based products, which is responsible for the moderate yields this reaction gives.<sup>170</sup> The proposed mechanism involves the activation and subsequent opening of the epoxide by acidified water, through hydrogen bonding (**Scheme 16**). This generates the carbocation **30**. This molecule is short-lived, undergoing a re-arrangement to relieve the ring strain of the cyclobutene ring, to result in the comparatively more stable para-menthane carbocation species, **31**. Water then attacks this cation, resulting in the formation of **12**. However, a number of other terpenoid products are also sometimes synthesised as a result of a number of side reactions/ alternative pathways. A different arrangement of **30** to an alternative cationic compound, **32**, is possible. This results in the formation of campholenic aldehyde, **33**.<sup>170</sup> It is also possible that if **31** does form, the cationic charge will be quenched through the formation of *trans*-carveol (**34**). Additionally, depending on the solvent polarity, or under reflux, **12** can isomerise to *cis*-sobreol (**35**), which in turn will convert to **36** through the loss of water.<sup>172</sup>



**Scheme 16.** Proposed mechanism for the synthesis of **12**, including the competing syntheses of campholenic aldehyde (**33**) and other terpenoids.<sup>172,173</sup>

In addition to the compounds formed in **Scheme 16**, a number of other minor isomerisation mechanisms are also possible, generating terpenes such as *para*-cymene, isopinocampheol and isopinocamphone.<sup>172</sup>

It was hypothesised that much of the yield in the synthesis of **12** was being lost in the formation of some of these terpenoid compounds, especially considering the two-phase nature of the reaction (between water and the hydrophobic **29** starting material). **12** is an unusual terpene in that it is not readily soluble in organic solvents, facilitating the facile purification step of washing with cold ethyl acetate. On the other hand, the by-products mentioned (including *cis*-sobrerol) are hydrophobic, yellow oils, likely to dissolve in EtOAc. To verify that these terpenes were being formed in the reaction, thus reducing the yield of **12**, the filtrate from the washing step was evaporated to dryness and analysed by NMR. The result was a complex mixture of terpenoid products; common products of the ring-opening reactions of **29**, particularly under acidic conditions.<sup>170,173</sup> These compounds and reactions have been extensively studied in the literature and so a number of them were easily identifiable according to resonances visible by <sup>1</sup>H NMR, without the requirement for their isolation (**Figure 32**).<sup>170</sup>

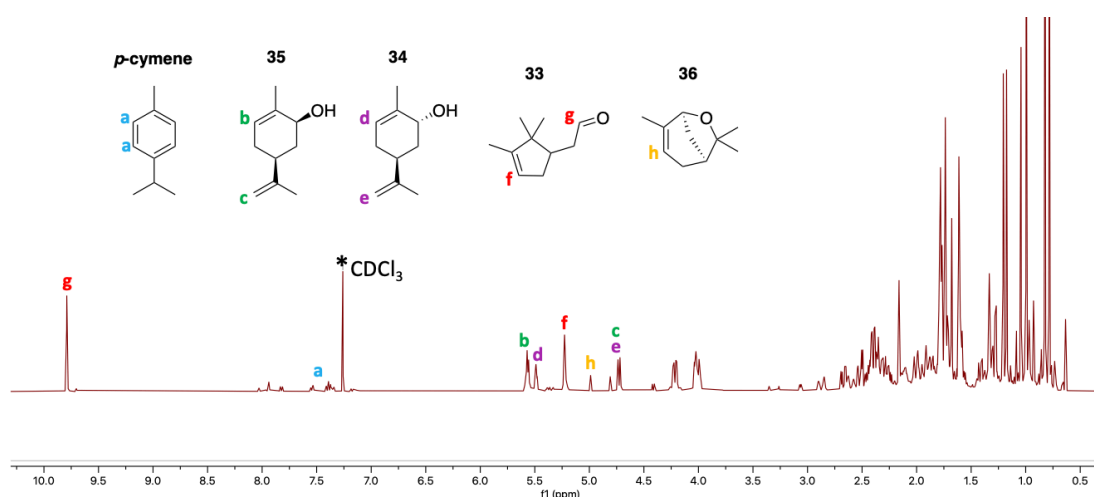


**Figure 32.** <sup>1</sup>H NMR spectrum in d-chloroform of the filtrate (washings) from the purification of **12**. A number of terpenoid isomer products were identified, as labelled.<sup>170</sup>



A quantitative yield was not determined for each of these terpenoid side products, however, together the crude mixture amounted to almost 2.2 g of material. Considering 5 g of starting material was used in this reaction and 47% of this was accounted for as the product **12**, it is reasonable to assume that these terpenoids constitute a considerable amount of the remaining 53% of material.

As anticipated, the sample was poorly soluble in a range of organic solvents, and as such NMR spectra were generally obtained in either deuterated methanol or DMSO. However, to compare to the starting material, an NMR in  $\text{CDCl}_3$  was desirable. Although poorly soluble, it was possible to obtain a  $^1\text{H}$  NMR spectrum of **12** in the deuterated solvent, and as such, the sample was found to be pure, and therefore brought forward for future reactions (**Figure 33**).

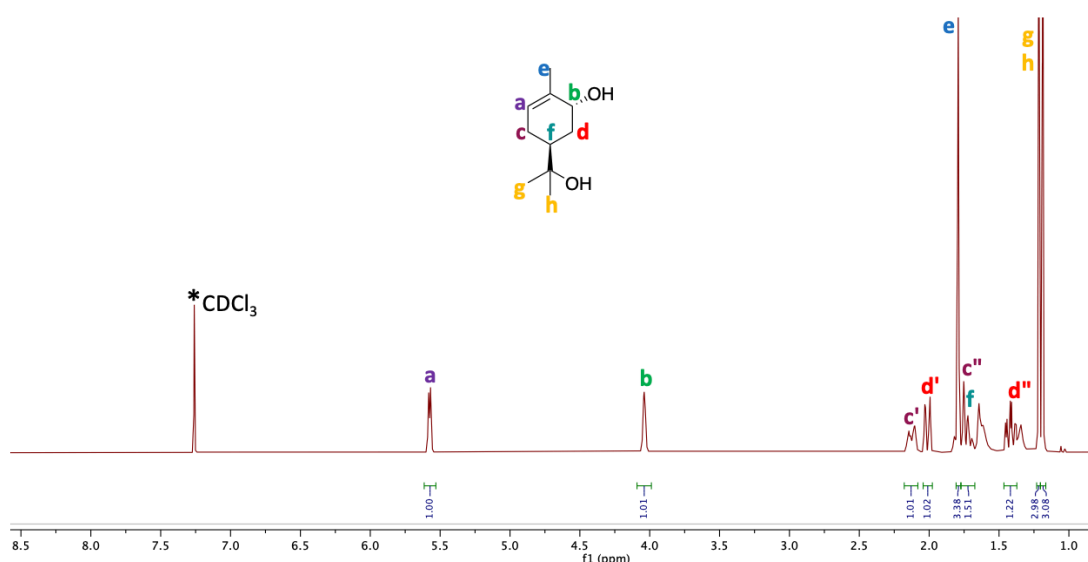
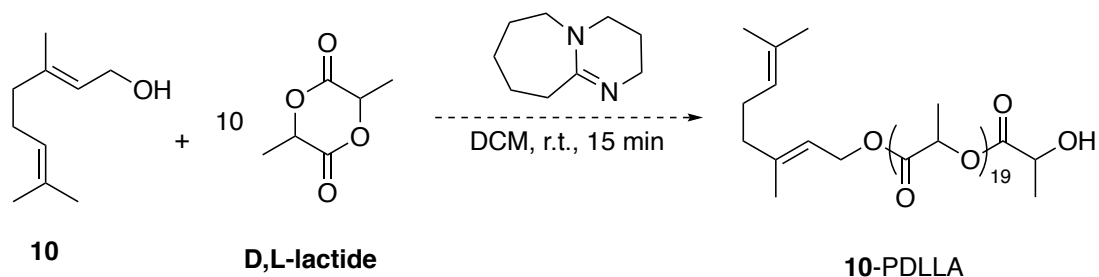


**Figure 33.**  $^1\text{H}$  NMR spectrum (in  $\text{CDCl}_3$ ) of trans-sobrerol (**12**).

Of the other intended initiators, carveol (**11**) and geraniol (**10**) are commercially available, natural products, so were purchased from chemical suppliers. Limonene-alcohol (**28**) was synthesised by members of the Howdle research group, *via* the hydroboration/oxidation of the exocyclic alkene moiety of (*R*)-limonene, using 9-Borabicyclo(3.3.1)nonane (9-BBN). These conditions were previously described by the group,

alongside an alternative, catalytic method.<sup>45</sup> As such, these three other terpenoids were readily available for synthetic use.

### 2.3.2 Synthesis of geraniol-initiated PDLLA oligomers



**Scheme 17.** Predicted ROP of lactide using **10** as the initiator species.

Pearce *et al.* recently published a facile synthesis of PLA-based oligomers employing the organocatalyst DBU, with dry DCM as the solvent and 10 equivalents of lactide monomer. In ambient conditions, the reaction went to >75% completion after only 15 minutes.<sup>168</sup> It was aimed in the first instance to employ these conditions in the ROP of lactide using **10** as the initiator species (**Scheme 17**), in order to determine that the reaction would proceed, and to act as a control experiment to determine the quality of polymers formed with respect to any made later using the greener solvent, 2-MeTHF. The aim was to generate similar-length oligomers to Pearce *et al.*, corresponding to 10 lactide monomers. In **Scheme 17** (and subsequent similar schemes in this thesis), the oligomers are drawn to show the constitutional repeating unit (CRU)<sup>174</sup> in its smallest possible format, i.e.  $n/2$ , rather than  $n$ , where  $n$  = number of monomers (i.e. the DP).

Consequently, the corresponding amounts of both monomer and initiator were measured into a vial which had been pre-dried, and dry DCM was added. A sample was taken at this point for <sup>1</sup>H NMR spectroscopy, of the monomer-initiator mixture in DCM, to serve as a 'zero' time point;  $t_0$ . DBU was then added (at 2 mol%) and the reaction was allowed to stir at room temperature for a total of 20 minutes. After this time the reaction

was stopped by precipitating the mixture into cold hexane. After cooling for approximately 1 hour in the freezer, the hexane was then decanted and replaced with diethyl ether. Following a further 2 hours of freezing, the Et<sub>2</sub>O was then decanted and the sample was dried in a vacuum oven for 24 hours.

<sup>1</sup>H NMR spectroscopy was used to determine the conversion of the monomer to oligomer. As anticipated, the *t*<sub>0</sub> sample indicated the presence of only monomer and initiator in the DCM solvent. Using a *t*<sub>end</sub> sample, taken after the washing steps, the conversion was found to be 70%, corresponding to a DP of 7. This was determined according to the integrals of the resonances corresponding to the alkene moieties of **10** in the PDLLA head group (**Figure 34**, resonances **a** and **c**), compared with the methyl group of the main oligomer chain (**Figure 34**, resonances **b** and **j**). DBU was also present, indicating that the washing steps may not have been sufficient to completely remove this leftover catalyst. However, there was no trace of any unreacted, leftover monomer or initiator.

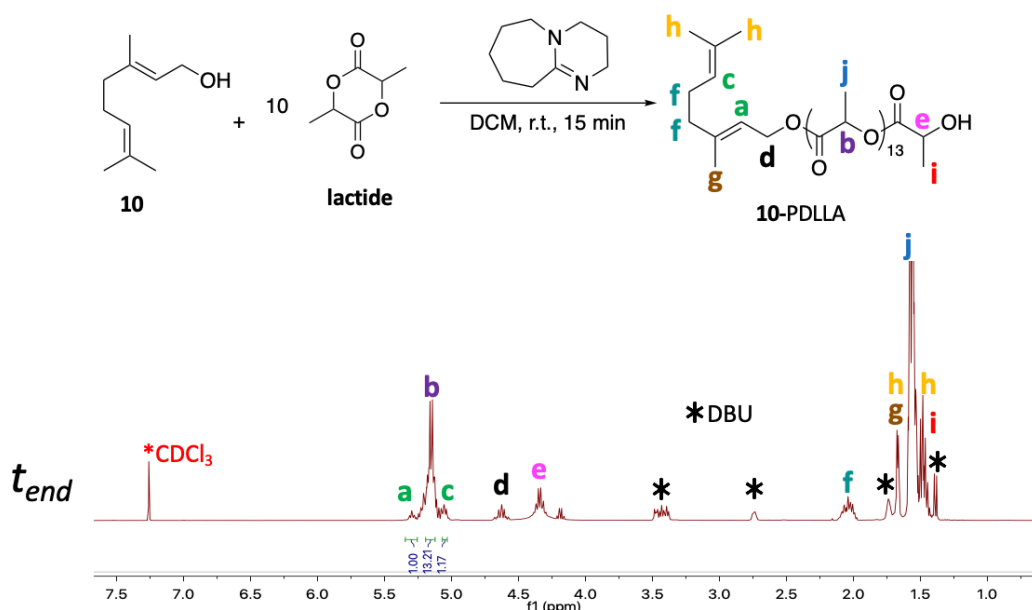


**Figure 34.** The conversion of racemic-lactide to PDLLA oligomers, using **10** as an initiator. The sample indicates a conversion of 70% monomer to oligomer, corresponding to 14 repeat units (including chain end).

The reaction was then conducted in the same way, replacing the DCM solvent with 2-MeTHF. This sustainable solvent has a much higher boiling point (80 °C) than DCM, which allowed for the reactions to be conducted at higher temperatures. This was fortunate, as it was found that at 60 °C, each of the reacting components (monomer, initiator and catalyst) were fully soluble, allowing the reaction to be conducted. The extra energy cost to run the reaction at 60 °C rather than in ambient conditions was considered negligible in terms of green chemistry, as avoiding the use of DCM is so favourable and 2-MeTHF is derived from bio-renewable sources rather than crude oil, making its use much more appealing for sustainable polymerisations.<sup>13,175</sup> After 20 minutes of reaction time, the oligomers were purified using the same washing steps as before.

Analysis of the sample by IR spectroscopy resulted in a spectrum which was superimposable to the sample made in DCM, confirming qualitatively the success of the green-solvent reaction in generating similar oligomers, without compromise to their chemical structure (**Figure 35**). In both spectra, the identifying sharp transition at 1750 cm<sup>-1</sup> is observed; a result of stretching of the ester carbonyl group. The C=C stretching of the alkene moieties of the terpene head group are also detected, at approximately 1650 cm<sup>-1</sup>. The fingerprint region of the spectra are similarly superimposable.

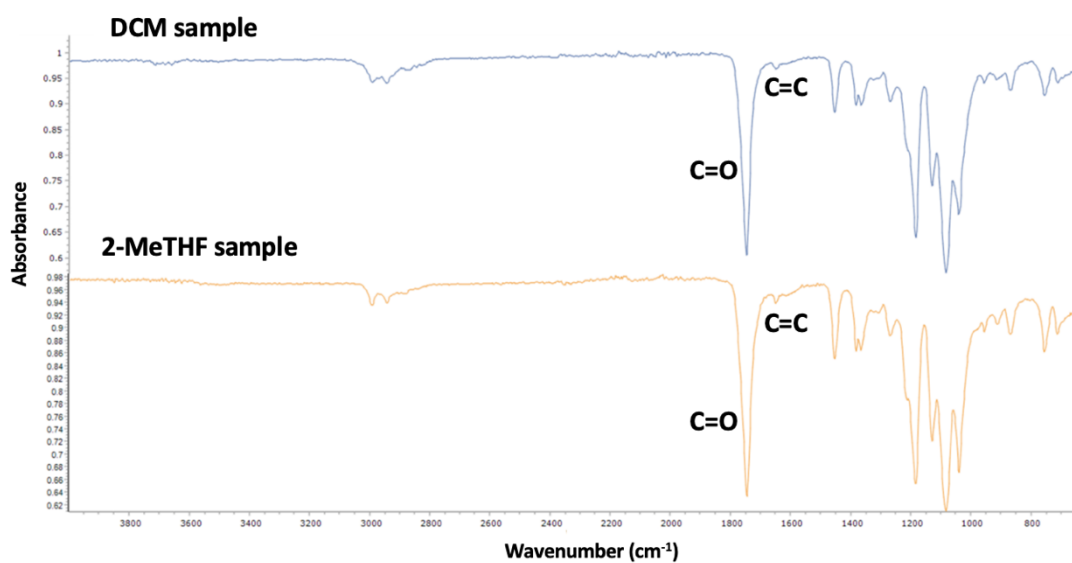


**Figure 35.** IR spectra of the geraniol-initiated PDLLA oligomers synthesised in DCM (top) and 2-MeTHF (bottom).<sup>176</sup>

<sup>1</sup>H NMR spectroscopy revealed a conversion of 70% (DP=7) for the sustainable synthesis of PDLLA oligomers in 2-MeTHF, matching the result in DCM. The <sup>1</sup>H NMR spectra resulted very similar for the two reactions, both featuring the characteristic peak shifts and broadening associated with polymerisation (**Figure 36**).

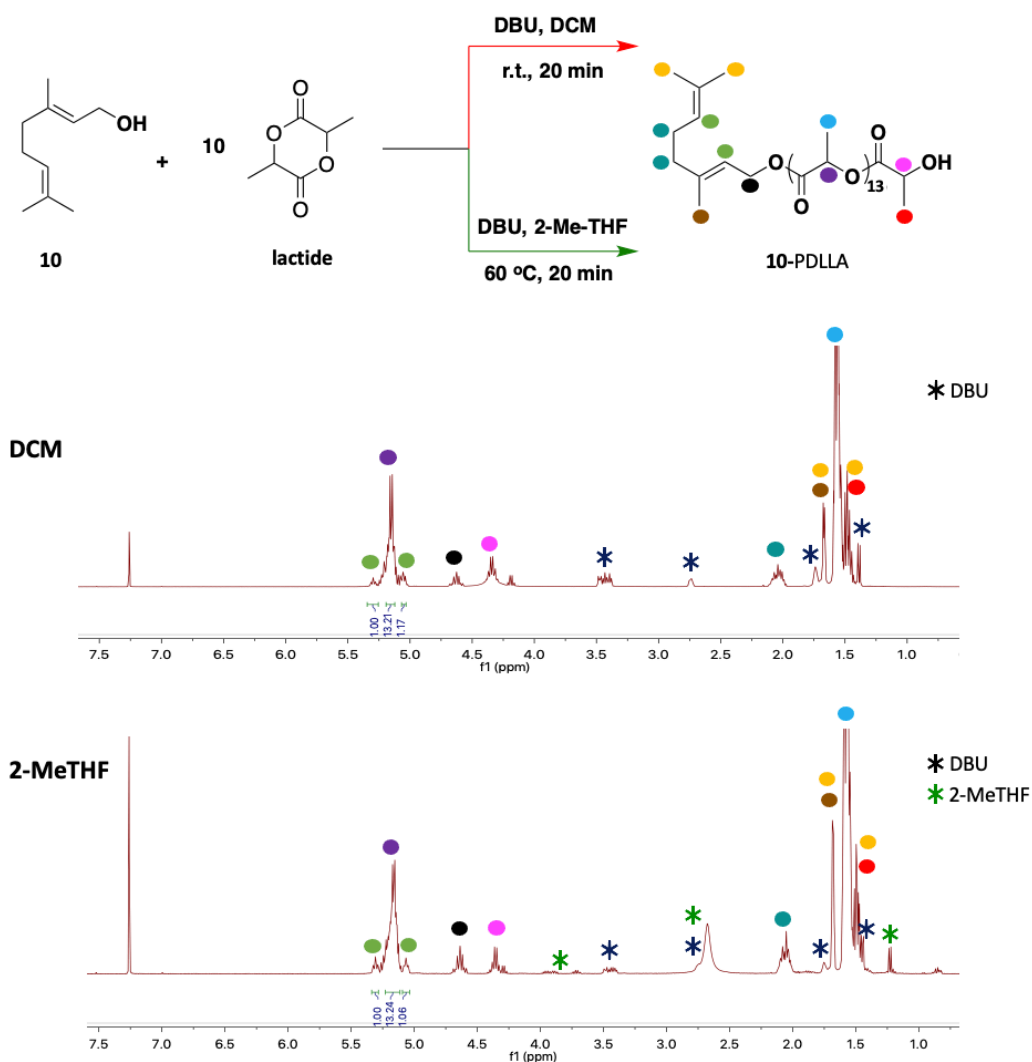


**Figure 36.** The conversion of racemic-lactide to PDLLA oligomers using **10** as an initiator, catalysed by DBU in DCM (top) and 2-MeTHF (bottom).<sup>176</sup>

The samples were then analysed by Gel Permeation Chromatography (GPC), using PDLLA standards on mixed-E columns (i.e. those optimised for systems  $<20,000 \text{ g}\cdot\text{mol}^{-1}$ ). Results indicated that the oligomers were approximately  $1330 \text{ g}\cdot\text{mol}^{-1}$ , which is in good agreement with the <sup>1</sup>H NMR result: a conversion of 70% would correspond to a molecular weight of  $1150 \text{ g}\cdot\text{mol}^{-1}$ . Additionally, the oligomers were relatively monodisperse,

with  $\bar{D} = 1.2$ , and featured only a single molecular weight distribution on the chromatogram, indicating the quality of the reaction (**Figure 37**).

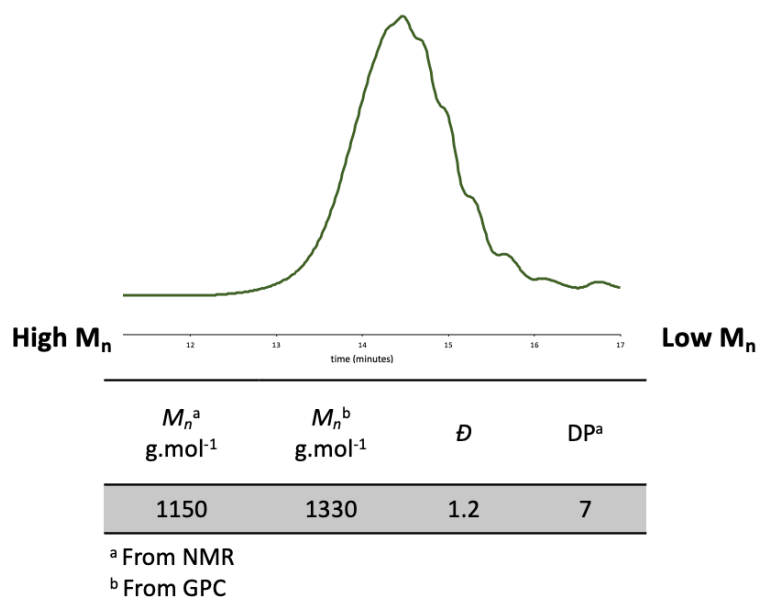


**Figure 37.** GPC Chromatogram and corresponding data from both GPC and NMR spectroscopy describing **10**-initiated PDLLA oligomers.<sup>176</sup>

Both Dynamic Mechanical Analysis (DMA) and Differential Scanning Calorimetry (DSC) techniques were employed to investigate the thermal nature of the oligomeric material. Both techniques revealed similar results, indicating the amorphous nature of the material, with glass transition temperatures ( $T_g$ ) of 0.3 °C and -4.6 °C observed for DMA and DSC, respectively.<sup>176</sup> While these results are quite similar, it is normal to expect a variation between the two analyses, due to the intrinsic difference between the static DSC and the dynamic DMA measurement, which leads to DSC observed  $T_g$ s being usually somewhat lower in absolute values than those of DMA.<sup>177</sup> The next step was to employ the three other identified terpenoids (**11**, **28** and **12**) using these fully green conditions, to prepare similar PDLLA oligomers and compare their properties, in order to gain an insight into the influence of the terpenoid head group on the overall oligomer chain.

### 2.3.3 Synthesis of PDLLA oligomers using green synthetic methods

Following the successful synthesis of PDLLA oligomers in 2-MeTHF, using **10** as an initiator, the remaining identified terpenoid products were then employed as initiators using similar conditions, in attempts to make oligomers of roughly the same molecular weight and chemical properties, with different terpene head groups.

First, limonene-alcohol, **28**, was used. At 60 °C, **28** and rac-lactide were dissolved in dry 2-MeTHF and a  $t_0$  sample was taken for  $^1\text{H}$  NMR analysis. This indicated the presence of only the monomer and initiator in the green solvent, as anticipated. DBU was then added and the mixture was stirred for 20 minutes, after which time the sample was precipitated into a cold 50:50 mixture of petrol and hexane. This mixture was changed slightly from the pure hexane solution used for oligomers made from **10**, in an attempt to draw out more of the deactivated catalyst from the oligomer product. The washing steps were then continued in the usual way as described for the geraniol-initiated sample, and the oligomer product was finally isolated as a white, solid powder.

$^1\text{H}$  NMR spectroscopy of this final product ( $t_{end}$ ) indicated that the reaction had been successful, and had reached a conversion of 80%, corresponding to a DP of 8 lactide monomers, a slight improvement from the geraniol-initiated oligomers (**Figure 38**). As before, 2D NMR techniques were used to identify a number of resonances in the  $^1\text{H}$  NMR spectrum, and to confirm that the terpenoid head group was covalently linked to the oligomer chain.



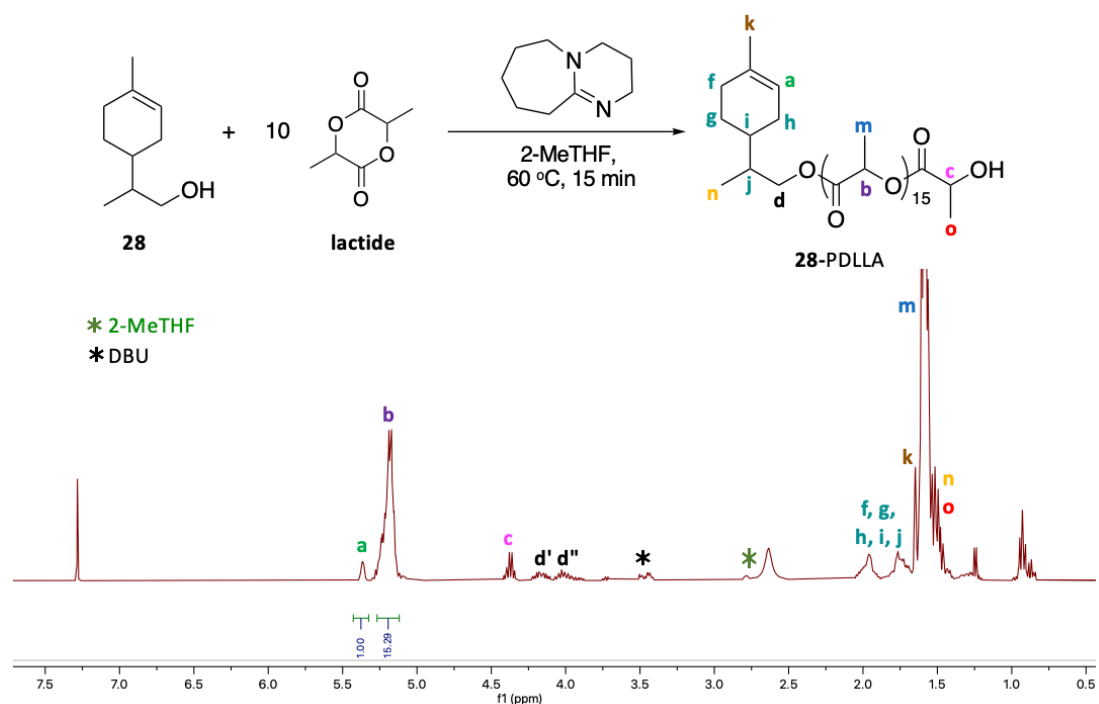


**Figure 38.** <sup>1</sup>H NMR spectrum of PDLLA oligomers made using limonene alcohol (**28**) as an initiator in 2-MeTHF. Conversion was found to be 80% (DP = 8), determined by integration of the resonance of the alkene bond of **28** (**a**), with respect to the -CH resonance of the PDLLA chain (**b**).<sup>176</sup>

A conversion of 80% would correspond to a molecular weight of approximately 1300 g·mol<sup>-1</sup>. Analysis by GPC (compared with PDLLA standards) revealed a good agreement with this, indicating an M<sub>n</sub> of 1670 g·mol<sup>-1</sup>, with a narrow dispersity of 1.2 (**Figure 41/ Table 1**). Thermal analysis revealed a T<sub>g</sub> of 25.7 °C or 31.3 °C, when measured by either DSC or DMA, respectively. These values are approximately 20 °C higher than the previous geraniol-based sample. It was hypothesised that this could be a result of the cyclic terpenoid head group bestowing more rigidity to the oligomers compared to the linear, aliphatic **10**.

The terpenoid carveol (**11**) was next investigated as an initiator, as a racemic mixture of cis/trans isomers (with the alcohol group in the up or down position on the ring). The same conditions were used; carveol and rac-lactide were dissolved in 2-MeTHF at 60 °C before DBU was added and the mixture was stirred for 20 minutes. The reaction was stopped by

deactivating the catalyst, precipitating the mixture into a 50:50 petrol/hexane mixture. After the washing steps were completed in the usual way, a solid, white powder was isolated.  $^1\text{H}$  NMR revealed a complete 100% conversion for this reaction, corresponding to a DP of 10, and a molecular weight of approximately  $1700\text{ g}\cdot\text{mol}^{-1}$  (**Figure 39**).

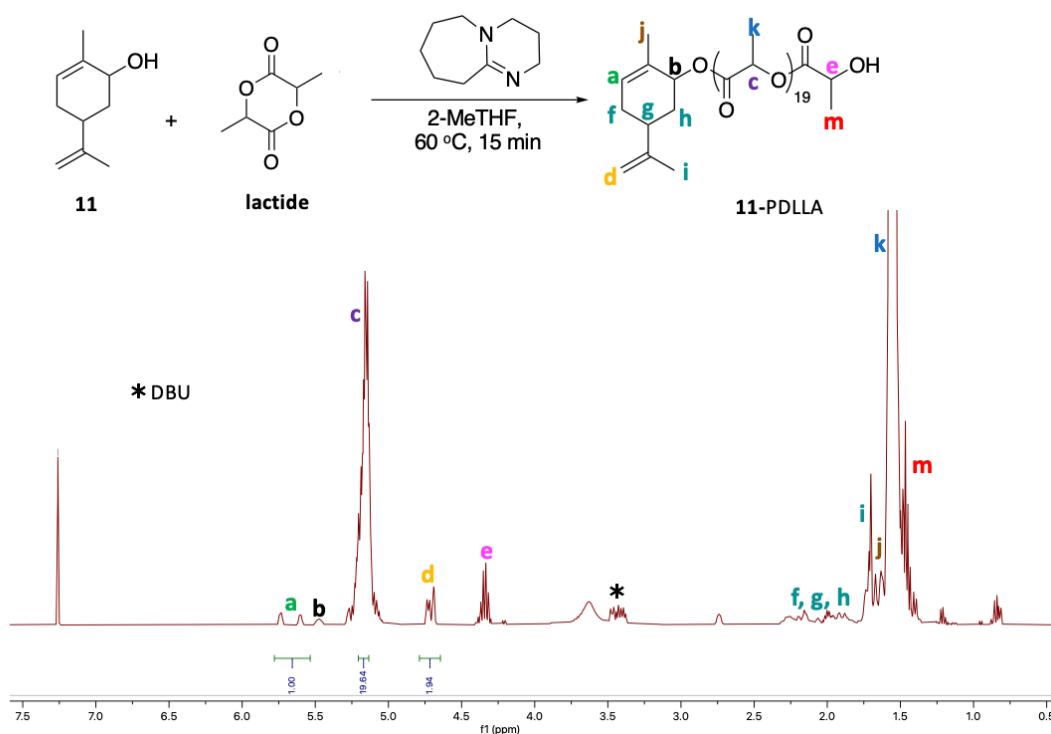


**Figure 39.**  $^1\text{H}$  NMR spectrum of **11**-initiated PDLLA oligomers in 2-MeTHF. Conversion was calculated to be 100% (DP = 100). **11** was used as a mixture of cis/trans isomers, resulting in two resonances for the endocyclic alkene **a** (one for each isomer).<sup>176</sup>

Once again the GPC results corroborated well with the  $^1\text{H}$  NMR data, indicating an  $M_n$  of  $2100\text{ g}\cdot\text{mol}^{-1}$ , once again with a narrow dispersity of only 1.2 (**Figure 41/ Table 1**). DSC and DMA results revealed  $T_g$ s of  $13.5\text{ }^\circ\text{C}$  and  $20.2\text{ }^\circ\text{C}$ , respectively. While slightly lower than the PDLLA oligomers with **28** as the head group, these results are still approximately  $15 - 20\text{ }^\circ\text{C}$  higher than the results shown for the **10**-initiated sample. The difference once again is hypothesised to be a result of the structurally different terpenoid head groups of the PDLLA chains.

Finally, the hydrophilic terpenoid *trans*-sobrerol (**12**) was investigated as an initiator for this reaction, using the green conditions. In this regard, the advantage of using the bio-based solvent is two-fold: not only is 2-MeTHF much more sustainable and less toxic, but additionally, **12** is particularly insoluble in DCM, as well as a variety of common organic solvents. However, at 60 °C, **12** was found to be fully soluble in 2-MeTHF, allowing the reaction to proceed, and thus expanding the library of available bio-based initiators with which to synthesise PDLLA.

Following the usual procedure, the reaction with **12** was found to proceed easily, resulting in a 100% conversion (DP = 10 lactide monomers), determined by <sup>1</sup>H NMR of the final white powder product (**Figure 40**).

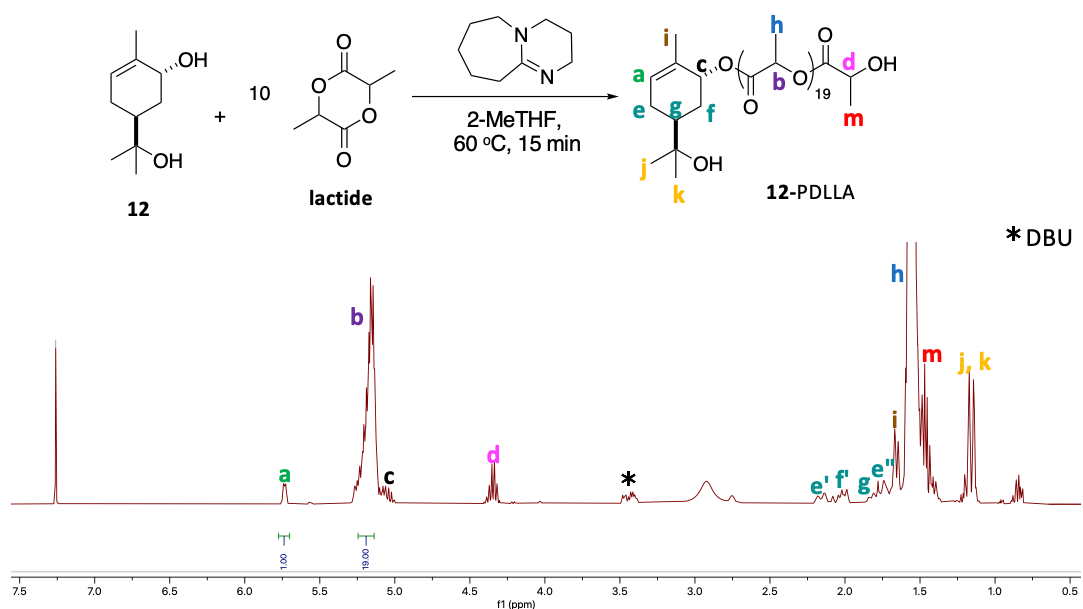
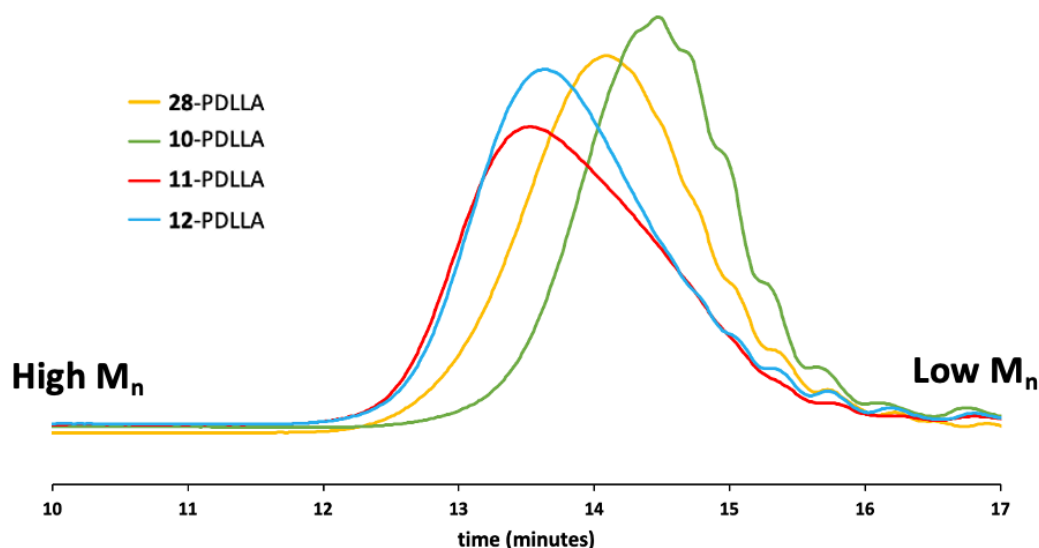


**Figure 40.** <sup>1</sup>H NMR spectrum of **12**-initiated PDLLA oligomers in 2-MeTHF. Conversion was calculated to be 100% (DP = 10) according to the resonance corresponding to the terpene alkene (**a**) compared to the -CH moiety of the polyester backbone (**b**).<sup>176</sup>

As before, the quality of the reaction was demonstrated by GPC, which showed a single, monodisperse molecular weight distribution of 1.2. The GPC data was in good agreement with that of NMR, with  $M_n$  values of 2050 g·mol<sup>-1</sup> and 1600 g·mol<sup>-1</sup> for either technique, respectfully (**Figure**

**41/ Table 1).** DSC and DMA analyses resulted in  $T_g$ s of 24.4 °C and 26.0 °C, respectfully. These values are in very good agreement with one another, and are within the expected range of results, indicating the amorphous nature of the material, and closely matching the other samples, particularly those with cyclic rings.



Oligomer	*Dp <sup>a</sup>	$M_n^a$ (g.mol <sup>-1</sup> )	$M_n^b$ (g.mol <sup>-1</sup> )	$\bar{D}$	$T_g^c$ (°C)	$T_g^d$ (°C)
10-PDLLA	7	1150	1330	1.2	-4.6	0.3
11-PDLLA	10	1700	2100	1.2	13.5	20.2
12-PDLLA	10	1600	2050	1.2	24.4	26.0
28-PDLLA	8	1300	1670	1.2	25.7	31.3

\*approximated to the closest & most sensible whole values.

<sup>a</sup> From NMR, <sup>b</sup> From GPC, <sup>c</sup> From DSC, <sup>d</sup> From DMA (1 Hz).

**Figure 41.** GPC chromatogram showing all four terpenoid-initiated PDLLA oligomers synthesised in 2-MeTHF, each with  $\bar{D} = 1.2$  (top).

**Table 1.** Data describing some of the physical characterisation of the four terpenoid-initiated PDLLA oligomers synthesised in 2-MeTHF (bottom).

Each of the four terpenoids were found to successfully initiate the ROP of rac-lactide, producing monodisperse oligomers ( $\bar{D}=1.2$ ) in conversions

ranging from 70-100%. The results are summarised in **Figure 41/ Table 1**. Thermal analysis by DSC and DMA gave results within the expected range of difference for the two techniques. Importantly, the trend in  $T_g$ s is the same for both techniques, with geraniol-PDLLA having the lowest and limonene-PDLLA having the highest  $T_g$ s.

As each of the oligomers were roughly the same length and size, it is hypothesised that the largest contributing factor to the difference in  $T_g$  of each sample is the nature of the terpenoid head group, especially given the relatively low molecular weights of PDLLA that were synthesised. A number of other factors might also be influenced by these groups, including how the oligomer chains pack together and orientate themselves in space, which will have knock-on effects on a number of other physical parameters. It was therefore endeavoured to investigate what other physical properties may also be altered as a result of these groups.

#### 2.3.4 Surface Activity Investigations

Water contact angles ( $\Theta_w$ ) were investigated to gain an insight into the hydrophilic/ hydrophobic character of the surface of each PDLLA sample. Surfaces are generally considered hydrophobic when the angle that the surface of a droplet of water makes with a material is greater than  $90^\circ$ , and similarly, if it is less than  $90^\circ$ , there is said to be 'good wetting' of the material, and it is considered hydrophilic.<sup>178,179</sup> Each of the surfaces of the four oligomers showed good wettability, with  $\Theta_w < 90^\circ$ , ranging from only approximately  $55^\circ$  to  $72^\circ$  (**Table 2**).<sup>176</sup> This is a relatively unusual result for PDLLA chains, which are usually hydrophobic: the literature reports long-chained, unfunctionalised PDLLA has  $\Theta_w$  values ranging from approximately  $80^\circ$  to  $90^\circ$ .<sup>180,181</sup>

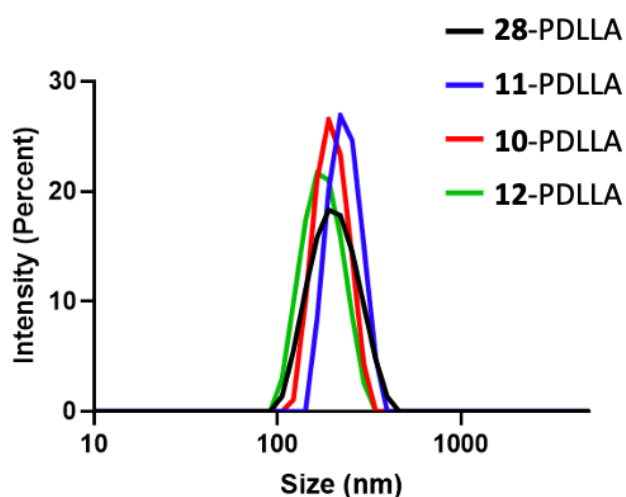
oligomer	$\Theta_w$ (°)
<b>10</b> -PDLLA	65 ±4
<b>11</b> -PDLLA	72 ±2
<b>12</b> -PDLLA	55 ±3
<b>28</b> -PDLLA	68 ±1

**Table 2.** Water contact angles ( $\Theta_w$ ) of each of the four terpenoid-initiated PDLLA oligomers.<sup>176</sup>

The relatively low  $\Theta_w$  values in this case suggest that the oligomers exhibit some amphiphilicity; they are not quite fully hydrophilic, though certainly are below the threshold of 90° for hydrophobic surfaces. This could possibly be explained by self-assembly behaviour of the material; in 2017, Yildirim *et al.* demonstrated that PLA polymers made using retinol as the initiator were found to self-assemble (following a nanoprecipitation technique) into small, monomodal sized nanoparticles with negative surface charges.<sup>182</sup> It was thus hypothesised that the water contact angles observed in this instance can be explained as a result of how the oligomer chains are arranged and organised in solution, particularly if the hydroxyl end-groups were to be orientated towards the surface, nearest the water droplets, with the polyester chain and terpenoid group contained in the inner, 'bulk' part. However, it is also worth noting that in the case of **12**-PDLLA, the oligomer which featured the most hydrophilic terpenoid head group (*trans*-sobrerol), this corresponded to the lowest  $\Theta_w$  value. This may suggest that the hydrophilic head group might be at the surface in this case, possibly alongside the hydroxyl end-groups of the PDLLA chains, rather than contained within the inner bulk as suggested for the other oligomers.

To investigate if self-assembly and surface activity of this nature was taking place, the oligomers were tested for nanoparticle formation *via* nanoprecipitation in water. The oligomers were dissolved in acetone at concentrations of 10 mg·mL<sup>-1</sup> and added dropwise to water under constant stirring. After stirring overnight to facilitate the evaporation of acetone, the colloid suspensions were studied *via* Dynamic Light Scattering (DLS). All four of the oligomer samples were found to self-assemble into well-defined

nanoparticles (NPs), with diameters ranging from c.175 nm up to 230 nm, with very narrow  $\mathcal{D}$ s of  $<0.1$  (**Table 3/ Figure 42**).<sup>176</sup> In addition to DLS analysis, the zeta potential (ZP) was also investigated, and was found to be considerably negative for each of the four NPs (**Table 3**). Negative ZPs indicate that a net-negative charge has developed at the surface of the NP, and the magnitude of the ZP gives an indication of the colloidal stability.<sup>183</sup> ZPs that are either greater than +25 mV or less than -25 mV are considered to have a high degree of stability: values between these parameters tend to form less stable NPs because the repulsive forces between the similarly-charged particles are not enough to prevent aggregation, flocculation or other processes which break down the nanoparticle suspensions, usually as a result of Van der Waals interactions between particles.<sup>183</sup>



oligomer	Size (nm)	PDI	ZP (mV)
10-PDLLA	201 ±8	0.08 ±0.02	-21 ±2
11-PDLLA	231 ±4	0.11 ±0.03	-32 ±3
28-PDLLA	195 ±3	0.04 ±0.01	-31 ±3
12-PDLLA	176 ±5	0.03 ±0.02	-27 ±4

**Figure 42.** DLS intensity of the terpene-initiated NPs formed via the nanoprecipitation technique (top).<sup>176</sup>

**Table 3.** Nanoparticle sizes, size distributions and Z-potentials. Measures performed in milliQ grade water (bottom).<sup>176</sup>

Each of the four NPs formed from the terpenoid-initiated PDLLA oligomers featured ZPs  $\leq -21$  mV, indicating good stability in the absence of additional stabilisers, and highlighting the potential of these materials to be used as new, bio-renewable surfactants. This is particularly significant when considering that PDLLA polymers of higher molecular weights cannot self-assemble into NPs without being co-polymerised with a second highly hydrophilic component (such as PEG), highlighting the advantage of this one-step, fully green synthesis.<sup>176</sup>

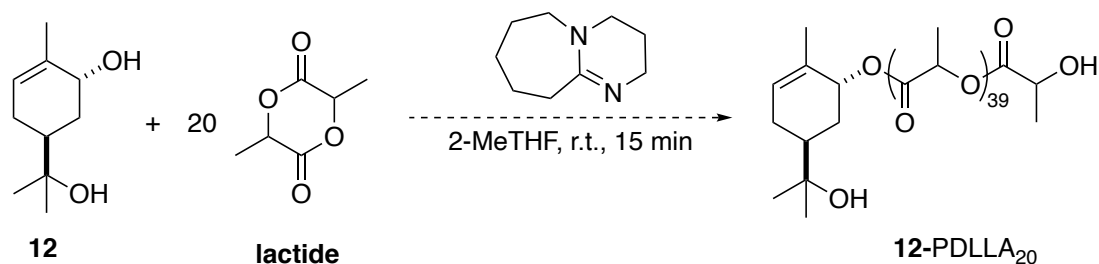
The negative ZP may be a result of the hydroxyl end-groups assembling toward the surface of the NP, as hypothesised. The **12**-PDLLA NP also resulted in the smallest of the NPs, which is likely a consequence of the *trans*-sobrerol head group bestowing enhanced hydrophilicity and thus better phase-separation between the hydrophilic and hydrophobic moieties of oligomer, resulting in smaller NPs.

### 2.3.5 Chain length investigations in **12**-PDLLA oligomers.

The hydrophobic/hydrophilic balance of the amphiphile is of critical importance for surfactants, with implications not only on the surface activity on the compound, but also on the shapes and geometries of the aggregates formed.<sup>144</sup> It was endeavoured to investigate this balance with **12**-PDLLA oligomers (which bear the hydrophilic **12** head group), by extending the length of the hydrophobic, polyester chain.

As such, it was aimed to synthesise oligomers with twice the PDLLA chain length as before, i.e. corresponding to 20 monomer units. It was aimed to do this employing the same, green conditions as before, with a molar ratio of 20:1 for the monomer/ initiator components (**Scheme 18**). The purpose of this was to demonstrate the robustness and versatility of the green ROP conditions.





**Scheme 18.** Proposed synthesis of **12**-initiated PDLLA oligomers with 20 monomer units.

The reaction was conducted in the usual way: the monomer and initiator components were dissolved together at 60 °C in 2-MeTHF before the catalyst was added and the mixture was stirred for approximately 20 minutes. After this time, the catalyst was deactivated by exposing the solution to air and precipitating into a 50/50 petrol/hexane mixture. Following the usual washing steps, the material was isolated as a white solid and analysed by <sup>1</sup>H NMR spectroscopy. This showed a DP of 20, i.e. a conversion of 100%, as determined by the integration of the alkene resonance in the terpenoid head group with respect to the integration of the CH proton in the PDLLA chain. Additionally, the spectrum was very similar to that of the **12**-PDLLA<sub>10</sub> system (**Figure 43**), indicating the retention of the resonances relating to the terpenoid head group, proving the robustness of the reaction conditions.

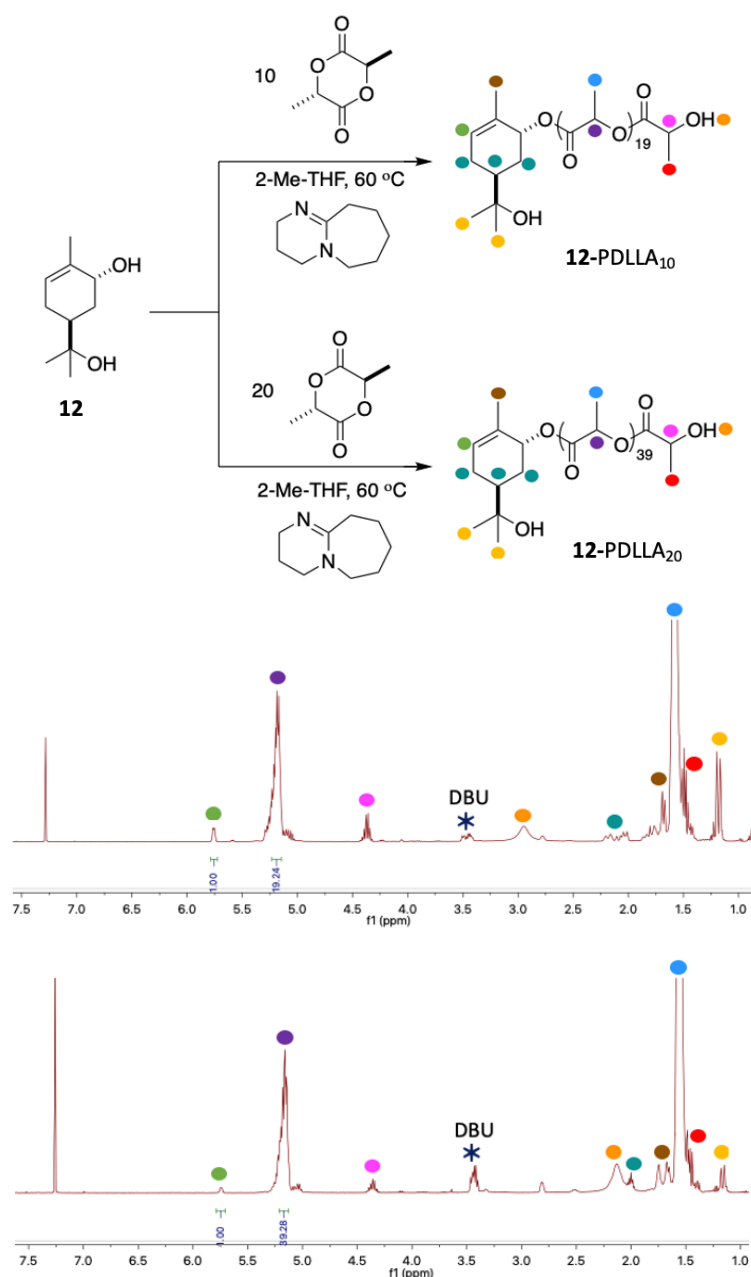


**Figure 43.** Reaction schemes for the synthesis of **12-PDLLA<sub>10</sub>** (top, left) and **12-PDLLA<sub>20</sub>** (bottom, left) using the green conditions. The respective <sup>1</sup>H NMR spectra are labelled, indicating similar results for both reactions.<sup>176</sup>

GPC analysis indicated that a single molecular weight distribution was present in the sample, with a molecular weight of 2200 g·mol<sup>-1</sup> (by M<sub>n</sub>) and a dispersity of 1.3, only slightly greater than that of the shorter **12-PDLLA<sub>10</sub>** sample, and still relatively monodisperse. This is in good agreement with the <sup>1</sup>H NMR calculated M<sub>n</sub>, of 3050 g·mol<sup>-1</sup>. In this way, it was shown that

using the reliable, green and sustainable ROP, the hydrophobic PDLLA chain could be doubled, which allows for precise control over the amphiphilicity of the oligomer samples when the hydrophilic **12** was employed as an initiator. The self-assembly and surfactant properties of **12**-PDLLA<sub>20</sub> were then investigated and compared to the **12**-PDLLA<sub>10</sub> sample, in order to further investigate how this change in hydrophobic/hydrophilic balance affected the overall amphiphilicity of the oligomer (**Table 4**).

oligomer	$\Theta_w$ (°)	ZP (mV)	Size (nm)	PDI
<b>12</b> -PDLLA <sub>10</sub>	55 ± 3	-27 ± 4	176 ± 5	0.03 ± 0.02
<b>12</b> -PDLLA <sub>20</sub>	c. 55.4	c. -40 mV	c. 103	c. 0.12

**Table 4.** Water contact angles ( $\Theta_w$ ), nanoparticle sizes and Z-potentials of the **12**-PDLLA<sub>10</sub> and **12**-PDLLA<sub>20</sub> samples. The **12**-PDLLA<sub>20</sub> sample was analysed by another member of the Howdle research group, and unfortunately the precise data including the error is no longer available.<sup>176</sup>

First, the water contact angle of **12**-PDLLA<sub>20</sub> was investigated and found to be c.55°, very similar to the **12**-PDLLA<sub>10</sub> sample. This value is significantly below the 90° threshold, indicating a hydrophilic surface. Given the similarities of the two samples, it is likely that the oligomers are arranging in such a way that the surface of both samples are similar. To investigate this self-assembly behaviour of the longer-chained oligomers, the nanoprecipitation method was employed using the same conditions as used for the **12**-PDLLA<sub>10</sub> sample: the oligomer was dissolved in acetone at a concentration of 10 mg mL<sup>-1</sup> and added dropwise to water under constant stirring. After stirring overnight to facilitate the evaporation of acetone, the colloid suspension was then studied *via* DLS (**Figure 44**). The results indicated the presence of nanoparticles with a size of c. 103 nm, which were monomodal with a  $\mathcal{D}$  of only 0.12. These nanoaggregates are almost 70 nm smaller than those produced from the shorter **12**-PDLLA<sub>10</sub> sample

(**Figure 44**),<sup>176</sup> indicating the significance of the balance of amphiphilicity within the surfactant molecules. This smaller nanoparticle aggregation size in the **12-PDLLA<sub>20</sub>** sample is favourable, as the preferred range for nanoparticle size should be 20-200 nm, particularly for biomedical applications such as drug delivery.<sup>115</sup>

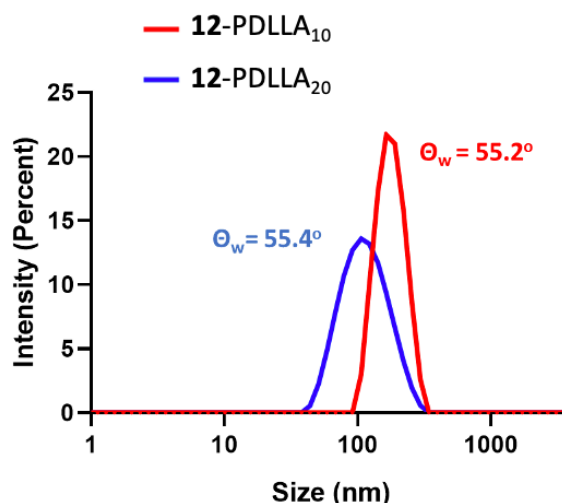


**Figure 44.** DLS intensity comparing the **12-PDLLA<sub>10</sub>** (red) and **12-PDLLA<sub>20</sub>** (blue) nanoparticle sizes and  $\Theta_w$ . The water contact angle  $\Theta_w$  of each sample is also included.

Measurement of the zeta-potential of the **12-PDLLA<sub>20</sub>** sample resulted in a very negative value of c. -40 mV. The magnitude of this result suggests a high degree of stability for these aggregates, further promoting their potential use as bio-based surfactants.<sup>183</sup> Additionally, when the CAC for this sample was calculated (by measuring the light scattering count rate intensity variation as a function of concentration), it was found to be  $70 \mu\text{g mL}^{-1}$  i.e. 0.032 mM. Comparatively, that of the **12-PDLLA<sub>10</sub>** sample was  $90 \mu\text{g mL}^{-1}$ , i.e. 0.053 mM. (**Figure 45**).<sup>176</sup> Both of these values are within a comparable range for commonly employed surfactants: Triton X100, for example, has a CMC of 0.22-0.24 mM, while Tween<sup>®</sup> 20 has a CMC of  $60 \mu\text{g mL}^{-1}$ , according to the values quoted in the Sigma Aldrich/ Merck catalogues.<sup>184,185</sup> Low CAC values of 70 or  $90 \mu\text{g mL}^{-1}$  are beneficial for surfactant molecules, as only a small concentration of the

oligomer or polymer is necessary for nanoparticle formation and moreover, high dilutions are required before disaggregation processes occur, which broadens the scope of applications and utility for these renewable materials.<sup>176</sup> In particular, for biomaterial applications such as drug delivery, smaller nanoparticles in the region of 30-100 nm in diameter are often preferred as they tend to exhibit better cytocompatibility profiles than larger ones,<sup>186</sup> and better uptake into cells without being rapidly eliminated from the body, as with nanoparticles <20 nm in size.<sup>115,187</sup>

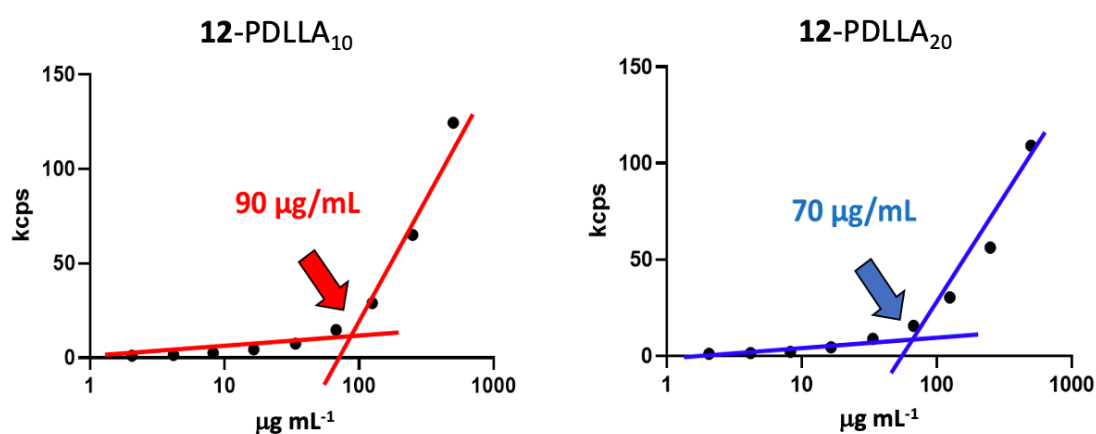


**Figure 45.** Graphs displaying count rate (measures in kcps) vs concentration ( $\mu\text{g mL}^{-1}$ ), used to measure the CACs of **12-PDLLA<sub>10</sub>** (left,  $90 \mu\text{g}\cdot\text{mL}^{-1}$ ) and **12-PDLLA<sub>20</sub>** (right,  $70 \mu\text{g}\cdot\text{mL}^{-1}$ ).<sup>176</sup>

The amphiphilic balance of the oligomer, between the hydrophilic **12** head-group and the length of the hydrophobic polyester chain, evidently has significant consequences on the colloidal properties of the material. Having established that the **12-PDLLA<sub>20</sub>** has very favourable surfactant properties in terms of its nanoparticle size and CAC, it was endeavoured to investigate further the stability of these particles. In particular, it was aimed to compare the stability of this oligomer to the other terpene-initiated oligomers, which were found to form nanoparticles (**Table 3**), but did not feature the hydrophilic **12** head-group, hypothesised to be imperative to the favourable colloidal properties of **12-PDLLA<sub>20</sub>**.

To test this, both **12**-PDLLA<sub>20</sub> and the limonene-initiated **28**-PDLLA<sub>10</sub> samples were dissolved in phosphate buffer saline (PBS), maintained at pH 7.4, at a concentration of 0.5 mg·mL<sup>-1</sup>, and their stability was monitored over 48 hours. **28**-PDLLA<sub>10</sub> was chosen as a suitable model to compare to **12**-PDLLA<sub>20</sub>, as they both featured similar zeta potentials (-31 mV and -40 mV, respectively), indicating a good degree of stability. A *t*<sub>0</sub> measurement showed that both samples formed nanoparticles upon dissolution in PBS, as expected. After 24 hours, both samples appeared stable, with no change to the nanoparticle sizes or distributions when measured by DLS (**Figure 46**). However, at 48 hours after dissolution, the **28**-PDLLA<sub>10</sub> sample began to show evidence of agglomeration and aggregation, with large changes in the particle sizes and size distribution. Alternatively, the **12**-PDLLA<sub>20</sub> sample did not feature any signs of nanoparticle breakdown, with the sample appearing to remain stable over this time (**Figure 46**).<sup>176</sup>

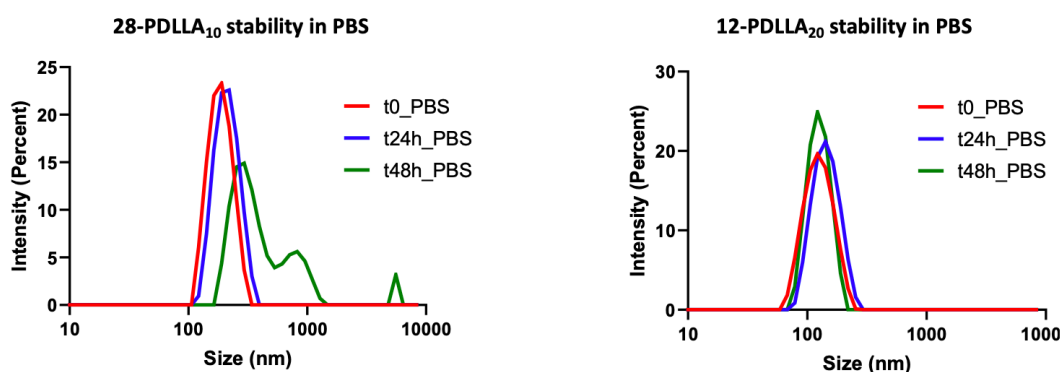


**Figure 46.** Stability profiles of **28**-PDLLA<sub>10</sub> (left) and **12**-PDLLA<sub>20</sub> (right) in PBS at 0.5 mg·mL<sup>-1</sup> over 0, 24 and 48 hours.<sup>176</sup>

The extra stability of the **12**-PDLLA<sub>20</sub> sample was thought to be a result of the better amphiphilic balance of these oligomers, as a consequence of both the longer hydrophobic polyester chain, as well as, critically, a more hydrophilic terpenoid head-group. The head group is considered critical in terms of the stability of the nanoparticles formed, as it is the interactions between the corona of the particles and the ionic strength of the medium which will induce agglomeration and disaggregation processes. It is

hypothesised that the tertiary hydroxyl group of **12** (and the overall, unusual hydrophilic nature of this molecule) contributes to better, more-stable interactions with PBS, allowing for the generation of stable nanoparticles. Importantly, PBS is a media which mimics biological environments, suggesting that the oligomers and their colloidal formulations may have applications as biological surfactants.<sup>176</sup>

### 2.3.6 Cytocompatibility Evaluation

Investigations into the colloidal properties of the oligomers suggested that these bio-based surfactants may have applications in biological or biomedical fields. However, in order for a material to have a practical use in biological applications, it is imperative that its cytocompatibility be determined; this is of paramount importance for a new material in determining if it will go on to have safe clinical use.<sup>117,188</sup> As such, a preliminary cytocompatibility screening of each oligomer was conducted using two *in vitro* assays, one to measure the metabolic activity of the cells following their exposure to the oligomers, and one which assesses plasma membrane disruption. Three human cell lines were investigated: lung epithelial cells (A549), skin epithelial cells (A431) and intestinal epithelial cells (Caco-2), in order to give a representation of the compatibility of the oligomers following exposure *via* inhalation, skin-contact and ingestion, respectively.

Cellular metabolic activity was measured by means of the Presto Blue cell viability assay. Each oligomer sample was dissolved in cell culture medium (DMEM) containing 10% FBS, and exposed to each cell line for 48 hours. A vehicle control containing no nanoparticles (DMEM only) was used as a negative control, while the commercial surfactant Triton X100 (TX) applied at 1% v/v was used as the positive control to induce cell death.

After 48 hours, each of the particles showed no significant decrease in cellular metabolic activity, indicating no major toxicity (**Figure 47A**).<sup>176</sup>

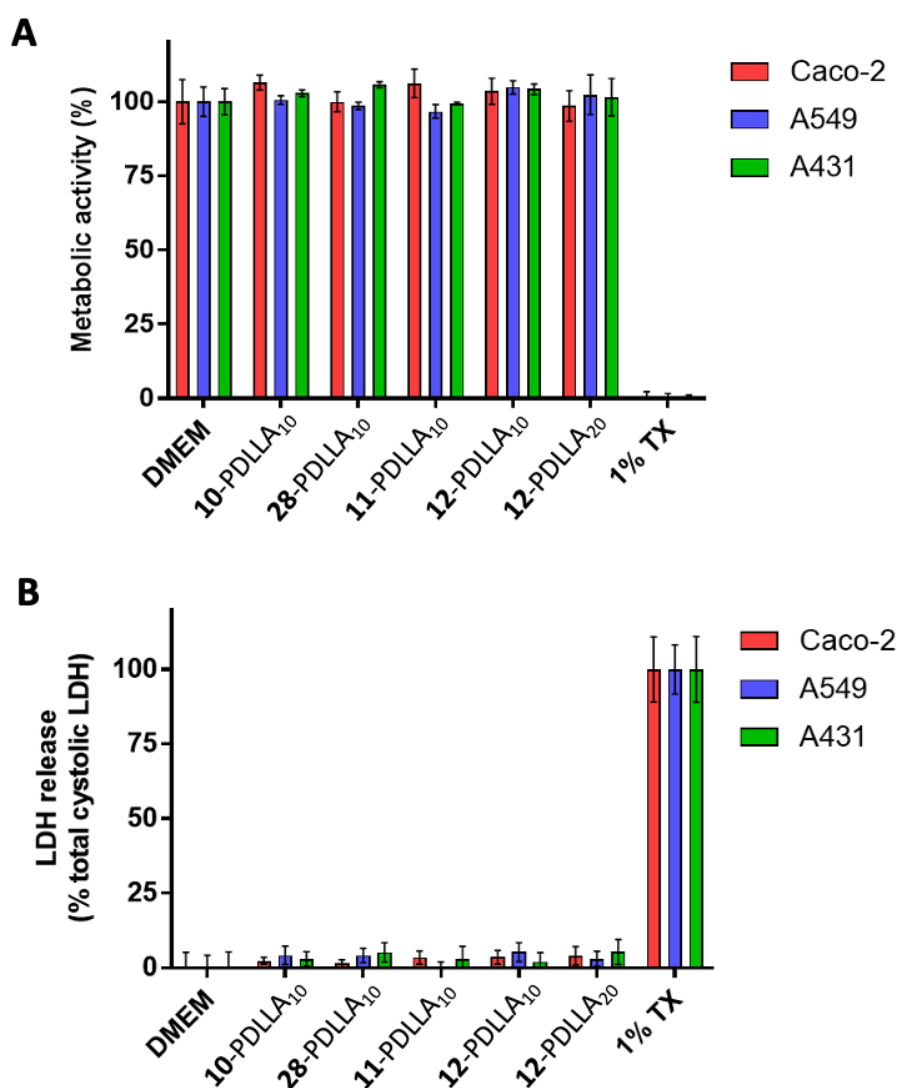


**Figure 47.** Cytocompatibility of nanoparticles on Caco-2 (intestinal), A549 (airway) and A431 (skin) epithelial cells. Cytotoxicity was determined by PrestoBlue metabolic activity (top, graph A) and LDH release as an indicator of membrane damage (bottom, graph B). DMEM treatment represents the vehicle control and Triton X-100 (TX) applied at 1% v/v was used as the cell death control. Data are presented as mean  $\pm$  S.D ( $n=3$ ).<sup>176</sup>

In addition to the PrestoBlue metabolic activity assay, cytotoxicity of the oligomers was also investigated by means of a lactate dehydrogenase (LDH) release assay, which is used to assess membrane damage



(**Figure 47B**). LDH is a ubiquitously present cytosolic enzyme in cells that is released into the cell culture medium upon substantial damage to the cell plasma membrane.<sup>189</sup> The extracellular LDH can then be detected by a coupled enzymatic reaction in which NAD<sup>+</sup> is reduced (by LDH) to NADH, which in turn acts as a reducing agent of a tetrazolium salt, resulting in a red formazan salt which can be measured spectrophotometrically. The amount of formazan salt present is directly proportional to the amount of LDH that has been released into the cell medium as a result of membrane damage.<sup>189</sup> This kind of cell damage is highly relevant for surfactants, which are known for causing membrane associated effects, such as disruptions in membrane fluidity, increases in membrane permeability and lysis.<sup>190-193</sup>

In the case of all five oligomer-based nanoparticles, no substantial membrane damage was observed using this assay, with only negligible levels of LDH present in the extracellular medium with respect to the controls (**Figure 28B**).<sup>176</sup>

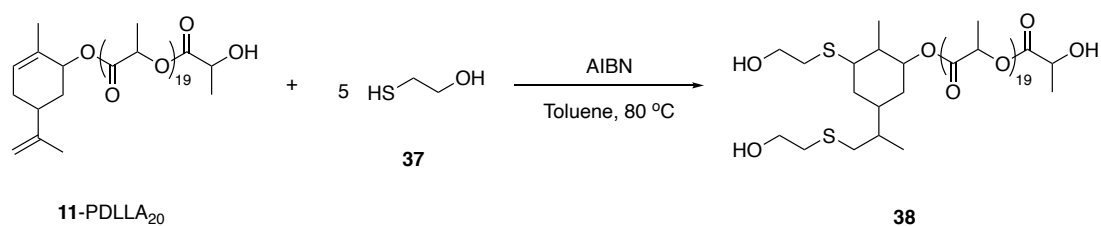
The absence of cytotoxicity, as demonstrated by both the cellular metabolic activity and membrane-disruption assays, indicates the materials can be considered cytocompatible, which is a good indication for their potential to be biocompatible *in vivo*. This, combined with the well-known biodegradability of PLA-based polymers, shows promising potential for the use of these materials as carriers in biomaterials or biomedical applications, including drug delivery, even in the absence of conjugation to another hydrophilic moiety.

### 2.3.7 Alkene functionalisation

The initial aim of using terpenes as initiators for the ROP of lactide was to provide the highly versatile and useful biocompatible polyester with an anchor from which the polymer could be easily functionalised. Commonly in the literature, PLA is functionalised or co-polymerised with PEG or a similar hydrophile to enable self-assembly, encapsulation of cargo within a hydrophobic core, and stealth-like behaviour *in vivo*.<sup>132,194</sup> In some respects, the discovery of the surfactant behaviour of the terpenoid-

functionalised oligomers removes the need for a hydrophile to be conjugated to the PDLLA chain, as this hydrophilic character is at least in part already bestowed onto the oligomer. Nonetheless, this conjugation might be important for other functional groups and compounds to be added to the polymer chain. Weems *et al.* demonstrated that the alkene functionalities of a number of terpenes could be exploited using thiol 'click' chemistry, employing a relatively facile and green reaction. This method was used to generate terpene-based resins for 3D printed thermosets.<sup>167</sup> Using an alternative method, the Meier group conducted a variety of thiol-click reactions on a various terpenes including limonene, showing that both the mono-addition and di-addition products could be made.<sup>66</sup>

It was decided to briefly investigate that the alkene moieties of the terpenoid oligomers were available to these kinds of reactions, by investigating the reaction of **11**-PDLLA<sub>10</sub> oligomer with 2-mercaptoethanol, **37** (Scheme 19).



**Scheme 19.** Proposed conjugation of 2-mercaptoethanol (**37**) to the **11**-PDLLA<sub>10</sub> terpenoid-initiated oligomer.

The conditions used were similar to those developed by the Meier group. In their paper, it is reported that in a reaction with limonene, 2.5 equivalents of **37** resulted in a 36% yield of the mono-addition product at the exocyclic alkene, and a 62% yield of the di-adduct. The two products were then separated and purified by column chromatography.<sup>66</sup> The terpenoid head group of **11**-PDLLA<sub>10</sub> is structurally very similar to limonene (despite being derived from carveol), and so in an effort to overcome this moderate 62% yield for the di-adduct, 5 equivalents (rather than 2.5) of **37** were used. The reacting components were stirred in toluene with AIBN at 80 °C for 24 hours, after which time the sample was studied by NMR. At

first glance, it was apparent that the reaction had not gone to completion, as the resonances of both alkene functionalities were still visible in the  $^1\text{H}$  NMR spectrum after 24 hours. However, upon investigating the ratios between the resonances, it became clear that the reaction was proceeding to a certain extent.

The analysis was complicated somewhat by the fact that the carveol terpenoid (**11**) used to generate **11**-PDLLA<sub>10</sub> was present as two isomers, and so two distinct resonances are present for the endocyclic alkene (one from each isomer), as well as two overlapping ones for the exocyclic alkene. Additionally, a very broad resonance is observed for the C-H proton in the backbone of the PDLLA oligomer (**Figure 48**). This is characteristic of PLA, though it complicates the analyses in this instance where more than one polymer product is present.

In order to analyse the success of the thiol click reaction, the ratio of alkene-to-polymer resonances were investigated. It was found that in the  $t_0$  sample (i.e. just before the reaction began, at time-zero), the endocyclic alkene was integrated to 14.35, while the exocyclic one was 12.18, when entirety of the broad polymer resonance was set to integrate to 100 (**Figure 48**). By comparison, after 24 hours, this ratio moved to just 5.62 : 100 : 7.48, for the endocyclic alkene : PDLLA oligomer : exocyclic alkene, respectively (**Figure 48**). This ratio shows that there has been a decrease in the alkene resonances with respect to the oligomer chain, indicating that although the reaction evidently did not go to completion after 24 hours, nonetheless the reaction does proceed. Unusually, this analysis indicates that the endocyclic alkene is depleting faster than the exocyclic one (a decrease of 61% and 39% is observed, respectively). However, this is likely not a true result, as the polymers (unreacted **11**-PDLLA<sub>10</sub> and **38**) are not isolated from one another, and so it is not possible to accurately conclude the true ratios or values of each resonance.

However, the depletion of the alkene resonances with respect to the oligomer backbone is evidence that the reaction does proceed, and while optimisation would be required to use this thiol-click chemistry to functionalise the alkene moieties effectively, it has been shown that the oligomers do have the potential to react in this way.

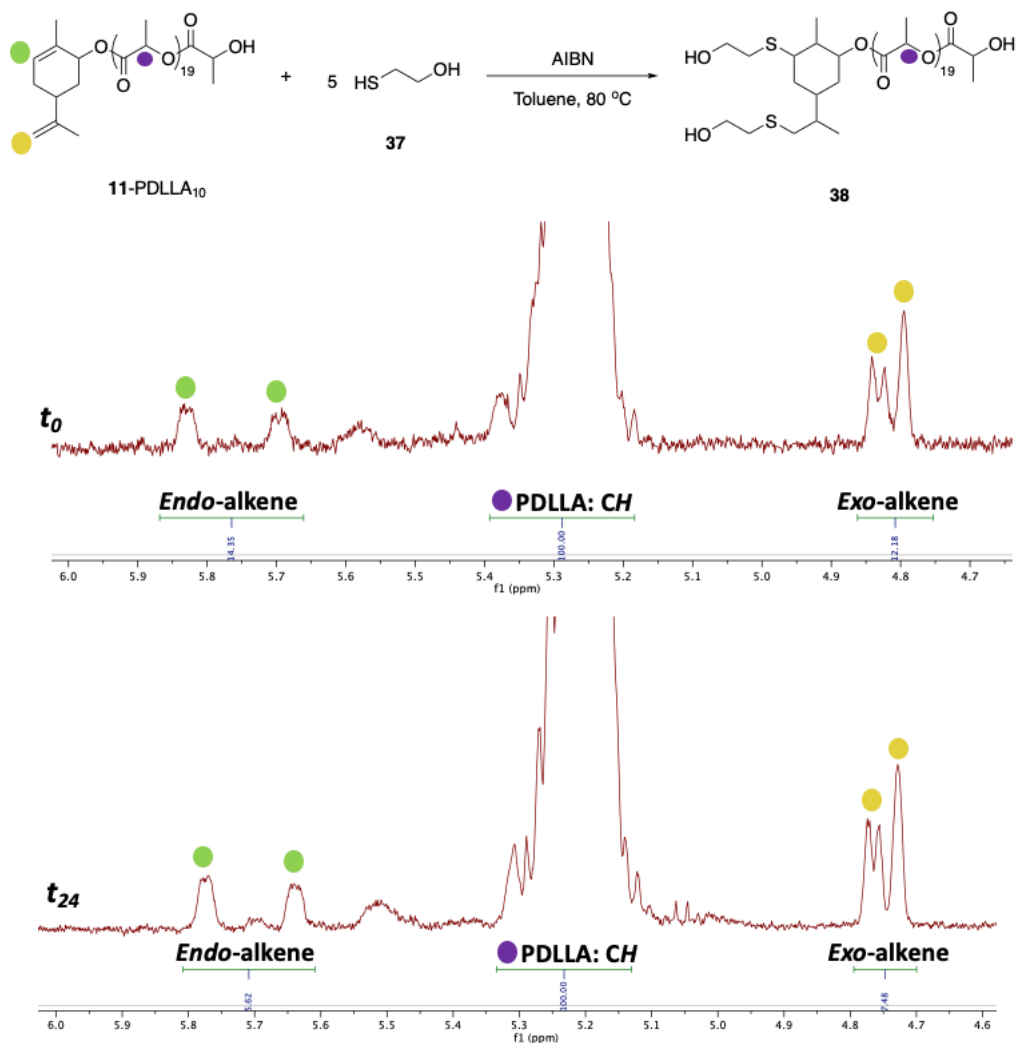
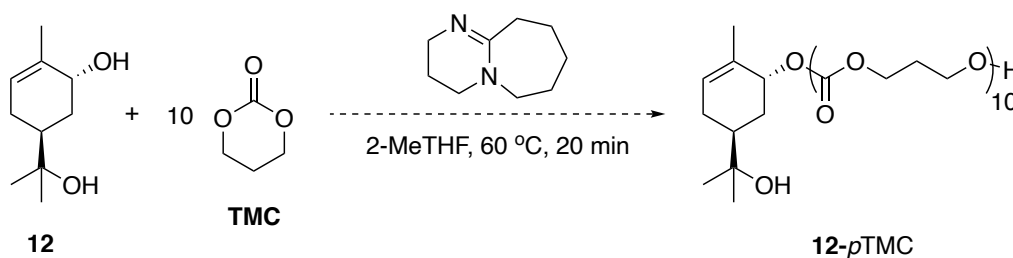


**Figure 48.** <sup>1</sup>H NMR spectra showing the reaction of mercaptoethanol (**37**) with **11**-PDLLA<sub>10</sub>. The top spectrum shows the reaction just before it began (i.e. *t*<sub>0</sub>), in which the ratio of endocyclic alkene : PDLLA-CH : exocyclic alkene is 14.35 : 100 : 12.18. The bottom spectrum ratio is 5.62 : 100 : 7.48 for the same resonances, indicating the depletion of both alkene moieties in the reaction.

### 2.3.8 Green ROP of Trimethylcarbonate (TMC)

In a bid to highlight the full utility and lack of limitations of the fully-green ROP reaction conditions, it was aimed to demonstrate that these conditions could be used to generate other polymers beyond PDLLA. As such, it was aimed to use the same conditions with an alternative monomer: trimethylcarbonate (TMC).

TMC is a popular cyclic monomer which can be considered bio-based, since the material used to make it (1,3-propanediol) can be derived from carbohydrates.<sup>195</sup> Like PLA, polymers of TMC are also biocompatible, a fact which has resulted in extensive studies of its use in biomaterials, in particular as a hydrophobic block for aliphatic drug-delivery scaffolds.<sup>196</sup> As with lactide, both conventional organometallic catalysts and emerging organocatalysts have been used to bring about polymerisation, as the monomer undergoes ROP to form aliphatic polycarbonates.<sup>136,195</sup> However, unlike PLA, TMC is a carbonate monomer (not a lactone), and so the polymers it makes are polycarbonates rather than polyesters. As a result, TMC based materials have been found to be more resistant to non-enzymatic hydrolysis (the process is much slower for carbonates),<sup>197</sup> allowing for its use in a wealth of applications that are not available to aliphatic polyesters such as PLA.<sup>195</sup> The carbonate monomer will also have a different reactivity profile to a lactone monomer, making it a suitable alternative with which to investigate the scope of the green ROP conditions.



**Scheme 20.** Proposed polymerisation of TMC using 'fully green' ROP conditions.

As such, it was aimed to form oligomers of *trans*-sobrerol initiated-poly-TMC (**12-pTMC**) in an analogous reaction to those formed from lactide

(**12**-PDLLA<sub>10</sub>). This meant employing **12** as the initiator species in a reaction with 10 equivalents of monomer in 2-MeTHF at 60 °C (**Scheme 20**). The reaction was conducted in the usual way, and was stopped after 20 minutes by exposing the reaction to air and precipitating into cold hexane. Analysis by <sup>1</sup>H NMR found that while there was unreacted monomer present in the final sample, most of the monomer was successfully converted to polymer, corresponding to a degree of polymerisation of 60% (DP=6) (**Figure 49**).

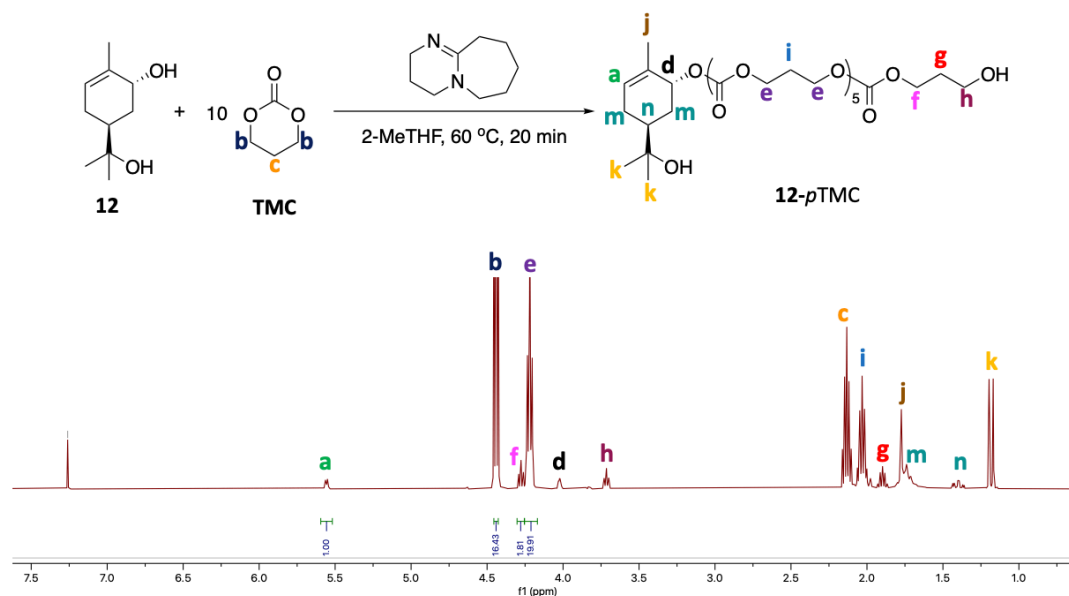


**Figure 49.** <sup>1</sup>H NMR spectrum showing the conversion of TMC to **12-pTMC**, using the terpenoid **12** as an initiator in green ROP conditions.

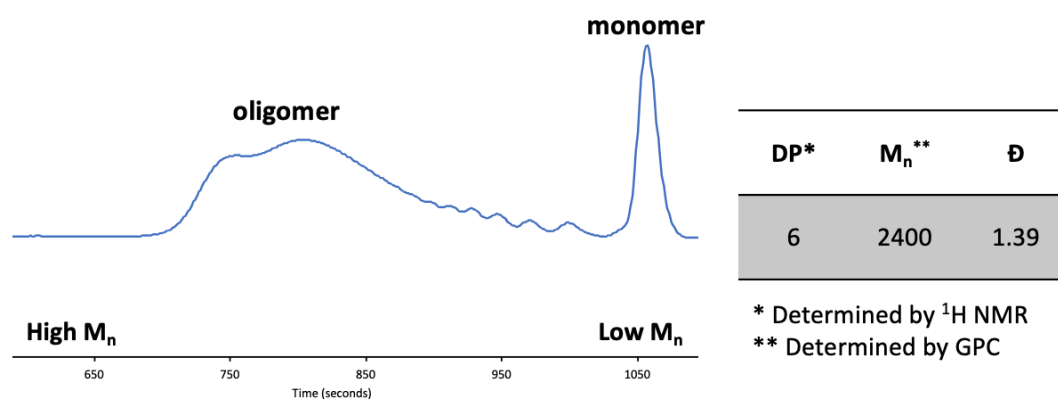
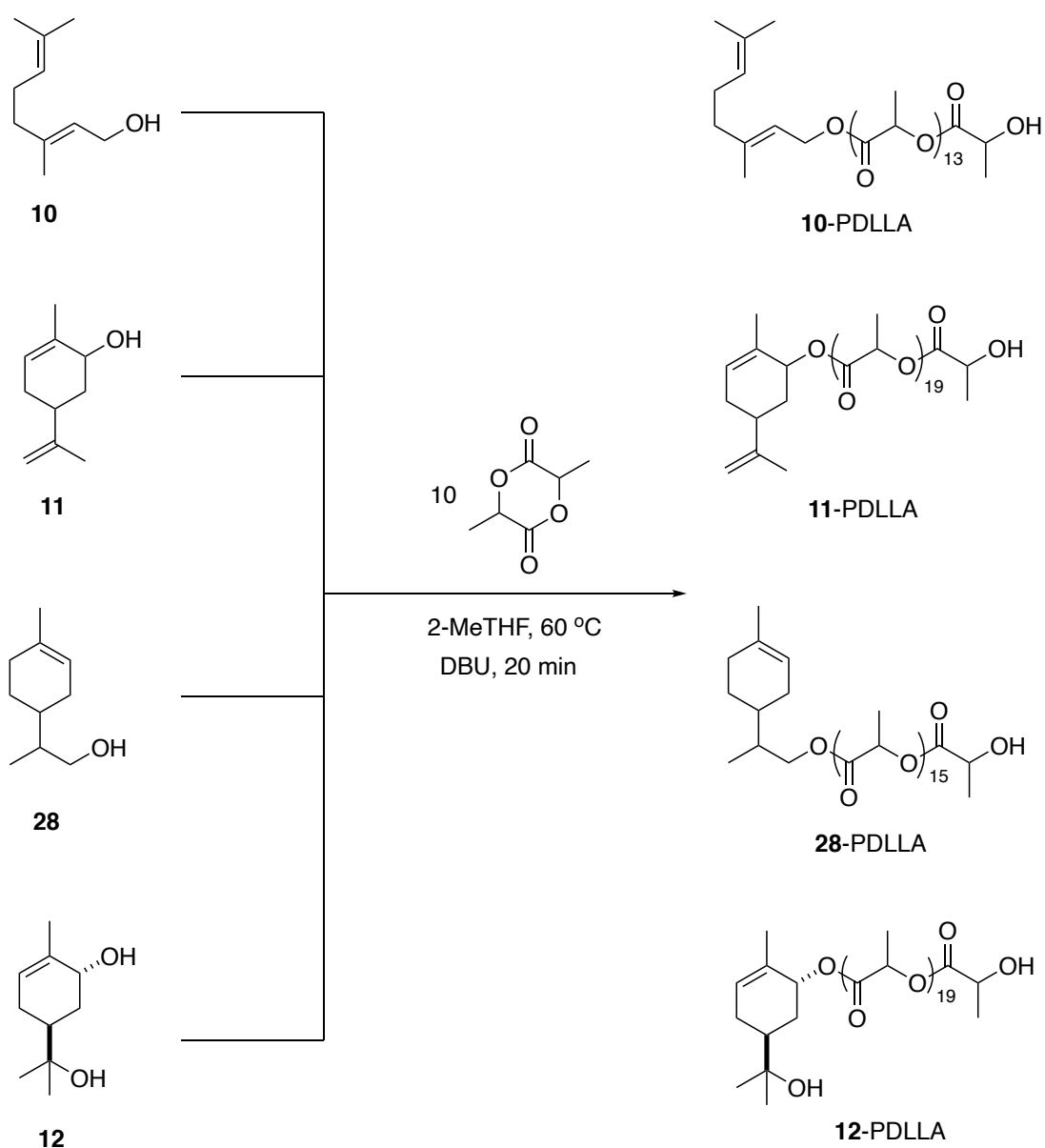


**Figure 50.** GPC chromatogram and corresponding data from the polymerisation of TMC using the green ROP conditions.

GPC analysis also confirmed the conversion of monomer to polymer, with a molecular weight ( $M_n$ ) of  $2400 \text{ g}\cdot\text{mol}^{-1}$  (compared to PDLLA standards), albeit with a slightly larger dispersity to that of the PDLLA oligomers, of 1.39 (**Figure 50**). However, this is a good result: the ROP mechanism is optimally used for the production of long polymers, with short-chain oligomers being harder to synthesise in this method.<sup>131</sup> 10 equivalents of monomer corresponds to only ten repeat units in the oligomer, which is difficult to achieve. Additionally, given the different reactivities of carbonates and esters, these conditions are not optimised for this type of polymerisation, and it would not be taken for granted that lactide and TMC monomers would react in the same way. While optimisation of this reaction would be required, a conversion of 60% and a dispersity of 1.39 can therefore be considered a positive preliminary result for oligomers of TMC synthesised in this method.

## 2.4 Conclusions

Four terpenoids were successfully employed as initiators in the ROP of rac-lactide, to generate a set of monodisperse PDLLA oligomers with terpenoid head groups, in good conversion. This was achieved in a way which adheres well with the concept of a circular economy and the 12 principles of green chemistry, employing bio-renewable solvents and catalysts (**Scheme 21**).



**Scheme 21.** The structures of the four terpenoid-initiated PDLLA<sub>10</sub> oligomers synthesised using fully-sustainable, green conditions.



It was shown that when 2-MeTHF was employed as the solvent, at 60 °C all reacting components could be dissolved and the reaction could take place to the same extent and quality as when DCM was employed. This is significant in terms of the sustainability of the reaction as 2-MeTHF is bio-based and renewable, but additionally, DCM is very toxic, so 2-MeTHF is a preferred alternative for a variety of applications such as polymers for biomaterials. One of the terpenoid head-groups that was employed, **12**, is completely insoluble in DCM, and so the switch to the bio-based solvent allowed for the generation of **12**-initiated PDLLA oligomers, which was significant in terms of the properties of the oligomers. Furthermore, the organobase DBU was successfully employed as a catalyst, avoiding the need for toxic metal-based alternatives.

Each of the four oligomers were found to self-assemble in water, producing well-defined nanoparticles *via* the nanoprecipitation method, without the need for additional stabilisers. This was determined using both DLS and zeta-potential analyses. To further demonstrate the robustness of the reaction conditions, and to probe the effect of the hydrophobic/hydrophilic balance of the oligomers on the overall physical properties, a 20-lactide oligomer was synthesised using the terpenoid **12**. In this instance it was shown that the reaction proceeded in a 100% conversion, resulting in a PDLLA oligomer with double the length of the hydrophobic chain to those synthesised previously, conjugated to the hydrophilic *trans*-sobrerol head group. It was then demonstrated that the amphiphilic balance of the bio-based surfactant was indeed altered by this longer hydrophobic chain: this **12**-PDLLA<sub>20</sub> surfactant resulted in smaller NPs of approximately 100 nm, and smaller CMCs of only 70 µg mL<sup>-1</sup>, which is comparable to marketable surfactants.<sup>176</sup> Additionally, these surfactants were found to be stable over a 48 hour period, and were shown to be more stable than the **28**-PDLLA<sub>10</sub> sample over this same timeframe, likely due to the extra hydrophilicity bestowed by the hydrophilic **12** head group.

Both LDH and PrestoBlue cell viability assays found that each of the bio-based surfactants were devoid of any major toxicity in three cell lines, indicating that there is possible applications for these materials in biomaterials such as drug delivery systems. Additionally, it was determined that the alkene functionalities of each of the terpenoids was retained in the

structure of each oligomer, confirmed by NMR and IR spectroscopy. In a brief study to investigate the functionalisation of these groups, it was shown that although the reaction would require optimisation, these alkenes are responsive to thiol-click chemistry, allowing for further functionalisation of the materials for specific applications.

Finally, the sustainable, 'green' ROP conditions were expanded for use with other types of monomers: when the bio-renewable solvent 2-MeTHF was employed alongside DBU as a catalyst, the terpenoid **12** was found to successfully initiate the polymerisation of TMC, a carbonate monomer. This resulted in bio-based and bio-degradable polycarbonate oligomers of 2400 g·mol<sup>-1</sup> (by GPC), corresponding to conversions of 60% and degrees of polymerisation of 6 (by NMR).

Ultimately, it has been demonstrated that monoterpenes (of a variety of chemical structures and features) can be considered a tool-box of renewable and highly functionalisable small-molecule initiators for ROP. Furthermore, these ROP reactions have been modified so that they align with the concept of the circular economy and the 12 principles of green chemistry,<sup>13</sup> which is of ever-increasing importance considering the environmental challenges of a growing, world-wide dependence on polymer and plastic materials.<sup>3</sup>

## 2.5 Experimental

### 2.5.1 *General Materials and Methods*

#### Materials

All reagents were purchased from a chemical supplier and used without further purification. Water was deionised before use. Dry solvents were obtained from solvent drying towers and contained <17 ppm of water. TLCs were performed on silica gel mounted on aluminium and visualised using potassium permanganate with gentle heating. Experiments carried out using inert conditions employed nitrogen by means of a Schlenk line, or an argon balloon.

#### Analytical Techniques

**<sup>1</sup>H NMR spectra** were recorded in deuterated chloroform (CDCl<sub>3</sub>) at 25°C, with Bruker 400 MHz spectrometers.

**<sup>13</sup>C NMR spectra** were recorded in CDCl<sub>3</sub> on 100 MHz spectrometers. <sup>1</sup>H NMR chemical shifts ( $\delta$ ) were recorded in parts per million (ppm), with the shift of CHCl<sub>3</sub> ( $\delta$  = 7.26 ppm) as the internal standard when CDCl<sub>3</sub> was used. <sup>13</sup>C NMR chemical shifts were reported using the central line of CHCl<sub>3</sub> ( $\delta$  = 77.0 ppm) when CDCl<sub>3</sub> was used as the internal standard. The following abbreviations are used to designate the multiplicity of each signal; s, singlet; d, doublet; dd, doublet of doublets; dddd, doublet of doublet of doublet of doublets; t, triplet; dt, doublet of triplets; ddt, doublet of doublet of triplets; q, quartet; m, multiplet; app, apparent; br, broad. Couplings (*J*) are given in Hertz (Hz).

**Infra-Red spectra** were carried out using a Bruker Tensor 27 using an ATR attachment and peaks are quoted as  $\nu_{\max}$  in cm<sup>-1</sup>.

**High Resolution Mass Spectrometry** was conducted using a Bruker MicroTOF spectrometer operating in electrospray ionisation (ESI) mode.

**Gel Permeation Chromatography (GPC)** was performed in THF (HPLC grade, Fisher Scientific) as the eluent at room temperature using two Agilent PL-gel mixed-E columns in series with a flow rate of 1 mL min<sup>-1</sup>. A

differential refractometer (DRI), was used for sample detection. The system was calibrated using polycaprolactone standards.

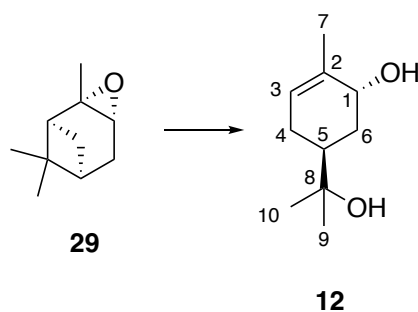
**Differential scanning calorimetry (DSC)** was used to determine the glass transition temperature ( $T_g$ ) of the polymers produced. The analysis was performed on a TA-Q2000 (TA instruments), which was calibrated with an indium standard under N<sub>2</sub> flow. The sample (1–3 mg) was weighed into a T-zero sample pan (TA instruments) with a reference T-zero pan remaining empty. Both pans were heated at a rate of 10 °C min<sup>-1</sup>, from –90 °C to 120 °C for all samples. To remove any thermal history of the individual samples two heating cycles were recorded with the  $T_g$  being measured from the second cycle.

**Dynamic mechanical analysis (DMA)** was used to determine the  $T_g$  of the polymers. Measurements were performed on a Triton Technologies DMA (now Mettler Toledo DMA1) using the powder pocket accessory. The sample (40 mg ± 5 mg) was weighed into a powder pocket. Samples were measured at 1 and 10 Hz in single cantilever bending geometry between –50–100 °C depending on the region of interest. The value of the  $T_g$  was taken as the peak of the tan delta (tan  $\delta$ ) curve.

**Water Contact Angle (WCA)** values were recorded at 25 °C by means of a KSV Cam 200 (KSV Instruments Ltd., Helsinki, Finland). Samples were prepared by solvent casting of polymer in acetone solutions, at 5 mg·mL<sup>-1</sup>, on cover slips. Polymer-coated slides were mounted horizontally on the stand of the instrument. A small drop of distilled water was dispensed by a syringe with a flattened tip needle onto the polymer film. Each droplet was allowed to settle and interact for 5 seconds. The tangent line was recorded using a camera and both shape and contact angle were analysed. Three measurements were repeated for each sample.

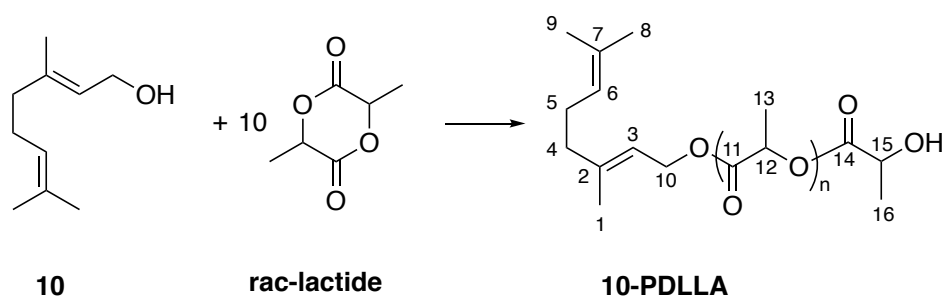
**Dynamic Light Scattering (DLS) and Z-potential:** Particle size analyses were performed by DLS utilizing a Zetasizer Nano spectrometer (Malvern Instruments Ltd) equipped with a 633 nm laser at a fixed angle of 173°. The same instrument was used to measure the Z-potential of the produced NPs. All experiments were performed in triplicate on the same sample.

### 2.5.2 Synthesis of trans-sobrerol (**12**)



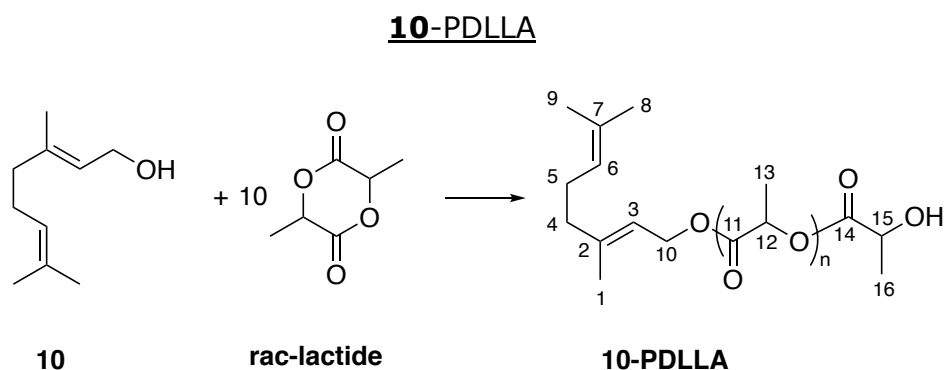
CO<sub>2</sub> was bubbled through water (66 mL) until pH=4 was reached, then  $\alpha$ -pinene oxide (**29**) (5.02 g, 33.03 mmol, 0.5 M) was added dropwise under vigorous stirring. The mixture was stirred overnight for 16 hours, before evaporation of the water under reduced pressure to yield a white solid. This was washed with cold ethyl acetate under Büchner filtration to yield the title compound as a white, crystalline solid (2.62 g, 15.41 mmol, 47%). **FTIR (ATR)**  $\nu_{\max}/\text{cm}^{-1}$  = 3323 (OH), 3006, 2973, 2960, 2933, 2921, 2887, 2652, 1713, 1471, 1442, 1429, 1402, 1376, 1360, 1312, 1294, 1253, 1220, 1183, 1154 (C-O), 1086 (C-O), 1052, 1038, 1027, 1003, 985; **<sup>1</sup>H NMR:** (400 MHz, CDCl<sub>3</sub>)  $\delta_{\text{H}}$  = 5.61 – 5.53 (m, 1H, H-3), 4.04 (t,  $J$  = 3.0 Hz, 1H, H-1), 2.18 – 2.08 (m, 1H, H-4'), 2.05 – 1.98 (m, 1H, H-6'), 1.79 (s, 3H, H-7), 1.77 – 1.67 (m, 2H, H-4'' and H-5), 1.41 (td,  $J$  = 13.2, 3.9 Hz, 1H, H-6), 1.21 (s, 3H, H-10 or H-9), 1.19 (s, 3H, H-10 or H-9); **<sup>13</sup>C NMR** (100 MHz, CDCl<sub>3</sub>)  $\delta_{\text{C}}$  = 134.5 (C-2), 125.5 (C-3), 72.4 (C-8), 68.8 (C-1), 39.0 (C-5), 32.8 (C-6), 27.8 (C-9 or C-10), 27.3 (C-4), 26.6 (C-9 or C-10). **HRMS (ESI<sup>+</sup>)**  $m/z$  [M+Na<sup>+</sup>] calculated for [C<sub>10</sub>H<sub>18</sub>O<sub>2</sub>Na]<sup>+</sup> 193.1204 found 193.1207 (M + Na<sup>+</sup>).

### 2.5.3 Synthesis of **10**-PDLLA using 'conventional' (DCM) method



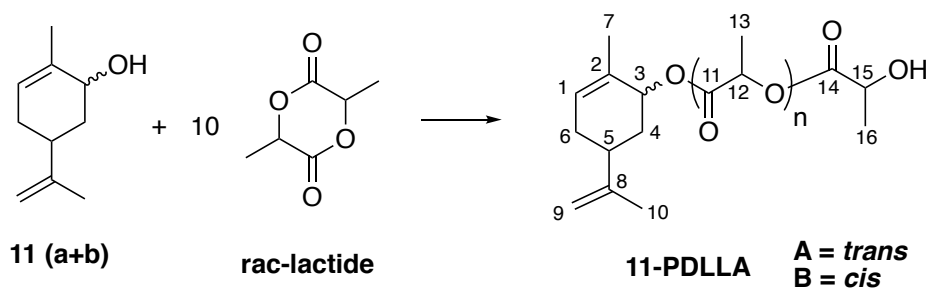
To an oven-dried glass vial charged with dry DCM (7 mL) was added geraniol (**10**) (106.6 mg, 0.69 mmol) and rac-lactide (1.07 g, 6.94 mmol). A  $t_0$  sample was taken for NMR analysis, and DBU was added (20  $\mu$ L, 0.14 mmol). The mixture was stirred at room temperature for 20 minutes before the reaction was stopped by precipitating into cold heptane. After cooling the sample at -20 °C for 2 hours, the heptane was decanted and replaced with Et<sub>2</sub>O. This was cooled to -20 °C for a further 2 hours before the organic solvent was decanted and the solid was dried in a vacuum oven to obtain the final oligomer as a white solid (70% conversion, 5.03 g, 63% yield). Calculated  $M_n$  from NMR: 1300 g·mol<sup>-1</sup>,  $M_n$  from **GPC**: 1650 g·mol<sup>-1</sup> and  $\bar{D}$  1.2. **FTIR (ATR)**  $\nu_{\max}/\text{cm}^{-1}$  = 2992, 2942, 2349, 1750 (C=O), 1650 (C=C), 1454, 1381, 1336, 1306, 1269, 1213, 1183, 1128, 1083 (C-O). **<sup>1</sup>H NMR**: (400 MHz, CDCl<sub>3</sub>)  $\delta_{\text{H}}$  = 5.33 – 5.25 (m, 1H, H-3), 5.20 – 5.12 (m, 6H, H-12), 5.08 – 5.02 (m, 1H, H-6), 4.72 – 4.55 (m, 2H, H-10), 4.38 – 4.30 (m, 1H, H-15), 2.15 – 1.95 (m, 4H, H-4 and H-5), 1.69 – 1.64 (m, 6H, H-9 or H-8, and, H-1), 1.58 – 1.55 (m, 21H, H-13), 1.49 – 1.45 (m, 6H, H-8 or H-9, and, H-16). **<sup>13</sup>C NMR** (100 MHz, CDCl<sub>3</sub>)  $\delta_{\text{C}}$  = 169.7 (C-11), 166.4 (C-14), 143.4 (C-2), 132.0 (C-7), 123.7 (C-6), 117.6 (C-3), 69.1 (C-12), 66.8 (C-15), 62.4 (C-10), 26.3 (C-4 or C-5), 25.8 (C-1), 20.6 (C-16), 19.6 (C-4 or C-5), 16.8 (C-13).

### 2.5.4 'Fully Green' ROP syntheses



To an oven-dried glass vial charged with dry 2-MeTHF (7 mL) was added geraniol (**10**) (107.3 mg, 0.69 mmol) and rac-lactide (1.07 g, 6.94 mmol). The vial was sealed and the mixture was heated to 60 °C, and a  $t_0$  sample was taken for NMR analysis. DBU was added (0.02 mL, 0.14 mmol, 2 mol%) and the reaction was stirred under argon for 20 minutes. The vial was then exposed to air to stop the reaction, and the mixture was precipitated into cold heptane. After cooling for 2 hours at -20 °C, the heptane was decanted and replaced with diethyl ether. This was cooled to -20 °C for a further 2 hours before the organic solvent was decanted and the solid was dried in a vacuum oven to obtain the final oligomer as a white solid (70% conversion, 5.12 g, 64% yield). Calculated  $M_n$  from NMR: 1150 g·mol<sup>-1</sup>,  $M_n$  from **GPC**: 1330 g·mol<sup>-1</sup> and  $\bar{D}$  1.2. **FTIR (ATR)**  $\nu_{\text{max}}$ / cm<sup>-1</sup> = 2992, 2942, 2350, 1750 (C=O), 1650 (C=C), 1453, 1381, 1366, 1307, 1268, 1183, 1127, 1083 (C-O), 1040; **<sup>1</sup>H NMR**: (400 MHz, CDCl<sub>3</sub>)  $\delta_{\text{H}}$  = 5.31 (t,  $J$  = 7.1 Hz, 1H, H-3), 5.23 – 5.12 (m, 6H, H-12), 5.06 (t,  $J$  = 6.8 Hz, 1H, H-6), 4.72 – 4.57 (m, 2H, H-10), 4.43 – 4.24 (m, 1H, H-15), 2.14 – 1.98 (m, 4H, H-4 and H-5), 1.72 – 1.64 (m, 6H, H-8 or H-9, and, H-1), 1.60 – 1.55 (m, 21H, H-13), 1.51 – 1.42 (m, 6H, H-8 or H-9, and H-16). **<sup>13</sup>C NMR** (100 MHz, CDCl<sub>3</sub>)  $\delta_{\text{C}}$  = 169.7 (C-11), 166.3 (C-14), 143.3 (C-2), 132.0 (C-7), 123.7 (C-6), 117.4 (C-3), 69.0 (C-12), 66.7 (C-15), 62.4 (C-10), 26.3 (C-4 or C-5), 25.7 (C-1), 20.5 (C-16), 19.4 (C-4 or C-5), 16.8 (C-13).

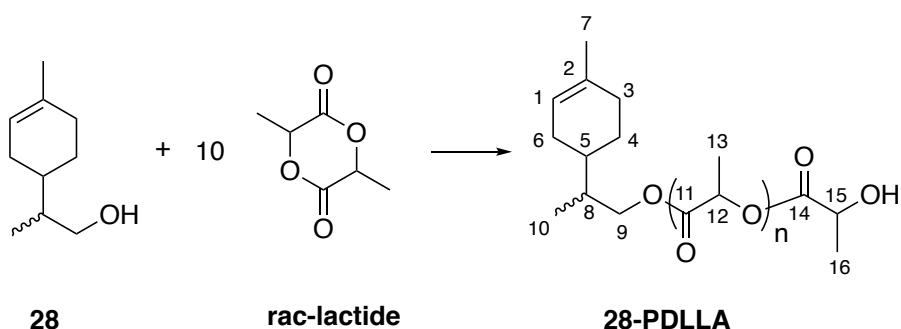
### 11-PDLLA



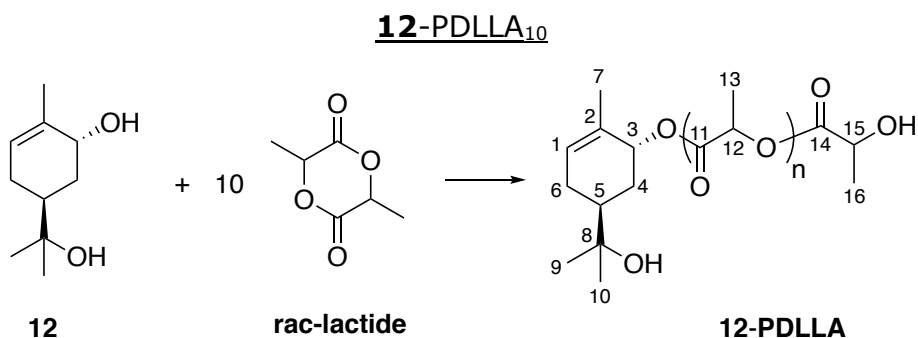
To an oven-dried glass vial charged with dry 2-MeTHF (7 mL) was added (106.7 mg, 0.69 mmol) and rac-lactide (1.12 g, 6.94 mmol). The mixture was heated to 60 °C, and a  $t_0$  sample was taken for NMR analysis. DBU was added (0.02 mL, 0.14 mmol, 2 mol%) and the reaction was stirred under argon for 20 minutes. The vial was then exposed to air to stop the reaction, and the mixture was precipitated into cold heptane. After cooling for 2 hours at -20 °C, the heptane was decanted and replaced with diethyl ether. This was cooled to -20 °C for a further 2 hours before the organic solvent was decanted and the solid was dried in a vacuum oven to obtain the final oligomer as a white solid (100% conversion, 4.86 g, 41% yield). Calculated  $M_n$  from NMR: 1700 g·mol<sup>-1</sup>,  $M_n$  from **GPC**: 2100 g·mol<sup>-1</sup> and  $\bar{D}$  1.2. **FTIR (ATR)**  $\nu_{\max}/\text{cm}^{-1}$  = 2993, 2944, 2335, 2189, 1981, 1750 (C=O), 1648 (C=C), 1452, 1381, 1362, 1267, 1183, 1127, 1082 (C-O), 1046; **<sup>1</sup>H NMR**: (400 MHz, CDCl<sub>3</sub>)  $\delta_H$  = 5.78 – 5.69 (m, 0.5H, H-1A), 5.66 – 5.57 (m, 0.5H, H-1B), 5.47 (s, 0.5H, H-3A), 5.30 – 5.26 (m, 0.5H, H-3B), 5.20 – 5.13 (m, 19H, H-12), 4.80 – 4.62 (m, 2H, H-9), 4.41 – 4.28 (m, 1H, H-15), 2.35 – 1.80 (m, 5H, H-4', H-4'', H-5, H-6' and H-6''), 1.72 – 1.69 (m, 3H, H-10), 1.68 – 1.65 (m, 1.5H, H-7A), 1.64 – 1.61 (m, 1.5H, H-7B), 1.59 – 1.53 (m, 57H, H-13), 1.49 – 1.46 (m, 3H, H-16). **<sup>13</sup>C NMR** (100 MHz, CDCl<sub>3</sub>)  $\delta_C$  = 175.2 (C-14), 169.7 (C-11), 148.5 (C-8), 128.6 (C-2A), 126.7 (C-2B), 109.7 (C-9A) 109.5 (C-9B), 74.8 (C-3A), 72.2 (C-3B), 69.1 (C-12), 66.8 (C-15), 40.3 (C-5A), 35.8 (C-5B), 33.9 (C-4 or C-6), 30.8 (C-4 or C-6), 20.9 (C-7 or C-10 or C-16) 20.6 (C-7 or C-10 or C-16), 20.4 (C-7 or C-10 or C-16), 16.8 (C-13).



## 28-PDLLA

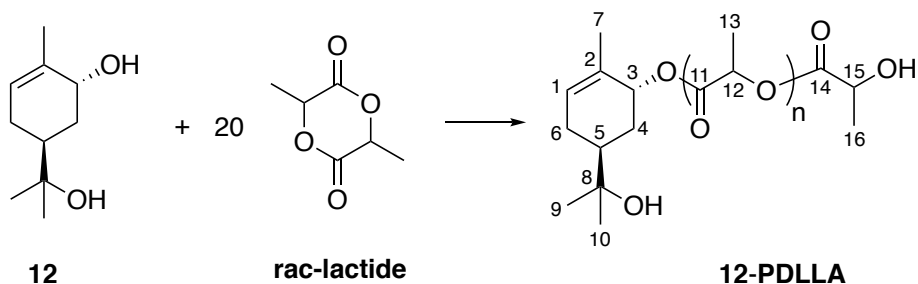


To an oven-dried glass vial charged with dry 2-MeTHF (7 mL) was added limonene-alcohol (**28**) (107.0 mg, 0.69 mmol) and rac-lactide (1.07 g, 6.94 mmol). The vial was sealed and the mixture was heated to 60 °C, and a  $t_0$  sample was taken for NMR analysis. DBU was added (0.02 mL, 0.14 mmol, 2 mol%) and the reaction was stirred under argon for 20 minutes. The vial was then exposed to air to stop the reaction, and the mixture was precipitated into cold heptane. After cooling for 2 hours at -20 °C, the heptane was decanted and replaced with diethyl ether. This was cooled to -20 °C for a further 2 hours before the organic solvent was decanted and the solid was dried in a vacuum oven to obtain the final oligomer as a white solid (80% conversion, 3.83 g, 53% yield). Calculated  $M_n$  from NMR: 1300 g·mol<sup>-1</sup>,  $M_n$  from **GPC**: 1670 g·mol<sup>-1</sup> and  $\bar{D}$  1.2. **FTIR (ATR)**  $\nu_{\max}/\text{cm}^{-1}$  = 2992, 2153, 1750 (C=O), 1649 (C=C), 1545, 1511, 1451, 1380, 1365, 1266, 1182, 1127, 1080 (C-O), 1041; **<sup>1</sup>H NMR**: (400 MHz, CDCl<sub>3</sub>)  $\delta_H$  = 5.38 – 5.29 (m, 1H, H-1), 5.25 – 5.11 (m, 15H, H-12), 4.42 – 4.30 (m, 1H, H-15), 4.21 – 4.07 (m, 1H, H-9'), 4.06 – 3.92 (m, 1H, H-9''), 2.06 – 1.66 (m, 8H, H-3, H-4, H-5, H-6 and H-8), 1.62 (s, 3H, H-7), 1.60 – 1.50 (m, 45H, H-13), 1.50 – 1.43 (m, 6H, H-10 and H-16).



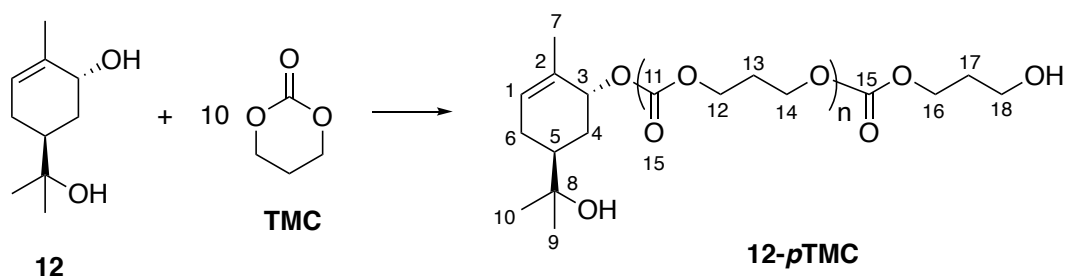
To an oven-dried glass vial charged with dry 2-MeTHF (7 mL) was added *trans*-sobrerol (**12**) (118.5 mg, 0.69 mmol) and rac-lactide (1.03 g, 6.94 mmol). The vial was sealed and the mixture was heated to 60 °C, and a  $t_0$  sample was taken for NMR analysis. DBU was added (0.02 mL, 0.14 mmol, 2 mol%) and the reaction was stirred under argon for 20 minutes. The vial was then exposed to air to stop the reaction, and the mixture was precipitated into cold heptane. After cooling for 2 hours at -20 °C, the heptane was decanted and replaced with diethyl ether. This was cooled to -20 °C for a further 2 hours before the organic solvent was decanted and the solid was dried in a vacuum oven to obtain the final oligomer as a white solid (100% conversion, 4.94 g, 44% yield). Calculated  $M_n$  from NMR: 1600 g·mol<sup>-1</sup>,  $M_n$  from **GPC**: 2050 g·mol<sup>-1</sup> and  $\bar{D}$  1.2. **FTIR (ATR)**  $\nu_{\max}/\text{cm}^{-1}$  = 3537, 2945, 2171, 2032, 1962, 1750 (C=O), 1650 (C=C), 1452, 1381, 1364, 1267, 1183, 1127, 1082 (C-O), 1046; **<sup>1</sup>H NMR**: (400 MHz, CDCl<sub>3</sub>)  $\delta_{\text{H}}$  = 5.73 (d,  $J$  = 5.4 Hz, 1H, H-1), 5.24 – 5.11 (m, 19H, H-12), 5.09 – 5.01 (m, 1H, H-3), 4.38 – 4.30 (m, 1H, H-15), 2.23 – 2.10 (m, 1H, H-6'), 2.04 – 1.95 (m, 1H, H-4'), 1.85 – 1.77 (m, 1H, H-6''), 1.66 (m, 3H, H-7), 1.59 – 1.51 (m, 57H, H-13), 1.48 – 1.44 (m, 3H, H-16), 1.43 – 1.39 (m, 1H, H-4''), 1.19 – 1.16 (m, 3H, H-9 or H-10), 1.15 – 1.13 (m, 3H, H-9 or H-10). **<sup>13</sup>C NMR** (100 MHz, CDCl<sub>3</sub>)  $\delta_{\text{C}}$  = 175.3 (C-14), 169.7 (C-11), 130.4 (C-2), 128.8 (C-1), 72.6 (C-3), 72.0 (C-8), 69.1 (C-12), 66.8 (C-15), 39.7 (C-5), 29.8 (C-4), 27.6 (C-9 or C-10), 27.0 (C-6), 26.4 (C-9 or C-10), 20.6 (C-7 or C-16), 20.4 (C-7 or C-16), 16.7 (C-13).

### 12-PDLLA<sub>20</sub>



To an oven-dried glass vial charged with dry 2-MeTHF (7 mL) was added *trans*-sobrerol (**12**) (61.6 mg, 0.35 mmol) and rac-lactide (1.03 g, 6.94 mmol). The vial was sealed and the mixture was heated to 60 °C, and a  $t_0$  sample was taken for NMR analysis. DBU was added (0.02 mL, 0.14 mmol, 2 mol%) and the reaction was stirred under argon for 20 minutes. The vial was then exposed to air to stop the reaction, and the mixture was precipitated into cold heptane. After cooling for 2 hours at -20 °C, the heptane was decanted and replaced with diethyl ether. This was cooled to -20 °C for a further 2 hours before the organic solvent was decanted and the solid was dried in a vacuum oven to obtain the final oligomer as a white solid (100% conversion, 7.76 g, 37% yield). Calculated  $M_n$  from NMR: 3050 g·mol<sup>-1</sup>,  $M_n$  from **GPC**: 2200 g·mol<sup>-1</sup> and Đ 1.2. **FTIR (ATR)**  $\nu_{\max}/\text{cm}^{-1}$  = 3537, 2947, 2171, 2033, 1750 (C=O), 1650 (C=C), 1451, 1380, 1364, 1266, 1182, 1127, 1082 (C-O), 1046; **<sup>1</sup>H NMR**: (400 MHz, CDCl<sub>3</sub>)  $\delta_H$  = 5.74 (d,  $J$  = 5.5 Hz, 1H, H-1), 5.22 – 5.13 (m, 39H, H-12), 5.05 – 5.01 (m, 1H, H-3), 4.41 – 4.30 (m, 3H, H-15), 1.80 – 1.64 (m, 5H, H-4, H-5, H-6), 1.62 – 1.51 (m, 117H, H-13), 1.51 – 1.35 (m, 6H, H-7 and H-16), 1.20 – 1.11 (m, 6H, H-9 and H-10). **<sup>13</sup>C NMR** (100 MHz, CDCl<sub>3</sub>)  $\delta_C$  = 177.1 (C-14), 169.5 (C-11), 130.7 (C-2), 127.8 (C-1), 71.9 (C-3), 72.0 (C-8), 69.2 (C-12), 66.8 (C-15), 39.5 (C-5), 29.3 (C-4), 27.6 (C9 or C10) 27.2 (C-6), 26.4 (C-9 or C-10), 20.5 (C7 or C-16), 20.3 (C-7 or C16), 16.8 (C-13).

## 12-pTMC



To an oven-dried vial charged with dry THF (7 mL) was added *trans*-sobrerol (**12**) (85.8 mg, 0.49 mmol) and TMC (0.50 g, 4.9 mmol). The vial was sealed and the mixture was heated to 60 °C, and a  $t_0$  sample was taken for NMR analysis. DBU was added (0.02 mL, 0.14 mmol, 2 mol%) and the reaction was stirred under argon for 20 minutes. The vial was then exposed to air to stop the reaction, and the mixture was precipitated into cold heptane. After cooling for 2 hours at -20 °C, the heptane was decanted and replaced with diethyl ether. This was cooled to -20 °C for a further 2 hours before the organic solvent was decanted and the solid was dried in a vacuum oven to obtain the final oligomer as a white solid (60% conversion). Calculated  $M_n$  from **GPC**: 2400 g·mol<sup>-1</sup> and  $\bar{D}$  1.39. **FTIR (ATR)**  $\nu_{\max}/\text{cm}^{-1}$  = 3328 (OH), 2972, 1732 (C=O), 1459, 1404, 1361, 1331, 1220, 1145, 1119, 1027; **<sup>1</sup>H NMR**: (400 MHz, CDCl<sub>3</sub>)  $\delta_H$  = 5.56 (dt,  $J$  = 5.9, 1.7 Hz, 1H, H-1), 4.28 (t,  $J$  = 6.2 Hz, 2H, H-16), 4.22 (td,  $J$  = 6.3, 2.1 Hz, 20H, H-12 and H-13), 4.04 – 3.99 (m, 1H, H-3), 3.71 (t,  $J$  = 6.0 Hz, 2H, H-18) 2.04 (m, 10H, H-13), 1.99 – 1.96 (m, 1H, H-4'), 1.90 (p,  $J$  = 6.1 Hz, 2H, H-17), 1.78 (m, 3H, H-7), 1.72 (m, 3H, H-2 and H-3) 1.40 (td,  $J$  = 13.2, 3.9 Hz, 1H, H-4''), 1.20 (s, 3H, H-9 or H-10), 1.17 (s, 3H, H-9 or H-10). **<sup>13</sup>C NMR** (100 MHz, CDCl<sub>3</sub>)  $\delta_C$  = 155.4 (C-15), 155.0 (C-11), 134.5 (C-2), 125.4 (C-1), 72.3 (C-6), 68.7 (C-3), 65.7 (C-16), 68.0 (C-12 and C-14), 65.3 (C-16), 64.4 (C-13), 59.0 (C-18), 38.9 (C-5), 32.78 (C-4), 31.7 (C-17), 28.1 (C-13), 27.7 (C-9 or C-10), 27.2 (C-6), 26.5 (C-9 or C10), 20.9 (C-7).

### *2.5.5 Nanoparticle Preparation and Stability Assay*

The polymeric nanoparticles (NPs) were formed *via* the nanoprecipitation method. More precisely, 1 mL of acetone solution containing 10 mg of polymer was added to 10 mL of HPLC filtered water under constant stirring (550 rpm). The water/acetone uncapped solutions were gently stirred over-night in order to facilitate acetone evaporation. Particle size analyses was then determined using DLS as described in the analytical techniques section. Stability tests were performed by diluting the NP suspensions with PBS and monitoring the variations in sizes via DLS in a period of 48 hours.

### *2.5.6 Critical Aggregation Concentration (CAC) calculation*

The Critical Aggregation Concentration (CAC) was calculated using a Zetasizer Nano ZS as described in Malvern application note AN101104. A constant attenuator was selected and the count rate in kcps of the scattered light was monitored for a range of diluted NP suspensions (1000–2.00  $\mu\text{g mL}^{-1}$ ). The intensity increases linearly with concentration above the CAC, while below the CAC the count rates reach a plateau. The CAC was then calculated by intersecting the two lines.<sup>198</sup>

### *2.5.7 Cell Culture*

Dr. Robert Cavanagh is acknowledged for conducting the cell culture analysis. Caco-2 human adenocarcinomic colon epithelial cells, A549 human adenocarcinomic alveolar epithelial cells and A431 human epidermoid carcinoma cells were obtained from the American Type Culture Collection (ATCC; Manassas, Virginia) and used at passages 30–35, 20–25 and 25–30, respectively. All cells were cultured in DMEM (Sigma-Aldrich) supplemented with 10% (v/v) FBS (Sigma-Aldrich) and 2 mM L-glutamine (Sigma-Aldrich), and at 37 °C with 5% CO<sub>2</sub>.

### 2.5.8 Cytocompatibility Evaluation

Dr. Robert Cavanagh is acknowledged for conducting the cytocompatibility evaluation. The lactate dehydrogenase (LDH) release assay (Sigma Aldrich, TOX7 kit) and PrestoBlue cell viability assay (Thermo Fisher Scientific) were performed to assess nanoparticles behaviour. All cells were seeded at  $1 \times 10^4$  cells per well in 96 well plates and cultured for 24 hours prior to assaying. Nanoparticles were exposed to cells for 48 hours and applied in 100  $\mu$ L phenol red free DMEM containing 10% (v/v) FBS and 2 mM L-glutamine. Triton X-100 (TX) applied at 1% (v/v) applied in phenol red free medium was used as a cell death (positive) control and a vehicle control containing no nanoparticles used as a negative control. Following exposure, 50  $\mu$ L of supernatant was collected per well for analysis of LDH content. Cells were then washed twice with warm PBS and 100  $\mu$ L 10% (v/v) PrestoBlue reagent diluted in phenol red free medium applied per well for 60 min. The resulting fluorescence was measured at 560/600 nm ( $\lambda_{\text{ex}}/\lambda_{\text{em}}$ ). Relative metabolic activity was calculated by setting values from the negative control as 100% and positive control values as 0% metabolic activity. Assessment of LDH release was performed according to the manufacturer's instructions and involved adding 100  $\mu$ L LDH reagent to collected supernatant samples and incubating at room temperature shielded from light for 25 min. Absorbance was then measured at 492 nm. Relative LDH release was calculated with the negative control absorbance at 492 nm taken as 0%, and the positive control, assumed to cause total cell lysis, as 100%.

### 3 Chapter Three: Epoxy-amine oligomers for synergistic antifungal applications

#### 3.1 Introduction: Epoxy-amine resins for antifungal applications

Since their commercialisation in the 1940s,<sup>83</sup> epoxy-resin materials have become a particularly well-developed area of polymer science. Strictly, 'epoxy resin' refers to unreacted monomers or oligomers featuring epoxide groups, which can undergo curing to form polymers and networks of crosslinked chains. However, in practise, the term has come to colloquially refer to the already-cured systems.<sup>83,87</sup> Epoxy resins are known for their excellent mechanical strength, electrical insulation and thermal resistance,<sup>88</sup> rendering the materials among the most versatile thermosetting polymers in the world.<sup>86</sup> But their applications are diverse and versatile, depending on the structure of both the epoxy-monomer and the curing agent, as well as the curing reaction conditions;<sup>83,88</sup> there is also evidence to suggest that these kinds of materials have suitable properties to be used in the biomaterials industry.<sup>89,90</sup>

Epoxy-amine networks are the most widespread of epoxy-resin systems<sup>93</sup> and curing is most usual with di- or poly-amines,<sup>92</sup> which may be aliphatic, cycloaliphatic or aromatic, and either primary or secondary.<sup>88</sup> While linear polymers are possible, it is more usual for branching to occur, generating networks of epoxy-resin polymers (**Figure 51**). This is particularly true where primary amines are used; a single addition of the amine to the epoxide results in a secondary amine with extra nucleophilicity, which thus will react with the remaining epoxides, inducing branching.<sup>93</sup> Networks such as these can also be formed by varying the epoxide/ amine stoichiometric ratio (**Figure 51**).<sup>92</sup>

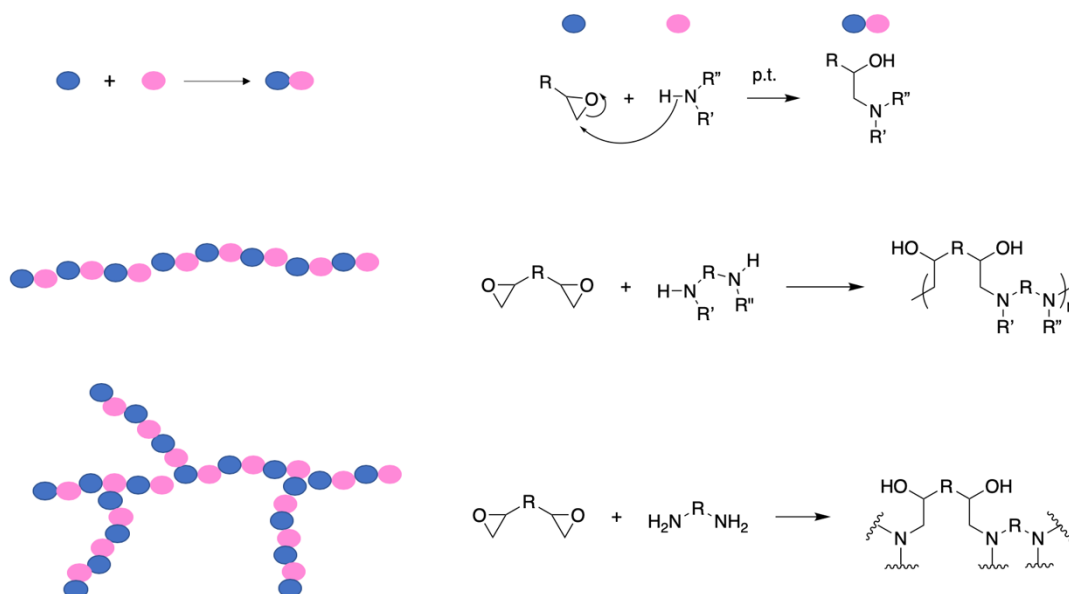


**Figure 51.** Cartoon representing the reaction of epoxides with amines to form linear polymers (middle) and networks (bottom).

The vast majority of commercially-available epoxy resins are derived from crude oil, but sustainability issues are driving the development of renewable alternatives.<sup>99</sup> Research into renewable epoxy resin materials have examined both the epoxide monomers as well as their curing agents from bio-based sources.<sup>84</sup> Amines have again proved a popular choice in the renewable curing agent market.

It is hypothesised that replacing the aromatic rings of common epoxy-resins with an aliphatic or cycloaliphatic alternatives could significantly alter the polymer properties, moving away from the toughness and rigidity to potentially render more supple materials that may be useful in biomaterials applications, particularly if coupled with aliphatic diamines. A number of studies have already suggested this.<sup>97,106</sup>

It is clear that epoxy resin chemistry is broad and versatile, lending itself to a variety of different monomers and a plethora of potential polymer systems, with diverse applications. While epoxy-resins evidently already account for a sizeable share of the polymer industry,<sup>107</sup> undoubtedly their full potential in the future of our polymeric systems is far from complete, particularly in regards to systems made from renewable sources of



biomass. It is the intention herein to investigate the use of terpenes in epoxy resin chemistry for antifungal applications.

Compared with antibacterial treatments, finding fungal-specific agents is considered more challenging. This is (at least in part) a result of fungi being eukaryotic, as are their human hosts, and so finding therapies which can effectively treat the fungus but not damage host cells can be difficult.<sup>153,154</sup> Additionally, the current arsenal of approved agents for anti-fungal or fungicidal use is quickly being eroded by fungal resistance.<sup>124</sup> The development of new antifungal therapeutics has been met with many challenges in recent decades, and there is now an urgent need for effective new treatments, particularly those with novel mechanisms of action.<sup>153,156</sup>

Of the approaches being researched to overcome fungal infections and biodeterioration, the use of biocidal polymers as an active mode of action against fungal growth and colonization is promising.<sup>126</sup> There are numerous advantages to using polymers for this strategy over small-molecules, not least because polymer materials can offer physical and chemical stability and usually a longer shelf-life, which results in long-lasting resistance against micro-organisms.<sup>146</sup> Additionally, the cost of biocidal polymers is generally much lower than advanced antibiotics. The versatile nature of polymers, including their facile synthesis methods, can enable the specific design of a high concentration of active components in the synthetic polymer materials.<sup>146</sup>

In addition to the use of biocidal polymers as a novel method of protecting against antimicrobial infections, synergistic and combination therapies may also offer a pragmatic approach to the problem, and is particularly attractive in terms of guarding against antimicrobial resistance.<sup>155</sup> This is particularly true of antifungals and fungicides: these therapies allow for the development of potent new formulations without the need for specific new agents (the development of which has been particularly slow for antifungals). This means that new therapies can potentially be facilitated by repurposing known antifungals, which is beneficial in terms of the timescale of approval and the cost.<sup>107,153</sup> Arguably the most attractive feature that synergistic therapies offer, however, is a lower likelihood of the fungi developing resistance to the therapy. This is because the evolution of resistance to more than one agent is much slower

than with a single one.<sup>155</sup> Furthermore, synergistic combinations enable lower amounts of active agents to be used, lessening potential concerns surrounding non-specific toxicity, or cost.<sup>107,155</sup>

The discovery of novel synergistic combinations is not a straightforward process however, and strong interactions between potential antifungals is not very common.<sup>153</sup> The biggest challenge for novel combination therapies now is thought to be the discovery of fungal-specific agents which can target the new antifungal mechanisms being discovered.<sup>165</sup> The discovery of these kinds of combinations could help to alleviate the pressing need to find strategies to combat microbial resistance. Combination therapies are already in use to treat many infectious diseases such as HIV, tuberculosis and malaria, and as such the area has garnered a lot of interest in the treatment of fungal pathogens.<sup>165</sup> While there has been research into synergistic combinations of known antifungal and fungicidal small molecules,<sup>153,166</sup> the use of biocidal polymers as one of the synergistic components has the potential to develop versatile and cost-effective antifungal formulations.

### 3.2 Aims and Objectives

The overall objective in this work is to produce new oligomers or polymers for antimicrobial applications. The antimicrobial nature of a variety of essential oils, namely terpenes, is well known. In particular, (*R*)-carvone exhibits antibacterial and antifungal activity against a variety of strains that are pathogenic to humans.<sup>199</sup> It was aimed to both capitalise upon and enhance the antimicrobial activities of this naturally occurring compound, by using facile epoxy-resin chemistry to couple the compound with co-monomers that, in a polymer system, might also be effective in enhancing these antimicrobial properties, as well as allowing for the generation of novel antimicrobial formulations. To achieve this, the terpene must first be converted to a monomer which could undergo epoxy-resin chemistry.

While much of epoxy-resin chemistry is focused on the use of aromatic monomers for hard, rigid materials, it is thought that aliphatic systems will display comparatively less rigidity and hardness,<sup>97</sup> and may have versatile applications in biomaterial or medical applications, as evidenced in some examples.<sup>87,97,200</sup> With this in mind, a route was designed to synthesise a bis-epoxide monomer *via* a facile synthesis from (*R*)-carvone, a naturally abundant terpenoid found in spearmint oil in concentrations of up to 80%.<sup>34</sup> Commercially, carvone is usually made from limonene,<sup>34</sup> making it an attractive starting point both economically and environmentally from which to form monomers. Carvone differs from limonene in that it contains a ketone functionality, which allows for the possibility of further post-polymerisation modifications of any resulting polymers, adding to its value as a monomer.

The syntheses of the monomer was designed *via* the epoxidation of the molecule's alkene functionalities (**Figure 52**). It was predicted that two separate oxidising agents would be required as the alkenes are electronically distinct from one another: a nucleophilic one for the endocyclic enone would be required, such as alkaline hydrogen peroxide, while it was anticipated the exocyclic alkene would require an electron deficient epoxidizing agent, such as *m*CPBA.

In designing the synthesis of this new epoxy monomer from renewable feedstocks, it was considered of paramount importance to seek

out either known or novel 'green' routes to these monomers. In this respect, it was aimed to adhere insofar as possible to the 12 Principles of Green Chemistry.<sup>13</sup> It was also important to try to ensure the use of non-toxic components in the synthesis, especially considering the intention to find use for these materials in biomedical, antimicrobial applications.

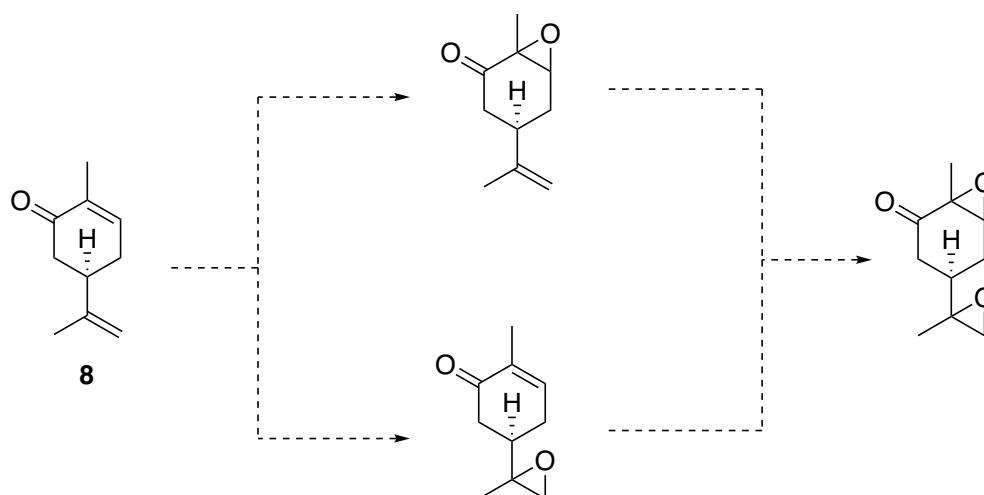


**Figure 52.** The predicted epoxidation routes of (R)-carvone to produce carvone bis-epoxide.

Following the successful synthesis of these terpene-based bis-epoxides, the aim was then to polymerise these monomers with amine-based co-monomers. Both primary and secondary amines would be employed, to investigate the difference in molar ratio of the reacting components on the overall structure and properties of the compounds formed. 1,6-hexane diamine and 1,6-dimethyl hexane diamine were identified as suitable co-monomers (**Figure 53**). Both feature a six membered, linear alkyl chain between two amine groups, the former being two primary amines, with two methylated secondary amines on the latter.

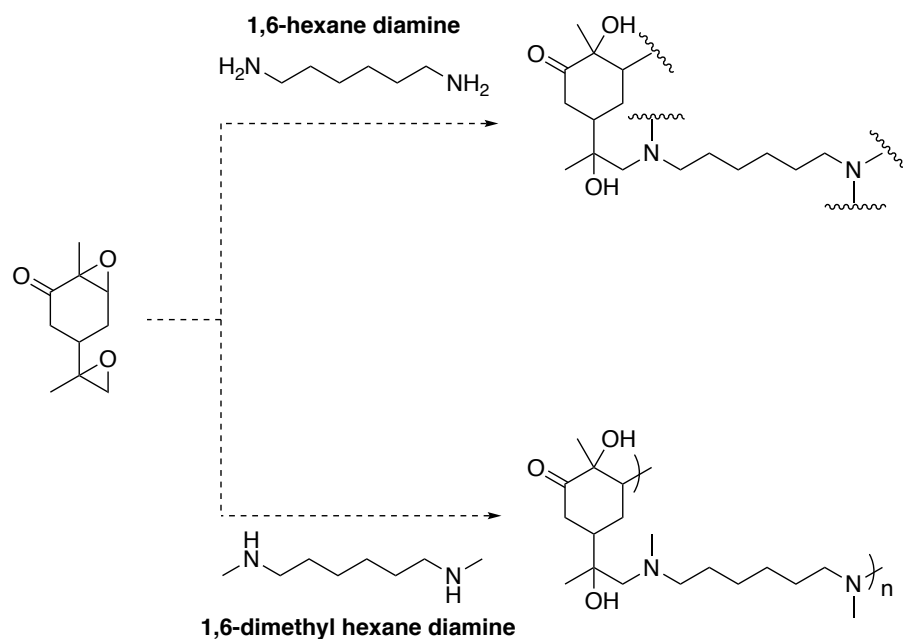


**Figure 53.** *The predicted polymerisation of terpene-based bis-epoxides with primary (top route) and secondary (bottom route) aliphatic diamines. It is anticipated that the primary diamine will form polymer networks, while the secondary diamine should form linear polymers.*

Aliphatic amines were identified as suitable co-monomers, not least because epoxy-resin systems are most usually cured with amines,<sup>92</sup> meaning the reaction is well-studied and documented in the literature.<sup>83,88,93,201</sup> Additionally, aliphatic amines have a suitable nucleophilicity to allow the reaction to occur at ambient temperature, in the absence of any additional catalysts or solvents.<sup>87,102</sup> This is favourable in the synthetic design when considering environmentally conscious chemistry: solvents present one of the most challenging aspects of green synthesis and where possible it would be ideal to avoid their use entirely.<sup>13</sup> Conveniently, hydroxyl groups have been found to catalyse the reaction of the amino group and the epoxide, and as the reaction itself generates these groups (**Figure 53**), the reaction is thus self-catalysed.<sup>102</sup> It is therefore anticipated that these polymer syntheses can avoid the use of additional components, ensuring a high atom economy and minimising waste, adhering well with the 12 principles of Green Chemistry.<sup>13</sup>

It is predicted that the diamines chosen in these syntheses may act as model systems for the reaction of a variety of primary and secondary diamines of similar structures. This would allow for an array of polymer systems to be synthesised by the same methods, including those, for example, derived entirely from renewable feedstocks. One way of doing this would be to use the 5-carbon cadaverine or the 4-carbon putrescine as the diamine co-monomer, both of which are derived from natural sources.<sup>104</sup> In the current syntheses however, diamines with 6-membered carbon alkyl linkers were chosen for a number of reasons. First of all, it was anticipated that using a long hexyl linker would introduce a degree of flexibility to any resulting structures, which is desired in the synthesis of new systems with less rigidity and toughness than conventional epoxy resin materials. Additionally, it also anticipated that the long alkyl chain would minimise the possibility of intra-molecular cyclisation, which may be more favourable with shorter chain alkyl linkers. On the other hand, there is evidence that the use of flexible, aliphatic amines can bring about *inter*-molecular cyclisation, resulting in the formation of oligo- or polymeric macrocycles.<sup>93</sup> While the aim in the first instance is to form linear polymers, this would not necessarily be problematic as macrocycles may also be useful, having been known to have useful applications in biomedical applications such as drug delivery systems.<sup>202</sup> Most significantly, the long 6-membered alkyl linker was desired when considering the hydrophobic/hydrophilic balance of the overall structures formed, known to be of paramount importance in antifungal or indeed any biocidal polymers.<sup>146</sup> It was hypothesised that generating compounds with an amphiphilic balance such as this, combined with the known antimicrobial nature of terpenes, could arrive at a material with considerable antimicrobial properties.

Employing conditions of the well-established epoxy-amine polymerisation reaction,<sup>87,102</sup> it was endeavoured to synthesise chains of oligomers rather than long-chain polymers, aiming to keep the DP to approximately  $\leq 10$ . The idea behind this was to mimic similar structural properties of antimicrobial peptides (AMPs), and more specifically, antifungal peptides (AFPs). AMPs are gene-encoded molecules produced by all organisms to defend against harmful micro-organisms.<sup>203</sup> These natural defence (poly-)peptides have been mimicked in the design of a

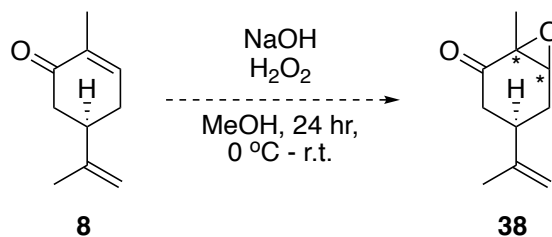
variety of synthetic polymers for the purpose of antimicrobial polymers,<sup>204</sup> and the peptide chain length is thought to be an important factor in the mode of action, with those containing 2-10 amino acids attracting attention as less-toxic and more-stable alternatives to longer chains.<sup>203,204</sup> While the terpene-amine oligomers in this project are not polypeptides, nonetheless it is anticipated that the same oligomer properties might result (i.e. hydrophobic segments and cationic charge), and so it is aimed to keep the oligomers within this same size range.

Upon a successful synthesis of new terpene-based epoxy oligomers, their solubility would need to be probed in order to identify any water-soluble systems. Initial biological screens that would test the suitability of a material for a biomedical application, such as a cytocompatibility assays, or more specifically, those used to investigate fungal inhibition, are conducted in water-based media. This is in order to provide the cells an environment in which to metabolise, grow and survive. As such, formulations of the polymers must be made up in water, DMSO or a similar non-toxic solution that is easily tolerated by the biological systems. The use of amines can sometimes ensure appropriate hydrophilicity is brought about; in hydrophilic media or solvent the amines will become protonated and generate quaternary cations which are water-soluble. However, the hydrophilicity or amphiphilicity is dependent on (and very sensitive to) the overall structures of the polymers, and quaternary amines alone are not promise of a suitable material for successful applications.<sup>146,161</sup>

Should any synthesised oligomers prove to have appropriate solubility for the required screenings, it is then aimed to probe their antifungal activity both alone and in combination with known antifungals. The development of new antifungal therapeutics has been met with many challenges in recent decades, and there is now an urgent need for effective new treatments, particularly those with novel mechanisms of action.<sup>153,156</sup> Terpenes are already known for their antimicrobial properties,<sup>199</sup> and it is anticipated that the diamine co-monomer could lead to the generation of a polycationic species, known for their ability to interact electrostatically with cell membranes.<sup>205</sup> The combination of an oligomer of this nature alongside a known, perhaps repurposed antifungal agent may present a novel combination or synergistic therapy, which is highly desirable.<sup>153,155</sup>

### 3.3 Results and Discussion

#### 3.3.1 Synthesis of carvone-based bis-epoxide monomer using mCPBA

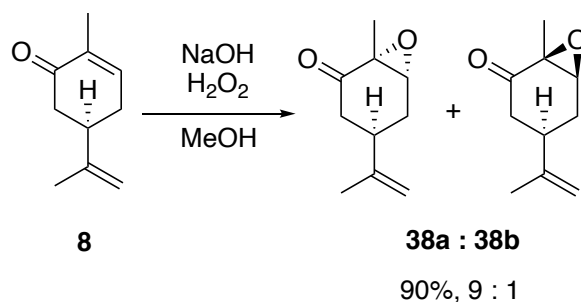


**Scheme 22.** The proposed epoxidation of the endocyclic double bond of (*R*)-carvone using alkaline hydrogen peroxide.

The double-bond moieties of carvone are electronically distinct from one another, and so different oxidising agents are required to epoxidise each one.<sup>70</sup> Initially, a route was designed to epoxidise the electron-deficient, endocyclic alkene using alkaline hydrogen peroxide in methanol (**Scheme 22**). This would provide a relatively green synthesis of the mono-epoxide: methanol can be produced from biomass,<sup>206</sup> making it a renewable solvent, while hydrogen peroxide is often regarded as the 'ultimate green reagent', as it is a relatively mild oxidant which does not produce an excess of toxic or wasteful by-products.<sup>206</sup>

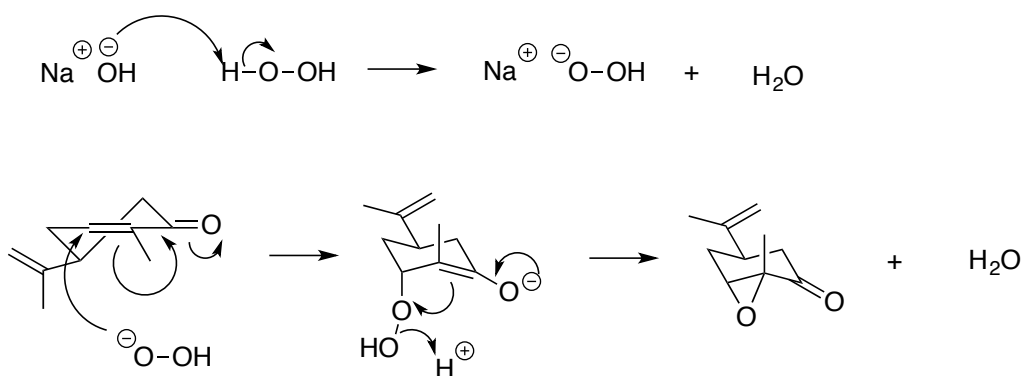
The reaction was initially conducted using well-established conditions from the literature.<sup>70</sup> Herein, (*R*)-carvone was stirred in methanol at 0 °C and 2 M aqueous sodium hydroxide solution (NaOH<sub>aq</sub>) was added. Hydrogen peroxide solution (30% v/v) was then added dropwise via syringe. After stirring for 3 hours the epoxidised product **38** was successfully isolated in a 90% yield, as a mixture of diastereomers **38a** and **38b**, in a 9:1 ratio, respectively, and without the need for further purification (**Scheme 23**).





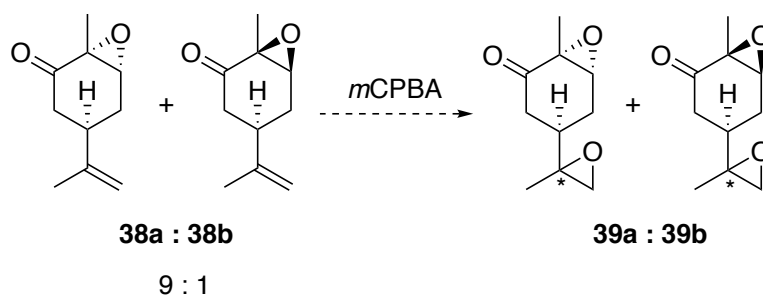
**Scheme 23.** Synthesis of mono-epoxides **38a** and **38b** via the epoxidation of the *exo*-cyclic double bond of (*R*)-carvone using alkaline hydrogen peroxide.

The 3D conformation of (*R*)-carvone is significant in relation to the stereochemical outcome of this reaction. Hydrogen peroxide (H<sub>2</sub>O<sub>2</sub>) is a nucleophilic oxidising agent, which attacks the enone moiety at the 1,4-position in a Michael-type addition.<sup>70</sup> Carvone has two sp<sup>2</sup> centres in its ring, which distort it away from a chair conformation to a much flatter structure (**Scheme 24**).<sup>207</sup> When the molecule undergoes 1,4-nucleophilic attack at the enone, the more favourable route is for the attack to occur axially rather than equatorially.<sup>207</sup> This allows for the most stable, chair-like transition state structure to form. Should the nucleophile attack from an equatorial angle, the structure would have to form a twist-boat transition state, which is highly disfavoured.<sup>207</sup> The stereochemical outcome is a consequence of this, with <sup>1</sup>H NMR spectroscopy indicating a diastereomeric ratio of 9:1 for the epoxide in the *R,R* (down) or *S,S* (up) positions, respectively (**Scheme 23**). Attempts were not made to separate or further isolate either diastereomer, but to carry forward the monoepoxide as a mixture of the two.



**Scheme 24.** Proposed mechanism for the endocyclic epoxidation of (R)-carvone with 3D structures accounting for the most favoured stereochemical outcome.<sup>207</sup>

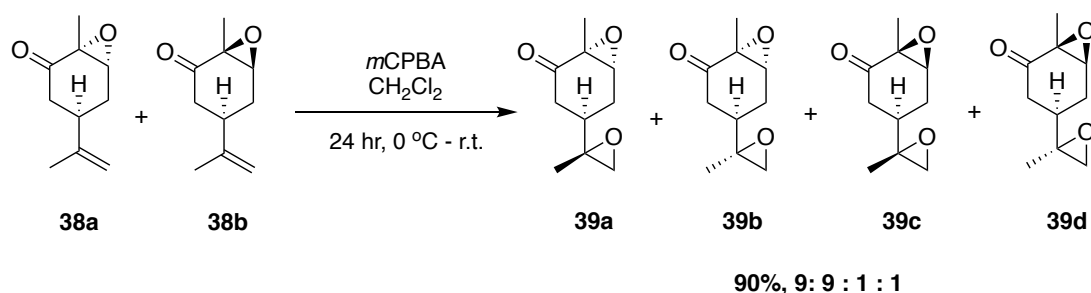
With this intermediate monoepoxide in hand, it was aimed to then form another epoxide at the exocyclic alkene using *meta*-chloroperbenzoic acid (*m*CPBA) to arrive at bis-epoxides **39a** and **39b** (**Scheme 25**).<sup>70</sup> Unlike hydrogen peroxide, *m*CPBA acts as an electrophilic oxidising species in a reaction with electron-rich alkenes,<sup>70</sup> thus making it a suitable epoxidising agent for the exocyclic alkene of **38**.



**Scheme 25.** Proposed synthesis of bis-epoxide **39**, using *m*CPBA to bring about the epoxidation of the exocyclic alkene of **38**.

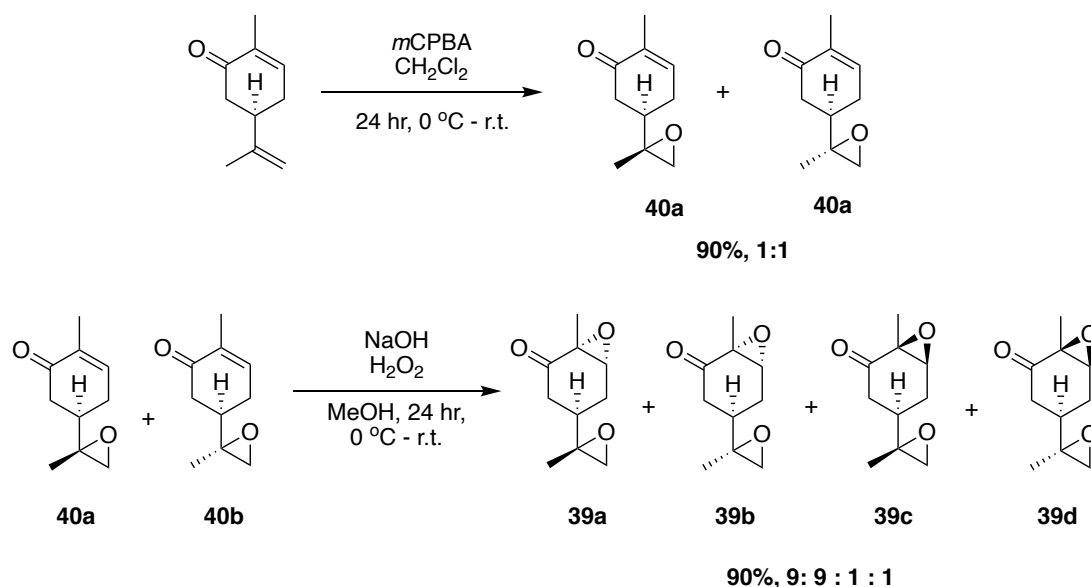
The reaction was conducted using 1.2 equivalents of *m*CPBA in dichloromethane (DCM), initially on ice and then brought to room temperature (**Scheme 26**). After 24 hours, the mixture was washed with saturated aqueous sodium bicarbonate solution (NaHCO<sub>3</sub>) to remove the

*meta*-chlorobenzoic acid (*m*CBA) side product, before the bis-epoxide product was isolated in a 90% yield. It was found by <sup>1</sup>H NMR analysis that, as expected, there was no stereochemical control to this reaction, resulting in a 9:9:1:1 mixture of bis-epoxides **39a** to **39d**, respectively (**Scheme 26**). By this route, the monomer was thus synthesised in an 81% yield over the two steps.<sup>107</sup>



**Scheme 26.** Epoxidation of the exocyclic, electron-rich alkene of **38** using *m*CPBA in DCM, in the synthesis of bis-epoxide monomer **39a** to **39d**.

It was investigated whether or not epoxidising the double bonds in the reverse order (i.e. the exocyclic one first with *m*CPBA, followed by the endocyclic one with alkaline hydrogen peroxide), might have any effect on either the stereochemical ratio of products, or on the yield. However, in each case, similar yields and diastereomeric ratios were observed for both reactions to form the alternative mono-epoxide **40a** and **40b**, as well as the bis-epoxide (**Scheme 27**). Once again, the monomer was synthesised in an 81% yield over the two steps.



**Scheme 27.** The epoxidation of (*R*)-carvone using *m*CPBA to first form the intermediate mono-epoxides **40a** and **40b**, followed by the epoxidation with alkaline hydrogen peroxide to generate the bis-epoxide monomer **39** in an overall yield over the two steps of 81%.

It was then investigated whether or not an excess of *m*CPBA could be used to bring about the epoxidation of both double bonds of (*R*)-carvone in one step. The reaction was first attempted with 2.5 equivalents of the peroxy-acid. After 24 hours, the product was isolated and found by  $^1\text{H}$  NMR analysis to be the mono-epoxide species **40a** and **40b**, with no trace of the bis-epoxide (**Figure 54**). A second attempt was made to form the bis-epoxide in one step using 2.5 equivalents of *m*CPBA, but this time in a more concentrated reaction and over a period of 7 days. This attempt also resulted in the isolated product **40a** and **40b**, with no trace of the intended bis-epoxide present. These unsuccessful attempts indicate the chemoselectivity of *m*CPBA for electron-rich double bonds, over electron poor ones.

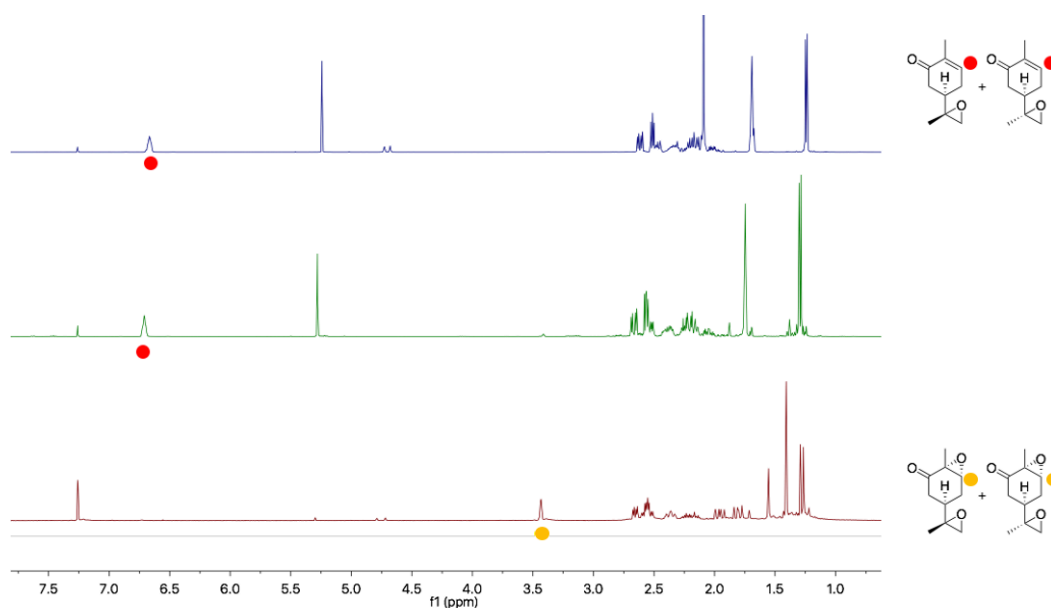
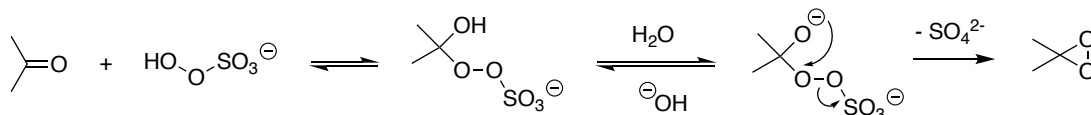


**Figure 54.**  $^1\text{H}$  NMR spectrum indicating the failed attempt to synthesis the bis-epoxide monomer **39** using 2.5 equivalents of *m*CPBA (green, middle trace). The resonance at approximately 6.75 ppm (red dot) indicates the enone functionality remained intact for the experiment, and only the exocyclic alkene was epoxidised, with no trace of the desired  $\alpha$ -epoxy proton (yellow dot).

### 3.3.2 Synthesis of terpene-based bis-epoxide monomer using Oxone<sup>®</sup>

The use of alkaline hydrogen peroxide in methanol in the epoxidation of the endocyclic alkene may be considered a relatively green reaction, however, the use of *m*CPBA in the exocyclic epoxidation is of some concern: most notably it is not an atom-economic reagent, producing a molecule of chlorobenzoic acid as stoichiometric waste.<sup>107</sup> Additionally, the reaction is exothermic which becomes significant when working on a large scale, and is conducted in DCM, which causes ozone depletion and is a suspected carcinogen.<sup>208</sup> To avoid the use of this reagent, an alternative synthesis using Oxone<sup>®</sup> was designed. Oxone<sup>®</sup> is the commercial name for potassium peroxydisulfate, an inexpensive and stable potassium-based salt.<sup>209</sup> It reacts *in situ* with acetone to form the oxidant dimethyl dioxirane (DMDO) (**Scheme 28**),<sup>210</sup> which is then used to epoxidise electron-rich

alkenes. This was first determined by Murray *et al.*, who showed that solutions of DMDO in acetone could be obtained through distillation and used to epoxidise alkenes, with *cis*-alkenes reacting about eight times faster than *trans*- ones.<sup>211</sup>



**Scheme 28.** Proposed mechanism for the *in situ* generation of DMDO using potassium peroxydisulfate and acetone.<sup>210,212</sup>

Studies into the *in situ* generation of DMDO have shown that the Bayer-Villiger oxidation of the ketone species (acetone, in this instance) is possible instead of the dioxirane formation, but disfavoured provided the pH levels of the mixture do not become too acidic.<sup>212</sup> Therefore, until the turn of the 21<sup>st</sup> Century, the common protocol involved biphasic conditions of Oxone<sup>®</sup> solution (in water) with acetone, in addition to an appropriate buffer, a phase-transfer catalyst and benzene as a solvent.<sup>212</sup> In 2000, however, Ferraz *et al.* published a far simpler (and greener) protocol, employing sodium bicarbonate (NaHCO<sub>3</sub>) to help buffer the mixture, which was added to a stirred solution of the substrate in acetone, acting as both a reagent and a solvent, at 0 °C. An aqueous solution of Oxone<sup>®</sup> was then added dropwise to this mixture, yielding a variety of epoxidised olefins in excellent yields.<sup>213</sup>

Accordingly, (*R*)-carvone was stirred in an excess of acetone at room temperature (23 °C) and solid NaHCO<sub>3</sub> was added. A 0.52 M solution of Oxone<sup>®</sup> (3 equivalents) was then added *via* syringe pump at a flow rate of 1 mL·min<sup>-1</sup>, using conditions adapted from a recently reported procedure for the exocyclic epoxidation of (*R*)-carvone.<sup>209</sup> Following the Oxone<sup>®</sup> addition, the reaction was stirred for a total of three hours before extracting the water layer with diethyl ether (Et<sub>2</sub>O). The organic extracts were then washed with brine and dried over MgSO<sub>4</sub> before evaporation of the volatiles to yield a yellow oil. <sup>1</sup>H NMR analysis revealed that, as expected, the exocyclic alkene had been completely consumed in the

reaction, while as expected, it appeared the endocyclic double bond remained intact, according to the resonance at 6.72 ppm (**Figure 55, a**).

However, by comparison with the NMR for **40**, the spectra were not identical and it was evident that another species was present, due to the resonance at 3.44 ppm (**Figure 55, blue-X**). When compared to the NMR spectrum for the bis-epoxide monomer **39** made previously using NaOH/H<sub>2</sub>O<sub>2</sub> and *m*CPBA, the two resonances seemed to correspond well, and so it was hypothesised that perhaps after the formation of the mono-epoxide **40** at the exocyclic position, the molecule was being further converted at the endocyclic position to the **39** monomer. The ratio between the two species was found to be 1:0.7 for the predicted product (**40**)/side product, respectively (according to the integration of the enone proton and the one at 3.44 ppm (**a** and **b** respectively in **Figure 57, vide supra**). The presence of the alternative mono-epoxide **38** (**Figure 55, third trace**) was ruled out as the characteristic alkene protons are found to have been completely consumed in this reaction.

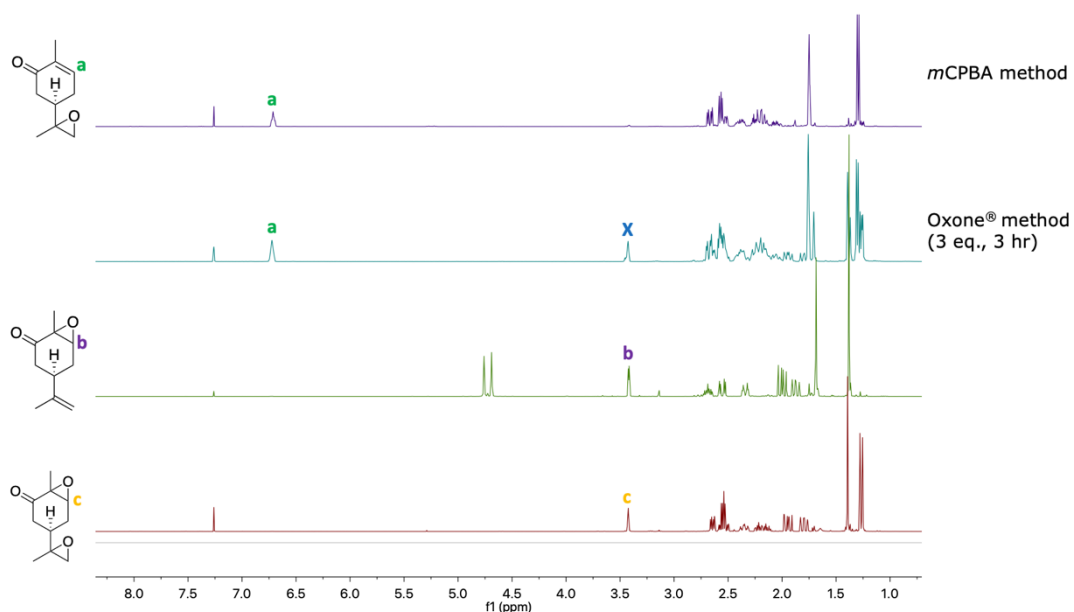


**Figure 55.**  $^1\text{H}$  NMR spectra showing the mono-epoxide **40** made using mCPBA (top trace), the ene-one resonance is indicated by the green letter **a**. This ene-one functionality is still present in the Oxone<sup>®</sup> method spectrum (second trace), alongside an unknown moiety indicated by the blue **X**. This corresponds well with the  $\alpha$ -epoxy proton of this bis-epoxide product **39** (bottom trace), the resonance for which is highlighted by the orange letter **c**. The mono epoxide **38** is ruled out (third trace); although the purple dot corresponds well, the exocyclic alkene resonances are missing.

It was thought that as there was already an excess of Oxone<sup>®</sup> present in solution (3 equivalents were used), perhaps instead longer reaction times could help fully convert mono-epoxide to the bis-epoxide, and so the reaction was conducted again and stirred for 48 hours, with samples taken at regular intervals (**Figure 56**). However, this proved unsuccessful, with no significant change in the ratio of the product **40** (**a**) to side-product (**b**) after two days compared with 3 hours (**Figure 56**). After 3 hours, the ratio of products is then 1:0.7, while at 5 hours, the ratio increases slightly in favour of the side product, to 1:0.9. However, this did not change after 24 hours and after 48 hours it had instead decreased slightly to 1:0.8.



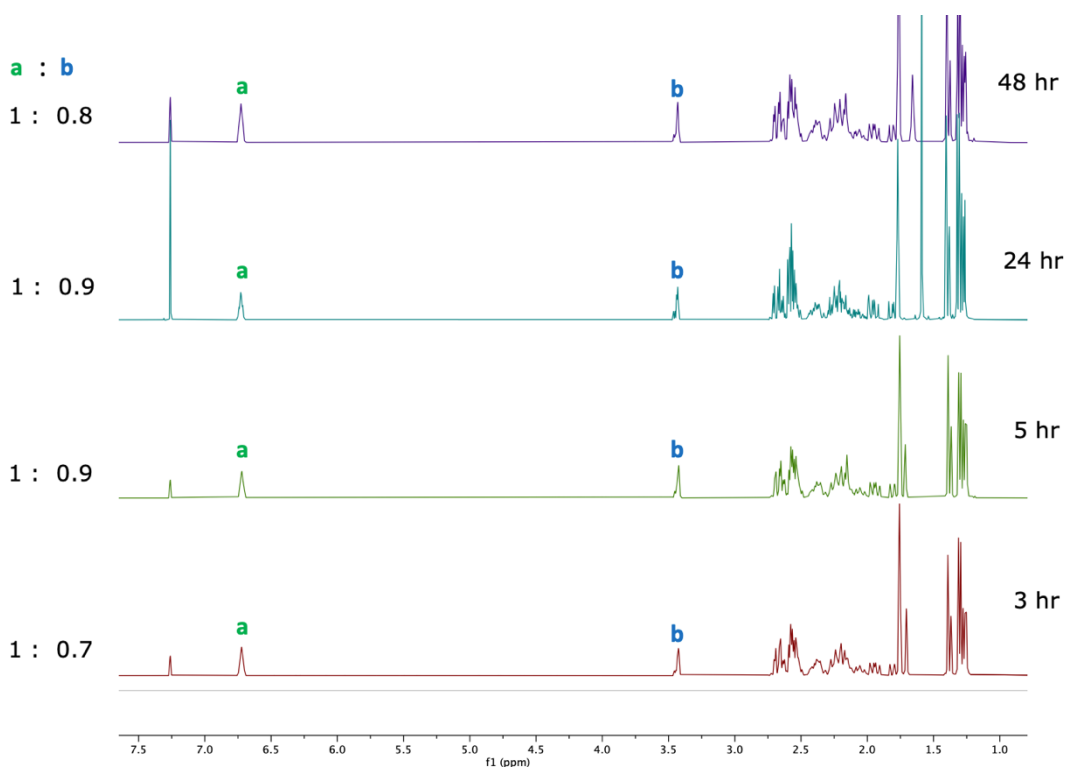


**Figure 56.** NMR spectra showing the reaction of (*R*)-carvone with Oxone<sup>®</sup> at 3 hours (bottom trace, red), 5 hours (second trace, green), 24 hours (third trace, teal) and 48 hours (top trace, purple). The integration ratios between the enone proton at 6.72 ppm (green **a**) and the unidentified resonance at 3.44 ppm (blue **b**) is indicated at each interval.

Upon further analysis of the reaction, it became evident that using these conditions, the reaction goes to completion consuming all the starting material and producing a clean sample of the mono-epoxide product **40** after just 30 minutes stirring, by which time only half the Oxone<sup>®</sup> solution had been added. Following the full addition of Oxone<sup>®</sup> after 60 minutes, even after immediate work up without further time stirring, the side-product corresponding to the resonance at 3.44 ppm is formed (**Figure 57**). It is not entirely surprising that the reaction would go to completion in the formation of **40** after only half the addition of Oxone<sup>®</sup>, as three equivalents are being used where only one would be required to do this reaction.

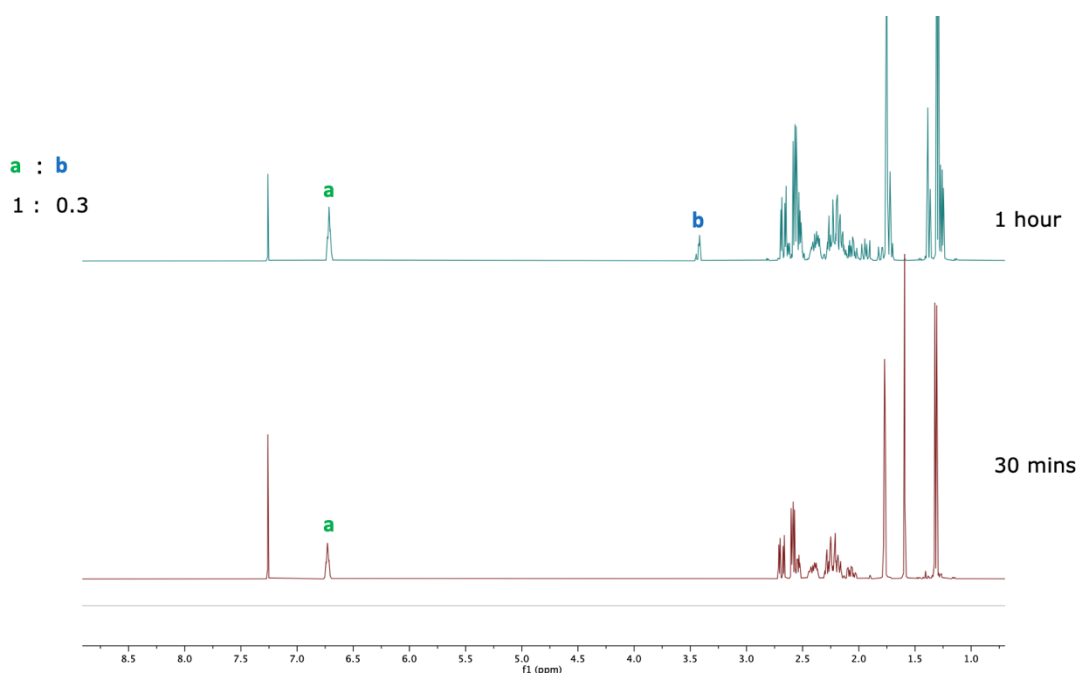
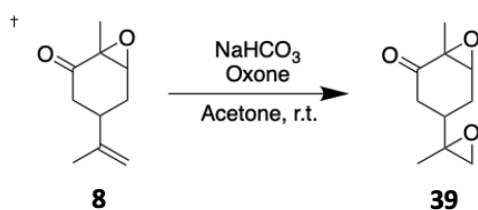


**Figure 57.**  $^1\text{H}$  NMR spectra of the epoxidation of (*R*)-carvone using 3 equivalents of Oxone<sup>®</sup> (as a 0.5 M aqueous solution), after 30 minutes (bottom trace, maroon) when half the Oxone<sup>®</sup> solution had been added.

The endocyclic alkene of (*R*)-carvone is known not to successfully undergo epoxidation using DMDO,<sup>209</sup> or other electron-deficient oxidising agents,<sup>70</sup> and given this lack of success over 48 hours and with excess equivalents of Oxone<sup>®</sup>, it was decided to not further investigate the formation of the bis-epoxide from (*R*)-carvone. Instead, attention turned to forming the bis-epoxide monomer using Oxone<sup>®</sup> from the previously-synthesised mono-epoxide **38**, formed with alkaline hydrogen peroxide. This could also be viewed as analogous to using a protecting-group strategy for the endocyclic enone: to investigate if the impurity found at 3.44 ppm would still be synthesised in this case too, even with the enone unavailable for reactions.

The same conditions (adapted from the literature protocol<sup>209</sup>) were used in the first instance, i.e. Oxone<sup>®</sup> solution (0.52 M, 3 equivalents) was added *via* syringe pump at 1 mL·min<sup>-1</sup> to a stirring solution of the mono-epoxide **38** in acetone with NaHCO<sub>3</sub>. NMR analysis indicated the completion of this reaction with the formation of the bis-epoxide **39** after 60 minutes,

with no additional side products forming after 72 minutes when the full amount of Oxone<sup>®</sup> was added, or if left stirring for an additional 3 hours. This would suggest that the resonance at 3.44 ppm seen previously is indeed a result of a reaction at the enone moiety. The reaction was stopped by extracting the water layer with Et<sub>2</sub>O and isolating the product in a 65% yield (**Table 5, entry 1**). It was thus shown that these conditions were relatively robust; the bis-epoxide product being stable enough to stir in the solution after the reaction completion, without requiring immediate work up and without the formation of additional side-products.



Entry	Scale (mmol)	Oxone (eq.)	Oxone (M)	NaHCO <sub>3</sub> (eq.)	Yield
<b>1</b>	12.05	3	0.52	4.8	65%
<b>2</b>	30.07	1.5	0.73	2.5	82%
<b>3</b>	29.94	1.5	0.32	4.8	83%

**Table 5.** Optimisation of the conversion of mono-epoxidized **38** to the bis-epoxide monomer **39** using Oxone<sup>®</sup>.

*†) Stereochemistry is not represented in this scheme.*

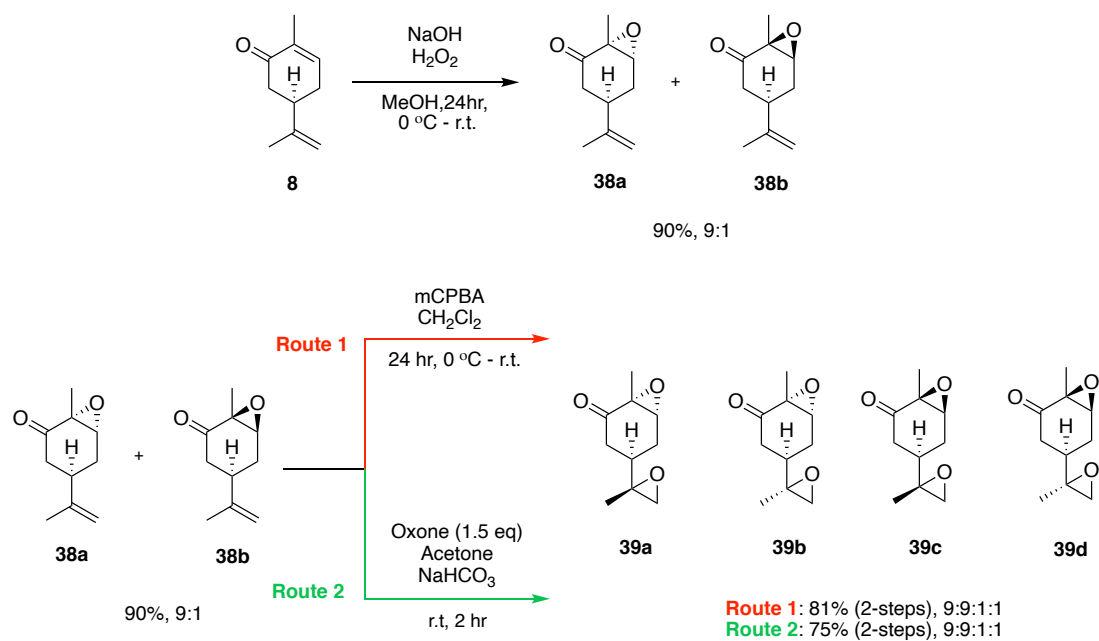
*‡) No yield was recorded in this instance*

When scaling up this reaction, the quantity of Oxone<sup>®</sup> used becomes significant as it equates to longer reaction times due to the addition of the 0.5 M solution at a flow rate of only 1 mL min<sup>-1</sup>. In an attempt to circumvent this and have shorter reaction times, increased concentrations of Oxone<sup>®</sup> were investigated. The amount of NaHCO<sub>3</sub> was also reduced from 4.8 equivalents to 2.5, due to the decrease in Oxone<sup>®</sup> being added when having changed from 3 to 1.5 equivalents. Unfortunately it was found that Oxone<sup>®</sup> would not fully dissolve in the amount of water required to form a 1 M solution, and so a reaction was conducted at 0.73 M, on a scale of 30.07 mmol (5 g). This resulted in the desired product with a yield of 82%

(**Table 5, entry 2**). Conversely, reactions were also conducted with weaker solutions of 0.32 M Oxone<sup>®</sup>. While the yield did not change significantly in this instance, this reaction brought about the best results, with the bis-epoxide product isolated in an 83% yield (**Table 5, entry 3**). While these results indicated that the molarity of Oxone<sup>®</sup> solution did not have a great effect on the yield or outcome of the reaction, it was found that when only 1.5 equivalents of NaHCO<sub>3</sub> were used, the reaction did not go to completion. In these cases starting material was also shown in the NMR, unless another equivalent of the base was added at a later point, which resulted in the full conversion to the bis-epoxide.

The route to the bis-epoxide **39** using alkaline hydrogen peroxide to first form intermediate **38** followed by Oxone<sup>®</sup> to fully convert the exocyclic alkene was found to produce the monomer in a good yield of 75% over the two steps (**Scheme 29**). While the overall yield using *m*CPBA is moderately higher (81% over the two steps), it is evident that the use of Oxone<sup>®</sup> is by far the more favourable route, as it is much 'greener'. Notably, it completely avoids the use of DCM, the danger of which was recently highlighted after severe necrosis occurred when it was accidentally injected sub-cutaneously.<sup>214</sup>

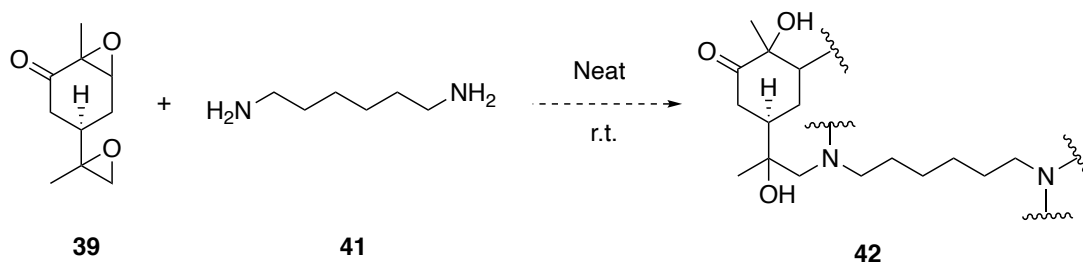
Attempts to separate the diastereomers of **39** were not conducted as the use of stereospecific monomers was not predicted to be necessary at this stage for the purpose of investigating polymerisation.



**Scheme 29.** Synthesis of bis-epoxide monomer (**39**) via epoxidation using alkaline hydrogen peroxide followed by either mCPBA (route 1) or Oxone<sup>®</sup> (route 2).<sup>107</sup>

### 3.3.3 Synthesis One of $\beta$ -amino alcohol oligomers

With the aim of keeping the synthetic methods as 'green' and non-toxic as possible, it was desired to cure the carvone bis-epoxide species, **39**, at ambient temperature and in the absence of solvents or catalysts. Investigations began with the aliphatic, di-primary 1,6-hexane diamine (**41**), in a 1:1 molar ratio for the terpene/ diamine species (**39:41**). It was anticipated that cross-linking or branching would occur in this system, as this stoichiometric ratio results in 1:2 for the epoxy:amine reactive components (**Scheme 30**). Two screens involving reaction temperature and time were designed to investigate how the reaction proceeds, and to explore the most optimal conditions. For simplicity, the full stereochemistry of the bis-epoxide monomer (as described in the previous section 3.3.2/**Scheme 29**) will not be drawn in future schemes.



**Scheme 30.** Proposed reaction of carvone bis-epoxide (**39**) with co-monomer 1,6-hexane diamine (**41**) to produce polymer networks described by structure **42**. 'Neat' conditions refer to the absence of additional components such as solvents or catalysts.

#### 3.3.3.1 Temperature screen

The reaction was conducted on a 0.5 g scale for the diamine species (i.e. 4.31 mmol), corresponding to 0.78 g/4.31 mmol of epoxide. Aliphatic amines are known to react with epoxides at ambient temperature,<sup>88</sup> and so a screen from 0 °C to 110 °C was designed. Lower temperatures were intended to investigate the limits of the nucleophilicity of the amine species

and the control of the polymerisation, while it was anticipated that higher temperatures might drive the polymers to higher molecular weights.

In each case, the samples were stirred together, in neat conditions (i.e. in the absence of any additional components), for 5 hours. The vials were capped but pierced with a needle to expose the reaction to air. At both 0 °C and 20 °C it was found that it was difficult to dissolve the solid diamine in the liquid terpene. After 5 hours, the resulting mixtures appeared to have an orange-brown colour, with those samples cured at higher temperatures appearing darker and more viscous or even, in some instances, hard or glassy by appearance. The exception was the sample cured at 0 °C, which remained mostly yellow in colour (**Figure 58**).

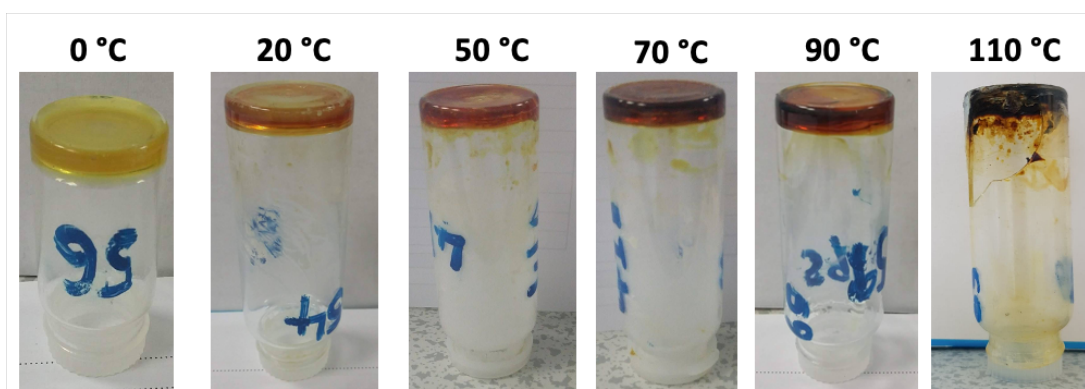


**Figure 58.** The results of the cured carvone bis-epoxide/ primary diamine systems, conducted from 0 °C to 110 °C, each for a period of 5 hours.

The resulting cured mixtures were found to be soluble in a selection of solvents, suggesting that the systems were not fully cross-linked. The  $^1\text{H}$  NMR spectra of each sample proved very complex and as such it was not a particularly useful analysis in determining the structures of the materials, except to indicate that the bis-epoxide monomer appeared to have been completely consumed in each reaction. This was concluded due to the characteristic  $\alpha$ -epoxy proton resonance at 3.44 ppm in the monomer being completely depleted in the polymer spectrum (**Figure 59**). For each temperature the spectra appeared very similar, indicating that the reaction had proceeded in a similar way in all cases.

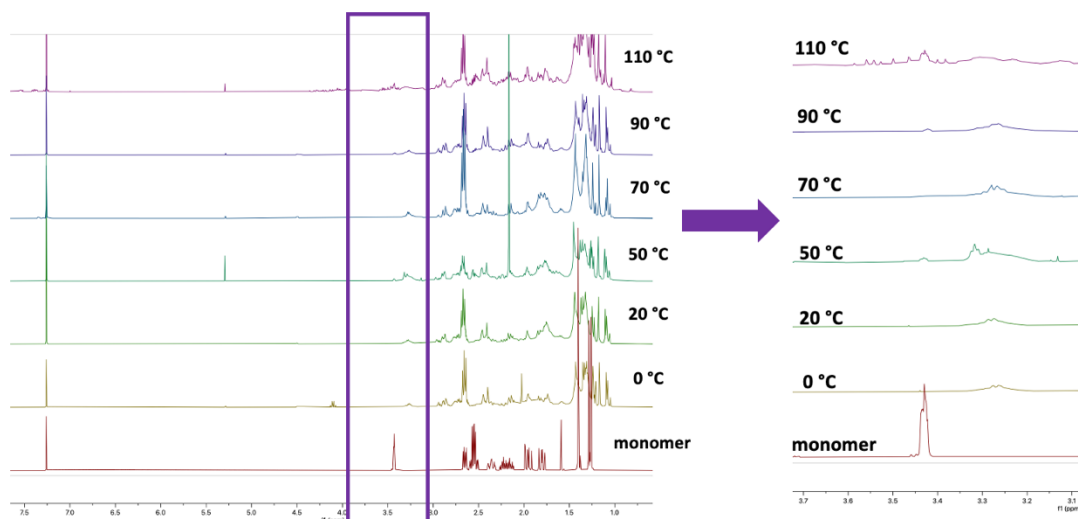


**Figure 59.**  $^1\text{H}$  NMR spectra of the cured carvone bis-epoxide/ primary diamine systems and the bis-epoxide monomer. Characteristic resonances of the bis-epoxide are missing at approximately 3.44 ppm, indicating the consumption of the monomer in each case.

While end-groups could not be distinguished by NMR, it was anticipated (given the bis-epoxide was completely consumed) that there would be amine-terminated chains, as the stoichiometric ratio was 2:1 for each N-H/epoxide group. IR spectroscopy confirmed the presence of N-H bending modes at approximately  $1656\text{ cm}^{-1}$ , though unfortunately the region in which to observe the N-H stretch ( $3300 - 3500\text{ cm}^{-1}$ ) was overlapped with the broad hydroxyl stretches ( $3200 - 3600\text{ cm}^{-1}$ ) and so these could not be observed. However, the IR spectra were also useful in showing that the reaction had occurred in each case; each one showing the characteristic hydroxyl and carbonyl stretches. For reactions at certain temperatures the carbonyl stretch is less distinct, and a second stretch at approximately  $1650\text{ cm}^{-1}$ , was equally strong. This second stretch is characteristic of an imine group, which traditionally appear at lower wavenumbers than the carbonyl equivalents, ranging from  $1649\text{-}1664\text{ cm}^{-1}$ .<sup>215</sup> Unfortunately, no pattern was discerned to link the occurrence of this IR stretch to the temperature of the reaction. To investigate this imine moiety (and the structure in general) further, the  $^{13}\text{C}$  NMR of each sample was obtained.



$^{13}\text{C}$  NMR was more useful in helping to determine the structure of the samples, in particular with the use of DEPTs, which were obtained for the systems formed at both 20 °C and 70 °C. A large number of resonances are present in both, indicating the presence of a mixture of products and/or complex products. A quaternary resonance in the  $^{13}\text{C}$  NMR (or DEPT-45) at 210.8/ 211.1 ppm in both the 20 °C and 70 °C samples respectively, indicates the presence of a ketone functionality, suggesting the preservation of the monomer-ketone during the reaction. This would suggest that if polymerisation has occurred, it must be *via* the ring-opening of the epoxide groups. It is predicted that the exocyclic epoxide will be the first to react, as it is less sterically hindered than the endocyclic one. Comparing the monomer and oligomer NMRs of the reaction at 20 °C, the corresponding resonance on the  $^{13}\text{C}$  NMR indicates that this exocyclic epoxide has fully reacted; similar resonances in the oligomer spectrum do not align with those of the monomer when the region is inspected closely (**Figure 60, d**).

The characteristic  $^1\text{H}$  NMR resonance at 3.44 ppm corresponding to the  $\alpha$ -epoxy proton of the endocyclic epoxide in the monomer was previously shown to have also been fully consumed, suggesting the endocyclic epoxide was also completely reacted. This is similarly confirmed with the  $^{13}\text{C}$  NMR, as the corresponding carbon resonance in the monomer does not correspond to any resonance in the oligomer sample (**Figure 60, c**).

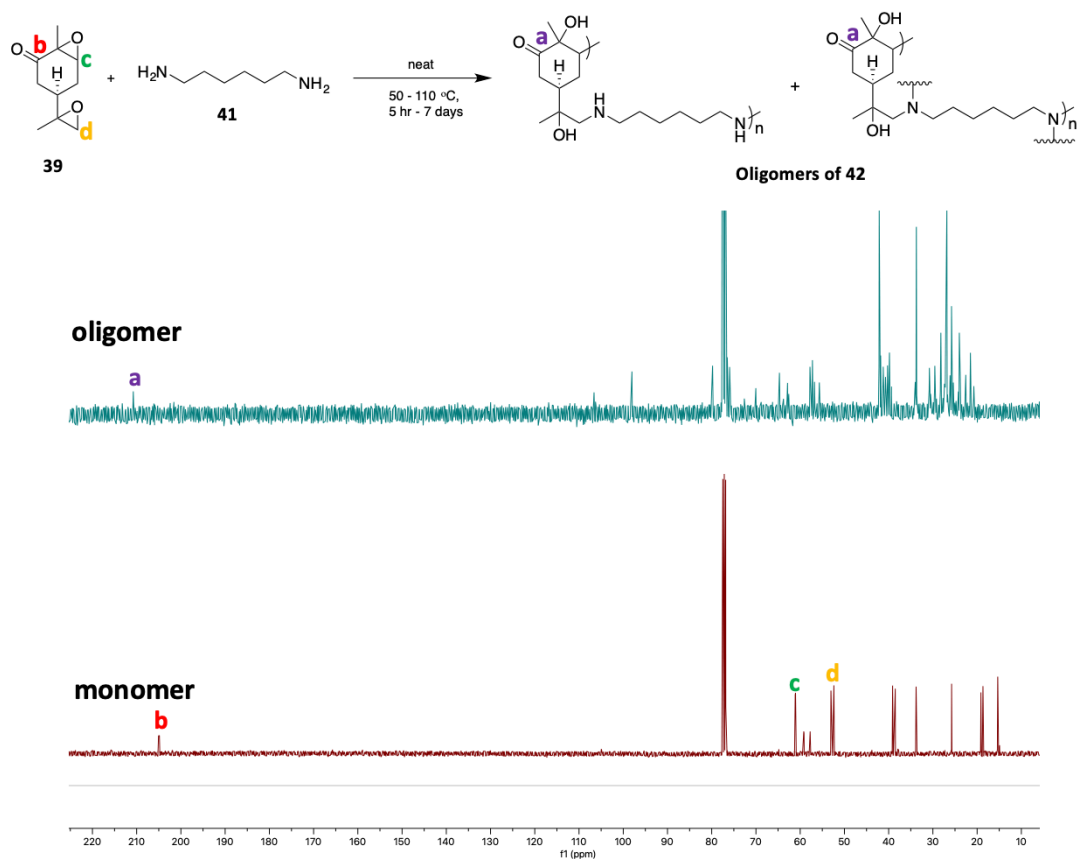


**Figure 60.** The reaction of carvone bis-epoxide with the primary diamine, showing predicted possible structures of the polymer networks formed (top). The  $^{13}\text{C}$  NMR for the sample conducted at 20 °C is shown below stacked against the bis-epoxide monomer. The resonance at 210.8 ppm indicates a ketone functionality (**a**), which is different from that of the monomer (**b**, 205.5 ppm).

Upon further inspection of the  $^{13}\text{C}$  NMR for the 70 °C reaction, another quaternary carbon peak was evident at 173.1 ppm which is not present in the sample conducted at 20 °C. This is the region where resonances relating to imines would occur, and as such it was hypothesised that at higher temperatures a condensation reaction was occurring between the primary amine and ketone resulting in the Schiff base moiety. It is clear that not all terpene monomers undergo this condensation, as the ketone resonance at 211.05 ppm is also visible in the NMR. It is likely that this condensation occurs after the initial polymerisation (*via* ring opening of the

epoxides), and probably as a form of cross-linking of the polymer structures. It is also possible that it occurs intra-molecularly. As a result, it is expected that the polymers conducted at temperatures above 70 °C are made up of combinations of the structures described in **Figure 46**.

Further analysis by 2D HSQC NMR showed that a resonance at 98.0 ppm on the  $^{13}\text{C}$  NMR was that of a primary C-H carbon, as determined by the corresponding DEPT spectrum (**Figure 46**). A primary carbon in this region is likely the result of the ring-opening of the endocyclic epoxide, resulting in a proton in the  $\alpha$ -position to an amine and  $\beta$ - to an alcohol. Ring-opening of the exocyclic epoxide would result instead in a secondary  $\text{CH}_2$  carbon. This is further evidence that the endocyclic epoxide is participating in the reaction, though again it is not clear whether or not this resonance occurs in the ketone-containing or imine-containing polymers (no correlation was seen in HMBC NMR for either).

It is reasonable to assume that if the endo-cyclic epoxide is participating in the reaction, then so too must the exocyclic one, as it is less sterically hindered and more likely to react first with the amine comonomer. The structures for these polymer networks are therefore predicted to be as described in **Figures 61** and **62**.

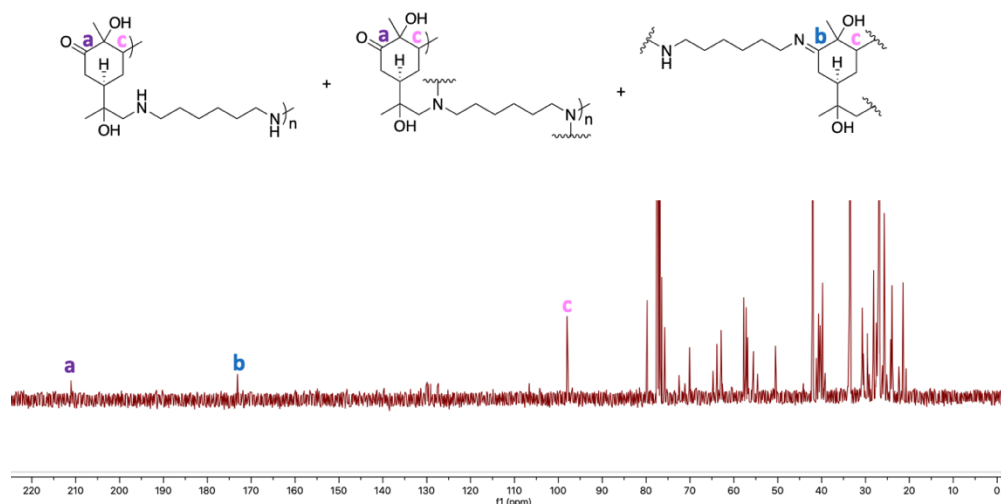
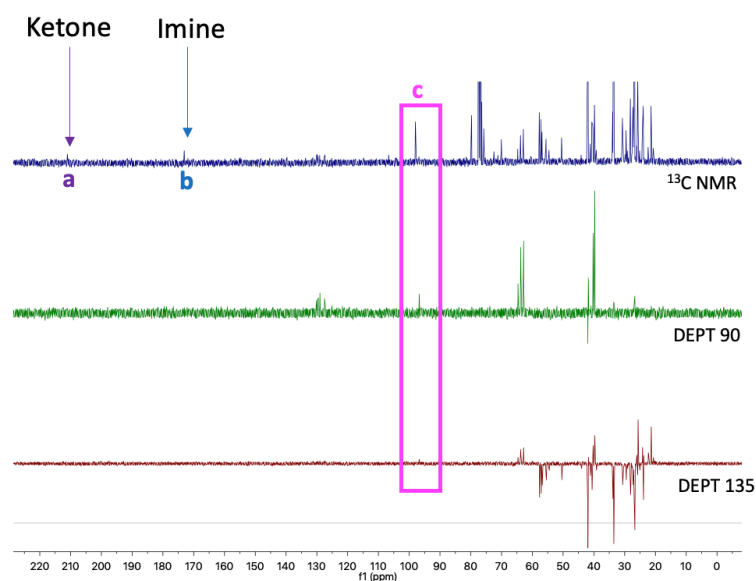
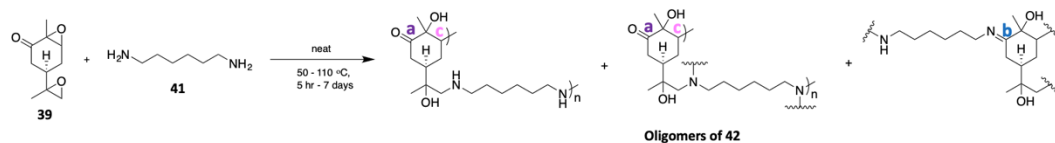


**Figure 61.**  $^{13}\text{C}$  NMR and corresponding predicted structures of the oligomer-42, cured at 70 °C over 5 hours. 'a' indicates a ketone resonance found at 211.05 ppm while 'b' indicates an imine at 173.1 ppm. 'c' corresponds to a CH resonance at 98.0 ppm which could be a result of either of the three structures.



HSQC:  $^1\text{H}$  vs  $^{13}\text{C}$  NMR

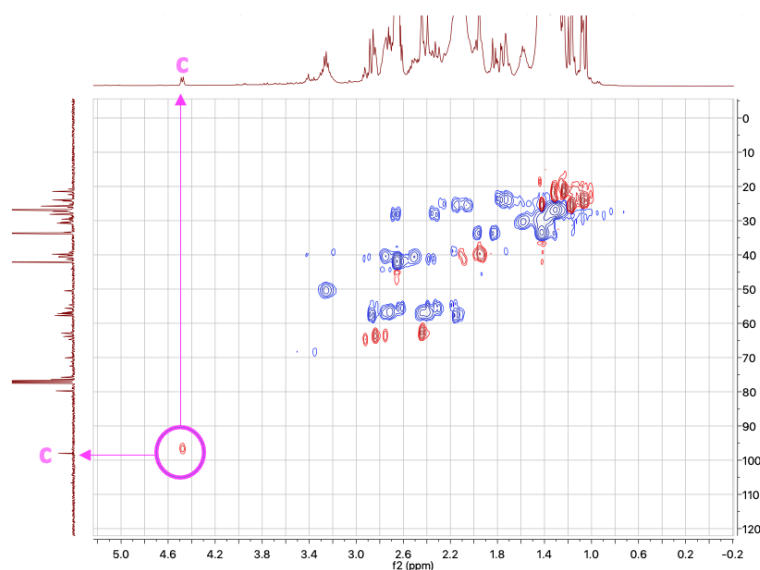


**Figure 62.** DEPT NMRs and HSQC NMR indicating that the resonance at 98.0 ppm ( $^{13}\text{C}$ )/ 4.45 ppm ( $^1\text{H}$ ) is that of a primary C-H carbon. This is likely to be the result of the ring-opening of the endocyclic epoxide in either the ketone-containing or imine-containing polymers.

The solubility of the polymer samples also proved suitable to allow their analysis by gel permeation chromatography (GPC). In each case, the

concentration was carefully maintained at  $2 \text{ mg}\cdot\text{mL}^{-1}$  for each sample, which were run on Mixed E columns (optimised for systems  $<20,000 \text{ g}\cdot\text{mol}^{-1}$ ), using THF as an eluent and analysed using polycaprolactone standards. The results indicated the presence of oligomers, ranging from  $\sim 1200\text{--}4500 \text{ g}\cdot\text{mol}^{-1}$  and with dispersities ( $\mathcal{D}$ ) ranging from 1.44 – 2.32 (**Table 6, Figure 63**). Unfortunately, no pattern could be distinguished from the data to correlate increasing temperature with increasing molecular weight. However, the polymerisations conducted at  $90 \text{ }^\circ\text{C}$  and  $110 \text{ }^\circ\text{C}$  appeared the most successful by GPC: given that the concentrations of each sample were kept the same, the chromatogram indicates these high temperature reactions contain higher mass fractions of higher molecular weight populations (**Figure 63**). It was also evident that reactions conducted between  $0 \text{ }^\circ\text{C}$  and  $50 \text{ }^\circ\text{C}$  contained very small concentrations of oligomers. It was anticipated that in these cases the reactions involved the formation of dimers or trimers only (given that NMR spectroscopy indicated that the reaction proceeded to some extent), while higher temperatures were required to form longer chains. However, it is important to consider that these oligomers are most likely highly branched and not best analysed by comparison to linear polycaprolactone chains.

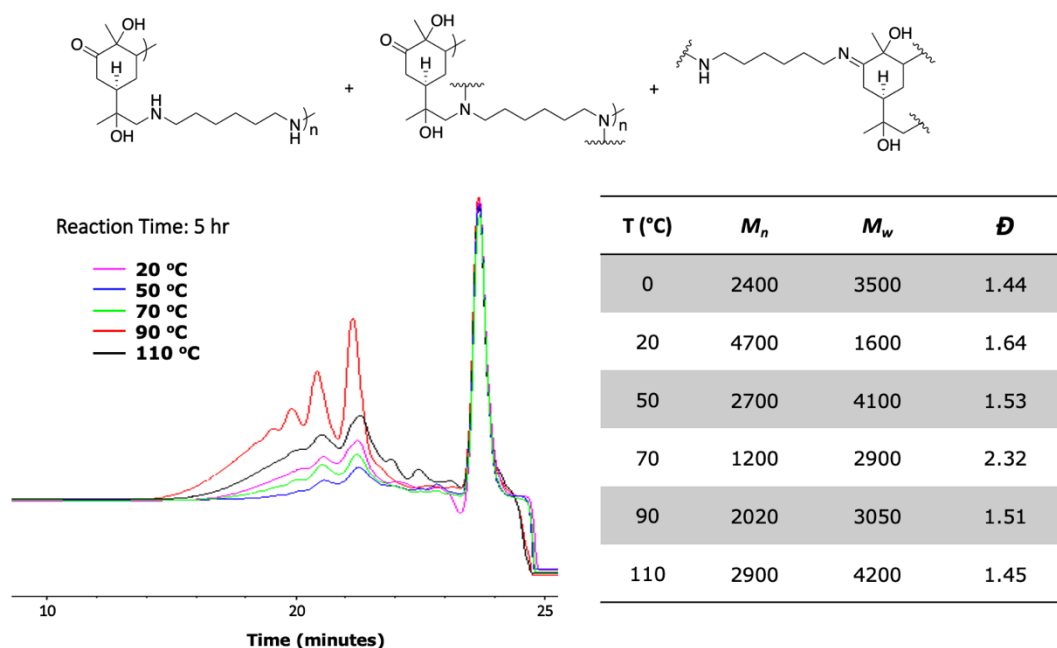


**Figure 63 and Table 6.** GPC chromatogram (left) of the  $\beta$ -amino alcohol oligomer networks formed from the curing of carvone-bis-epoxide with 1,6-hexane diamine, at temperatures ranging from 20 °C to 110 °C, over five hours. The corresponding data obtained from the GPC analysis is presented in **Table 6** (right).

As the oligomers were found to be of low molecular weight and most likely branched structures, mass spectrometry was investigated in order to gain precise insight into both the structures and lengths of each samples. In each case, the smallest addition product involving the reaction of one amine moiety with one terpene was present. There are three ways in which this could occur: first, by the reaction of the amine with the exocyclic epoxide or, second, with the endocyclic epoxide (**Figure 64 compounds A and B**). These addition products have identical masses and so it is not possible to distinguish between the two using mass spectrometry. A third product is also possible, involving the condensation of the ketone with the amine (**Figure 64, compound C**). This product has a different mass to the epoxide-addition products, allowing its identification.

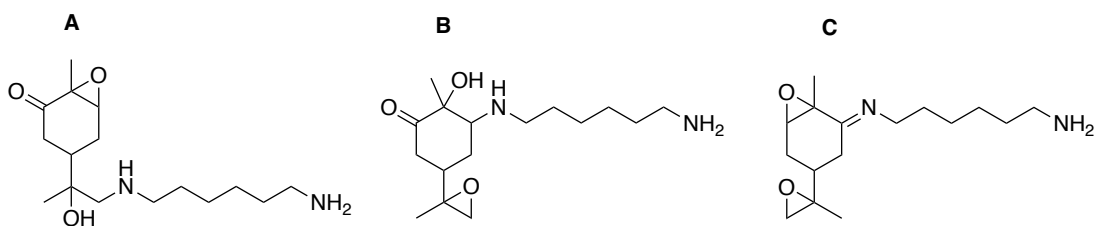


**Figure 64.** The three possible products following a single reaction of 1,6-hexane diamine with carvone bis-epoxide.

In the case of each reaction at the given temperatures, masses for both the epoxide addition reaction and the ketone condensation were found, indicating all three mechanisms (or at least the imine formation and one of the epoxide-additions) were occurring in the first instance in the reaction. The possible growth of these 'dimers' to longer oligomers of these compounds was then looked for, keeping in mind the general mechanism of step-growth polymerisation, in which small oligomers are first formed which then react together to form longer chains.<sup>216</sup> This differs from chain-growth in which the growth of the polymers occurs sequentially from only one reactive point in the chain. Again, in each case a number of  $m/z$  compounds were identified relating to the oligomeric structures, corresponding to degrees of polymerisation (DPs) up to 7 (where one amine added to a terpene, i.e. the structures in **Figure 65**, would have DP=2). In each of these cases it was interesting to note that polymerisation seemed to proceed *via* the condensation reaction and one epoxide ring-opening reaction (assumed to be the exocyclic one), rather than by the ring-opening of the epoxides alone (**Figure 65**). It was found that there were more examples by mass spec. of oligomeric combinations in samples conducted at lower temperatures, with only a selection of oligomers with DPs of 5 found in samples conducted above 70 °C (**Figure 66**). This is hypothesised to be because at higher temperatures the chains will have sufficient energy to react together to form longer oligomers, which are then not detected by mass spec. Instead, these longer chain oligomers are seen by GPC, corresponding to the higher mass fractions of higher molecular weights (**Figure 63**).

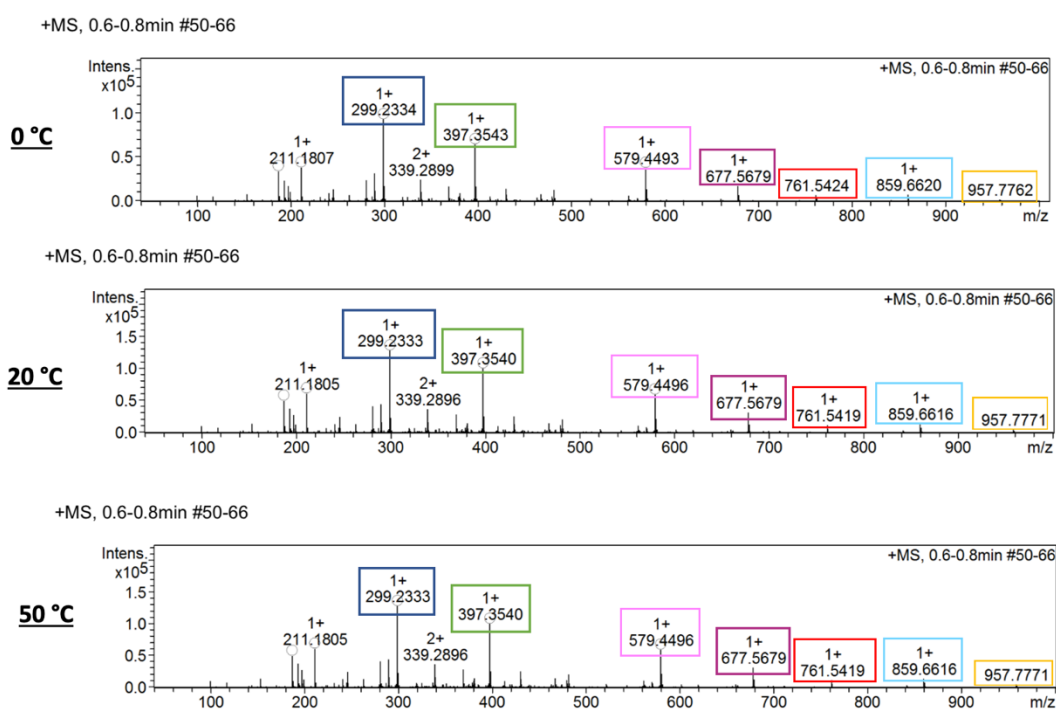
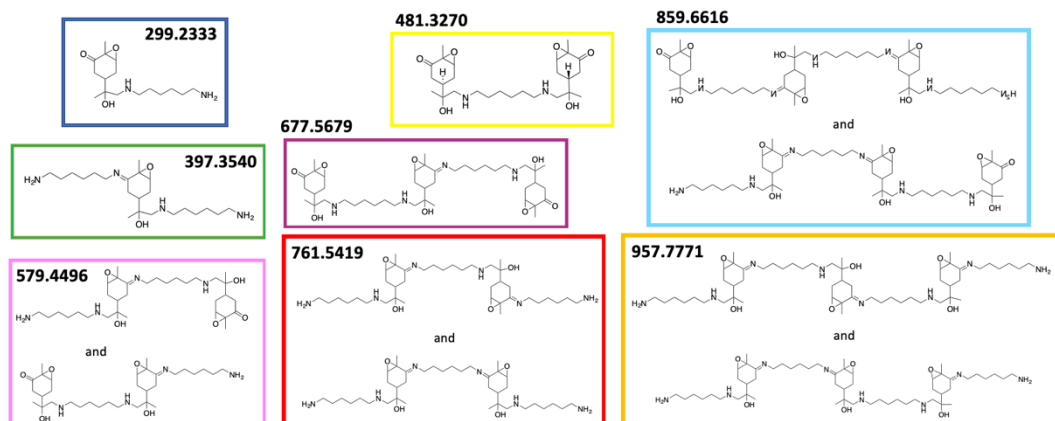
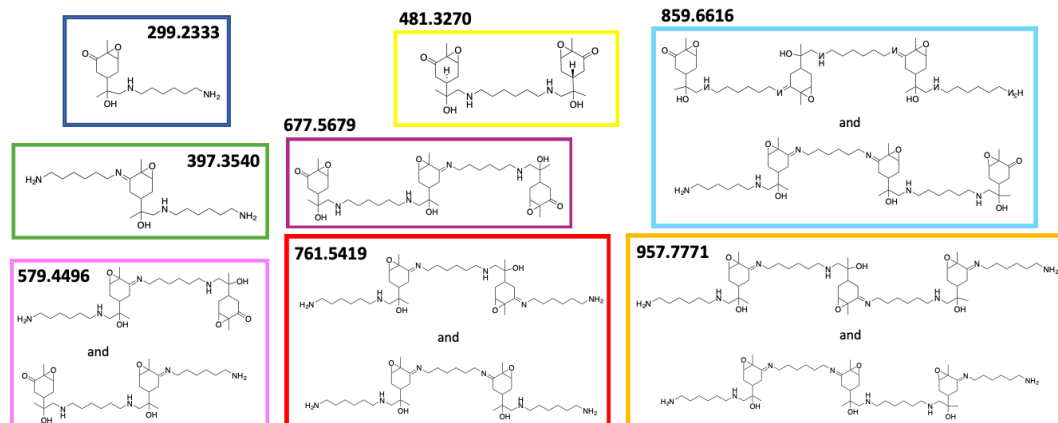
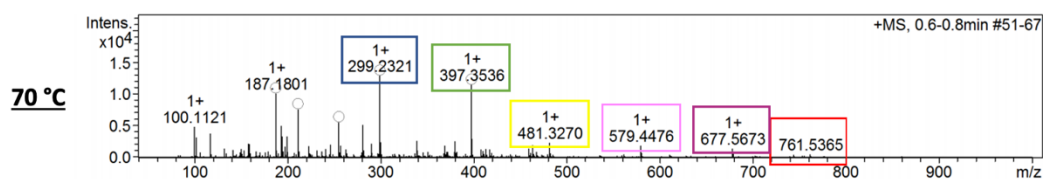


**Figure 65.** Mass spectrometry results from the reactions conducted at 0 °C, 20 °C and 50 °C, of carvone bis-epoxide and 1,6-hexane diamine. Oligomers up to DP = 7 were identified.

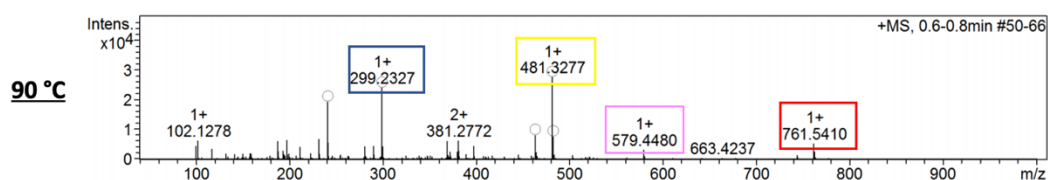




+MS, 0.6-0.8min #51-67



+MS, 0.6-0.8min #50-66



+MS, 0.6-0.8min #51-67

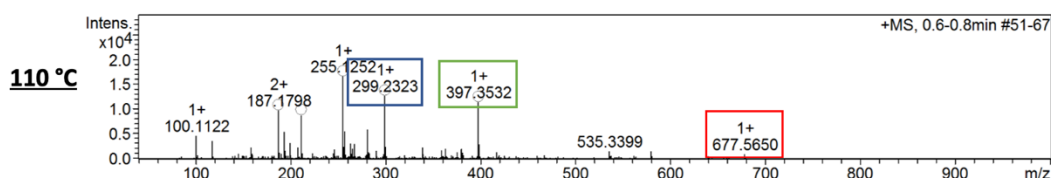


**Figure 66.** Mass spectrometry results of the reactions conducted at 70 °C, 90 °C and 110 °C, of carvone bis-epoxide and 1,6-hexane diamine. Oligomers of up to DP = 5 were found. It is anticipated that these samples did contain higher molecular weight oligomers, which were not detectable by mass spectrometry.

There were some discrepancies between the conclusions drawn between the mass spectrometry results and those of the NMR, for example in the  $^{13}\text{C}$  NMR of the sample conducted at 50 °C, no imine resonance was visible, though according to mass spectrometry this group is central to the progression of the polymerisation. It is important to remember that while

mass spectrometry is very precise, it is also not quantitative, and only molecules which can 'fly' well will be detected. It is possible that the results shown are of smaller quantities of the oligomers that were not fully reacted, which were not able to be removed from the sample by precipitation, as an adequate solvent/ antisolvent system was not found. The samples cured at higher temperatures also proved much less soluble in the required solvents for sample analysis than the ones cured  $\leq 50$  °C, which may have affected the data that resulted, as the samples obtained may have not been a true representation of the entire product. It is likely that all three reactions (condensation of the ketone and ring opening of the exo- and endo-cyclic epoxides) occur to bring about polymerisation. It was concluded that higher reaction temperatures resulted in higher degrees of branching; evidence for this is that these samples were less soluble than the others in a range of solvents, and became darker in colour with increasing temperature. It is likely that the formation of networks of oligomers rather than linear ones was highly likely in *each* case, as there are a variety of reactive groups in each of the monomer components. As such, references to linear molecular weights (for example using polycaprolactone standards in GPC analysis) become less relevant to these types of polymer samples, and their exact structures become harder to determine.

### 3.3.3.2 Time Screen

Considering the general mechanism for step-growth polymerisations, when the molecular weight is plotted against monomer conversion, it is found that the  $M_n$  does not increase rapidly in the initial and middle stages of the reaction, but accelerates rapidly towards the end.<sup>217</sup> It was therefore investigated whether longer reaction times could bring about more uniform populations with dispersities close to 2, as would be considered ideal for step-growth systems.<sup>217,218</sup> As such, the reaction was conducted in the same way: 4.31 mmol of the terpene was mixed with the same molar ratio of amine and they were stirred together in a vial over a 24, 48 and 72 hours. The temperature for each was maintained at 20 °C.

In each case, oligomers ranging from 1000 – 4500 g·mol<sup>-1</sup> were detected (**Table 7**), but with no trend found to correlate the increase of molecular weight with increase of reaction time. The chromatograms showed the results were very similar to those seen for the reaction conducted over 5 hours, with a single population of a broad dispersity of molecular weights (**Figure 67**).

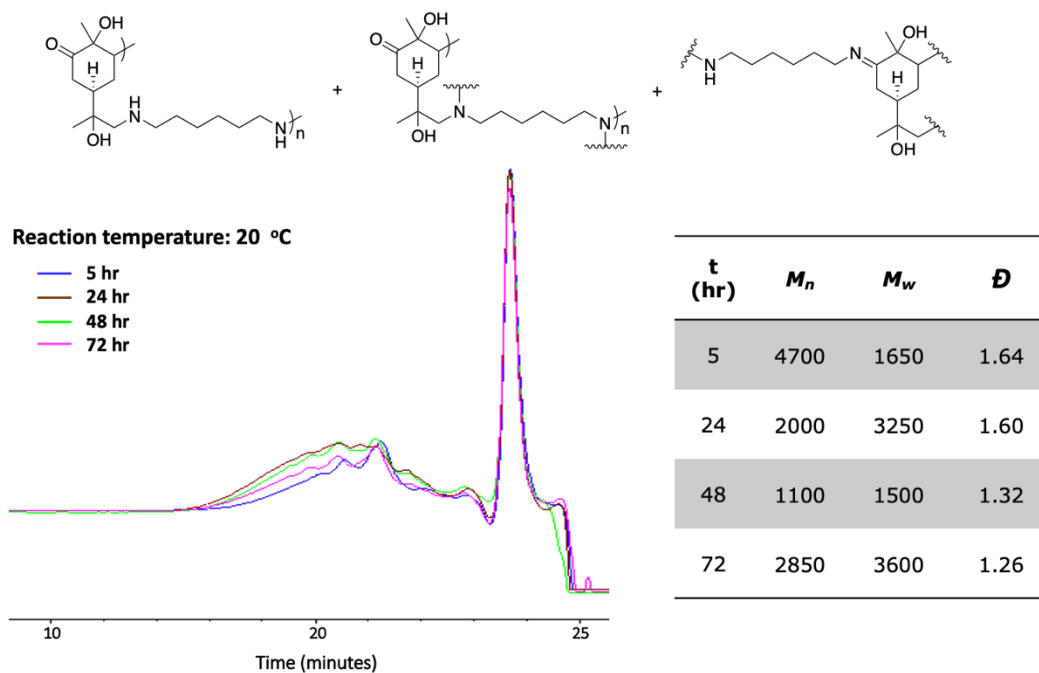


**Figure 67.** GPC chromatogram of the  $\beta$ -amino alcohol oligomers formed from the curing reaction between carvone bis-epoxide and 1,6-hexane diamine at 20 °C over a range of times from 5 – 72 hours and the corresponding data (**Table 7**, right).

All of the polymers synthesised over the range of temperatures and times were found to be soluble in only a small selection of solvents. It was found that most of the systems were not water-soluble at all, with only a small subset of those cured at low temperatures (50 °C) dissolving poorly in water. This was attributed to the high number of reactive sites of both the terpene and diamine co-monomer, which was likely to have caused branching and crosslinking in the oligomers. In future works, it could be possible to monitor these reactions with FTIR, or react-IR. However, as a result of this branching, the likelihood of taking these oligomers forward for the purpose of biomaterials was therefore slim, and so it was decided to instead focus attention on the synthesis of similar systems composed of ideally only linear polymers, with the aim of generating water-soluble material that could be easily analysed and used to investigate antimicrobial and biomaterial applications.

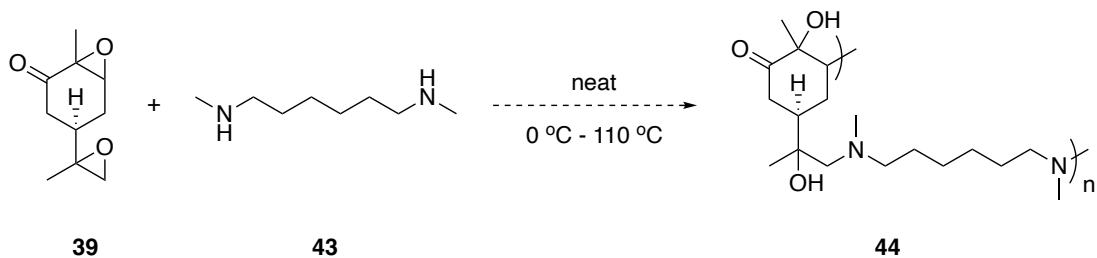
### 3.3.4 Synthesis Two of $\beta$ -amino alcohol oligomers

The curing of carvone bis-epoxide with 1,6-hexane diamine resulted in complex products that were difficult to analyse. This was a result of three reactive groups in the terpene monomer (the ketone and both epoxides), in addition to four points of reactivity in the diamine (each primary amine can react twice to form polymers), resulting in hyperbranched systems. It was decided to focus instead on the synthesis of polymers that would react in a more simple, linear mechanism, minimising the possibility of branching occurring. It was hypothesised that this would produce polymers that were easier to analyse and more soluble in a wider variety of biologically compatible solvents.

It was decided therefore to substitute the di-primary diamine used in the previous studies with *N,N*-dimethyl-1,6-hexane diamine (**43**), in similar curing reactions with carvone bis-epoxide (**39**). In this instance, each amine moiety in the compound has already been methylated once, resulting in two di-secondary amine reactive groups. This is advantageous for two reasons:

1. It is anticipated that each amine will only react once with an epoxide, meaning the molar ratio of epoxide/ amine reactive groups is 1:1 rather than 1:2 as before. In this way the generation of hyperbranched systems *via* the amine moieties is much less likely.
2. It is anticipated that in these reactions the condensation of the ketone is unlikely to occur, as it would result in the formation of an iminium ion, which is much less energetically favourable to form than an imine, as it is a charged species.

For these reasons it is predicted therefore that exclusively linear polymers will form in these reactions, which it is anticipated should be easier to analyse (**Scheme 31**).



**Scheme 31.** The proposed reaction of carvone bis-epoxide (**39**) with N,N-dimethyl-1,6-hexane diamine (**43**) to produce linear polymer (**44**).

In aiming to keep the reaction as 'green' as possible in terms of the synthesis, and following the results seen with the primary diamine system in the previous section, it was decided to investigate the reaction of these compounds in the absence of additional components such as catalysts or initiators. Similar reaction conditions to those used previously were therefore investigated in this case: 3.47 mmol (0.5 g) of the liquid diamine was added to the same molar ratio (3.47 mmol/ 0.63 g) of the bis-epoxide and three screens were then conducted: a temperature screen, a time screen, and additionally, a solvent screen.

#### 3.3.4.1 Temperature screen

The temperature screen was conducted in a similar way to that of the di-primary diamine systems: the two components were stirred together at temperatures ranging from 0 °C to 110 °C, for 5 hours in the absence of additional components such as catalysts or solvents. The vials were once again capped but pierced with a needle to expose the reaction to air, which was found to help reduce the product condensation seen forming on the edges of the vial.

After 5 hours each of the samples appeared orange-brown in colour (with the exception of the sample conducted at 0 °C), with samples appearing darker or more brown as the reaction temperature increased. This darkening appeared to correspond to an increase in viscosity of the samples: the sample conducted at 0 °C which was more orange-yellow in

colour and very non-viscous; the vial could not be inverted without spilling the sample (**figure 68**). All other samples could be inverted however the samples conducted at 20 °C and 50 °C could not be kept like this for long periods, as the mixtures quickly began to drip down the sides of the vial. It was anticipated that both the colours and the viscosities of the samples was a result of either higher molecular weight oligomers or polymers in the samples conducted at higher temperatures, and/or, higher mass-fractions of these higher molecular weight populations in these samples (as seen in the previous study with the di-primary diamine). A number of analytical studies were therefore conducted to investigate this. Beforehand, a range of solvent/antisolvent systems were investigated in order to try and separate out any high molecular weight portions from the rest of the sample by precipitation. However, unfortunately no reliable method could be established, with most solvents dissolving both the polymer and monomer species. Instead, as there were no coupling agents, catalysts or solvents used in the reaction, and the samples were thus made up entirely of the reacting components (and their products), it was decided to take forward the entirety of the sample for analysis and further investigation without purification.

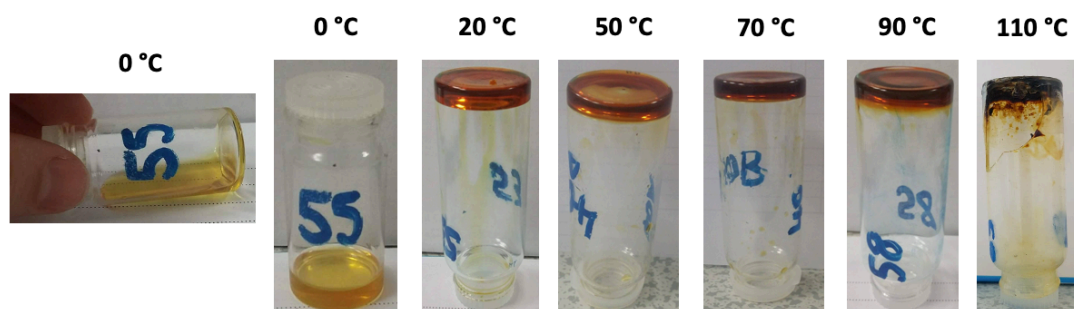


**Figure 68.** The results of carvone-bis epoxide cured with di-secondary diamine, *N,N*-dimethyl-1,6-hexane diamine, for 5 hours at temperatures ranging from 0 °C to 110 °C.

In the first instance, NMR and IR analyses were used to determine the structures of the samples and to investigate if the reaction had successfully proceeded in each case. Both of these techniques confirmed that for the

samples conducted at 0 °C and 20 °C, no reaction had occurred, and the spectra were simply the sum of the two monomers together in solution (**Figure 69**).

The  $^1\text{H}$  NMR revealed similar, complex spectra for samples conducted at temperatures  $\geq 50$  °C. These spectra were found to be absent of any trace of the bis-epoxide monomer, according to the disappearance of the characteristic monomer resonance at 3.44 ppm (representing the proton  $\alpha$ - to the endocyclic epoxide). This would indicate that the terpene monomer had been completely consumed in each case (except those conducted at 0 and 20 °C) (**Figure 69**).

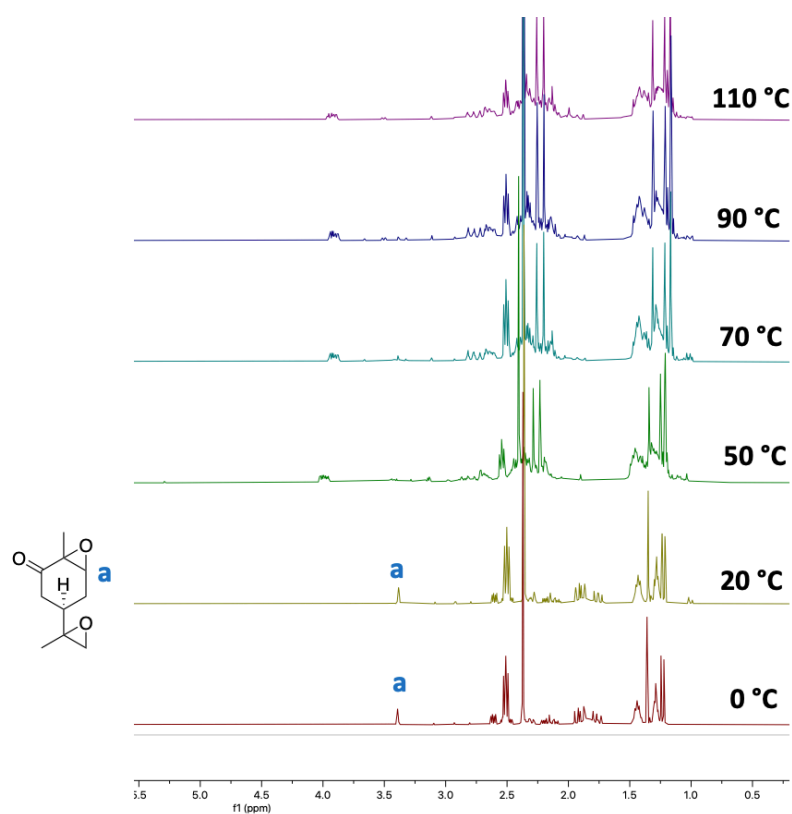


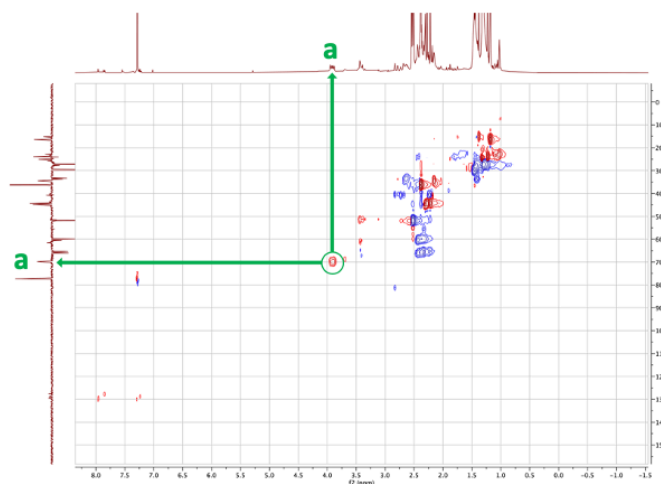
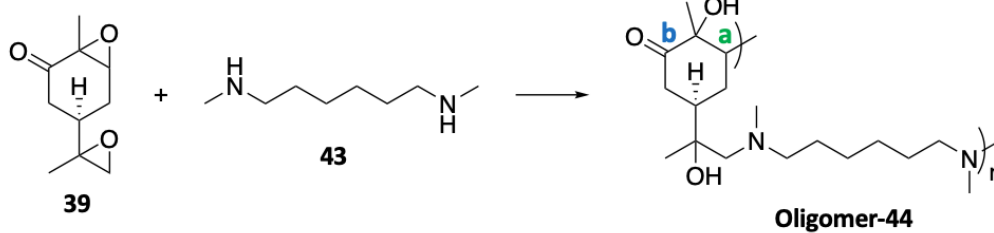
**Figure 69.**  $^1\text{H}$  NMR spectra of the curing of carvone bis-epoxide with di-secondary diamine **43** over 5 hours at temperatures ranging from 0 °C to 110 °C. Samples conducted  $< 50$  °C returned the two monomers with no reaction while samples conducted above 50 °C did react, revealing similar complex spectra in each case.



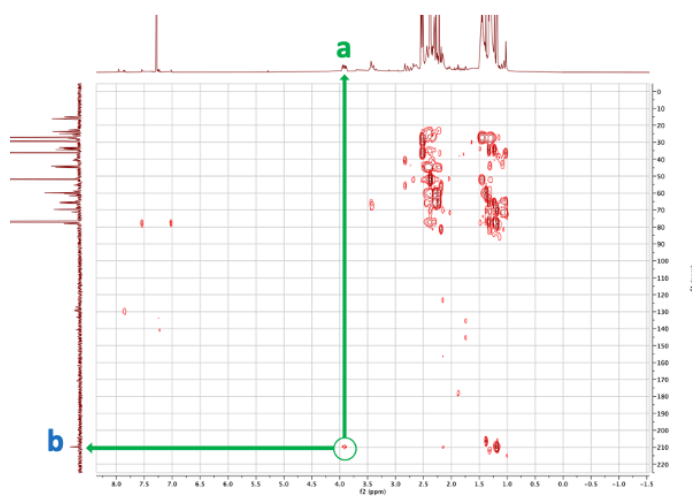
The IR spectra for samples conducted  $\geq 50$  °C showed the presence of the characteristic carbonyl stretch at  $\sim 1731$   $\text{cm}^{-1}$ ; a shift from  $1704$   $\text{cm}^{-1}$  in the monomer. As expected, there was no evidence to suggest condensation of the ketone was occurring in this instance, with no iminium stretch identifiable in any of the samples' spectra.<sup>215</sup> The hydroxyl stretch appeared slightly lower than expected, with a broad stretch at  $\sim 3300$   $\text{cm}^{-1}$  for samples conducted  $\geq 50$  °C, suggesting intermolecular hydrogen bonding between the oligomer or polymer chains.

As with the oligomers formed from the di-primary diamine, the  $^1\text{H}$  NMR spectra for each successfully-reacted sample was quite complex and end groups could not be distinguished. As such, the spectra were not diagnostic in terms of determining the degree of polymerisation, and similarly yields for the oligomers could not be accurately obtained in the usual way, especially considering the oligomers could not be separated or purified by precipitation.

While much of the  $^1\text{H}$  NMR spectrum was complex and indecipherable, nonetheless it was useful in determining the mode of propagation of the polymerisation. In the spectra of each of the successful polymer samples (i.e. those conducted  $\geq 50$  °C), a multiplet was evident by  $^1\text{H}$  NMR ranging from 3.97 – 3.83 ppm, which was found using DEPT and 2D techniques to be that of a tertiary C-H carbon. This resonance was therefore assigned to the proton  $\alpha$ - to the amine and  $\beta$ - to the tertiary alcohol, formed as a result of ring opening of the endocyclic epoxide (**Figure 70, a**). As before with the primary amine resins (section 3.3.3), where ring-opening of the endocyclic epoxide occurs, it is reasonable to assume that this will also occur at the exocyclic epoxide, which is more likely to undergo the reaction due to both steric and electronic factors. The use of 2D HMBC NMR shows that this multiplet correlates with a quaternary centre at 210.0 ppm on the  $^{13}\text{C}$  NMR, indicating the retention of the ketone in the polymer chains (**Figure 70, b**). No iminium resonance is present in the  $^{13}\text{C}$  NMR, and as such it can further be deemed unlikely that propagation occurs *via* the formation of an iminium bond, leaving ring-opening of both epoxides as the most likely modes of polymerisation. It may therefore be concluded that the oligomer structures are as predicted (shown in **Figure 70**).



**HSQC NMR:  $^1\text{H}$  v  $^{13}\text{C}$ ; 1-J**



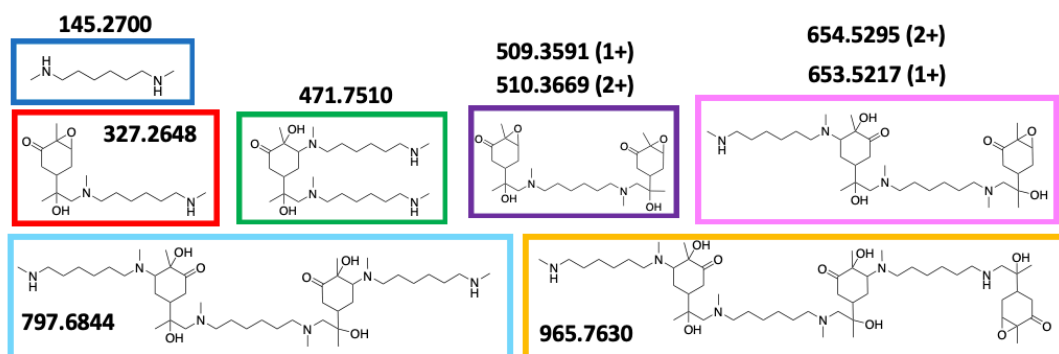
**HMBC NMR:  $^1\text{H}$  v  $^{13}\text{C}$ ; 3-J**

**Figure 70:** The 2D HSQC (left) and HMBC (right) NMR spectra used to confirm the structure of the oligomer **44**. The HSQC shows that the multiplet 'a' on the  $^1\text{H}$  NMR is shown to be 1-bond from a CH tertiary carbon, while the correlation on the HMBC indicates it is 3-bonds away from the ketone (b).

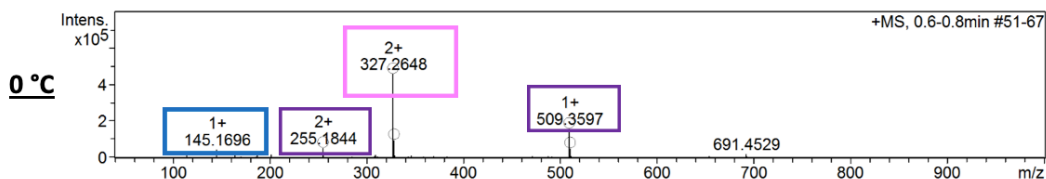
It was considered unlikely that crosslinking or branching was occurring in these reactions: each secondary amine becomes tertiary after a single addition to an epoxide group, rendering the species unlikely to undergo nucleophilic attack a second time. The ratio of reactive-amine/epoxy groups was therefore closely kept 1:1 (taking the purity of the epoxide into consideration), so consequently minimal cross-linking would be expected to occur between the end groups of the oligomers.<sup>107</sup> Additionally, when considering the base-catalysed method for the ring-opening of epoxides, this would generate only tertiary alcohol groups in this instance, which are sterically hindered and do not readily undergo nucleophilic attack.<sup>219</sup> While the acid-catalysed product would, on the other hand, generate a primary and secondary alcohol with greater potential for crosslinking, the probability of these species forming is considered highly unlikely, due to the presence of the basic diamine monomer.<sup>107</sup> As such, crosslinking or branching in the samples was ruled out, and it was concluded that exclusively linear oligomer chains were forming in this instance.

To begin to get an insight into the lengths of polymer samples, mass spectrometry analysis was first employed. In each case (regardless of temperature), oligomers up to approximately  $500 \text{ g}\cdot\text{mol}^{-1}$  were detected, corresponding to trimers. Each sample (except for the one at  $110 \text{ }^\circ\text{C}$ ) also contained dimers, and the diamine monomer (**Figures 71** and **72**). With leftover, unreacted diamine detected by mass spec, it is likely that the end groups of the oligomers are also amine-terminated, rather than epoxide-terminated. This corresponds to the data observed in NMR.

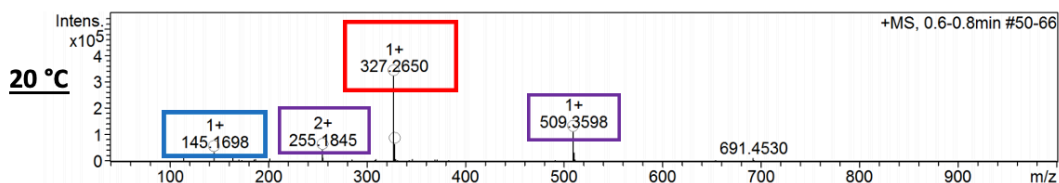
Generally speaking, the mass spec. results were relatively uniform in the species detected for each sample, without great variation based on the temperature of the reaction. However, it is important to remember that mass spectrometry is not quantitative and techniques such as NMR would be much more accurate in describing the species present. This is evident in the fact that by NMR, no reaction seemed to have occurred at  $0 \text{ }^\circ\text{C}$  and  $20 \text{ }^\circ\text{C}$ , however the samples by mass spec reveal trimers and even tetramers are forming. The  $m/z$  results detected by mass spec may be very minute traces being detected.



+MS, 0.6-0.8min #51-67



+MS, 0.6-0.8min #50-66



+MS, 0.6-0.8min #51-67

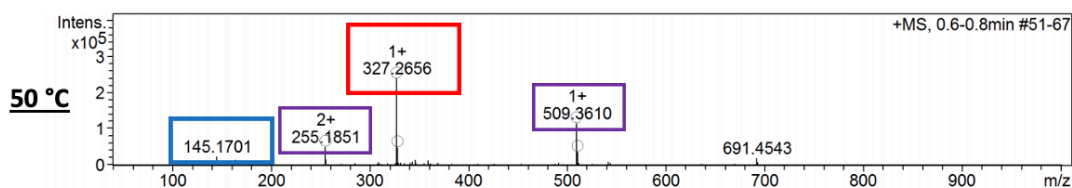


**Figure 71.** Mass Spectrometry results of the oligomer-44 sample. Oligomers of up to DP = 3 were found. It is anticipated that these samples did contain higher molecular weight oligomers, which were not detectable by mass spectrometry.

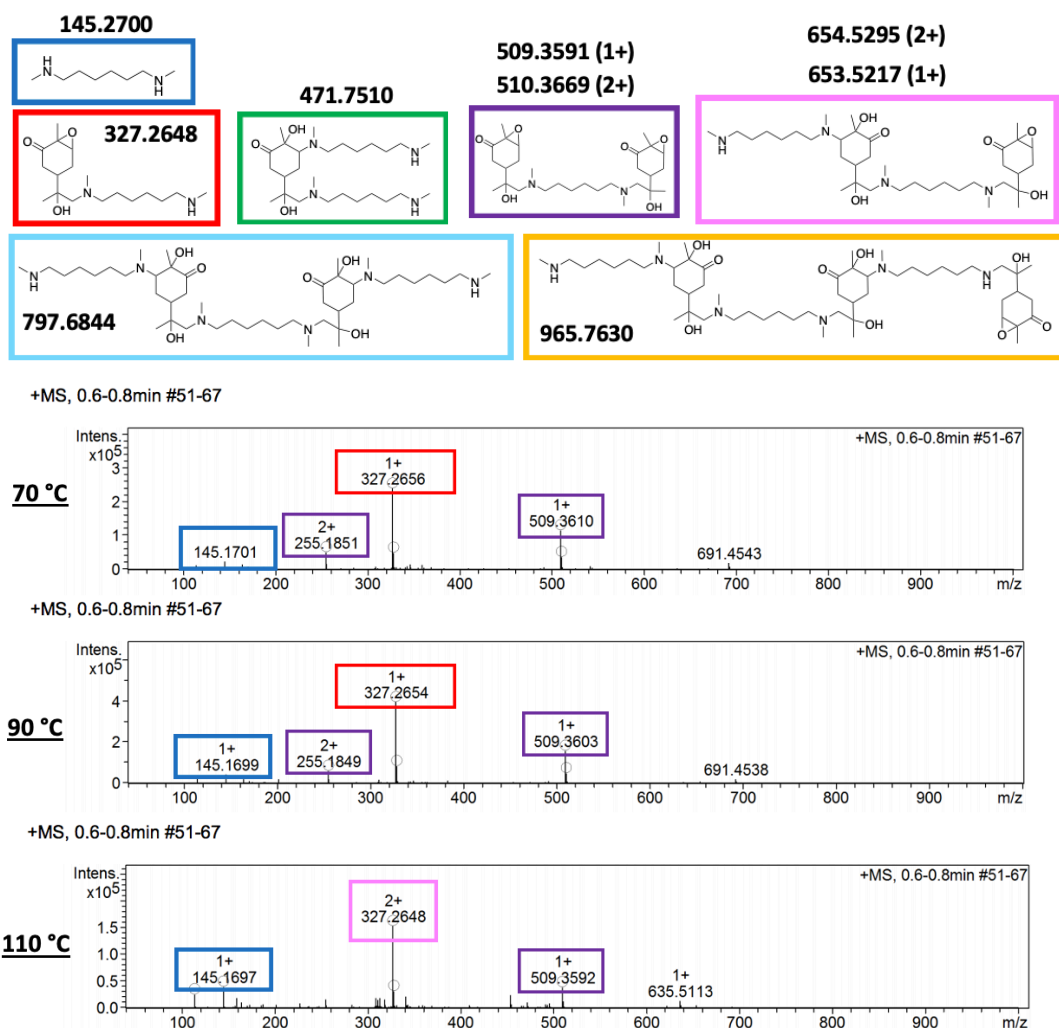


**Figure 72.** Mass spectrometry results of the oligomer **44** sample. Oligomers up to DP = 3 were detected. It is anticipated that these samples did contain higher molecular weight oligomers, which were not detectable by mass spectrometry.

As in the previous study (section 3.3.3), it is hypothesised that samples of larger molecular weights do not fly well or are outside of the detectable limit of mass spectrometry. As such, the samples were also analysed by GPC. As before when analysing the systems made from the di-primary diamine (section 3.3.3), the samples were run on mixed E columns using THF as an eluent. The  $dn/dc$  for these particular systems was not determined, so polycaprolactone standards were used to identify the

molecular weights of the species. Each of the samples were made to the same concentration of 3 mg mL<sup>-1</sup> in THF.

The results confirmed that samples conducted at temperatures of 0 °C and 20 °C did not form any oligo- or polymeric material, corresponding to the NMR results and suggesting that the masses found in mass spectrometry are only minute traces. Reactions conducted  $\geq 70$  °C successfully underwent the polymerisation reaction, while the sample at 50 °C featured only a small population of low molecular weight material which had undergone the reaction (**Figure 73**). Correlating this to the NMR results, it is likely that in this case only dimers or trimers were forming: the bis-epoxide is completely consumed (by <sup>1</sup>H NMR), although the material is not of very high molecular weight (by GPC), nor is the mass-fraction of this material in the sample very significant.

In each case where the reaction was found to have occurred, a broad dispersity of molecular weights was formed rather than a single population. In each case the samples were made to be the same concentration (3 mg·mL<sup>-1</sup>), which allowed for the comparison of the mass-fractions in each sample. It was thus shown that an increase in temperature was found to correspond to an increase in the mass fraction of oligomers of higher molecular weights (**Figure 73**); the sample conducted at 110 °C in particular was found to contain significantly higher mass-fractions of oligomers of higher molecular weights.

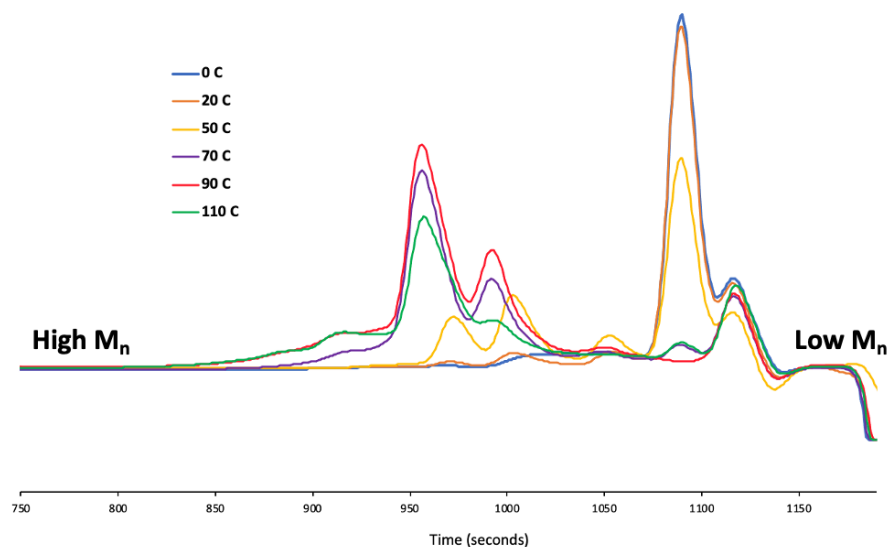


**Figure 73.** GPC chromatogram resulting from the curing of carvone bis-epoxide with 1,6-dimethyl hexane diamine for five hours, at temperatures ranging from 0 °C to 110 °C. No polymerisation occurred for samples conducted below 50 °C (orange and blue traces). The rest were found to form populations of short chain oligomers.

While the GPC traces suggest the presence of multiple populations of oligomers (as often seen on Mixed E columns<sup>220</sup>), to establish molecular weights of the samples the chromatogram was integrated over all of these populations, encompassing the full dispersity of molecular weights. In the case of the samples conducted at 0 °C and 20 °C, no populations of polymers could be detected by GPC analysis; these traces found only monomer units (**Table 8**). The sample conducted at 50 °C was found to contain these monomer units, as well as small populations of low molecular weight oligomers, with an average molecular weight over all populations of approximately 260 g·mol<sup>-1</sup> (by  $M_w$ ), indicating DPs of <2 units, where one terpene and one alkyl-amine moiety would have DP = 2 (**Table 8**). The  $M_w$  and DP figures are not exact and are seemingly very small, as the data is taken an average over all populations in the sample.

The samples conducted at 70 °C and 90 °C featured broadly similar results to one another, with oligomers of approximately 460 and 520 g·mol<sup>-1</sup> by  $M_w$ , respectively. The final sample conducted at 110 °C may

be considered the most successful in terms of polymerisation, with DPs of 4 corresponding to molecular weights of  $\sim 670 \text{ g}\cdot\text{mol}^{-1}$  (by  $M_w$ ).

All of the samples had dispersities  $\leq 2$ . This figure is lower than what would be considered optimal for step-growth polymerisation according to the Flory and Carothers' equations.<sup>221-223</sup> Ideally, when the stoichiometry of the reacting components is kept 1:1 (as in this case), taking into account the purity of the samples, it follows that the dispersity of the samples should grow towards 2. A lower dispersity may refer to a stoichiometric imbalance, or that unreacted monomers remain in solution, or further reaction would be possible for the low molecular weight oligomers present in solution. The results are summarised in **Table 8**.

39 + 43  $\xrightarrow[\text{t (}^\circ\text{C)}]{\text{neat}}$  Oligomer-44

T (°C)	$M_n$ (g mol <sup>-1</sup> )	$M_w$ (g mol <sup>-1</sup> )	$\overline{D}$	DP
0	160	170	1.1	0
20	160	170	1.1	0
50	210	260	1.2	2
70	400	460	1.2	3
90	440	520	1.2	3
110	520	670	1.3	4

**Table 8.** GPC results from the curing of carvone bis-epoxide with 1,6-dimethyl-hexane diamine at temperatures ranging from 0 °C to 110 °C over 5 hours. GPC was conducted on mixed E columns using THF as an eluent and compared to polycaprolactone standards.

The values given in **Table 8** are rather imprecise as they refer to the  $M_w$  or 'weight-average' molecular weight of the entire population which, as



mentioned, is shown to be made up of different populations of oligomers. To gain a better insight into the lengths of oligomers that were present in each sample, in what amounts (by mass fraction), each somewhat-distinct segment on the chromatogram was integrated separately. Three distinct regions were thus identified amongst the samples: the first peak, **A**, was present in samples conducted from 0 °C – 50 °C, and considered to be the unreacted monomers. This sample constituted 100% of the mass-fractions of the samples conducted at 20 °C and below, with the increase in temperature corresponding to the decrease in mass fraction of this population to 52.9% for the 50 °C sample (see **Table 9** for specifics).

The second region, **B**, was present in all samples conducted  $\geq 50$  °C (**Figure 74**), and represented oligomer populations with an average molecular weight in this region ranging from  $\sim 750$  to  $1500 \text{ g}\cdot\text{mol}^{-1}$  by number-average molecular weight ( $M_n$ ) depending on which sample was being considered. This sample represented the highest mass fraction for all samples (except those conducted at 0 °C and 20 °C), making up between 47–100% of the samples  $\geq 50$  °C (**Table 9**).

For the samples conducted at 90 °C and 110 °C, a third population, **C**, was identified, which consisted of a shoulder to region **B**, but which was only present for reactions at these high temperatures. This region was found to contain higher molecular weight material (**Figure 74**), corresponding to  $M_n$  values of  $2720 \text{ g}\cdot\text{mol}^{-1}$  and  $4495 \text{ g}\cdot\text{mol}^{-1}$ , and mass fractions of 15.8% and 18.5%, for the two samples, respectively (**Table 9**). It is remarkable that the two  $M_n$  values for oligomers in this region are so different, despite overlapping on the chromatogram and being run at the same concentration, on the same column on the same day and analysed in the same way. It is concluded that these results show the 'crudeness' of GPC as a measure of the molecular weights of short oligomers, and the large margin of error that may arise as a result.

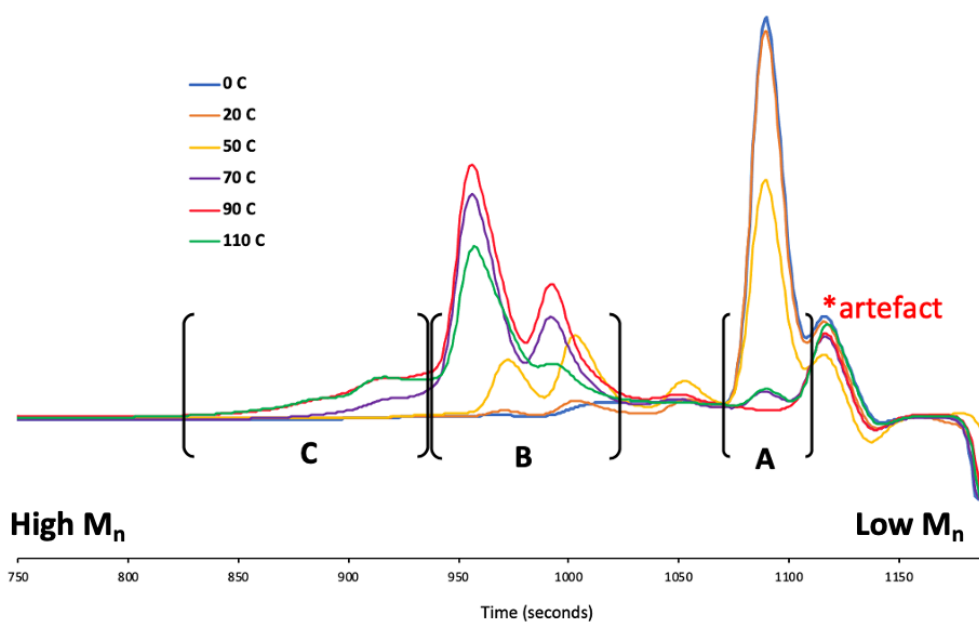


**Figure 74.** GPC results for the curing of carvone bis-epoxide with 1,6-dimethyl hexane diamine for 5 hours. To assist the analysis, the chromatogram was split into sections **A**, **B** and **C** to better predict the length of the polymer chains in the samples.

T (°C)	Peak A				Peak B				Peak C			
	Mn (g mol <sup>-1</sup> )	PDI	Mass Fraction (%)	DP	Mn (g mol <sup>-1</sup> )	PDI	Mass Fraction (%)	DP	Mn (g mol <sup>-1</sup> )	PDI	Mass Fraction (%)	DP
0	352	1.48	100	1	-	-	-	-	-	-	-	-
20	272	1.40	100	0	-	-	-	-	-	-	-	-
50	490	1.39	52.9	3	753	1.66	47.1	5	-	-	-	-
70	-	-	-	-	825	1.27	100	5	-	-	-	-
90	-	-	-	-	940	1.12	84.2	6	2720	1.07	15.8	17
110	-	-	-	-	1489	1.08	60	9	4495	1.21	18.5	28

**Table 9.** GPC results from the curing of carvone bis-epoxide with 1,6-dimethyl hexane diamine, obtained when the chromatogram is split into three segments as described in **Figure 74**. GPC was conducted on mixed E columns using a THF eluent and analysed using PCL standards.

In spite of discrepancies and difficulties analysing the GPC results, in each case it can be concluded that low molecular weight oligomers rather than polymers are formed from these reaction conditions. The majority of the oligomer chains in each sample (conducted above 50 °C) are likely to have DPs of up to 5 or 6, i.e. two or three terpenes with two or three alkyl-amine linker moieties which are likely to be the end groups. However, at this length the resolution of GPC is not optimised to distinguish between oligomers of this size, even using mixed E columns. It is important to bear this in mind and consider that there is likely a large degree of error involved in these data, as a result. The GPC data should be interpreted as a guideline as to the lengths and weights of the oligomer chains. Nonetheless, given the range of solubility of these oligomer samples in a wide range of solvents and even water, this is a good indication that the material might be suitable to be used in anti-fungal studies.

#### *3.3.4.2 Reaction Time Screen*

It was then decided to investigate whether the length of reaction time would have an effect on the chain length and  $M_n$  of the oligomers. The aim was two-fold:

1. To simply increase the molecular weight ( $M_w$  and  $M_n$ ) of the oligomers in general, seeing their conversion to longer oligomers.
2. To increase the mass fraction of oligomers of higher molecular weights, such as those in region **C** (**Figure 74**), especially where conversion to longer oligomers was not possible.

It was thought that perhaps this could be achieved through longer reaction times, giving the reacting species sufficient time to enter the exponential growth phase, according to the general step growth mechanism for polymers (in which the low molecular weight species join together to form longer polymer chains in the final stages).<sup>217</sup>

The reactions were conducted in the usual way: the two monomers were added together, neat, and stirred this time for up to 7 days, with samples also taken after 1 day and 4 days. This was repeated for temperatures of 20, 50 and 70 °C.

In each case it was evident by the GPC chromatograms that the longer reaction times allowed for the conversion of lower molecular weight materials to longer oligomer chains: a pattern emerges showing the decrease in the mass fraction of the lower molecular weight samples, as these are converted to longer chains, in turn growing the mass fractions of higher molecular weight material (**Figure 75**). As expected, the increase in temperature was also found to have an influence, with those samples conducted at highest temperatures and longest times producing the highest molecular weights, as well as the highest mass fractions for these weights (**Figure 75**).

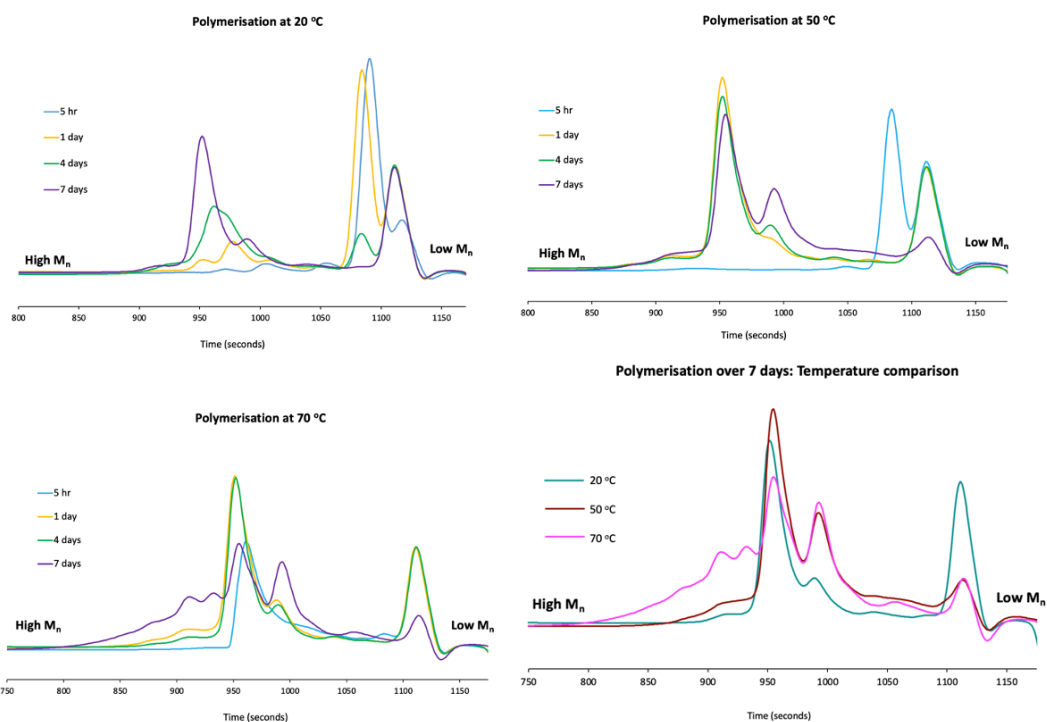
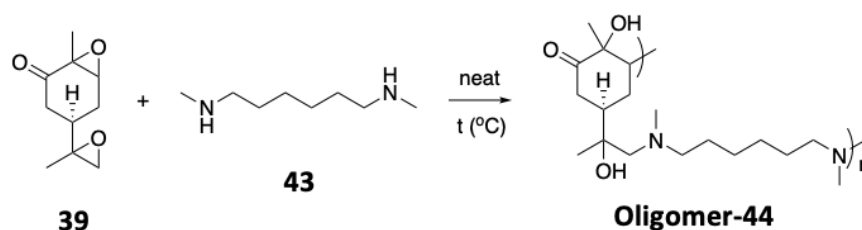


**Figure 75.** GPC chromatograms showing the effect that the length of reaction time had on the molecular weight of the oligomer species. At all temperatures (20, 50 and 70 °C), higher mass fractions of higher molecular weight species were obtained when the reaction was conducted over longer time periods (up to 7 days). A comparison of the results over 7 days indicates the reaction conducted at highest temperature (70 °C) was most successful in generating the longest oligomers over this time frame.

Analysis of the corresponding data from these GPC results indicated that in these reactions, oligomers of up to approximately  $730 \text{ g}\cdot\text{mol}^{-1}$  (by  $M_w$ ) are evidenced, when the reaction is conducted for up to 7 days at  $70 \text{ }^\circ\text{C}$  (**Table 10**). This corresponds to DPs of about 5. As before, the chromatograms indicate that the samples are polymodal, being made up of multiple populations. The data represented in **Table 10** are the averages taken over the full range of populations visible in the chromatogram.



Reaction conditions		Results		
t (°C)	Time	$M_n$ (Da)	$M_w$ (Da)	$\bar{D}$
<b>20</b>	<b>5 hr</b>	162	164	1.01
	<b>1 day</b>	420	455	1.09
	<b>4 days</b>	470	512	1.09
	<b>7 days</b>	535	560	1.05
<b>50</b>	<b>5 hr</b>	160	162	1.02
	<b>1 day</b>	562	598	1.06
	<b>4 days</b>	511	554	1.08
	<b>7 days</b>	502	543	1.08
<b>70</b>	<b>5 hr</b>	440	469	1.07
	<b>1 day</b>	553	600	1.09
	<b>4 days</b>	542	572	1.06
	<b>7 days</b>	580	733	1.26

**Table 10.** GPC results from the curing of carvone bis-epoxide with 1,6-dimethyl hexane diamine over a range of temperatures and times. GPC was performed on Mixed E columns using THF as an eluent and compared to polycaprolactone standards.

It was considered perhaps the oligomers would be better soluble in an alternative GPC eluent to THF (although by eye, THF didn't appear problematic in terms of solubility). It was also considered that the amine

moieties may be 'sticking' to the columns, causing them to elute more slowly and appear as lower molecular weights. A variety of samples were therefore re-analysed by GPC, this time using DMF containing 0.1% lithium bromide as an eluent. Unfortunately, in this case the results showed no trace of oligomers of any length could be found, indicating that the samples were even less suited to the DMF columns than the THF ones.

While it is likely that the molecular weights determined from GPC are imprecise and inaccurate, the data do nonetheless allow for a picture to be formed of what the oligomer samples probably look like. Most likely, this is that they contain short chains made up of oligomeric material or 'pre-polymers', most likely trimers and tetramers in length. Mass spectrometry confirmed the presence of up to tetramers in length, though beyond this could not be detected most as the samples would be too heavy to 'fly' in the machine optimised for small molecules. Oligomers of this length are suitable to be brought forward for antifungal testing.

Structurally, it is most likely that linear oligomers are being formed. Given that no end-groups are visible by NMR analysis, it is also possible that these oligomers have cyclised. However, it is more likely for entropic reasons that they are end-terminated with amine groups (which are also not visible by NMR); over time the oligomers do grow (albeit marginally) in length, which would not be possible if they were cyclising. It was ruled-out that the structures would be end-terminated with epoxide groups, as the terpene bis-epoxide appears to have been completely consumed according to  $^1\text{H}$  NMR analysis.

#### *3.3.4.3 Solvent screen*

It was observed that as the reaction proceeded, the samples gradually became more viscous and the magnetic stirring bar did not appear to be effective. It was thought that the use of a solvent might help to overcome this by providing a reaction medium in which the oligomeric chains could move around in solution and potentially increase the number of collisions, leading to higher molecular weights.

The reactions were conducted in the same way as before, this time in a 1 M solution: 3.47 mmol each of the terpene and the diamine was dissolved in 3.5 mL of solvent. Ethanol was chosen in the first instance as it can be obtained by fermentation and is therefore considered a 'bio-solvent', with a low environmental impact compared to other solvents.<sup>224</sup> Similar reactions were also performed using THF and 2-methyl-THF (2-MeTHF), the latter of which is also bio-renewable.<sup>175</sup> The reactions were conducted at 50 °C for 5 hours for ethanol reaction, while the THF and 2-MeTHF reactions were conducted at just 20 °C, and stirred for 4 days. When the reactions were complete, the solvent was removed by a flow of air, and a sample was taken to compare with the results of the corresponding neat reactions over similar temperatures and time frames.

Analysis by GPC revealed from the chromatogram that the results were, at best, very similar to those samples conducted under neat conditions (**Figure 76**). In each case, the samples conducted in solvent appeared significantly more polydisperse, with populations observed at lower molecular weights than the samples with no solvent.

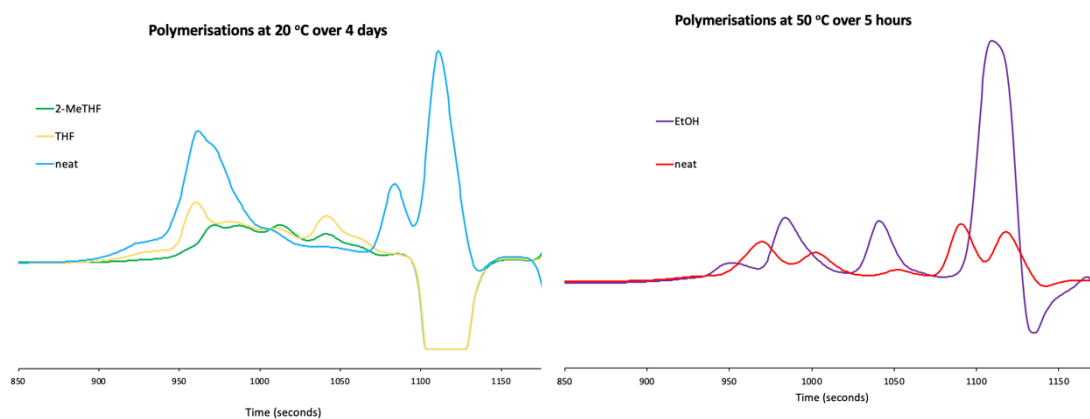


**Figure 76.** GPC chromatograms showing the samples conducted in solvents. The left-hand side shows the reactions conducted over 4 days at 20 °C in THF (yellow), 2-MeTHF (green) and in the absence of solvent (i.e. neat, blue trace). The right-hand side shows the samples conducted at 50 °C in ethanol (purple) and neat (red).

As a result of these reactions, it was concluded that the use of a solvent in this way was not effective in increasing the molecular weights of the oligomer chains. Owing to the added cost and difficulty in removing the solvent, further conditions were not investigated or attempted.

There is certainly scope remaining for these studies to investigate better reaction conditions, including the use of catalysts and solvents, to push these oligomers to higher molecular weight, linear polymers. However, for the purpose of antifungal testing, oligomer chain lengths of 2-10 were sought to be brought forward for antifungal testing, as these are the lengths that are aimed for in the synthesis of antimicrobial peptides.<sup>203,204</sup> Additionally, at this point it was decided that enough facile and 'green' routes had been exhausted, so as to conclude these investigations and focus on the applications of the oligomers that were forming instead.

It was concluded that the most effective synthesis of these oligomers was neat, at 70 °C and over 7 days, as this seemed to give the best balance between high molecular weights, while also forming samples that were not too viscous. This meant that the sample was soluble in a wider range of solvents, importantly including water and DMSO, identifying the oligomers as candidates for investigations into fungal inhibition studies, and their potential as a new biomaterial.



### 3.3.5 Synergistic Antifungal Investigations

Of the polymer systems studied, those made from carvone bis-epoxide and the di-secondary diamine were identified as suitable candidates for testing in antifungal studies (oligomer **44**, **Figure 77**). The samples conducted at 70 °C over 7 days were found to be the most optimal to study for these purposes as these appeared to strike the best balance between high molecular weights, while also forming samples that were not too viscous, so that the oligomers were soluble in DMSO and water, an important aspect of these formulations.

It was decided to test the synergy of these oligomers in combination with the antifungal drug Amphotericin B (AmB) and the fungicide iodopropynyl butylcarbamate (IPBC) (**Figure 77**). The antifungal activity was investigated against two fungal strains, *Candida albicans* and *Trichoderma virens* (with AmB and IPBC, respectively).

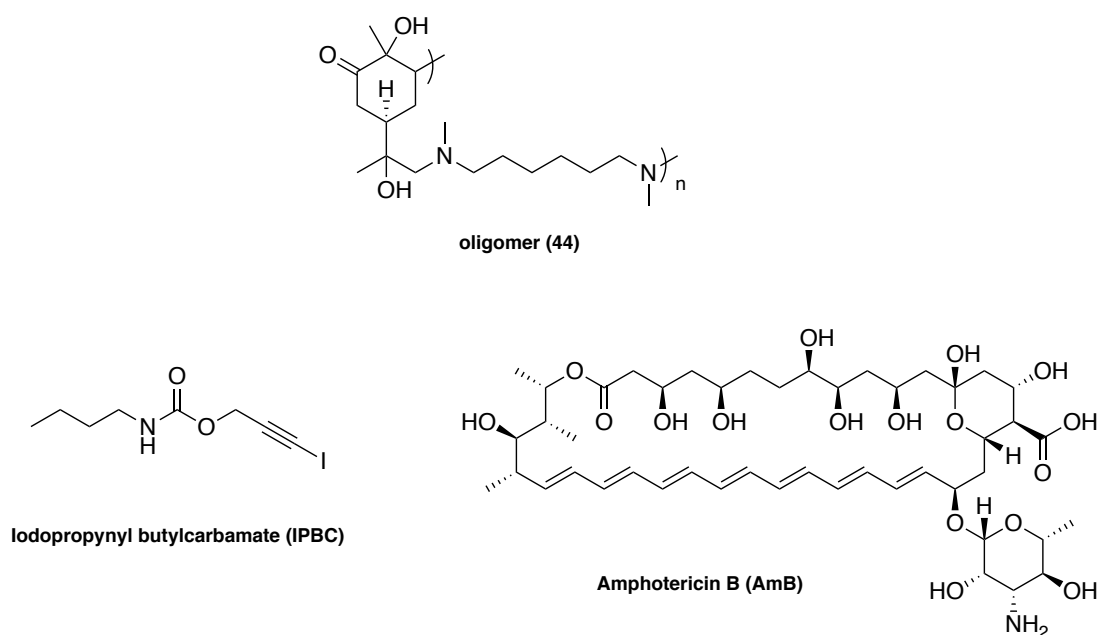


**Figure 77.** The structures of the terpene-based oligomer **44**, the fungicide iodopropynyl butylcarbamate (IPBC) and the antifungal drug Amphotericin B (AmB).

### 3.3.5.1 Synergistic investigations of iodopropynyl butylcarbamate (IPBC) and oligomer **44** against *Trichoderma virens*

*Trichoderma virens* is a species of fungus which is not pathogenic to humans, however, it is associated with promoting plant growth which can cause problems for certain materials.<sup>225</sup> As such, fungicidal treatments against it could be used for materials applications, for example, in protecting paints, sealants or coatings from fungal colonisation. It was decided to investigate any potential synergistic antifungal activity of oligomer **44** against *T. virens*, in combination with the fungicide iodopropynyl butylcarbonate (IPBC).

IPBC is widely used as a preservative in the cosmetics industry. It is also used in painting, textiles and adhesives, and is considered a wood preservative, as it is added to paints and treatments to control the growth of microbes.<sup>226</sup> Although the mechanisms of action are not fully understood for IPBC, its antifungal properties are thought to be a result of iodine toxicity.<sup>227</sup> Known since the 1970s, it has been a popular fungicide to work with due to its material properties, including that it is water soluble and stable to hydrolysis and degradation processes in pH 5 buffered solution.<sup>228</sup> However, in spite of its widespread use, IPBC has also been known to cause allergic reactions, and thus there is a need to reduce the levels of IPBC incorporation in formulations for more widespread applications. Its use is already limited to only 0.05% in cosmetics.<sup>226</sup> A synergistic therapy is therefore of interest to try to enhance the antimicrobial properties of the fungicide, without the need for large amounts of it.

In order to begin investigating a synergistic effect of the oligomer **44** with IPBC against *T. virens*, the minimum inhibitory concentrations (MICs) of both compounds first needed to be determined. The fungus would then be supplied with sub-inhibitory concentrations of these compounds, both individually and combined, in order to determine any synergistic activity.

Growth assays to determine the MICs were conducted in potato dextrose broth, i.e. PDB. Concentrations of 14.06 - 900  $\mu\text{g}\cdot\text{mL}^{-1}$  of **44** were supplied to the fungus in PDB and its growth was monitored over three days (**Figure 78**).

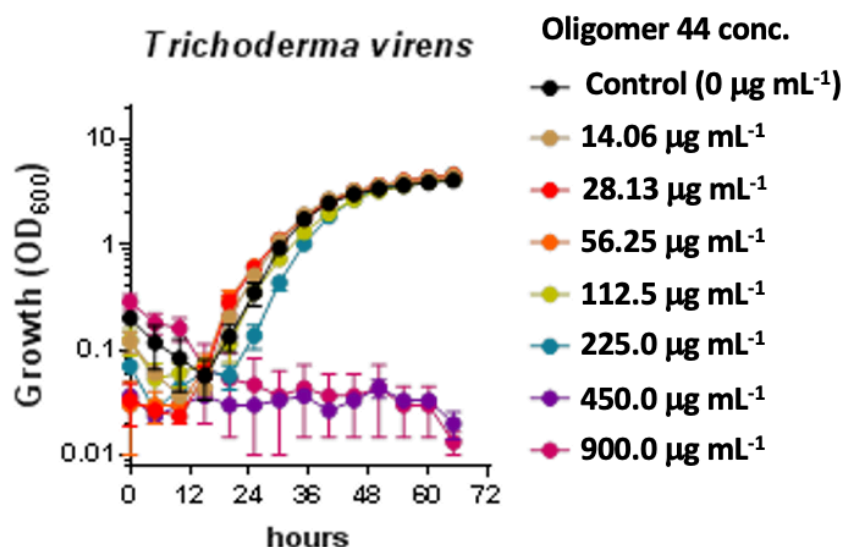


**Figure 78.** Growth assay conducted to determine the minimum inhibitory concentration (MIC) of oligomer **44** against *T. virens* in YPD broth.

After 72 hours, it was apparent that concentrations  $\leq 225 \mu\text{g}\cdot\text{mL}^{-1}$  were not sufficient to inhibit the growth of the fungus relative to the control, but that this occurred for concentrations  $\geq 450 \mu\text{g}\cdot\text{mL}^{-1}$ . The MIC was thus determined to be  $450 \mu\text{g}\cdot\text{mL}^{-1}$ .

Using a similar method, the MIC of IPBC against *T. virens* in PDB was determined to be  $1600 \text{ ng}\cdot\text{mL}^{-1}$ . With these two MIC values in hand, synergistic activity could be probed by supplying the fungus with concentrations below these values and investigating fungal growth inhibition. As such, growth assays were conducted in PDB in which *T. virens* was supplied with just  $200 \text{ ng}\cdot\text{mL}^{-1}$  of IPBC both alone and in combination with varying concentrations of **44**, ranging from 14 to  $900 \mu\text{g}\cdot\text{mL}^{-1}$ . It was determined that just  $220 \mu\text{g}\cdot\text{mL}^{-1}$  of **44** in combination with the  $200 \text{ ng}\cdot\text{mL}^{-1}$  of IPBC were together sufficient to produce a complete inhibition of fungal growth (**Figure 79**).

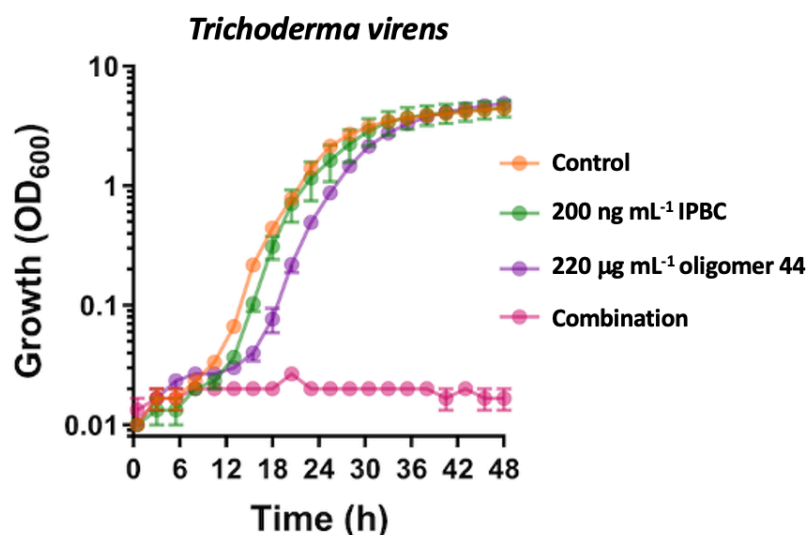


**Figure 79.** Growth inhibition assay indicating the synergistic antifungal activity of oligomer **44** and IPBC against *T. virens*: The fungus was cultured in PDB in the presence of **44** and/or IPBC, supplied at the indicated sub-inhibitory concentrations. These had no inhibitory effect on the fungus when supplied alone, but when combined, a complete growth inhibition was observed. The values are means  $\pm$  SEM from three replicate experiments.<sup>107</sup>

Given that neither component at the supplied concentrations had any effect on the growth of the fungus, but together they did, this is evidence of synergistic activity. Following these positive results, standard 'checkerboard' assays were conducted in order to quantify the synergy (and formally rule out an additive effect). These were conducted according to the general culturing and preparation guidelines according to EUCAST,<sup>229</sup> and meant that in this instance RPMI medium was used rather than PDB as with the growth assays. This resulted in the same MIC for IPBC (1600 ng·mL<sup>-1</sup>), and a slight increase for **44** to 0.5 mg·mL<sup>-1</sup>, which is not unusual (**Figure 80**).

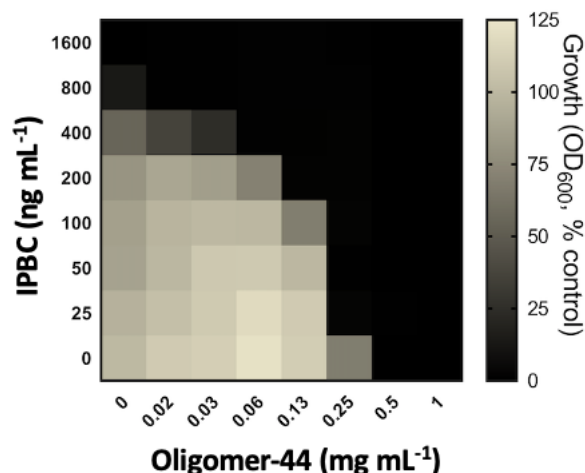


**Figure 80.** Checkerboard assay performed in RPMI, indicating the synergistic relationship between IPBC and oligomer **44**, resulting in antifungal activity ( $FICI = 0.38$ ). The values are means from three replicate experiments.<sup>107</sup>

Quantitatively, the checkerboard assays indicated that the presence of just  $250 \mu\text{g}\cdot\text{mL}^{-1}$  of **44** resulted in a decrease in the MIC of IPBC by up to 64-fold: from  $1600 \text{ ng}\cdot\text{mL}^{-1}$  to  $25 \text{ ng}\cdot\text{mL}^{-1}$ . This is significant; an MIC which is shown to decrease by up to 5-fold with the addition of another compound is considered a 'strong' synergy, and these are not very common.<sup>155</sup> To determine the synergistic affect, the fractional inhibitory concentration index (FICI) was determined as described by Hseih *et al.* according to the following equation:<sup>230</sup>

$$FICI = FIC_X + FIC_Y = \frac{X}{MIC_X} + \frac{Y}{MIC_Y}$$

Taking X to be IPBC and Y to be oligomer **44**, the parameters of this equation can now be filled according to the data obtained from the checkerboard, as follows:

$$FICI = FIC_{AmB} + FIC_{44} = \frac{200}{1600} + \frac{0.13}{0.5} = 0.38$$

An FICI value of 0.38 (which is unitless) indicates a synergistic effect, as combinations are usually considered synergistic for values  $\leq 0.5$ .<sup>231</sup> Therefore, it is possible to quantitatively and formally conclude that the

combination of oligomer and fungicide at these concentrations induces a synergistic antifungal result.

However, given that after the synthesis the oligomers were not purified (as methods of precipitation were not effective), it was important to determine if this synergy was definitely occurring as a result of the oligomer contribution and not any leftover monomer in solution, or simply the monomer repeat units within the oligomer chains which could be enhanced by using the monomer alone. This was considered particularly important bearing in mind the known antimicrobial effects of amine compounds,<sup>104,146</sup> considering the use of the diamine co-monomer. Terpenes, including both isomers of carvone, have also known antifungal and antimicrobial effects,<sup>199</sup> and so it was similarly important to determine whether or not the effect was from any remainder bis-epoxide component in solution. This is important in determining if the synergistic effect truly warranted the synthesis of the oligomers, or if it could be achieved with only the monomer components. As such, checkerboard analyses were also conducted for the monomer compounds (**Figure 81**).

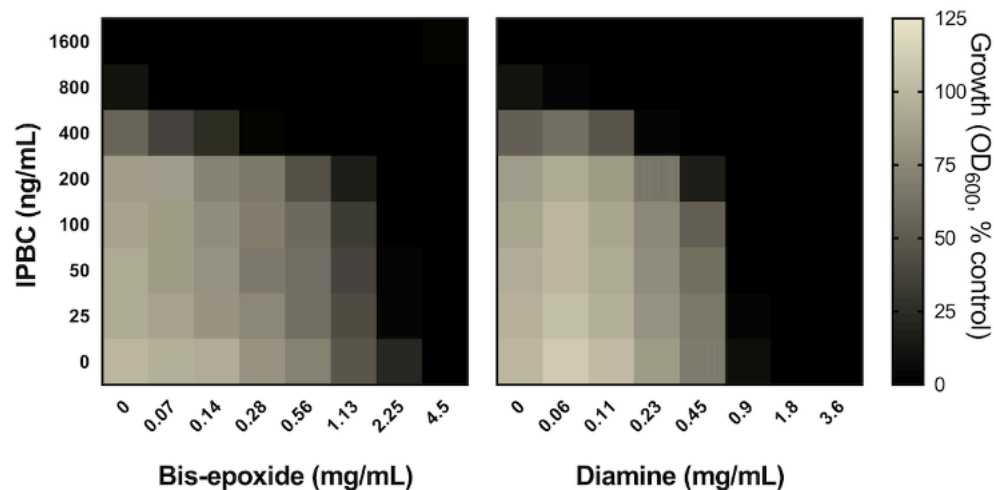


**Figure 81.** Checkerboard assay performed in RPMI, indicating a moderate synergistic relationship between IPBC and monomers bis-epoxide **39** (left) and diamine **43** (right) against *T. virens*. The values are means from three replicate experiments.<sup>107</sup>

The checkerboards revealed that for both the bis-epoxide compound (**39**) and the diamine (**43**), synergy was observed in both cases, with FICIs of 0.31 and 0.38 for each compound, respectively. However, the MICs of each were  $4.5 \text{ mg}\cdot\text{mL}^{-1}$  for **39** and  $1.8 \text{ mg}\cdot\text{mL}^{-1}$  for **43**, which is significantly higher than the MIC of the oligomer, which was just  $0.5 \text{ mg}\cdot\text{mL}^{-1}$ . Also, as mentioned, the addition of just  $0.25 \text{ mg}\cdot\text{mL}^{-1}$  of **44** demonstrated a huge 64-fold reduction in the amount of IPBC required in order to observe fungicidal activity, while neither monomer had an effect to match this significance. As such there is an advantage in using the oligomer system over the small molecules, not least as this uses much less material. In addition, the oligomers appear to provide more favourable material properties, for example their water solubility allowing for easy formulation compared to the small molecules.

Finally, to further visually demonstrate the synergistic relationship between **44** and IPBC, an agar disk diffusion assay was conducted. Sterile filter papers were soaked with  $1 \text{ mg}\cdot\text{mL}^{-1}$  **44**, with and without two concentrations of IPBC:  $25 \text{ }\mu\text{g}\cdot\text{mL}^{-1}$  and  $50 \text{ }\mu\text{g}\cdot\text{mL}^{-1}$  (in addition to a third control sample of  $0 \text{ }\mu\text{g}\cdot\text{mL}^{-1}$ ). These filter papers were laid on PDA agar plates inoculated with *T virens* (**Figure 82**).

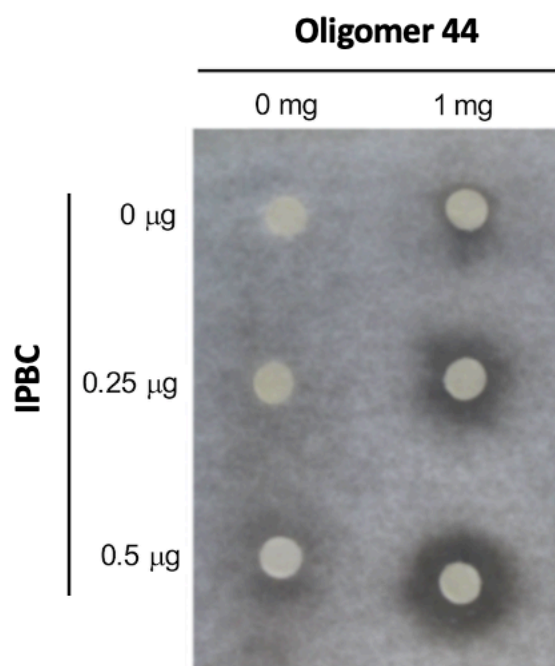


**Figure 82.** The agar disk diffusion assay on PDA agar, indicating the susceptibility of *T. virens* to **44** in combination with IPBC. The zones of inhibition became visible after 48 hours.<sup>107</sup>

The susceptibility of the fungus to the combination of inhibitors became visible after incubation of the agar plate at 30 °C for 48 hours. As predicted, the combination of inhibitors at higher concentrations inhibited the fungus to a greater extent than at lower concentrations. High (or low) levels of the inhibitors on their own were not shown to be effectively antifungal, with no distinct zones of inhibition visible compared to the combinations. This study visually demonstrates the effectiveness of this fungicidal combination, offering an insight into the possible function of these formulations in a fungicidal treatment/ application for materials.



### 3.3.5.2 Synergistic investigations of Amphotericin B and oligomer **44** against *Candida albicans*

Amphotericin B is a polyene, one of the major classifications of antifungal agents.<sup>156</sup> Although it has been known for over 50 years, the full extent of its antifungal activity has only recently come to light.<sup>232</sup> In the classical mechanism, the mycosamine sugar moiety of AmB binds with ergosterol, an essential membrane-lipid in the fungus. Ion channels are then formed as eight AmB molecules aggregate into 'pores' of approximately 1 nm, with the ergosterol lipids interdigitated with AmB molecules. These channels then insert into the membrane perpendicular to its extracellular surface, which results in ion leakage (**Figure 83, mechanism A**).<sup>233</sup> However, it was later determined that ion leakage from this pore formation is not the ultimate cause of cell death, but rather it is through a second mechanism which sees the polyene form large extra-membranous aggregates that act like a sponge, and extract ergosterol from the membrane (**Figure 83, mechanism B**).<sup>165</sup>

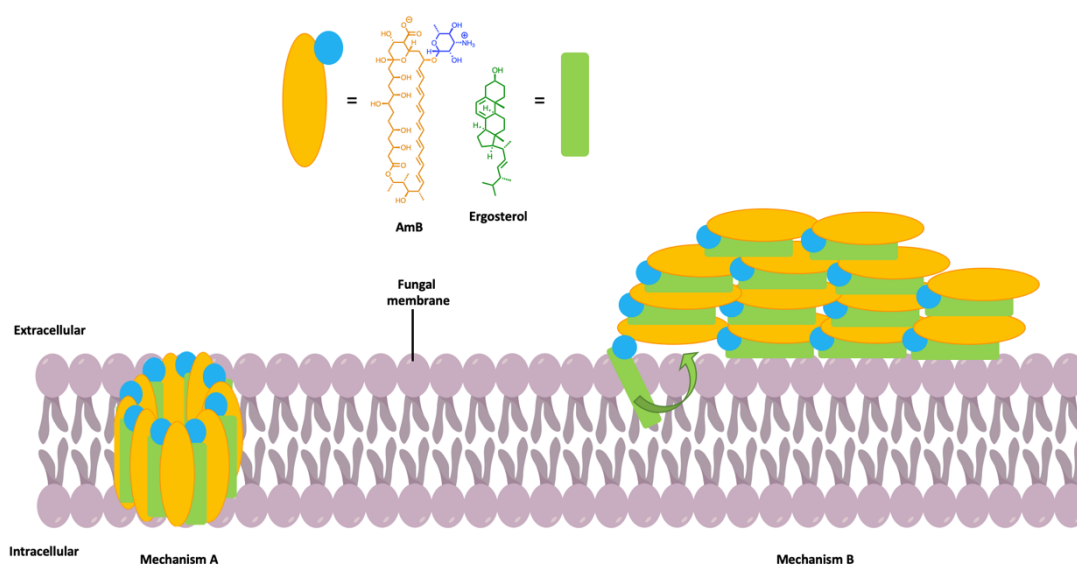


**Figure 83.** The mechanisms of antifungal activity by amphotericin B (AmB). Mechanism A shows the classic ion channel model in which AmB forms pores by binding with the membrane-lipid ergosterol. Mechanism B shows the newer 'sponge' model in which AmB forms large extra-membranous aggregates that extract ergosterol from the membrane, ultimately resulting in cell death.<sup>165,232,233</sup>

Studies show that while mechanism A is certainly damaging to the fungus, it is not required for antifungal activity, but that binding of ergosterol is essential.<sup>233</sup> Ergosterol is important for many essential cellular processes, meaning the cause of death is multifactorial, but ultimately without it the fungus cannot survive.<sup>165</sup> As a result, AmB is the most clinically relevant polyene for invasive fungal infections.<sup>156</sup> However, ergosterol is structurally very similar to cholesterol, and as a result the molecule is responsible for systemic toxicity to mammals, and is particularly nephrotoxic to humans.<sup>165</sup> Its dose is therefore limited to between 3 – 5 mg·kg<sup>-1</sup>,<sup>234</sup> and attempts to overcome this have been limited both in terms of cost of the treatment, and its effectiveness.<sup>235</sup>

It was decided to investigate the synergistic antifungal activity of AmB with oligomer **44** against *Candida albicans*. This is a human pathogen that can cause severe mucosal infections, and can be lethal if the immune system is impaired.<sup>236</sup> A synergistic therapy therefore presents an attractive possibility for treatment of *Candida* species.

To investigate the synergistic activity of **44** with AmB against *C. albicans*, the minimum inhibitory concentration (MIC) of both compounds were first determined, as done in the previous study against *T. virens*. For *C. albicans*, these studies were conducted in yeast extract peptone dextrose, i.e. YPD medium. After the MICs of both compounds were determined, the fungus was then supplied with sub-inhibitory concentrations of each inhibitor.

It was observed that when 4 µg·mL<sup>-1</sup> of AmB was supplied to the fungus in YPD broth, there was no inhibition of the fungus relative to the control (in which neither drug nor oligomer was supplied). Similarly, a concentration of 1.25 mg·mL<sup>-1</sup> of the oligomer **44** was, as predicted, not sufficient to inhibit the fungal growth, being below the pre-determined MIC threshold. However, when these concentrations were supplied to the fungus in combination, a total inhibition of fungal growth was observed (**Figure 84**).

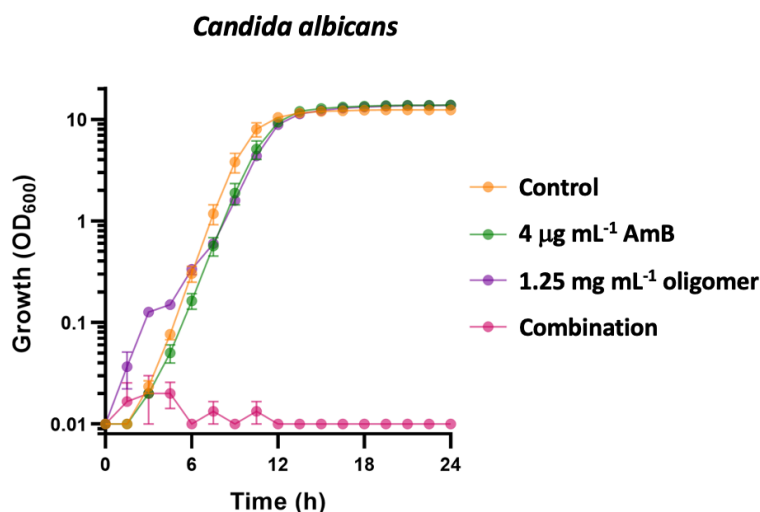


**Figure 84.** Growth inhibition assay indicating the synergistic antifungal activity of oligomer **44** and AmB: *C. albicans* was cultured in YPD in the presence of **44** and/or AmB, supplied at the indicated sub-inhibitory concentrations. These had no inhibitory effect on the fungus when supplied alone, but combined, a complete growth inhibition was observed. The values are means  $\pm$  SEM from three replicate experiments.<sup>107</sup>

These findings are indicative of synergistic activity between the oligomer and drug, and so a checkerboard assay was conducted in order to quantify the synergy and rule out an additive effect. These checkerboard assays were conducted according to the general culturing and preparation guidelines according to EUCAST,<sup>229</sup> and meant that in this instance RPMI medium was used. This resulted in lower inhibitory concentrations than those conducted in the rich YPD medium, which is not unusual. In this medium, the MICs of AmB and the oligomer were found to be  $1 \mu\text{g}\cdot\text{mL}^{-1}$  and  $2.5 \text{ mg}\cdot\text{mL}^{-1}$ , respectively.

Visually, the checkerboard was found demonstrate the synergy between the two compounds, given the convex pattern of growth that resulted.<sup>237</sup> Quantitatively, it was found that the presence of the oligomer resulted in an 8-fold reduction in the MIC for AmB: from  $1 \mu\text{g}\cdot\text{mL}^{-1}$ , to  $0.13 \mu\text{g}\cdot\text{mL}^{-1}$  (**Figure 85**).

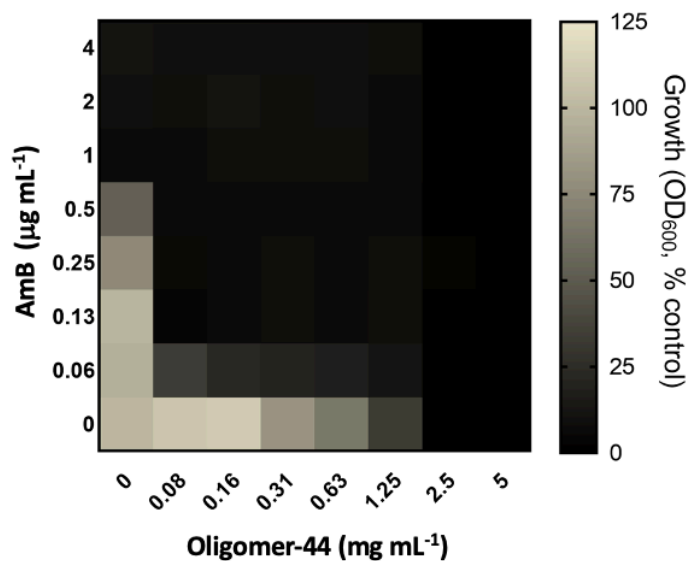


**Figure 85.** Checkerboard assay performed in RPMI, indicating the synergistic relationship between AmB and oligomer **44**, resulting in antifungal activity ( $FICI = 0.16$ ). The values are means from three replicate experiments.<sup>107</sup>

The fractional inhibitory concentration index (FICI) was then determined as described by Hsieh *et al.* using the same equation as was used for the studies with *T. virens.*, given below.<sup>230</sup> Taking  $X$  to be AmB and  $Y$  to be oligomer **44**, the parameters of this equation were filled according to the data obtained from the checkerboard, as follows:

$$FICI = FIC_{AmB} + FIC_{44} = \frac{0.13}{1} + \frac{0.08}{2.5} = 0.16$$

An FICI value of 0.16 indicates a strong synergistic effect,<sup>231</sup> making this a very promising result. However, as previously, it was important to determine if this synergy was definitely occurring as a result of the oligomer contribution and not any leftover monomer in solution, and whether or not this synergistic effect truly warranted the synthesis of the oligomers rather than using the small molecules. As such, checkerboard analyses were also conducted for the monomer compounds (**Figure 86**). The MICs for the bis-epoxide and the diamine were found to be  $5.0 \text{ mg}\cdot\text{mL}^{-1}$  and  $2.5 \text{ mg}\cdot\text{mL}^{-1}$ , respectively. The FICI was then calculated

for AmB in combination with the bis-epoxide and found to be 0.62, while the combination with the diamine was found to be 1.0. Neither of these values are indicative of synergy, but only of an additive effect. With no other components in the polymerisation reaction, it was therefore concluded that the oligomers were a fundamental component of the synergistic effect exhibited with AmB.

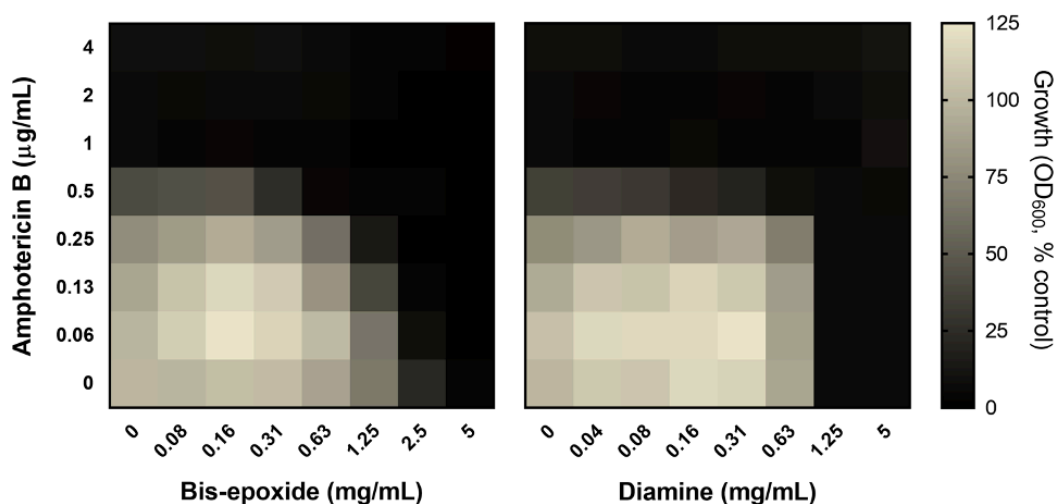


**Figure 86.** Checkerboard assay performed in RPMI, indicating no synergy evident between AmB and the two monomers, bis-epoxide **39** (left) and diamine **43** (right). The values are means from three replicate experiments.<sup>107</sup>

Finally, to further illustrate this synergistic relationship, agar disk diffusion assays were conducted. Sterile filter papers were soaked with the oligomer at  $1.4 \text{ mg}\cdot\text{mL}^{-1}$ , and no AmB, in addition to two with  $0.5 \text{ }\mu\text{g}\cdot\text{mL}^{-1}$  and  $0.05 \text{ }\mu\text{g}\cdot\text{mL}^{-1}$  AmB. Similarly, a second trio of filter papers were not soaked with the oligomer, but instead  $0.5 \text{ }\mu\text{g}\cdot\text{mL}^{-1}$  and  $0.05 \text{ }\mu\text{g}\cdot\text{mL}^{-1}$  of AmB, and a third control with neither drug nor oligomer (**Figure 87**).

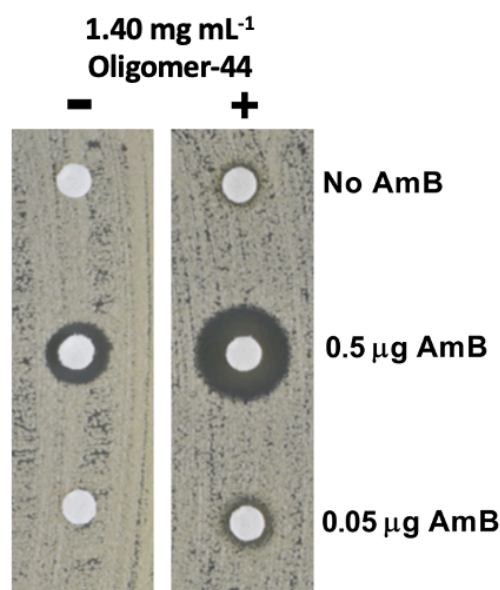


**Figure 87.** The agar disk diffusion assay on YPD agar, indicating the susceptibility of *C. albicans* to **44** in combination with AmB. The zones of inhibition became visible after 24 hours.

The susceptibility of the fungus to the combination of the two components became visible after 24 hours, at which point zones of inhibition were visible. In the control case, as expected, there was no inhibition to the growth of the fungus, and similarly with the oligomer and no AmB, or  $0.05 \mu\text{g}\cdot\text{mL}^{-1}$  of AmB but no oligomer, there did not appear to be any zone of inhibition formed. The presence of the oligomer in combination with this low concentration of AmB resulted in a very small inhibition zone compared to the control, which could not be considered effectively antifungal. A concentration of  $0.5 \mu\text{g}\cdot\text{mL}^{-1}$  AmB with no oligomer was enough to generate a small zone of inhibition, however when the oligomer was added to this concentration, a much larger zone was visible.

These results demonstrate the effectiveness of the synergistic relationship between **44** and AmB. It is also evident that the fungus is more susceptible to the combined drug and oligomer than by a simple product of their individual effects at those doses; further evidence of synergy.

### 3.3.5.3 Cytocompatibility test

The oligomer **44** was found to act in synergy with the fungicide IPBC and antifungal drug AmB against two different fungal strains *Trichoderma virens* and *Candida albicans*, respectively. These results demonstrated promising preliminary data indicating that formulations of these combinations may have future use in antifungal material and biomaterials applications. The data relating to *C. albicans* were particularly promising, with the combination of oligomer and AmB producing a significant synergistic antifungal response to the human pathogen. However, in order for the oligomer to have a practical use in biomaterials applications, it is imperative that its cytocompatibility be determined; this is of paramount importance for a new material in determining if it will go on to have a practical clinical use.<sup>188</sup> Similarly, while *T. virnes* is not a human pathogen and applications for the synergy of IPBC and **44** would likely lie outside of healthcare applications, it is nonetheless important to determine the toxicity or cytocompatibility of the material to determine the scope of the applications available.

As such, a preliminary investigation into the cytotoxicity of the new material, oligomer **44**, was conducted, by measuring the metabolic activity of human cells following their exposure to **44**. Cellular metabolic activity was thus studied using the Alamar Blue cell viability assay. This assay functions on the basis of the cellular reduction of a non-fluorescent resazurin salt by NADH-dependent enzymes, to the fluorescent resorufin salt.<sup>238,239</sup> Through the measurement of the reductive environment of cells, this assay provides an indirect measure of the redox reactions involved in the generation of cellular energy and thus serves as an indication of cell health and viability.<sup>240</sup>

As such, human lung fibroblasts (MRC-5) were selected to give an indication of the human cellular response to the material. In a previous, similar study, human fibroblasts were used to determine the concentration-dependant toxicity of thymol, a terpene found in the essential oil of oregano with antifungal activity.<sup>241</sup> This is particularly useful should the formulation prove useful for a spray therapy application.

The cells were incubated with concentrations ranging from 0.1 to 0.8 mg·mL<sup>-1</sup> of **44** applied in DMEM culture medium, for 24 hours.

Results indicated that no significant toxicity was demonstrated with **44** at a concentration of 0.1 mg·mL<sup>-1</sup>, with metabolic activity measured at 89.4 ± 2.7% relative to the vehicle control (**Figure 88**). Statistically significant cell toxicity is, however, observed with the application of concentrations ≥0.2 mg·mL<sup>-1</sup>, with 0.2 mg·mL<sup>-1</sup>, 0.5 mg·mL<sup>-1</sup> and 0.8 mg·mL<sup>-1</sup> reducing metabolic activity of the fibroblast cells to 80.3 ± 10.3, 69.3 ± 5.8 and 62.7 ± 3.6%, respectively (**Figure 88**).

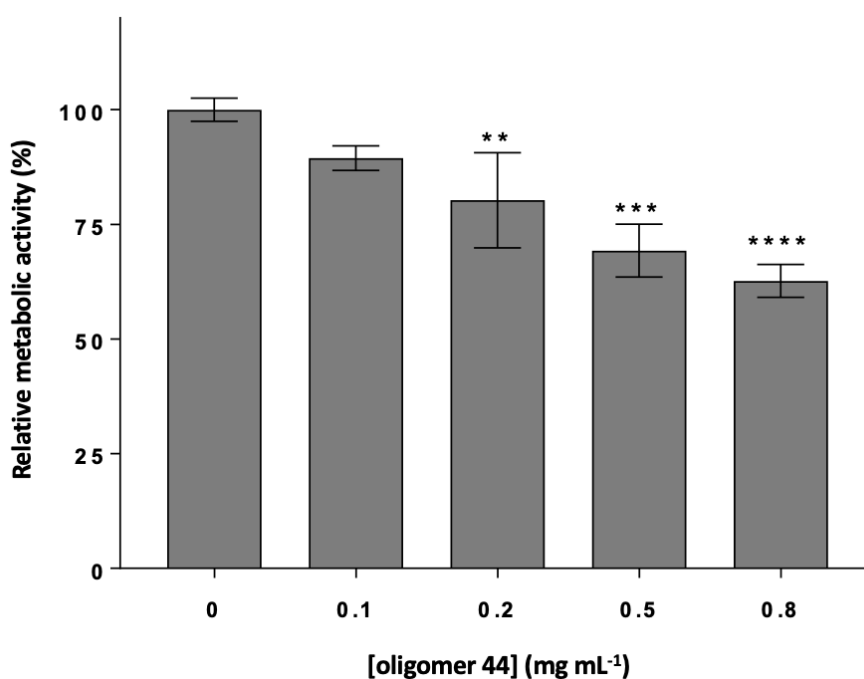


**Figure 88.** Cytocompatibility of oligomer **44** on MRC-5 human lung fibroblasts. Cytotoxicity was assessed by measuring cellular metabolic activity using the Alamar Blue assay: **44** was applied to cells for 24 hours in culture medium. Data is presented as mean ± S.D (n=3). Statistical significance was determined between the vehicle control group (0 mg mL<sup>-1</sup>) and treated groups by one-way ANOVA followed by Dunnett's post hoc test for multiple comparisons (\*p < 0.05; \*\*p < 0.01; \*\*\*p < 0.001; \*\*\*\*p < 0.0001).



While there is statistically significant cell toxicity found for samples  $\geq 0.2 \text{ mg}\cdot\text{mL}^{-1}$ , only  $0.08 \text{ mg}\cdot\text{mL}^{-1}$  of the oligomer in RMPI medium was required to induce synergistic antifungal activity against *C. albicans*. The results therefore suggests that the required concentration is cytocompatible, and may have potential use in a formulation or therapy (of course following the further standard, more-detailed testing).

Furthermore, through the imaging of MRC-5 cells following exposure to **44**, concentration-dependent cell toxicity is elicited (**Figure 89**). For example, at  $0.1 \text{ mg}\cdot\text{mL}^{-1}$  (**Figure 89B**) and  $0.2 \text{ mg}\cdot\text{mL}^{-1}$  (**Figure 89C**) it can be observed that the morphology of the fibroblasts remains unchanged compared to that of the vehicle control (**Figure 89A**), indicating absence of substantial toxicity with these concentrations. This would suggest that the material remains cytocompatible at higher concentrations than what the Alamar blue assay results indicated, which is not unusual considering the metabolic assay is an indirect measure of cell health and viability. However, the application of  $0.5 \text{ mg mL}^{-1}$  (**Figure 89D**) and  $0.8 \text{ mg}\cdot\text{mL}^{-1}$  (**Figure 89E**) of the oligomer to the fibroblast cells appear to change their morphology: a loss of elongation and spindle-like shape is observed, and instead a more rounded morphology, with a lack of processes extending out from the ends of the cell body, are shown. The loss of such morphological features in fibroblasts is indicative of cytotoxicity.<sup>242,243</sup>

Despite the discrepancy for the sample at  $2 \text{ mg}\cdot\text{mL}^{-1}$ , the observations made *via* assessment of cellular morphology (**Figure 89**) appear to support the metabolic activity data obtained from the Alamar blue test (**Figure 89**) of concentration-dependent toxicity with **44**. It is therefore concluded that cytocompatibility is only achieved at concentrations  $< 0.2 \text{ mg}\cdot\text{mL}^{-1}$ . This finding of the non-toxic dosing range should therefore be used to inform future testing for applications of **44**.

As the synergistic antifungal formulation with AmB against *C. albicans* required much less than  $0.2 \text{ mg}\cdot\text{mL}^{-1}$  of **44**, these results can therefore be interpreted as a positive initial indication of the

cytocompatibility of the combination-formulations. While further testing would be required with more complete and robust formulation studies to fully determine biocompatibility, these results show that applications in the biomaterials field isn't yet ruled out.

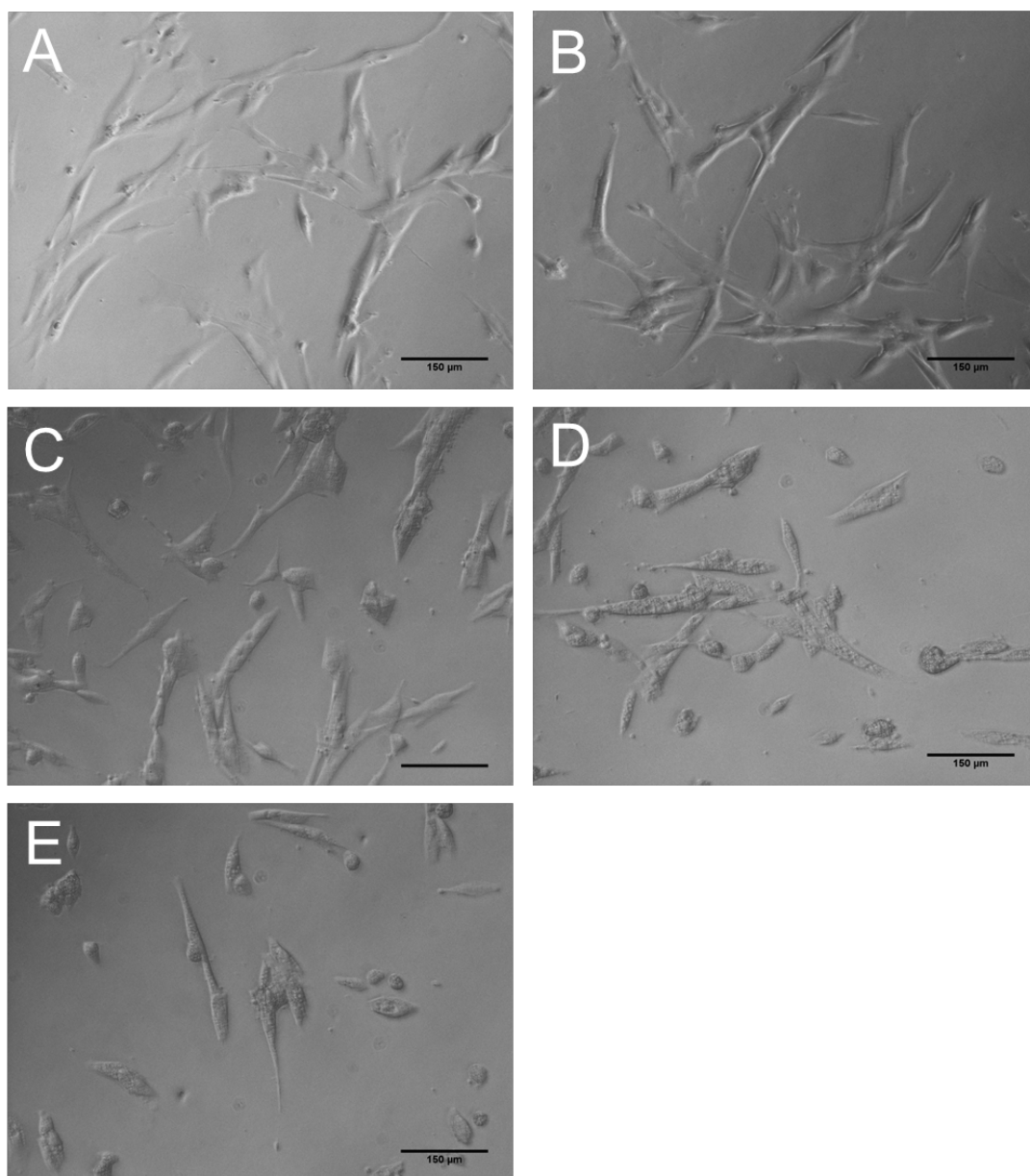


**Figure 89.** Bright field micrographs of MRC-5 human lung fibroblasts following exposure to (A) vehicle control ( $0 \text{ mg}\cdot\text{mL}^{-1}$ ), (B)  $0.1 \text{ mg}\cdot\text{mL}^{-1}$ , (C)  $0.2 \text{ mg}\cdot\text{mL}^{-1}$ , (D)  $0.5 \text{ mg}\cdot\text{mL}^{-1}$  and (E)  $0.8 \text{ mg}\cdot\text{mL}^{-1}$  of oligomer **44**, for 24 hours. Images shown are representative of three independent repeats performed. Scale bar is  $150 \mu\text{m}$ .

#### 3.3.5.4 Mechanism Discussions

There have been a number of proposed mechanisms for antifungal synergy, depending greatly on the nature of the two components being studied.<sup>244</sup> One such mechanism relies on the two components causing the inhibition of different stages of the same biochemical pathway. As an example of this, in 2015, Moreno-Martinez *et al.* found a range of undesirable fungi were susceptible to synergistic inhibition when exposed to combinations of aminoglycoside antibiotics and sulfate-transport inhibitors. The two components work together by different mechanisms, both causing errors in mRNA translation: Aminoglycosides are thought to induce a structural alteration in the small ribosomal subunit decoding centre, while sulfate-transport inhibitors are thought to cause translation errors by limiting the availability of sulfur-containing amino acids for cognate tRNAs.<sup>155</sup> The result is a synergistically increased error-rate of translation, and ultimately, fungal death.<sup>155</sup> Other examples include methods in which compounds prevent the biosynthesis of ergosterol, thus impairing the function of cell membranes.<sup>244</sup>

Mechanisms of synergy can also be achieved when the interaction of one component with the fungal cell wall or membrane results in an increased penetration and uptake of a second component.<sup>244</sup> This has been proposed for the synergistic activity between AmB and flucytosine, in which the polyene damages the fungal membrane and allows for greater uptake of flucytosine.<sup>244</sup> Alternatively, a transport interaction mechanism has also been proposed between AmB and flucytosine, in which AmB acts on the cell membrane, inhibiting the release of flucytosine across the membrane and out of the yeast cell. Flucytosine therefore remains at the site of its action within the cell and is available to kill any remaining, surviving fungus when AmB degrades the cell membrane.<sup>244</sup>

These do not constitute a complete or exhaustive list of mechanisms in which combinations can induce synergistic antifungal effects, but demonstrate that the interactions depend on a variety of factors, including the fungal species and the mode of action of individual antifungal agents.<sup>244</sup>

The potential mechanisms responsible for the observed synergy of the antifungal agents IPBC and AmB with **44** is hypothesised to be

underpinned by the amphiphilic nature of the oligomer, resulting in membrane disruption.

The hydrogen-bonding hydroxyl groups and tertiary amine groups, in combination with the hexane repeat units, provide the oligomer **44** a degree of amphiphilicity, a well-known factor which greatly influences biocidal activity.<sup>146</sup> Furthermore, it has been established that a degree of membrane activity from amphiphilic components can enhance the efficacy of anti-fungal agents,<sup>166,244</sup> which is ultimately very relevant to the results observed in this project.

In addition to this, the oligomers are likely cationic at the pH values of the antifungal assays (a result of the amine groups); another well-established antimicrobial property.<sup>146</sup> Importantly, cationic polymers have recently demonstrated membrane-disrupting effects on *C. albicans*.<sup>236</sup> However, the synergy indicates that the oligomers alone at the given concentrations do not induce antifungal activity, but instead must be combined with the respective antifungal agent. It is anticipated therefore that the mechanism of synergy results from both membrane disruption in combination with the conventional antifungal activity associated with the specific antifungal agent.

As the mechanism(s) underlying the antifungal activity of IPBC are not fully understood,<sup>227</sup> this synergistic mechanism is more difficult to predict. However, the mechanism underlying the antifungal activity of AmB involves the molecule accumulating at the membrane and acting as a 'sponge', extracting the essential membrane-lipid ergosterol.<sup>165</sup> It is likely therefore that the interaction between AmB and the oligomer **44** stems from a co-ordinated membrane and sterol disruption such as this.

In a recent study by de Castro *et al.*, a synergistic antifungal relationship was found between thymol, a terpene-derived small molecule, and nystatin, a polyene which is structurally very similar to AmB. In the study, the authors determined that the mode of action for this antifungal relationship involves the inhibition of ergosterol formation.<sup>241</sup> In another study, Liu *et al.* found a synergistic antifungal relationship between glabridin, an isoflavane, and fluconazole, a popular antifungal medicine based on azoles. The authors tested the membrane sterols of *C. albicans* treated with glabridin alone and in combination with flucazole, and found

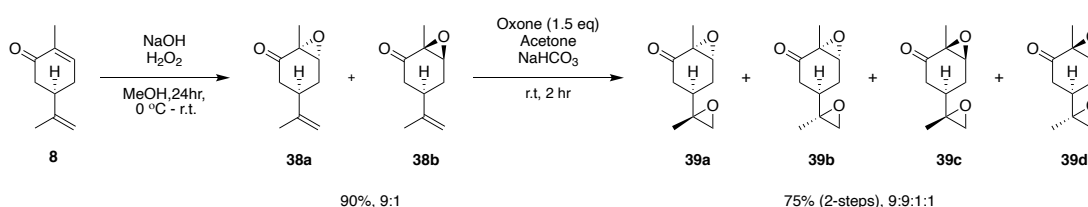
that there was no obvious change in the sterols of the fungal membrane observed, suggesting the synergy may not have been related to the inhibition of membrane sterol synthesis. Instead, the synergy was thought to be a result of direct membrane damage.<sup>166</sup>

Evidently, the mechanism of the specific antifungal agent individually is an important underlying factor in a synergistic mechanism. In this case, it is reasonable to suggest that the mechanism of synergistic antifungal activity between **44** and AmB is more similar in mechanism to the former study by de Castro *et al.*, given the structural similarities between AmB and nystatin. However, given the amphiphilic nature of **44**, membrane damage is also a reasonably likely.

In order to prove or determine the mechanism of synergy involved in this project, a systematic evaluation of both AmB and **44** (both individually and combined as a formulation) would need to be conducted. This is because the make-up of fungal cell walls and membranes vary not only with the specific fungal strain, but also on their local environment, which means assigning a precise membrane-effect is challenging and would likely be inaccurate without investigation.<sup>107</sup> Unfortunately, time restrains in relation to the recent COVID-19 pandemic meant that it was not possible to investigate the mechanism of action in this case. The hypothesis remains that the oligomer interacts with the cell membrane and inhibits the fungus, which results in increased efficacy of AmB. A similar hypothesis stands for the case of IPBC against *T. virens*, in which the membrane is disrupted, allowing for greater uptake of the fungicide.

### 3.4 Conclusions

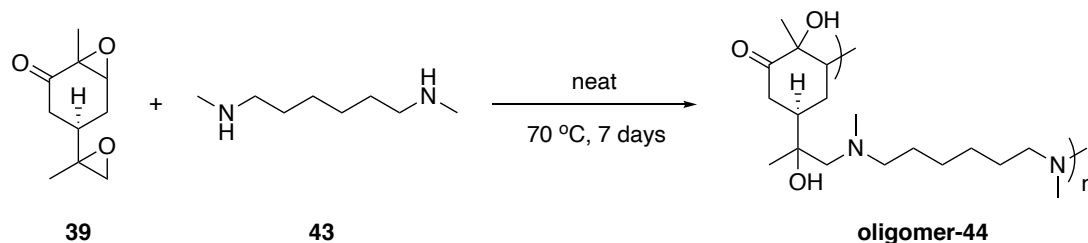
A bis-epoxide monomer was successfully synthesised from (*R*)-carvone (**8**), a terpenoid renewable feedstock that remains somewhat under-explored in terms of its application in polymer chemistry, compared to other terpenes. While the synthesis of this compound has been known in the literature for some time,<sup>70</sup> it has traditionally employed chlorinated solvents and toxic, atom-inefficient oxidising agents. In this project, the bis-epoxide **39** has been synthesised for the first time using known, mild conditions over the two steps, with inexpensive and facile, sustainable synthetic methods (**Scheme 32**). This resulted in a high yield of 75% for the monomer compound over the two synthetic steps, produced on a multigram scale.



**Scheme 32.** The sustainable synthesis of the bis-epoxide monomer **39** from (*R*)-carvone (**8**), via epoxidation of the alkene moieties.

This compound was then investigated as a monomer in the well-established step-growth polymerisation with two commercially available diamine co-monomers, hexane diamine (**41**) and 1,6-dimethyl hexane diamine (**43**). In the absence of solvents, catalysts or any additional components, these reactions were found to produce low molecular weight oligomers. Those made from the di-primary diamine **41** were found to form branched oligomers (determined given their poor solubility in a variety of solvents), with molecular weights ranging from approximately 1000 – 4500 g·mol<sup>-1</sup>. With their lack of solubility making their future in biomaterials applications unlikely, focus turned instead to the oligomers produced using the di-secondary diamine **43**. A subset of these oligomers, those synthesised at 70 °C over 7 days (**Scheme 33**), were found to be

approximately  $700 \text{ g}\cdot\text{mol}^{-1}$  (by  $M_w$ ), (indicating a DP of  $\sim 4$ ), and were found to dissolve in water and DMSO, a promising characteristic allowing for their testing for antifungal studies.



**Scheme 33.** The synthesis of terpene-based epoxy-amine oligomer-**44**, identified as suitable candidates for antifungal studies.

The oligomer **44** was then tested for antifungal activity in combination with the fungicide IPBC and the antifungal drug AmB against *Trichoderma virens* and *Candida albicans*, respectively. In the first study, it was shown that the presence of just  $250 \mu\text{g}\cdot\text{mL}^{-1}$  of **44** was found to decrease the MIC of IPBC by up to 64-fold, when supplied against *T. virens*. A synergistic relationship was detected between the two compounds, with an FICI of 0.38. In the second study, **44** was found to reduce the MIC of AmB by up to 8-fold against *C. albicans*, when only  $0.08 \mu\text{g}\cdot\text{mL}^{-1}$  was supplied in combination with the antifungal drug. This combination produced a highly synergistic relationship with an FICI of 0.16.

The synergy was demonstrated using growth inhibition assays, checkerboard assays and disk diffusion assays in both cases. It is hypothesised that this synergistic anti-fungal relationship is the result of a combination of membrane disruption and conventional antifungal activity between the combined components. However, unfortunately, time restrains in relation to the recent COVID-19 pandemic meant that it was not possible to explore these mechanism studies.

To investigate the possibility of using these oligomers in biomaterials applications, an Alamar blue assay was conducted in order to probe the cytocompatibility of the oligomer **44**. It was found that concentrations of up to  $0.2 \text{ mg}\cdot\text{mL}^{-1}$  of **44** did not damage or inhibit the metabolic activity of

human lung fibroblasts compared to the vehicle control. This concentration is above that required to induce antifungal activity with AmB against *C. albicans*. As such, these can be considered positive preliminary results for the future use of these oligomers in antifungal materials and biomaterials applications.



## 3.5 Experimental

### 3.5.1 *General Materials and Methods*

#### Materials

All reagents were purchased from a chemical supplier and used without further purification. Water was deionised before use. Dry solvents were obtained from solvent drying towers and contained <17 ppm of water. TLCs were performed on silica gel mounted on aluminium and visualised using potassium permanganate with gentle heating. Experiments carried out using inert conditions employed nitrogen by means of a Schlenk line, or an argon balloon

#### Analytical Techniques

**<sup>1</sup>H NMR spectra** were recorded in deuterated chloroform (CDCl<sub>3</sub>) at 25°C, with Bruker 400 MHz spectrometers. <sup>1</sup>H NMR chemical shifts ( $\delta$ ) were recorded in parts per million (ppm), with the shift of CHCl<sub>3</sub> ( $\delta$  = 7.26 ppm) as the internal standard when CDCl<sub>3</sub> was used. The following abbreviations are used to designate the multiplicity of each signal; s, singlet; d, doublet; dd, doublet of doublets; dddd, doublet of doublet of doublet of doublets; t, triplet; dt, doublet of triplets; ddt, doublet of doublet of triplets; q, quartet; m, multiplet; app, apparent; br, broad. Couplings (*J*) are given in Hertz (Hz). **<sup>13</sup>C NMR spectra** were recorded in CDCl<sub>3</sub> on 100 MHz spectrometers. <sup>13</sup>C NMR chemical shifts were reported using the central line of CHCl<sub>3</sub> ( $\delta$  = 77.0 ppm) when CDCl<sub>3</sub> was used as the internal standard.

**Infra-Red spectra** were carried out using a Bruker Tensor 27 using an ATR attachment and peaks are quoted as  $\nu_{\max}$  in cm<sup>-1</sup>.

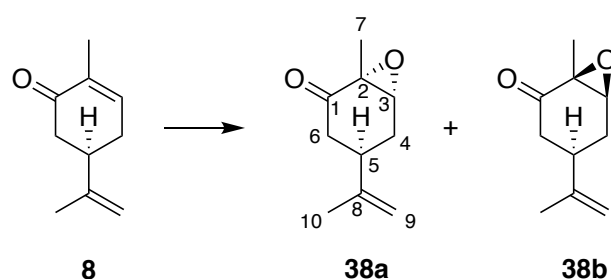
**High Resolution Mass Spectrometry** was conducted using a Bruker MicroTOF spectrometer operating in electrospray ionisation (ESI) mode.

**Gel Permeation Chromatography (GPC)** was performed in THF (HPLC grade, Fisher Scientific) as the eluent at room temperature using two Agilent PL-gel mixed-E columns in series with a flow rate of 1 mL min<sup>-1</sup>. A

differential refractometer (DRI), was used for sample detection. The system was calibrated using polycaprolactone standards.

### 3.5.2 Experimental procedures for monomer syntheses

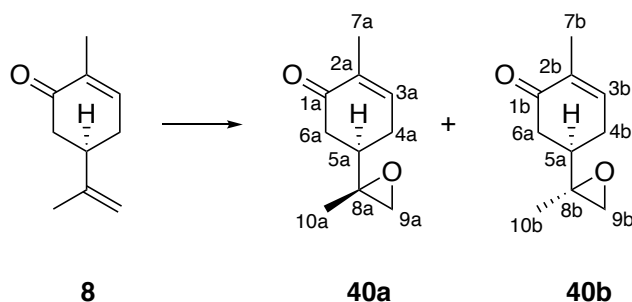
Synthesis of (1R,4R,6R)-1-methyl-4-(prop-1-en-2-yl)-7-oxabicyclo[4.1.0]heptan-2-one, (**38a**) and (1S,4R,6S)-1-methyl-4-(prop-1-en-2-yl)-7-oxabicyclo[4.1.0]heptan-2-one (**38b**).



To a solution of (*R*)-carvone (19.0 mL, 120.48 mmol) in MeOH (180 mL) was added 3M NaOH solution (12 mL, 36.15 mmol) and H<sub>2</sub>O<sub>2</sub> (30% w/w, 15 mL, 144.58 mmol). The mixture was stirred for 4 hours before quenching excess peroxides with sat. aq. Na<sub>2</sub>SO<sub>3</sub> (100 mL). The aqueous layer was extracted with ethyl acetate (2 x 100 mL) and the combined organic extracts were washed with sat. aq. Na<sub>2</sub>CO<sub>3</sub> (2x 100 mL) and brine (2x 100 mL) before drying over Na<sub>2</sub>SO<sub>4</sub>. Volatiles were removed under reduced pressure and the product was then concentrated *in vacuo* to afford the title compound as a yellow oil (17.95 g; 108.13 mmol, 90%) as a mixture of diastereomers (9:1, **38a**:**38b**), only peaks for the major diastereomer (**38a**) are reported. **FTIR (ATR)**  $\nu_{\max}/\text{cm}^{-1}$  = 3083, 2978, 2936, 1705 (C=O), 1646 (C=C), 1439, 1377, 1323, 1270 (C-O), 1117, 1047; **<sup>1</sup>H NMR**: (400 MHz, CDCl<sub>3</sub>)  $\delta_{\text{H}}$  = 4.78 – 4.74 (m, 1H, H-9'), 4.70 – 4.67 (m, 1H, H-9''), 3.42 (dd, *J* = 3.1, 1.2, 1H, H-3), 2.74 – 2.64 (m, 1H, H-5), 2.55 (ddd, *J* = 17.6, 4.7, 1.4, 1H, H-6'), 2.38 – 2.30 (m, 1H, H-4'), 2.00 (dd, *J* = 17.7, 11.6, 1H, H-6''), 1.87 (ddd, *J* = 14.7, 11.1, 1.2, 1H, H-4''), 1.68 (s, 3H, H-10), 1.38 (s, 3H, H-7); **<sup>13</sup>C NMR** (100 MHz, CDCl<sub>3</sub>)  $\delta_{\text{C}}$  = 205.5 (C-1), 146.4 (C-8), 110.6 (C-9), 61.4 (C-3), 58.9 (C-2), 41.9

(C-6), 35.1 (C-5), 28.8 (C-4), 20.7 (C-10), 15.4 (C-7); **HRMS (ESI<sup>+</sup>)**  $m/z$  [M+Na<sup>+</sup>] calculated for [C<sub>10</sub>H<sub>14</sub>NaO<sub>2</sub>]<sup>+</sup> 189.0891 found 189.0886 (M+Na<sup>+</sup>).

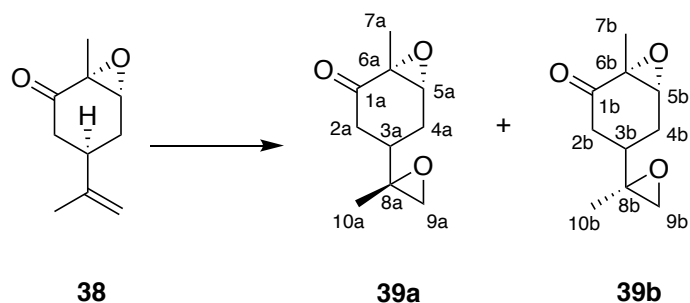
Synthesis of (*R*)-2-methyl-5-((*S*)-2-methyloxiran-2-yl)cyclohex-2-en-1-one (**40a**) and (*R*)-2-methyl-5-((*R*)-2-methyloxiran-2-yl) cyclohex-2-en-1-one (**40b**) (***m*CPBA method**)



To a solution of (*R*)-carvone (4.70 mL, 30.12 mmol) in CH<sub>2</sub>Cl<sub>2</sub> (28 mL, 0.5 M) was added *m*CPBA (70% w/w, 8.91 g, 36.15 mmol) in portions, at 0 °C. The reaction brought to room temperature and stirred for 5 hours before Na<sub>2</sub>S<sub>2</sub>O<sub>4</sub> (sat. aq.) (50 mL) was added to quench excess peroxides. The aqueous layer was extracted with CH<sub>2</sub>Cl<sub>2</sub> (2 x 50 mL), and the organic layer washed with excess NaHCO<sub>3</sub> (sat. aq.) (3 x 50 mL), and brine (2x 50 mL) before drying over MgSO<sub>4</sub>. Volatiles were removed under low pressure and the product was concentrated *in vacuo* to produce the title compounds as a yellow oil (4.502 g, 27.12 mmol, 90%) as a mixture of diastereomers (1:1/ **40a:40b**). **FTIR (ATR)**  $\nu_{\max}/\text{cm}^{-1}$  = 2977, 2924, 1754, 1667 (C=O), 1445, 1435, 1383, 1365, 1282, 1249 (C-O), 1106, 1072, 1026; **<sup>1</sup>H NMR** (400 MHz, CDCl<sub>3</sub>)  $\delta_{\text{H}}$  = 6.75 – 6.66 (m, 2H, H-3a and H-3b), 2.69 (dd,  $J$  = 4.4, 0.8 Hz, 1H, H-9a' or H-9b'), 2.65 (dd,  $J$  = 4.6, 0.8 Hz, 1H, H-9a' or H-9b'), 2.59 – 2.56 (m, 2H, H-9a'' and H-9b''), 2.56 – 2.49 (m, 2H, H-6a' and H-6b'), 2.44 – 2.33 (m, 2H, H-4a' and H-4b'), 2.30 – 2.18 (m, 4H, H-6a'', H-6b'', H-4a'' and H-4b''), 2.18 – 2.04 (m, 2H, H-5a and H-5b), 1.77 – 1.73 (m, 6H, H-7a and H-7b), 1.30 (d,  $J$  = 0.7 Hz, 3H, H-10a or H-10b), 1.29 (d,  $J$  = 0.7 Hz, 3H, H-10a or H-10b); **<sup>13</sup>C NMR** (100 MHz, CDCl<sub>3</sub>)  $\delta_{\text{C}}$  = 198.94 (C-1a or C-1b), 198.89 (C-1a or C-1b), 144.2 (C-3a or C-3b), 144.0 (C-3a or C-3b), 135.8 (C-2a or C-2b), 135.7

(C-2a or C-2b), 58.1 (C-8a or C-8b), 58.0 (C-8a or C-8b), 53.1 (C-9a or C-9b), 52.5 (C-9a or C-9b), 41.5 (C-5a or C-5b), 40.8 (C-5a or C-5b), 40.5 (C-6a or C-6b), 40.1 (C-6a or C-6b), 28.0 (C-4a or C-4b), 27.8 (C-4a or C-4b), 19.1 (C-10a or C-10b) 15.8 (C-10a or C-10b); **HRMS (ESI<sup>+</sup>)**  $m/z$  [M+Na<sup>+</sup>] calculated for [C<sub>10</sub>H<sub>14</sub>NaO<sub>2</sub>]<sup>+</sup> 189.0891 found 189.0886 (M+Na<sup>+</sup>).

Synthesis of (1*R*,6*R*)-1-methyl-4-((*R*)-2-methyloxiran-2-yl)-7-oxabicyclo[4.1.0]heptan-2-one (**39a**) and (1*R*,6*R*)-1-methyl-4-((*S*)-2-methyloxiran-2-yl)-7-oxabicyclo[4.1.0]heptan-2-one (**39b**) (mCPBA method)

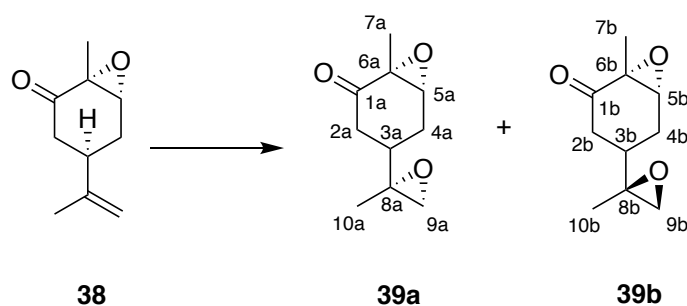


To a solution of **38** (9.37 g, 56.47 mmol) in CH<sub>2</sub>Cl<sub>2</sub> (60 mL, 1 M) at 0 °C was added meta-chloroperbenzoic acid (mCPBA) (70% w/w, 16.71 g, 67.77 mmol) slowly over 10 minutes. The solution was stirred for 16 hours at room temperature before excess peroxides were quenched with sat. aq. Na<sub>2</sub>S<sub>2</sub>O<sub>3</sub> solution (100 mL). The aqueous layer was then extracted with CH<sub>2</sub>Cl<sub>2</sub> (2 x 75 mL) and washed with NaHCO<sub>3</sub> (3 x 150 mL), and brine (100 mL) before drying over MgSO<sub>4</sub>. The solvent was removed under reduced pressure to yield title compound as a mixture of diastereomers, as a yellow oil (8.82 g, 50.82 mmol, 90%, dr = 1 : 1 for **39a** : **39b**). Only peaks for the two major diastereomers (**39a** and **39b**) are reported. **FTIR (ATR)**  $\nu_{\text{max}}$ / cm<sup>-1</sup> = 2979, 2943, 1704 (C=O), 1440, 1380, 1253, 1222, 1105, 1067; **<sup>1</sup>H NMR:** (400 MHz, CDCl<sub>3</sub>)  $\delta_{\text{H}}$  = 3.40 – 3.37 (m, 2H, H-5a and H-5b), 2.62 (dd,  $J$  = 4.5, 0.8 Hz, 1H, H-9a' or H-9b'), 2.59 (dd,  $J$  = 4.5, 0.8 Hz, 1H, H-9a' or H-9b'), 2.55 – 2.44 (m, 4H, H-9a'', H-9b'', H-2a' and H-2b'), 2.36 – 2.26 (m, 2H, H-4a' and H-4b'), 2.21 – 2.05 (m, 2H, H-3a and H-3b), 1.96 – 1.86 (m, 2H, H-2a'' and H-2b''), 1.81 – 1.72 (m, 2H, H-4a'' and H-4b''), 1.35 (s, 3H, H-7a and H-7b), 1.24 (s, 3H, H-10a or

H-10b), 1.21 (s, 3H, H-10a or H-10b). **<sup>13</sup>C NMR** (100 MHz, CDCl<sub>3</sub>) δ<sub>C</sub> = 205.0 (C-1a or C-1b), 204.8 (C-1a or C-1b), 61.5 (C-5a or C-5b), 61.0 (C-5a or C-5b), 59.1 (C-6a or C-6b), 59.0 (C-6a or C-6b), 57.8 (C-8a or C-8b), 57.7 (C-8a or C-8b), 53.0 (C-9a or C-9b), 52.3 (C-9a or C-9b), 39.0 (C-2a or C-2b), 38.4 (C-2a or C-2b), 31.0 (3a and 3b), 25.7 (C-4a or C-4b), 25.5 (C-4a or C-4b), 19.0 (C-10a or C-10b), 18.6 (C-10a or C-10b), 15.27 (C-7a and C-7b); **HRMS (ESI<sup>+</sup>)** *m/z* [M+Na<sup>+</sup>] calculated for [C<sub>10</sub>H<sub>14</sub>NaO<sub>3</sub>]<sup>+</sup> 205.0841 found 205.0830 (M+ Na<sup>+</sup>).

Synthesis of (1*R*,6*R*)-1-methyl-4-((*R*)-2-methyloxiran-2-yl)-7-oxabicyclo[4.1.0]heptan-2-one (**39a**) and (1*R*,6*R*)-1-methyl-4-((*S*)-2-methyloxiran-2-yl)-7-oxabicyclo[4.1.0]heptan-2-one (**39b**) (Oxone<sup>®</sup>)

**method**

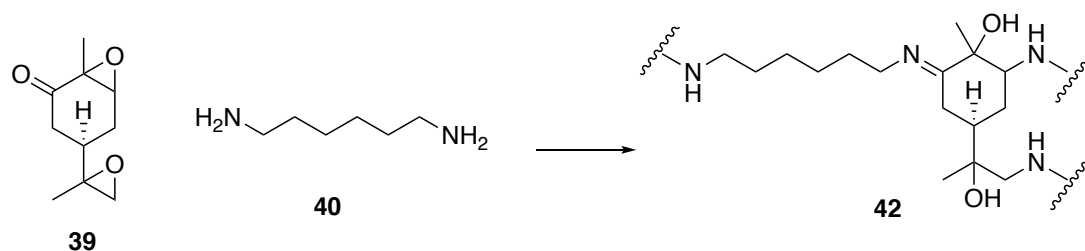


To a solution of **38** (3.715 g, 22.14 mmol) in acetone (90 mL) was added NaHCO<sub>3</sub> (8.95 g, 106.57 mmol). A solution of aqueous Oxone<sup>®</sup> was added (0.32 M, 106 mL) at a constant flow rate of 1 mL min<sup>-1</sup>, at room temperature. After the addition, the aqueous layer was extracted from the biphasic reaction medium into diethyl ether (2 x 75 mL) and the combined organic extractions were washed with brine (2 x 75 mL), dried over MgSO<sub>4</sub> and the solvent was removed under reduced pressure to yield the title compound as was a yellow oil consisting of a mixture of diastereomers (3.36 g, 20.23 mmol, 83%, dr = 1 : 1 for **39a** : **39b**). Only peaks for the two major diastereomers (**39a** and **39b**) are reported. **FTIR (ATR)** ν<sub>max</sub>/ cm<sup>-1</sup> = 2978, 2943, 1704 (C=O), 1441, 1380, 1253, 1223, 1105, 1066; **<sup>1</sup>H NMR:** (400 MHz, CDCl<sub>3</sub>) δ<sub>H</sub> = 3.48 – 3.39 (m, 2H, H-5a and H-5b), 2.66 (dd, *J* = 4.5, 0.8 Hz, 1H, H-9a' or H-9b'), 2.64 (dd, *J* = 4.4, 0.8 Hz, 1H, H-9a' or H-9b'), 2.60 – 2.49 (m, 4H, H-10a'', H-10b'', H-2a'

and H-2b'), 2.42 – 2.30 (m, 2H, H-4a' and H-4b'), 2.27 – 2.11 (m, 2H, H-3a and H-3b), 2.00 – 1.90 (m, 2H, H-2a'' and H-2b''), 1.86 – 1.75 (m, 2H, H-4a'' and H-4b''), 1.40 (d,  $J = 0.9$  Hz, 3H, H-7a and H-7b), 1.29 (s, 3H, H-10a or H-10b), 1.26 (s, 3H, H-10a or H-10b);  **$^{13}\text{C}$  NMR** (100 MHz,  $\text{CDCl}_3$ )  $\delta_{\text{C}} = 205.0$  (C-1a or C-1b), 204.8 (C-1a or C-1b), 61.5 (C-5a or C-5b), 61.0 (C-5a or C-5b), 59.1 (C-6a or C-6b), 59.0 (C-6a or C-6b), 57.8 (C-8a or C-8b), 57.7 (C-8a or C-8b), 53.0 (C-9a or C-9b), 52.3 (C-9a or C-9b), 39.0 (C-2a or C-2b), 38.4 (C-2a or C-2b), 31.0 (3a and 3b), 25.7 (C-4a or C-4b), 25.5 (C-4a or C-4b), 19.0 (C-10a or C-10b), 18.6 (C-10a or C-10b), 15.27 (C-7a and C-7b); **HRMS (ESI<sup>+</sup>)**  $m/z$  [ $\text{M} + \text{Na}^+$ ] calculated for  $[\text{C}_{10}\text{H}_{14}\text{NaO}_3]^+$  205.0841 found 205.0853 ( $\text{M} + \text{Na}^+$ ).

### 3.5.3 Experimental Procedures for polymer syntheses

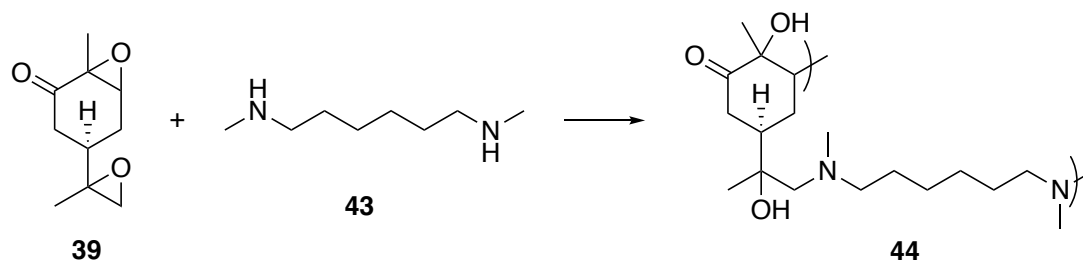
#### Synthesis of Oligomer **42**



To a glass vial charged with **39** (3.47 mmol, 0.632 g) was added 1,6-hexane diamine (**43**) (3.47 mmol, 0.51 g). The mixture was heated to 70 °C for 5 hours to yield an orange-brown solid.  $M_n$  from **GPC**: 1235  $\text{g}\cdot\text{mol}^{-1}$  and  $\text{Đ} = 2.3$ . **FTIR (ATR)**  $\nu_{\text{max}}/\text{cm}^{-1} = 3374$  (OH), 2927, 2855, 1707 (C=O), 1646 (C=N), 1450, 1371, 1337, 1286, 1256, 1090 (C-O), 1034;  **$^1\text{H}$  NMR**: (400 MHz,  $\text{CDCl}_3$ )  $\delta_{\text{H}} = 4.46$  (d,  $J = 6.8$  Hz), 3.34 – 3.10 (m), 2.97 – 2.80 (m), 2.78 – 2.56 (m), 2.55 – 1.63 (m), 1.63 – 1.49 (m), 1.47 – 1.34 (m,  $\text{CH}_2$ ), 1.29 (m,  $\text{CH}_2$ ), 1.14 (s,  $\text{CH}_3$ ), 1.10 – 0.97 (m,  $\text{CH}_3$ );  **$^{13}\text{C}$  NMR** (100 MHz,  $\text{CDCl}_3$ )  $\delta_{\text{C}} = 211.1$  (C=O), 173.1 (C=N), 98.0 (C-H), 79.7 (C-OH), 76.4 ( $\text{CR}_3\text{OH}$ ), 75.7 ( $\text{CR}_3\text{OH}$ ), 70.1 ( $\text{CR}_3$ ), 67.8 (CH), 63.8 (CH), 62.9 (CH), 57.7 ( $\text{CH}_2$ ), 56.8 ( $\text{CH}_2$ ), 56.7 ( $\text{CH}_2$ ), 55.6 ( $\text{CH}_2$ ), 54.6 ( $\text{CH}_2$ ), 50.5 ( $\text{CH}_2$ ), 42.1 ( $\text{CH}_2$ ), 39.8 (CH), 33.6 ( $\text{CH}_2$ ), 30.7, 26.9, 25.7

(CH<sub>3</sub>), 24.0; **HRMS (ESI<sup>+</sup>)**  $m/z$  [M+H<sup>+</sup>] calculated for [C<sub>37</sub>H<sub>73</sub>N<sub>6</sub>O<sub>4</sub>]<sup>+</sup> 677.5693 found 677.5697 (M + H<sup>+</sup>).

#### Synthesis of Oligomer **44**



To a glass vial charged with **39** (3.47 mmol, 0.632 g) was added 1,6-dimethyl hexane-1,6-diamine (**43**) (3.47 mmol, 0.62 mL). The mixture was heated to 70 °C for 7 days to yield a viscous, dark-brown oil.  $M_w$  from **GPC**: 733 g·mol<sup>-1</sup> and  $\bar{D} = 1.26$ . **FTIR (ATR)**  $\nu_{\max}/\text{cm}^{-1} = 3304$  (OH), 2930, 2855, 2791, 1731 (C=O), 1649, 1576, 1449, 1407, 1372, 1353, 1305, 1240, 1117, 1077 (C-O), 1050, 1005; **<sup>1</sup>H NMR**: (400 MHz, CDCl<sub>3</sub>)  $\delta_H = 4.06 - 3.87$  (m), 3.02 - 1.88 (m), 1.66 - 0.92 (m); **<sup>13</sup>C NMR** (100 MHz, CDCl<sub>3</sub>)  $\delta_C = 209.7$  (C=O), 70.6 (C-OH), 67.1, 66.3, 65.6, 60.1, 60.0, 52.2, 52.1, 44.6, 41.3, 40.9, 40.5, 36.5, 34.7, 33.8, 33.4, 29.8, 27.4, 27.36, 25.4, 25.2, 24.1, 17.4, 16.5, 16.4; **HRMS (ESI<sup>+</sup>)**  $m/z$  [M+H<sup>+</sup>] calculated for [C<sub>28</sub>H<sub>49</sub>N<sub>2</sub>O<sub>6</sub>]<sup>+</sup> 509.3591 found 509.3587 (M + H<sup>+</sup>).

### 3.5.4 Experimental Procedures for antifungal studies

#### Growth inhibition assays

Dr. Cindy Vallières is acknowledged for conducting the growth inhibition assays. For growth assays with *Candida albicans* SC5314, a standard laboratory strain, single colonies from YPD agar plates were used to inoculate YPD broth cultures [2% peptone (Oxoid, Basingstoke, UK), 1% yeast extract (Oxoid), 2% D-glucose] in Erlenmeyer flasks and incubated overnight at 37 °C, with orbital shaking at 120 rpm. Overnight cultures were diluted to OD<sub>600</sub> ~ 0.5 and cultured for a further 4 hours in fresh medium. The 4 hour mid/late exponential cultures were diluted to OD<sub>600</sub> ~ 0.01 and 100 mL aliquots transferred to 96-well microtiter plates (Greiner Bio-one; Stonehouse, UK), with drugs and oligomer added to final concentrations as specified in the Results and Discussion section 3.3.5.1. Plates were incubated at 37 °C with shaking in a BioTek Powerwave XS microplate spectrophotometer and OD<sub>600</sub> was recorded every 30 min.

For growth assays with *Trichoderma virens* CBS 430.54, spores were harvested from 7 d PDA (Oxoid) plates and inoculated to PDB (Sigma-Aldrich) broth to a concentration of 15 000 spores per mL. Aliquots (100 mL) of the diluted culture plus any chemical supplements, as specified in the Results and Discussion section 3.3.5.1, were transferred to 96-well plates and cultured statically for up to 65 hours at 30 °C in a BioTek Powerwave XS microplate spectrophotometer. For assaying antifungal combinations, concentrations of agents used were those determined from preliminary assays to be just sub-inhibitory or slightly inhibitory when supplied individually.

#### Checkerboard Assays

Dr. Cindy Vallières is acknowledged for conducting the checkerboard assays. General culturing and preparation for yeast 'checkerboard' assays was according to EUCAST guidelines.<sup>229</sup> Briefly, yeast cells from single



colonies were inoculated from 2-d PDA plates to RPMI 1640 medium + 2% glucose and cell concentration adjusted to a final inoculum of  $10^5$  cells mL<sup>-1</sup>. All culturing for checkerboard assays with *T. virens* was as described above. Culture aliquots (100 µL) were transferred to 96-well microtiter plates with chemicals added at the concentrations specified in the checkerboard figures (below). The inoculated plates were incubated statically for 48 hours at 30 °C (*T. virens*) or 24 hours at 37 °C (*C. albicans*). OD<sub>600</sub> was then measured with a BioTek EL800 microplate spectrophotometer. Fractional Inhibitory Concentration (FIC) as an indicator of synergy was calculated as described.<sup>230</sup>

#### Disk Diffusion Assays

Dr. Cindy Vallières is acknowledged for conducting the disk diffusion assays, PDA and YPD medium were inoculated with 10<sup>6</sup> spores per mL (*T. virens*) from 7 d-PDA plates and 10<sup>7</sup> cells per mL from exponential growth-YPD broth cultures (*C. albicans*), respectively. Sterile Whatman paper filter disks loaded with 10 mL inhibitor(s) were laid on the plates and incubated at 30 °C for 48 hours (*T. virens*) or at 37 °C for 24 hours (*C. albicans*).

#### Cytocompatibility Analysis

Mr. Arsalan Latif is acknowledged for conducting the cytocompatibility analysis. Cellular metabolic activity was studied using the Alamar Blue cell viability assay (ThermoFisher Scientific, UK) in order to assess polymer cytocompatibility. The cytotoxicity of oligomer **44** was studied on MRC-5 human lung fibroblasts. Cells were cultured in Dulbecco's Modified Eagle's Medium (DMEM; Sigma-Aldrich) supplemented with 10% (v/v) Foetal Bovine Serum (FBS; Sigma-Aldrich), 0.1 mg·mL<sup>-1</sup> streptomycin, 100 units/mL penicillin, 0.25 µg·mL<sup>-1</sup> amphotericin (Sigma-Aldrich) and 2 mM L-glutamine (Sigma-Aldrich) at 37 °C with 5% CO<sub>2</sub>.

For assaying, MRC-5 cells were seeded at density of 5x10<sup>4</sup> cells/well in a 24 well plate and cultured for 24 hours prior to testing. Dosing of cells

was initiated by removing culture medium, washing cells with phosphate buffered saline (PBS; Sigma-Aldrich) and the application of 2.0 mL per well of **44** (0.1 - 0.8 mg·mL<sup>-1</sup>) for 24 hours at 37 °C with 5% CO<sub>2</sub>. Polymer solutions were applied to cells diluted in culture medium. Treatment of cells with media alone served as the vehicle control. Following exposure, 200 µL Alamar Blue solution was applied per well, achieving a final Alamar Blue concentration of 9%, and incubated for 4 hours at 37 °C with 5% CO<sub>2</sub>. Solution fluorescence was then measured at 535/590 nm ( $\lambda_{\text{ex}}/\lambda_{\text{em}}$ ) using a Promega microplate reader, and relative metabolic activity calculated by setting the values of the negative control as 100% and values of Alamar Blue solution without cells as 0%.

## 4 Chapter Four: A brief insight into polymerisations using oxidised terpenes

### 4.1 Introduction: alcohol-based terpene monomers

The Introduction chapter of this thesis discusses in detail the environmental problems associated with polymer materials derived from crude oil. That chapter described how the global population has come to rely on polymers at a rate which is rapidly depleting the world's crude oil reserves, as the materials delve into ever-broad and versatile applications.<sup>2</sup> Given that crude oil feedstocks are expected to become depleted within the next century,<sup>8</sup> bio-based raw materials are now considered the preferred alternative to fossil-fuel carbon sources.<sup>6,12</sup>

Terpenes and terpenoids have been introduced as an attractive source of renewable, bio-based polymeric building blocks for polymer chemistry. Chapters 2 and 3 of this thesis deal with some of the ways in which the small-molecules can be used for polymer chemistry for biomedical applications, and in the literature, the renewable biomass has been the subject of many reviews with a great variety of applications.<sup>6,8,9,15</sup> As discussed in the introduction, terpene feedstocks offer an array of small molecules with a variety of double bonds and chiral centres,<sup>31</sup> that are naturally abundant, inexpensive and do not compete directly with food sources.<sup>35,68</sup> Many of them are already produced on industrial scales, as they are used in fragrance and flavouring industries.<sup>169</sup>

However, despite significant efforts to make polymers directly from terpenes,<sup>43</sup> results show that the materials do not readily homopolymerize, and the polymers lack the desired properties to compete with commercial alternatives.<sup>35,45</sup> On the other hand, the functionalisation of terpenes has shown the feedstock has huge potential for polymerisation.<sup>46</sup> Synthetic methods have been developed which over the past 20 years have seen terpenes undergo facile and robust (as well as bespoke) chemical modifications, to arrive at a wealth of monomer compounds. Primarily, this has been achieved *via* oxidation of the alkene moieties, which has been particularly successful. To give only a small handful of examples which are each described in more detail in the introduction chapter: The

Baeyer-Villiger oxidation has been employed by the Hillmyer group to arrive at a number of terpene-based lactones, derived from carvone and menthone. These were used to produce polyesters by Ring Opening Polymerisation (ROP).<sup>11,43,67-69</sup> Similarly, terpenoids with a ketone functionality can be converted to oximes, which can in turn undergo the Beckmann rearrangement, resulting in the corresponding lactams. These can undergo ROP to produce polyamides.<sup>43,71-73</sup> Epoxidation of terpenes has resulted in polycarbonates,<sup>28,49-51</sup> polyurethanes,<sup>52,53</sup> and polyethers.<sup>54,55</sup> Epoxidised terpenes also have applications as bio-based crosslinkers in epoxy-resin chemistry.<sup>56,57</sup>

Evidently, the oxidation of terpene-based biomass has huge potential for polymerisation, and as a result, much research now exists into green and sustainable methods of accessing these monomers, often independent to the investigations into their polymerisations.<sup>47,48</sup> In 2019, Drosbeke *et al.* synthesised a variety of terpene-based (meth)acrylate monomers employing sustainable synthetic methods, using the green metrics toolkit.<sup>47</sup> In 2020, Löser *et al.* demonstrated a catalytic synthesis of bis-carbonyl monomers from terpene-derived epoxides, and in 2018, Hernandez-Ortega *et al.* developed a library of diverse, oxidised monoterpenes which were all synthesised using a cytochrome P450 enzyme collection.<sup>245</sup>

To tap into the full potential of terpene-based polymers, research into the polymerisation of these (and other such) monomers has focused on methods that can 'drop' these terpenes and terpenoids into well-established polymerisation methods.<sup>35,45</sup> A variety of examples exist of terpenes, and frequently, their (meth)acrylate derivatives, used in RAFT polymerisations.<sup>77,78</sup> The Stockman and Howdle groups at the University of Nottingham have made progress over the last decade in generating (and capitalising upon naturally occurring) alcohol-functionalised terpenes. In 2016, it was demonstrated that the Brown hydroboration/oxidation could be used to produce a number of terpene-alcohols, which were in turn easily converted to (meth)acrylate monomers for free radical polymerisation.<sup>45</sup> In 2019, similar conditions were employed in the synthesis of a limonene-based diol, which could be further oxidised to the hydroxy-acid, or used as the diol with a diacid co-monomer, in the synthesis of bio-based polyesters

by condensation polymerisation methods.<sup>35</sup> More detail of these polymerisations can be found in the Introduction chapter ( section 1.0).

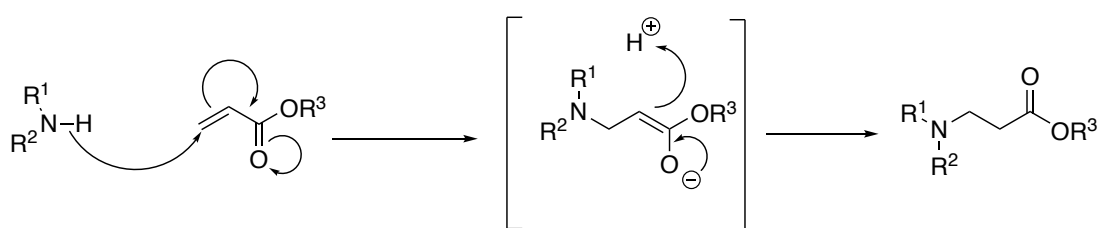
With a wealth of sustainable oxidative (and other) synthetic methods being developed,<sup>47,48</sup> it is evident that oxidised terpenes, in particular, alcohols, have much untapped potential as starting materials in polymer chemistry. This chapter is intended as an epilogue to the overall thesis: smaller than the previous chapters (as a result of the COVID-19 pandemic), it aims to briefly introduce a small library of novel terpene-based diols and triols, and demonstrate some of their potential in polymer chemistry. This will focus on two polymerisation types: polyesterification, for which diols can be used as monomers, and Michael-type polyaddition, for which the diols are twice-acrylated to produce the monomer compounds.

Polyesterification is a specific type of condensation polymerisation, a classification first coined by Carothers in 1929, to describe the reaction in which monomers react together to form polymers with the loss of a small molecule by a condensation mechanism.<sup>246</sup> By definition, the polymer chains are then available to undergo depolymerisation back to the monomer building blocks by hydrolysis or an equivalent chemical degradation reaction.<sup>246,247</sup> Condensation polymerisations have been used to generate polyesters, polyamides and polyethers, and it follows that polyesterification specifically refers to condensation polymerisations which result in polymers based on ester bonds.<sup>247</sup>

Polyaddition is an alternative method of polymerisation, also coined by Carothers in 1929.<sup>246</sup> In this case there is no loss of a small molecule by condensation, instead, the molecular formula of the monomer is identical with that of the structural unit.<sup>246</sup> Often this results practically in a proton transfer or rearrangement of the atoms from the monomer to the polymer.

Michael-type polymerisation is an example of a polyaddition mechanism which is used to generate poly( $\beta$ -amino ester)s. The Langer group was the first to use the Michael addition of a bifunctional amine with diacrylate esters to generate these polymers in 2000,<sup>248</sup> however, a similar reaction was reported by Ferruti *et al.* as early as 1970, employing bisacrylamides as alternatives to acrylates.<sup>249</sup> As with polyesterification,

the polymerisation works on the same principle as the small molecule reaction, with the bis-functionality of the monomers allowing for the formation of polymers.<sup>250</sup> In the case of the Michael-addition, this involves the coupling of electron poor alkenes or alkynes with a nucleophile.<sup>251</sup> This reaction is reported to be catalysed by either acids or bases, whereby the former is used to activate the Michael donor and the latter activates the acceptor.<sup>252</sup> However, the reaction is known in some cases to proceed in the absence of catalysts, especially with increasing nucleophilicity of the donor and electrophilicity and steric accessibility of the acceptor.<sup>252</sup> Where the nucleophile involved is an amine, this is known as the aza-Michael reaction (**Scheme 34**).



**Scheme 34.** Mechanism for the aza-Michael reaction of a generic amine with a generic acrylic ester, forming a  $\beta$ -amino ester.

While the aza-Michael polymerisation can take place at ambient conditions, recent work by Blakney *et al.* found that the use of triethylamine was an effective Lewis-base catalyst, resulting in a doubling of the molecular weight of the polymer material, although up to 14 days was the required reaction time.<sup>253</sup> More recently, Gurnani *et al.* reported an improved synthesis of the analogous bis-acrylamide reaction to produce poly(amidoamine)s, with triethylamine in a microwave synthesis, which significantly reduced reaction times.<sup>254</sup>

Since Langer's initial works, the aza-Michael polymerisation has been used to generate highly functional, biocompatible polymers.<sup>255</sup> An additional attractive feature is the ester bond in the polymer backbone, rendering the material biodegradable *via* hydrolysis.<sup>248</sup> The potential applications for these materials are vast, though they are currently

receiving a lot of attention for their potential to act as gene delivery vectors.<sup>253,254</sup> In fact, the motivation behind the original work was to enable the synthesis of cationic polymers for use in biomaterials and biomedical applications, that were available to undergo (bio)degradation. This is particularly important for applications such as gene delivery, which requires not only the complexation of the RNA to the cationic polymer vector, but it also must undergo “vector unpacking” in order to be able to deliver the gene, which can be facilitated by degradation of the polycation.<sup>248</sup>

However, the situation remains in that the next generation of polymer materials must endeavour to use green and sustainable approaches, in addition to bio-renewable starting materials, to try and reach circularity in these materials. As of yet, terpenes have not been investigated as a feedstock for these polymerisation types.

## 4.2 Aims and Objectives

Brown's hydroboration/ oxidation mechanism has proved a robust and facile method in which to add alcohol groups across alkenes *via* an anti-Markovnikov mechanism.<sup>256</sup> This is highly practical as it allows for the synthesis of the *least* hindered alcohol to form, often a primary or secondary (rather than tertiary) one, which means it is available for nucleophilic reactions, for example, in condensation reactions with carboxylic acids. The Howdle and Stockman groups at the University of Nottingham have previously reported the successful syntheses of alcohol-derived terpenes using these conditions.<sup>35,45</sup>

As such, it was aimed to expand upon the library of terpene-derived diols and triols synthesised using these methods, which have a huge potential for polymer chemistry. Previous work in the group has shown that limonene (**4**) and *trans*-sobrerol (**12**) can be converted to their corresponding diol (**20**) and triol (**45**) compounds,<sup>171</sup> and so it was decided in this project to use these conditions with  $\gamma$ -terpinene (**7**), citronellol (**13**), and linalool (**46**), aiming to synthesise compounds **47**, **48** and **49**, respectively (**Figure 90**).

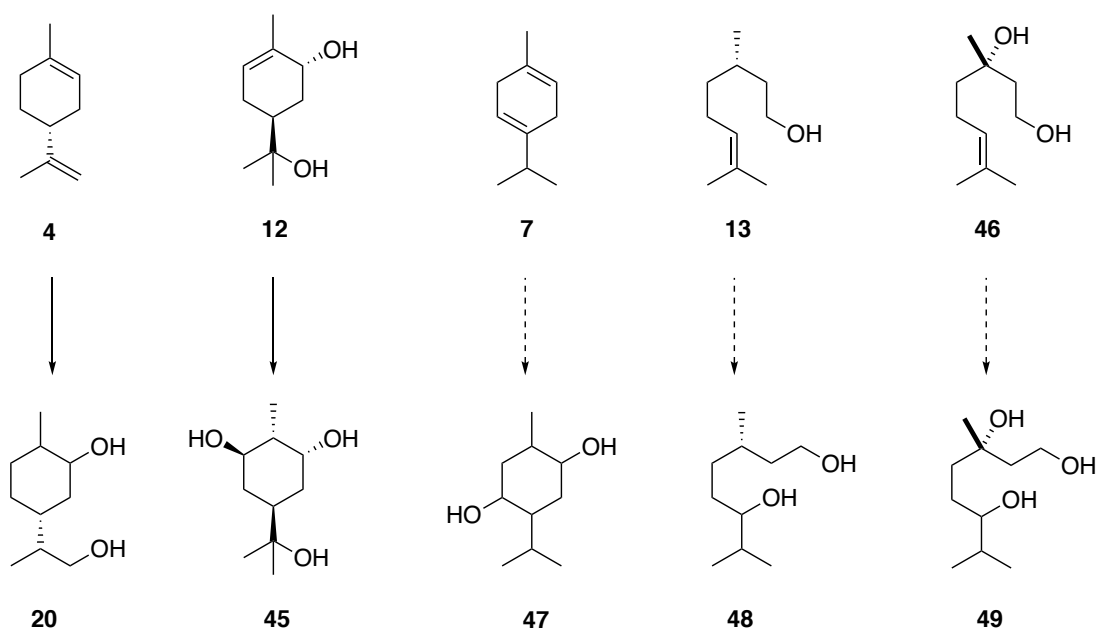
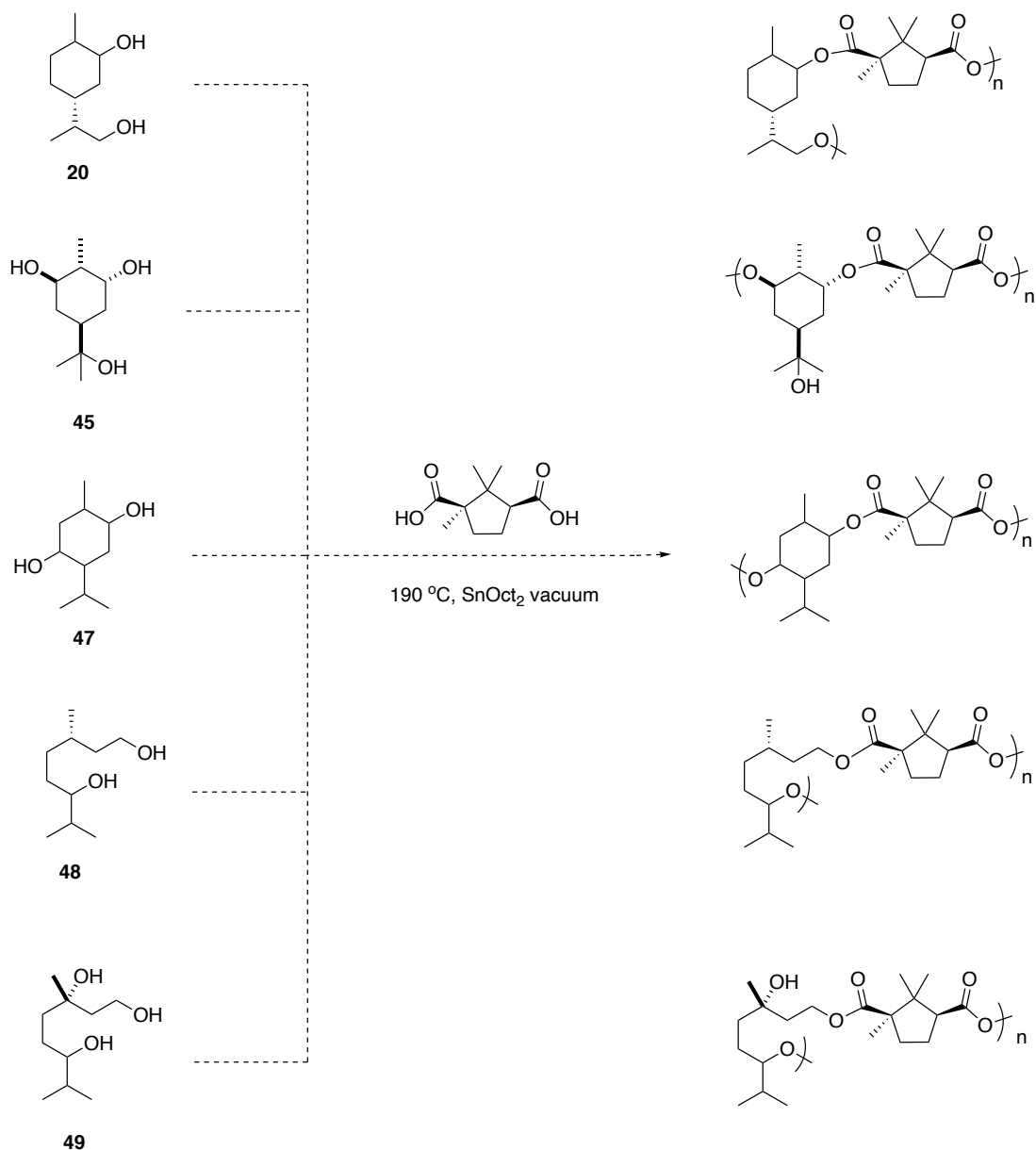


**Figure 90.** The proposed synthesis of terpene-derived diols and triols via the hydroboration/oxidation mechanism.



Following a successful synthesis of these five poly-ols, it was intended to investigate their use as monomers in polycondensation reactions. These terpenes were specifically chosen as their oxidised alcohol equivalents were predicted to form linear polymers with di-carboxylic acid co-monomers, avoiding branching reactions that might occur with more than two reactive alcohol functionalities. The triols **45** from *trans*-sobrerol and **49** from linanlool were not predicted to undergo branching, as the third alcohol in their structure is tertiary, and therefore unlikely to undergo nucleophilic addition.<sup>107</sup>

While the previous studies by Thomsett *et al.* has employed succinic acid as a co-monomer,<sup>35,171</sup> in this project it was decided instead to use camphoric acid, a di-acid made from the oxidation of the terpenoid camphor.<sup>257</sup> In 2019, Nsengiyumva *et al.* employed this monomer in the synthesis of linear polyesters with glass transition temperatures ranging from -16 °C to 125 °C.<sup>257</sup> By employing camphoric acid as a co-monomer with the terpenoid poly-ols in **Figure 75**, it was aimed to achieve five new polyesters fully derived from terpene-based biomass (**Scheme 35**). Additionally, it was envisaged that in the cases where there would be two hydrocarbon rings per repeat unit in the backbones of the resulting polymers (one from the poly-ol and one from the di-acid), this would further increase the rigidity of the polymers with respect to other common polyesters, which rarely include such features. It is hypothesised that this may in turn impart desirable properties to the polymers, such as high glass transition temperatures.<sup>257</sup>



**Scheme 35.** The proposed synthesis of five novel, fully terpene-based polyesters using melt conditions from Thomsett et al.<sup>171</sup>

The functionalisation of terpenes with (meth)acrylate groups has also proved a successful way in which to polymerise this renewable feedstock, by a variety of polymerisation techniques.<sup>78,258,259</sup> Using this toolbox of terpene-based poly-ols (**Figure 90**), it was intended to demonstrate a new, untapped method in which terpene-based acrylates can be polymerised: by the aza-Michael polymerisation. To achieve this, it was

endeavoured to convert each of the poly-ols to their corresponding di-acrylate compounds (**Figure 91**).

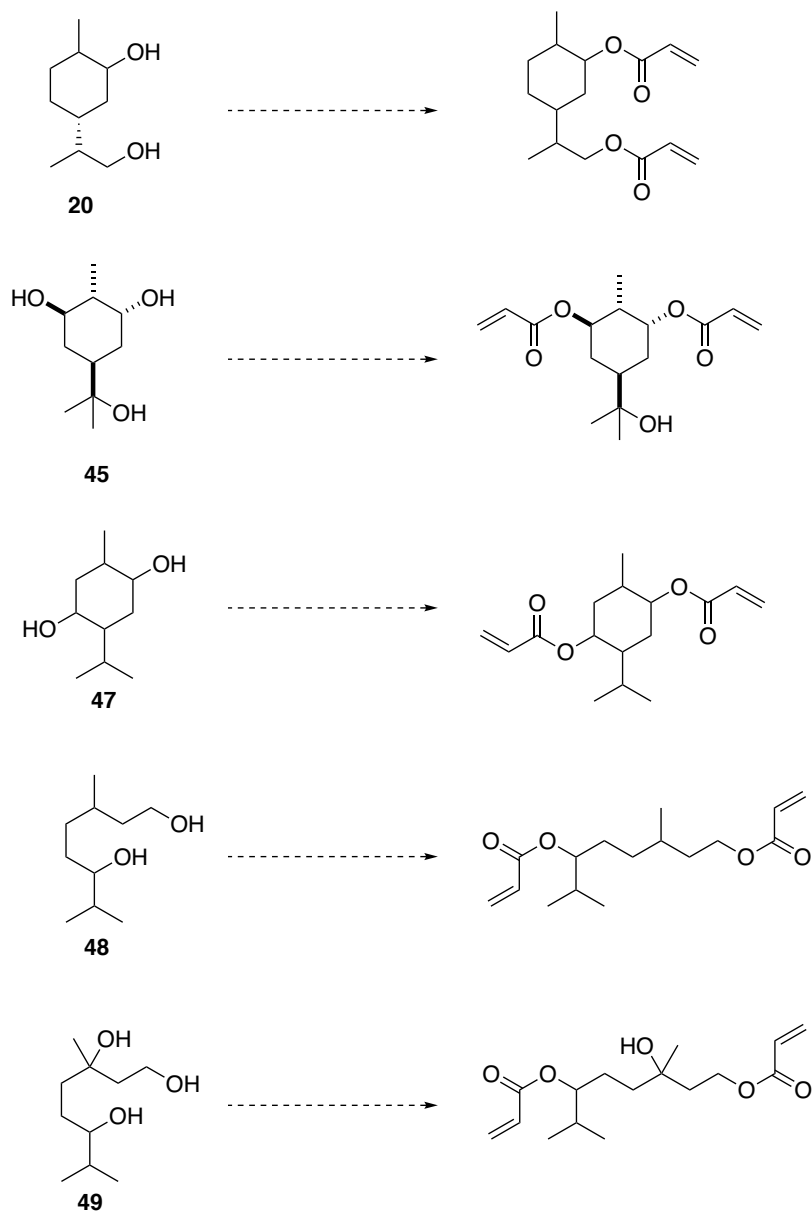
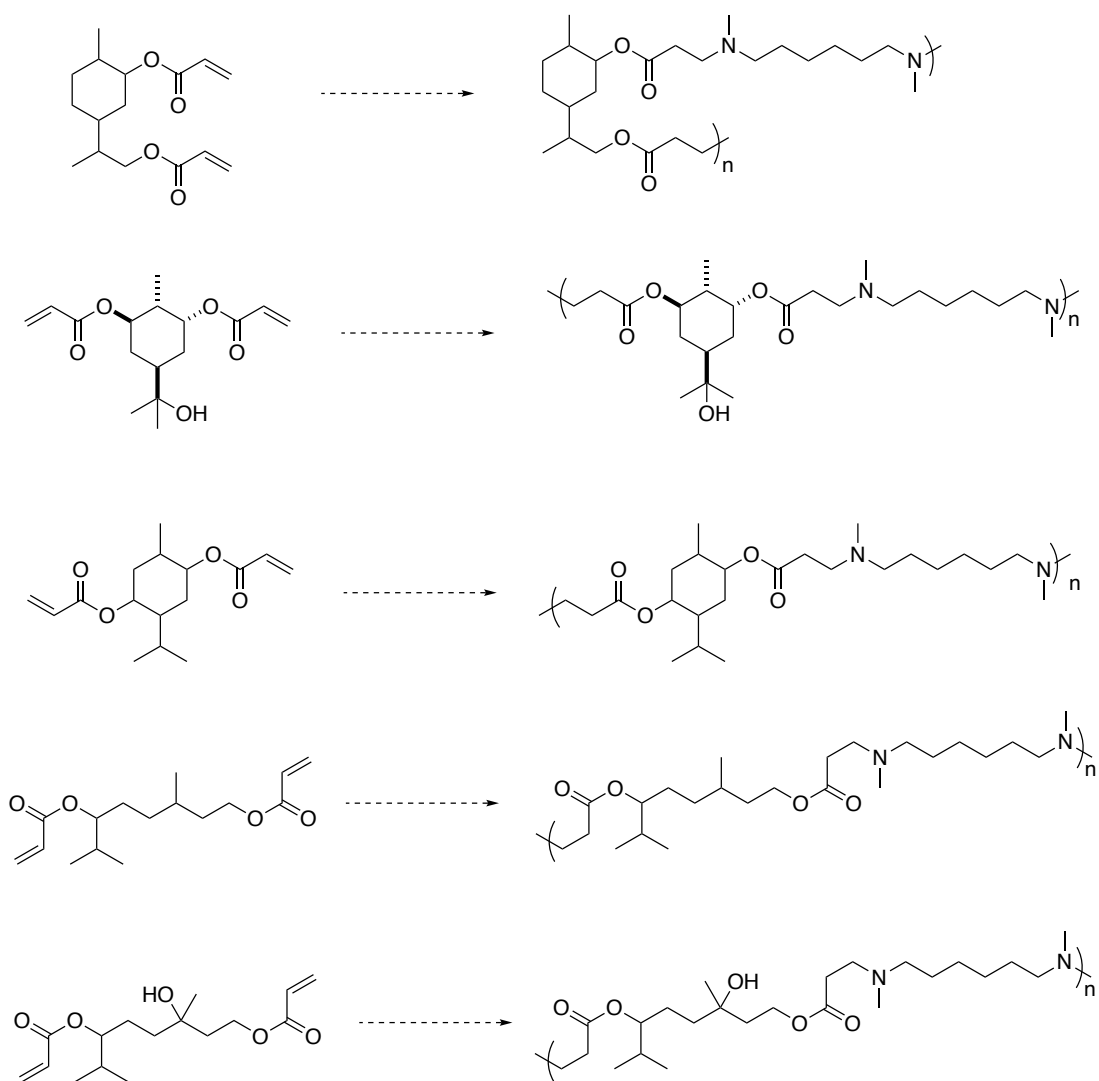


**Figure 91.** The proposed conversion of terpene-based poly-ols to five novel terpene-based diacrylate monomers.

Being mindful of the 12 Principles of Green Chemistry,<sup>13</sup> it was endeavoured to keep these reactions as non-toxic and sustainable as possible. As such, it was proposed to conduct the esterifications of the terpene diols to the corresponding di-acrylates using acrylic acid, which is bio-renewable, and propyl phosphonic anhydride (T3P®) which promotes

ester coupling. This reagent produces an environmentally benign, water-soluble triphosphate by-product, which is considerably more sustainable than the chlorinated alternatives when acryloyl chloride is used.<sup>45</sup>

Following a successful synthesis of these compounds, the next step would be to investigate their use as monomers in step-growth aza-Michael polymerisations with 1,6-dimethyl hexane diamine (**43**) as a co-monomer (**Scheme 36**). This is a linear, di-secondary diamine with a six-membered aliphatic alkyl chain between the two amine moieties. Owing to the previous success with this compound in the generation of  $\beta$ -amino alcohol oligomers from terpenes for anti-fungal purposes<sup>107</sup> (Chapter 3 of this thesis), it was sought to use **43** again in this work in order to capitalise upon the hydrophobic/hydrophilic balance between the alkyl chain and the amine groups. Amine moieties become cationic and hydrophilic in physiological conditions,<sup>260</sup> and the amphiphilic balance of polymers is known to play an important role in terms of any biocidal or anti-microbial activity,<sup>146</sup> which it is envisaged could be a potential application of any polymer materials formed in this instance.

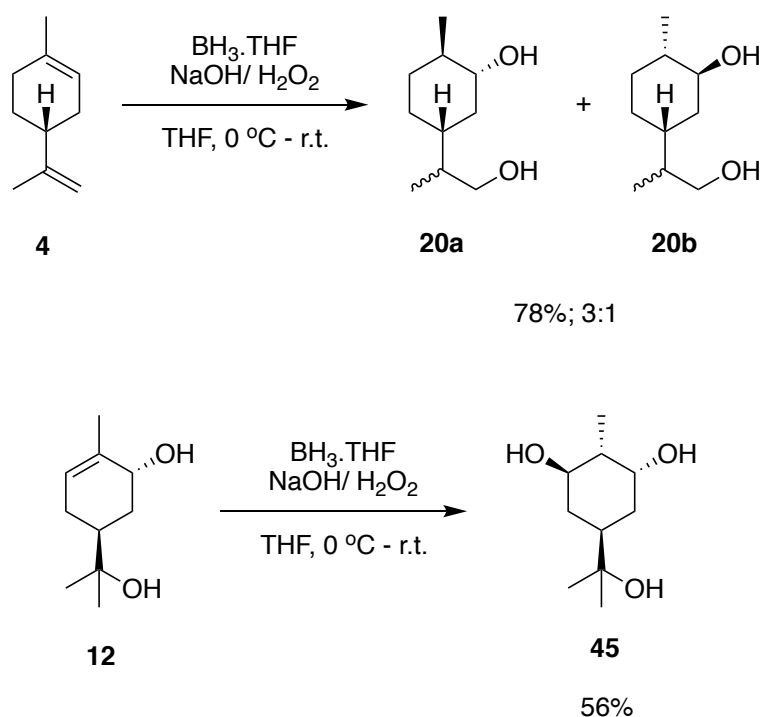


**Scheme 36.** The proposed synthesis of novel  $\beta$ -amino ester polymers from terpene-diacrylates and **43**.

### 4.3 Results and Discussion

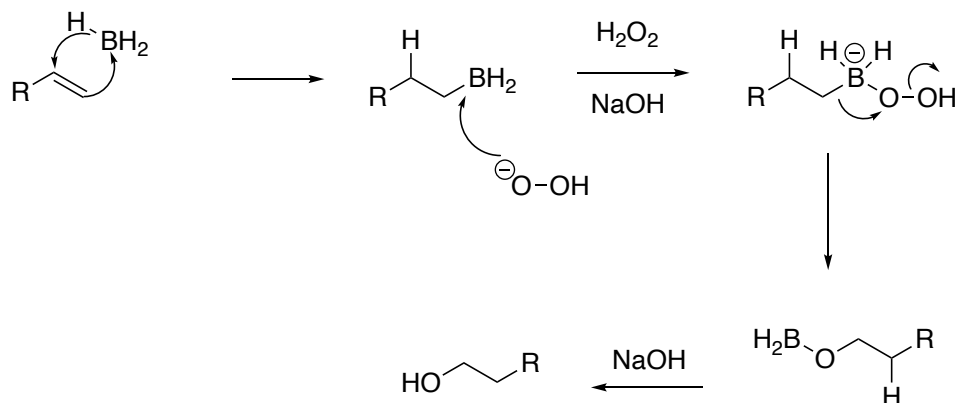
#### 4.3.1 Synthesis of terpene-based diols

A small library of poly-ol monomers for use in the synthesis of polyesters by polycondensation was designed, consisting of diols and triols derived from terpene-based biomass (**Figure 75**). Two of these monomers, limonene-diol (**20**) and *trans*-sobrerol-diol (**45**), are known compounds, having been previously synthesised by the Stockman and Howdle groups at the University of Nottingham.<sup>35,171</sup> Both are accessed *via* the Brown hydroboration/oxidation reaction conditions<sup>256</sup> on limonene (**4**) and *trans*-sobrerol (**12**). As such, these monomers were synthesised according to this protocol, which resulted in 78% and 56% yields for **20** and **45**, respectively (**Scheme 37**).



**Scheme 37.** The synthesis of limonene-diol (**20**) and *trans*-sobrerol triol (**45**) following conditions by Thomsett et al.<sup>171</sup> The synthesis of **20** introduces mixtures of new stereocentres to the molecule, while **45** is synthesised as a single diastereomer, purified by recrystallisation.

The hydroboration/oxidation follows an anti-Markovnikov mechanism, meaning that the alcohol group is added across the double bond to the least-hindered carbon atom. This is a result of the hydroboration step of the reaction: as the alkene  $\pi$ -electrons are donated into the empty p-orbital of the boron atom, a partial positive charge builds up at the other, more substituted carbon. Simultaneously, a hydride is transferred to this carbon atom, quenching this partial positive charge (**Scheme 38**).<sup>261</sup>



**Scheme 38.** The generic hydroboration/oxidation mechanism.<sup>261</sup>

The result of this regioselective mechanism is that the alcohol will end up on the same face as the one the hydride is added to. In the case of both **4** and **12**, when the endocyclic alkene undergoes the reaction, this means that the methyl group in the ring will end up on the opposite face to alcohol group. In the original studies, Thomsett *et al.* determined that in the case of limonene, the more favourable face for the boron to add is from the bottom face, resulting in the alcohol in the equatorial position.<sup>171</sup> This is a result of an intermediate borane complex which forms, and where more than one equivalent of  $\text{BH}_3$  is used, the result is a 3:1 ratio of **20a**:**20b**.

It was also determined in a similar study that the stereocentre surrounding the other, exocyclic methyl group of **20** is enriched in the *S*-diastereomer,<sup>262</sup> and Thomsett *et al.* reported that their conditions followed this trend.<sup>171</sup> The  $^1\text{H}$  NMR resonances for the mixture synthesised in this project matched those reported by Thomsett *et al.*, and so it was concluded that in this case, **20a** and **20b** was also enriched in the *S*-diastereomer at this position.





It was anticipated that the generation of the triol **49** from linalool would be water soluble and difficult to isolate, however, it was happily observed that this was not the case: the molecule was readily extracted with diethyl ether. Purification by silica gel chromatography yielded the product in a modest yield of 33%, as determined by quantitative NMR.

The reaction is not stereoselective, and so a new stereocentre was introduced to the molecule in a 1:1 ratio at the C-7 position of the secondary alcohol. Additionally, the linalool starting material used was an enantiomeric mixture, resulting in the pure product consisting of a mixture of 4 diastereomers. As these are two pairs of enantiomers, only signals for the **49a** and **49b** diastereomers are reported, as **49c** and **49d** are their respective enantiomers (**Figure 93**). It was not attempted to further separate any of these diastereomers.

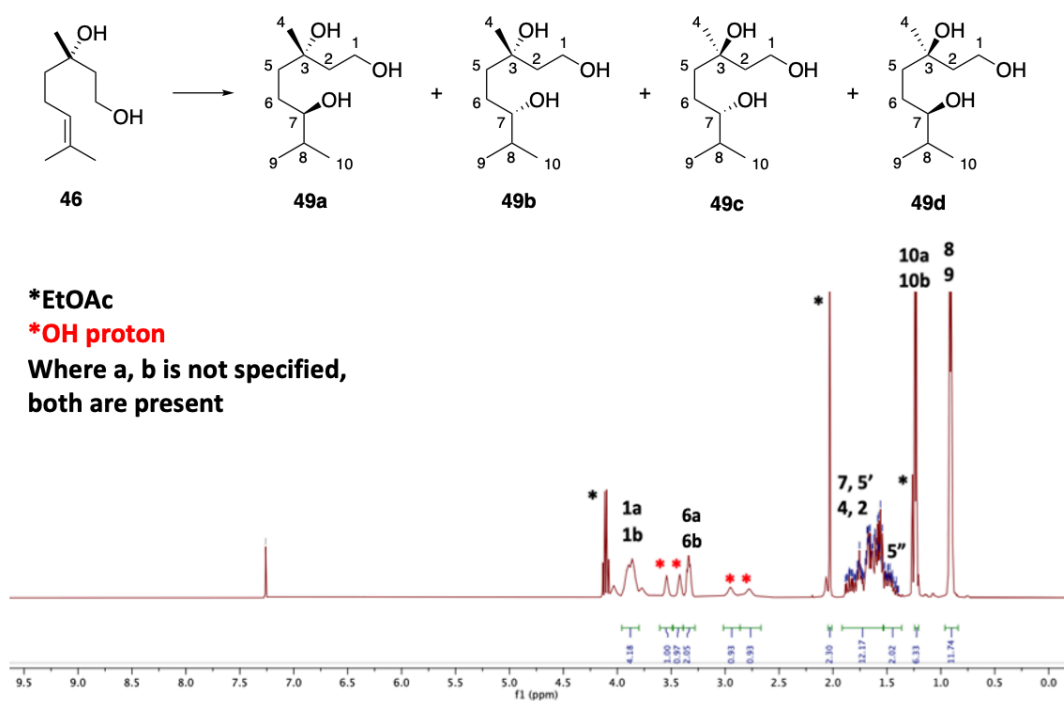


**Figure 93.** The synthesis of triol **49** from linalool. Diastereomers **49a** and **49c** are enantiomers, as are **49b** and **49d**. As a result, only one of each is detected and reported by  $^1\text{H}$  NMR spectroscopy.

Finally, the hydroboration/ oxidation of  $\gamma$ -terpinene (**7**) was investigated. This resulted in a yellow oil which, when investigated by  $^1\text{H}$  NMR, was found to be a mixture of products. It was found that these were able to be separated by silica gel chromatography, allowing for the isolation of two separate samples of the diastereomeric products **47a** and **47b** in 27% and 28% yields, respectively (**Figure 94**). However, using conventional through-bond NMR techniques, it was not possible to assign the specific diastereomers to either spectrum.

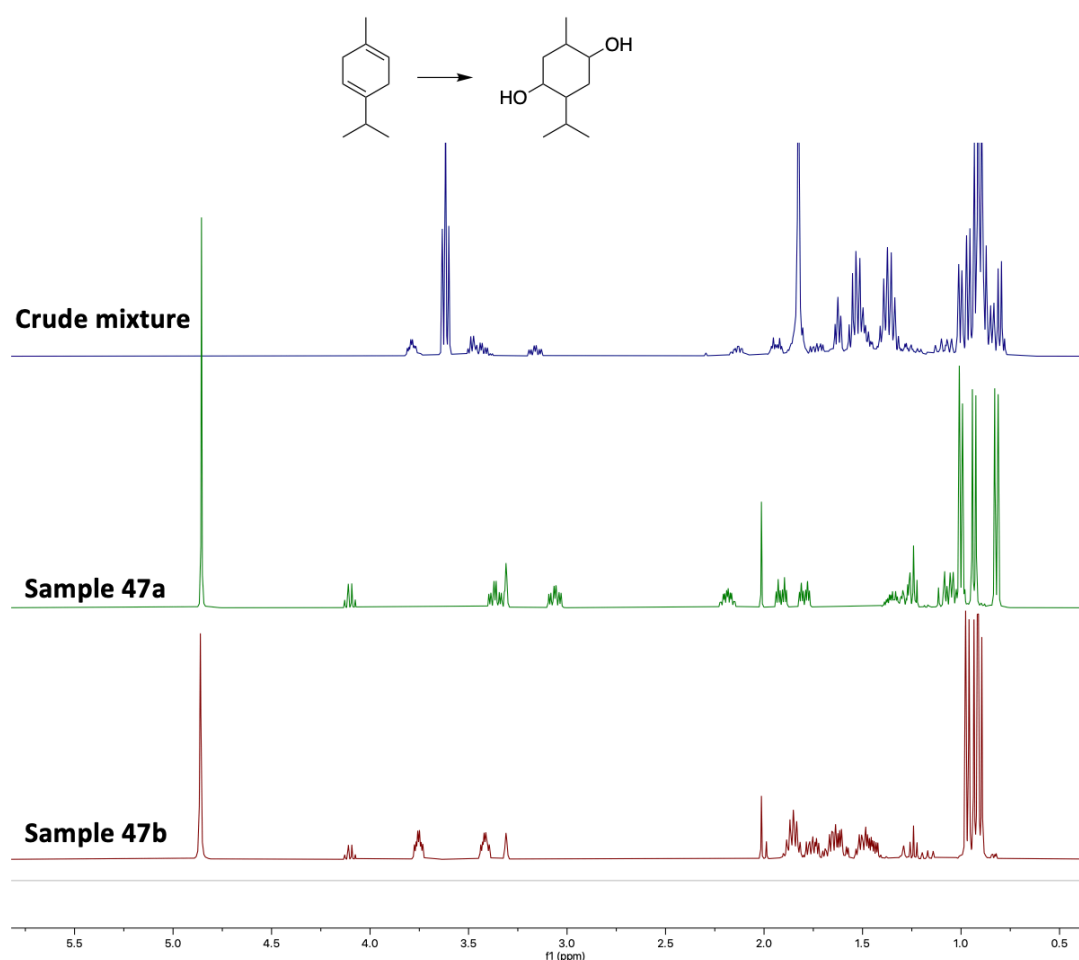
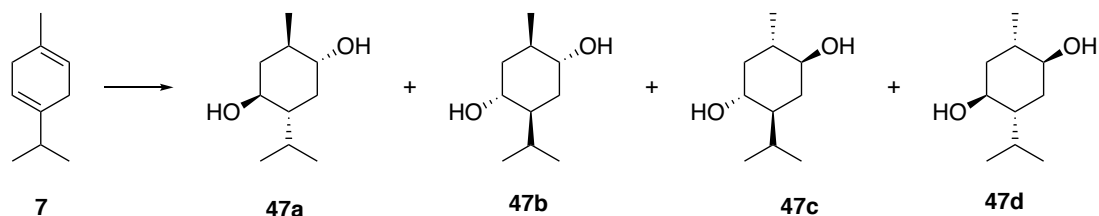


**Figure 94.**  $^1\text{H}$  NMR spectrum of the second diastereomeric sample isolated from the hydroboration/ oxidation of  $\gamma$ -terpinene.

When **7** undergoes the hydroboration/oxidation, the resulting diol product will contain four newly introduced stereocentres. However, the regioselectivity of the reaction is such that only four possible diastereomers

are formed (**Scheme 39**). Furthermore, two of these diastereomers are enantiomers of the other two, which results in only two samples being isolated following column chromatography, and only two NMR traces.



**Scheme 39.** *The possible diastereomers formed following the hydroboration/ oxidation of **7** to **47**. **47a** and **47c** are enantiomers of one another, as are **47b** and **47d**.*

Other conformations of the stereocentres are not possible because during the hydroboration step the hydride and borane must add from the same face of the molecule in a concerted reaction (**Schemes 38** and **40**).<sup>261</sup> The result is that the alcohol group will always be on the opposite face of the molecule to its neighbouring methyl or isopropyl group. As such, there are only four conformations of the product, depending on whether each  $\text{BH}_3$  equivalent will attack each alkene of **7** from either the bottom or top face.

As mentioned, through-bond NMR techniques were not sufficient to determine which isolated sample contained **47a** and which contained **47b** (and their respective enantiomers **47c** and **47d**). Instead, Nuclear Overhauser Effect Spectroscopy (NOESY) was employed, which shows  $^1\text{H}$ - $^1\text{H}$  through-space coupling. The spectrum for the first sample featured a number of correlations which allowed its identification as the sample with the alcohols having been added on opposite faces of the molecule, i.e., **47a** and **47c** (**Figure 95**).

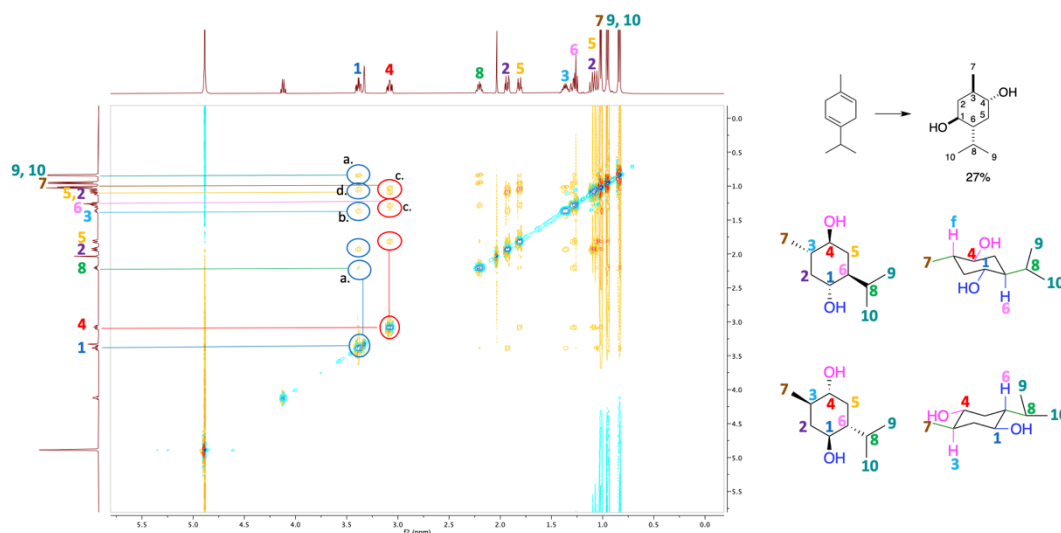


**Figure 95.** NOESY NMR of the first sample of **47** isolated from column chromatography, confirming this product as **47a** and **47c**.

The  $\alpha$ -OH proton at C-1 shows a correlation to the heptet-of-doublets resonance at the C-8 position (**Figure 95, correlation 'a'**). Similarly, a second correlation for this C-1 proton shows coupling with the proton at C-3 (**correlation 'b'**). This would indicate that each of these protons are on the same face of the ring, resulting in the stereochemistry being that of **47a** (and **47c**), as indicated in **Figure 95**. Similarly, the other  $\alpha$ -OH proton at C-4 shows a correlation to the methyl group at C-7 as well as the proton at C-6 (**correlations 'c'**). A number of other correlations also appeared on the spectrum however these were not diagnostic in determining the stereochemistry of the structure (e.g. **correlation 'd'**).

A NOESY spectrum for the second sample isolated from column chromatography was also obtained. Unfortunately, in this case the areas of correlation were not diagnostic in determining the structure, as too many of the unique, identifying resonances overlapped with the non-diagnostic ones by  $^1\text{H}$  NMR (**Figure 96**). However, by process of elimination, it follows that if the other sample has been identified as **47a** and **47c**, then this one must be enantiomers **47b** and **47d**.

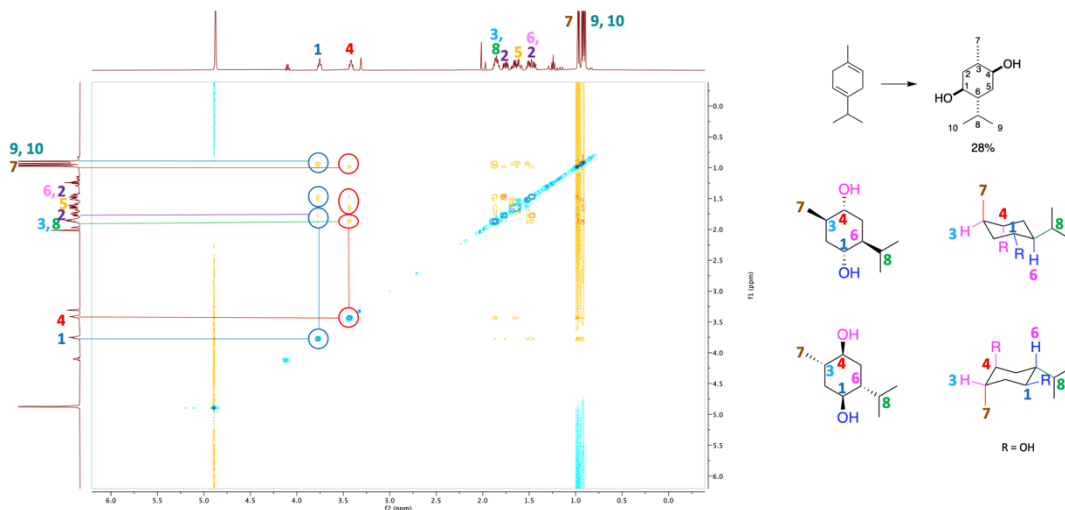


**Figure 96.** NOESY NMR of the second sample isolated from column chromatography, compounds **47b** and **47d**.

The isolation of two separate samples of **47** meant that a total of six potential monomers for polycondensation had been synthesised: four of which are cyclic and two\* linear (**Figure 97**). For simplicity, the complete stereochemistry for samples containing mixtures of diastereomers will not be drawn in future schemes, but will be drawn as indicated in **Figure 97**. Similarly, in the case of **47**, for simplicity only samples **47a** and **47b** will be referred to, though it should be noted that each sample will feature the respective **47c** and **47d** enantiomers too.

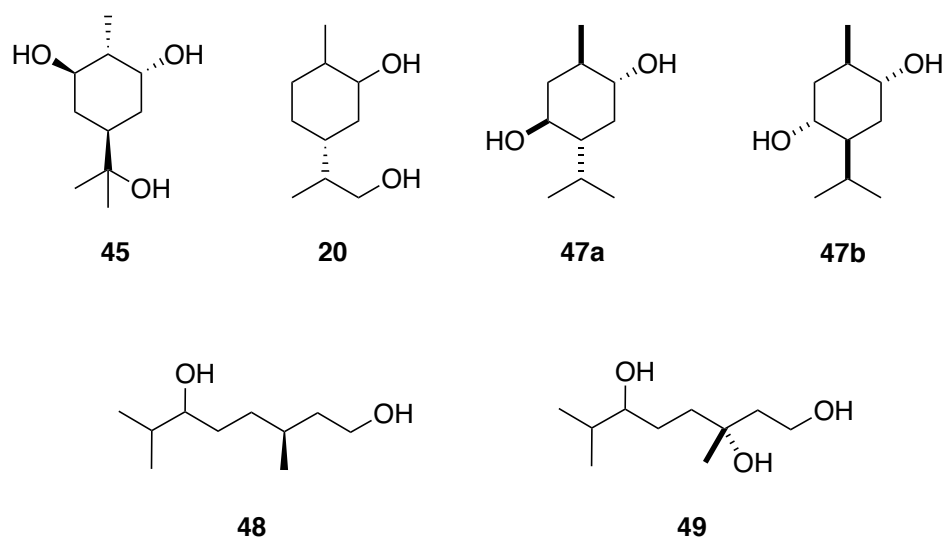


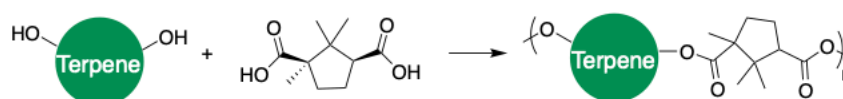
**Figure 97.** The six poly-ol monomers synthesised from terpene biomass via the hydroboration/ oxidation reaction. \*

\*See Missing and Future Works Caveat section relating to this work

#### 4.3.2 Attempted polycondensation of terpene-based poly-ols with camphoric acid

Previously, Thomsett *et al.* reported the use of monomers **20**<sup>35</sup> and **45**<sup>171</sup> in polycondensation reactions employing succinic acid as a co-monomer, using conventional 'melt' polymerisation conditions.<sup>35</sup> It was endeavoured in this project to instead employ camphoric acid in place of succinic acid, to achieve new polymers fully derived from terpene-based biomass. As such, with the six monomers in hand, the conventional 'melt' conditions employed by Thomsett *et al.* were investigated first.<sup>35</sup>

In each case, the terpene poly-ol and di-acid were heated together to 190 °C. SnOct<sub>2</sub> was added as a catalyst in 1.5 mol%, and the mixture was purged with argon. After approximately 20 minutes, the flow of argon was removed, and the mixture was put under vacuum for 24 hours to drive off the condensed water. After this time, samples were taken for GPC and NMR analysis (Table **11**), with the exception of the sample made using **45**, which was not soluble in chloroform or a variety of other solvents. This led to the hypothesis that this sample had crosslinked under the harsh, hot conditions. However, this wasn't certain and seemed unlikely, as unfortunately no polymerisation was found to have occurred in any of the other samples, when analysed by GPC (Table **11**).



Monomer	GPC	NMR
<b>45</b>	n/a	n/a
<b>20</b>	Nothing	No reaction
<b>47a</b>	Nothing	No reaction
<b>47b</b>	Nothing	No reaction
<b>48</b>	Nothing	Minimal reaction
<b>49</b>	Nothing	No reaction

**Table 11.** GPC and NMR results following the attempted polyesterification of the terpene-derived diols with camphoric acid. \*

\*See Missing Data Caveat section 4.4 relating to this work

The only reaction which appeared to have proceeded to a certain degree was that of the citronellol diol, **48**.\* This was determined by NMR, as the resonance corresponding to the CH<sub>2</sub> protons alpha to the primary alcohol seemed diminished and shifted (**Figure 98, resonance 1**). It was concluded that this reaction was not going to completion as the resonance was not completely diminished. It was also concluded that this primary alcohol was available to react with camphoric acid as it is less sterically hindered than the secondary alcohol, which did not appear to have undergone the esterification.

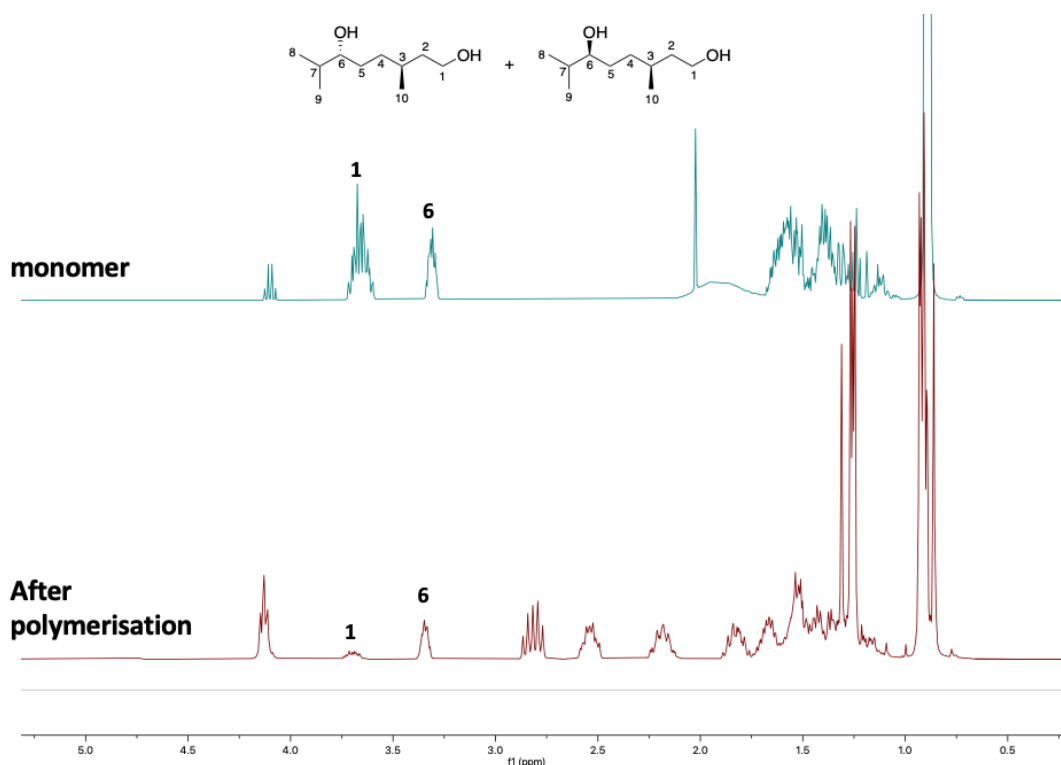


**Figure 98.** <sup>1</sup>H NMR spectrum of the citronellol diol monomer, **48**\* (top), and the <sup>1</sup>H NMR spectrum following its reaction with camphoric acid using melt polymerisation conditions.\*

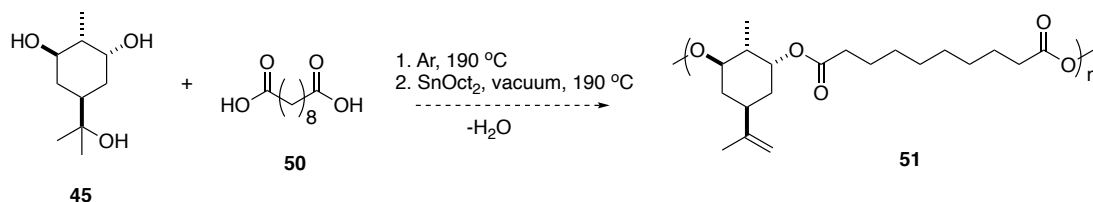
Despite the structural similarities of the citronellol diol **48** and the one made from linalool, **49**, in the latter case, no significant change in the <sup>1</sup>H NMR was observed which would allow for the conclusion that the reaction was taking place. It was thus concluded that the steric bulk of camphoric

\*See Missing Data Caveat section 4.4 relating to this work



acid was such that the esterification reaction was prevented with these relatively-bulky terpenes, particularly with secondary alcohols.

Instead, it was decided to focus on the polymerisation of these poly-ols with other bio-based diacids. As mentioned, Thomsett *et al.* has already demonstrated the use of **20** and **45** in the synthesis of bio-derived polyesters when coupled with succinic acid.<sup>171</sup> In the case of **45**, when exposed to melt conditions, the terpene triol underwent an elimination reaction at the tertiary alcohol, losing water and forming an alkene.<sup>171</sup> It was decided in this work to use sebacic acid (**50**), a 10-carbon bio-based diacid, under the same conditions, to investigate if the longer, aliphatic carbon chain would undergo the same elimination reaction.



**Scheme 41.** The proposed synthesis of novel polyesters from the terpene-based triol **45** with the bio-based diacid **50**. Following an elimination of water, the predicted polyester was anticipated to contain an alkene.

The reaction was first conducted over 24 hours, in the absence of a catalyst (**Table 12, entry 1**). The resulting polymer was analysed by GPC and found to contain oligomers up to 1200 g·mol<sup>-1</sup> (by M<sub>n</sub>), corresponding to a DP approximately 3, and with Đ = 1.9. By NMR, no alkene moiety was present, and so it was concluded in this case that the product forming was instead **52**, with the tertiary alcohol moiety intact in the end product.

To investigate if the catalyst was responsible or would help the formation of the terminal alkene, the reaction was conducted again, this time adding SnOct<sub>2</sub> (at 1.5 mol%) (**Table 12, entry 2**). This resulted in oligomers of approximately double the length: up to 2,200 g·mol<sup>-1</sup> or DP of 6, albeit with a slightly larger dispersity of 2.7. However, given that polycondensation reactions should ideally have a dispersity of 2, this can be considered a good result.<sup>221–223</sup> Additionally, an alkene moiety was

present by NMR, though the ratio of the  $\alpha$ -ester protons on the terpene ring to the alkene was 1:0.5, indicating the formation doesn't go to completion (**Figure 100, resonances a:b**). In an effort to drive the formation of this alkene, the reaction was conducted in the same way but over 48 hours rather than 24, as before. The result was a marginally longer oligomer of  $2700 \text{ g}\cdot\text{mol}^{-1}$ , with a dispersity of 2.3 (**Table 12, entry 3**). While an alkene resonance was visible on the NMR for this sample, unfortunately it was overlapped with the resonance of one of the  $\alpha$ -ester protons, and so it was not possible to quantify its presence (**Figure 100**). Finally, it was decided to conduct a polymerisation over a long period of 4 days (96 hours), to see if times of this length had an influence over the alkene formation. In this case it was found that the oligomers formed were up to  $3200 \text{ g}\cdot\text{mol}^{-1}$ , corresponding to a DP of approximately 9 (**Table 12, entry 4**). However, by NMR, no improvement was observed regarding the formation of the alkene, with a ratio of 0.45:1 for the alkene: $\alpha$ -ester protons (**Figure 100**).

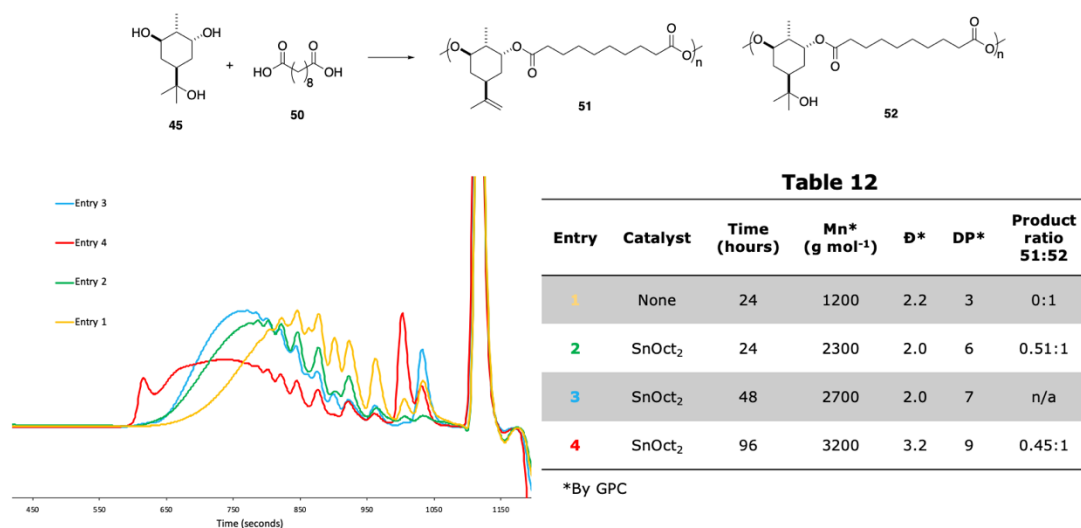


**Figure 99.** Reaction scheme (top) and GPC chromatogram (left) indicating the formation of oligomers **51** and **52**, following the condensation of sebacic acid **50** with terpene triol **45**. The data corresponding to the GPC analysis is given in **Table 12**.

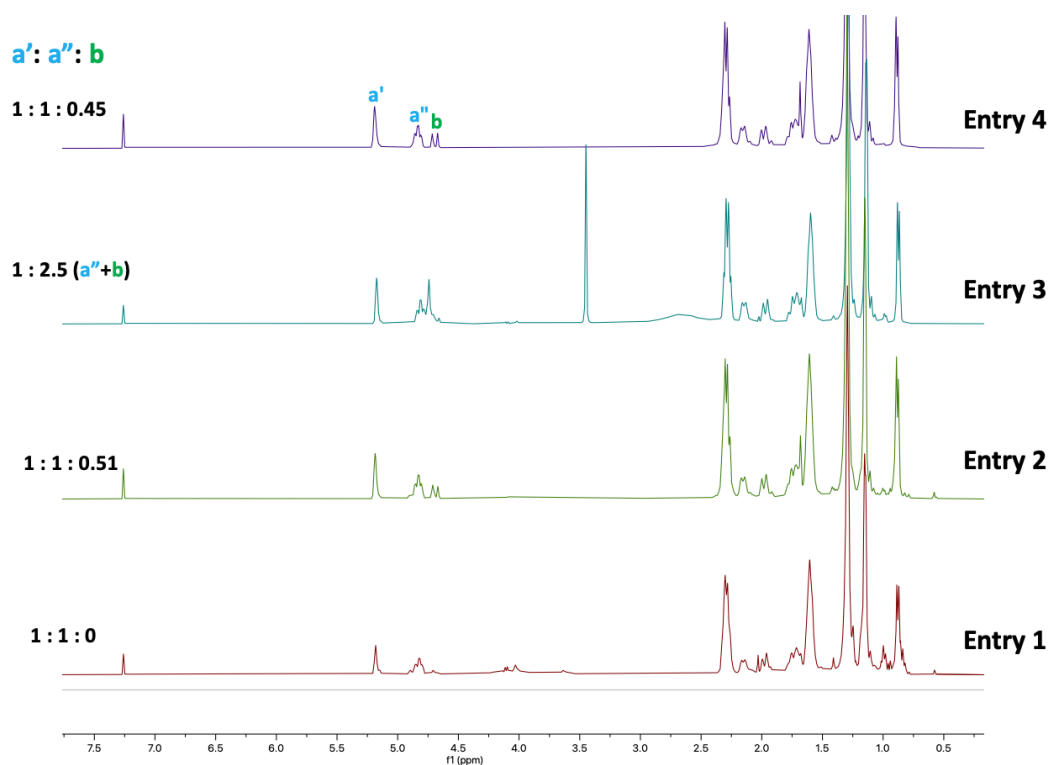
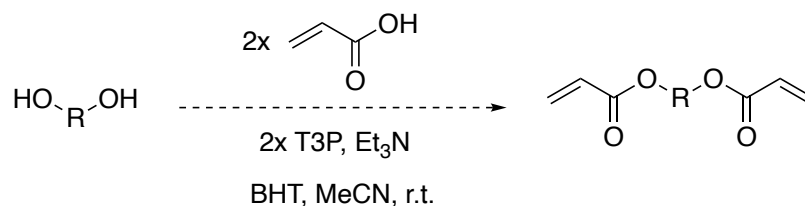


**Figure 100.** Stacked NMRs of the four polymerisation reactions between **45** and **50**. The alkene moiety is present in entries 2,3 and 4 at 4.69 ppm.

There is much research that still needs investigating with this reaction, including optimisation of the reaction conditions, and the characterisation of the resultant polymers to determine their use in any potential applications. However, unfortunately as a result of the COVID-19 pandemic, further investigations into this particular reaction were not possible. Similarly, the five other remaining poly-ol monomers remain untested in these condensation reactions.

However, with what time remained, attention turned instead to the use of these poly-ol compounds as starting materials for aza-Michael polymerisations.

### 4.3.3 Synthesis of terpene-derived diacrylate monomers



**Scheme 42.** The proposed general syntheses of terpene based diacrylates from the previously synthesised terpene poly-ols.

In 2000, the Langer group published for the first time the facile synthesis of poly-( $\beta$ -amino ester)s through the aza-Michael addition polymerisation.<sup>248</sup> This was achieved *via* the conjugate addition of bis-secondary amines to 1,4-butanediol diacrylate. Since then, extensive research has been conducted into these polymerisations and the resulting polymers, from a range of both bis-acrylate and bis-acrylamide monomers.<sup>251,254,255,263</sup> However, terpenes have yet to be used in this facile and robust polymerisation mechanism. As such, the aim in the first instance was to esterify the terpene-derived poly-ols (synthesised in section 4.3.1) to terpene-based diacrylate compounds which could be employed as monomers in these reactions.

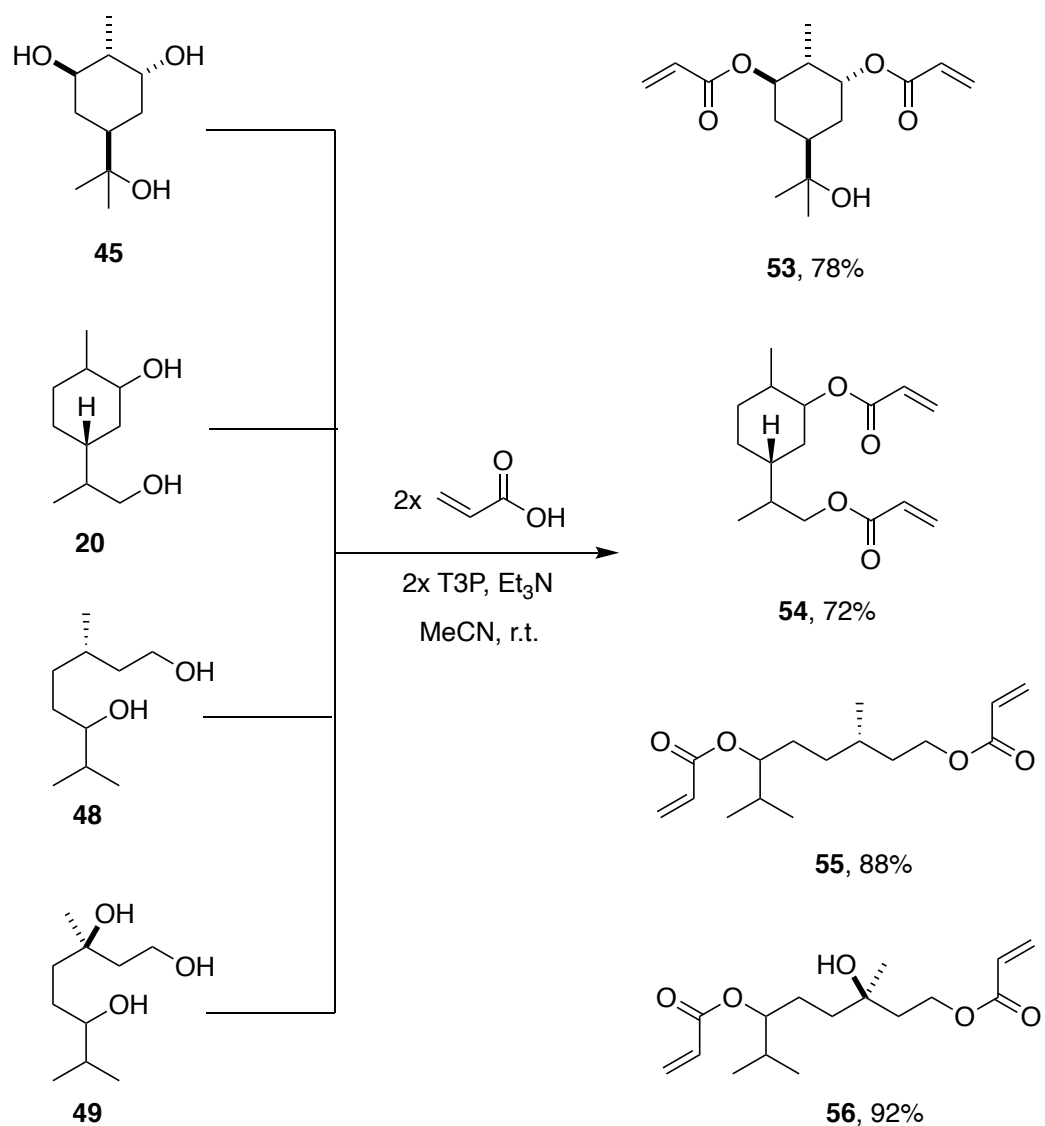
The reactions were designed to employ the same conditions of Sainz *et al.*, in which a variety of terpene-based mono-acrylate molecules were synthesised for free radical polymerisation.<sup>45</sup> This involves the use of bio-based acrylic acid and, importantly, eliminates the need for acryloyl chloride, which is toxic. In this work, two equivalents of acrylic acid and the ester coupling agent T3P<sup>®</sup> would be used in order to bring about the acrylation of two alcohol groups (**Scheme 42**).

Investigations began with the triol **45** from *trans*-sobrerol. This was conducted on a multi-gram scale (7.23 g/ 38.56 mmol), employing acetonitrile as a solvent due to its favourable solubility properties. Additionally, acetonitrile is considered one of the more green dipolar aprotic solvent options.<sup>208</sup> The radical inhibitor butylated hydroxy toluene

(BHT) was also added to the reaction to prevent radical polymerisation of either the monomer product or of acrylic acid. This inhibitor requires oxygen to be present, and as a result, when the reaction was complete the volatiles could not be removed by rotary evaporation, and so instead a flow of air was used to drive off the solvent in a fume cupboard. The resulting diacrylate compound **53** was successfully isolated in a 78% yield (**Scheme 44**).

Following this synthesis, this protocol was extended to the other poly-ols **20**, **48** and **49**. Each of these three monomers easily underwent the reaction forming the corresponding diacrylates **54**, **55** and **56** in 72%, 88% and 92% yields, respectively. These results are summarised in **Scheme 44**.

Unfortunately, due to the COVID-19 pandemic, time did not allow for the synthesis of acrylated diols **47a** or **47b**.



**Scheme 44.** The terpene-derived poly-ols **45**, **20**, **48\*** and **49** and their corresponding diacrylates **53-56** formed *via* esterification using acrylic acid and T3P<sup>®</sup>.

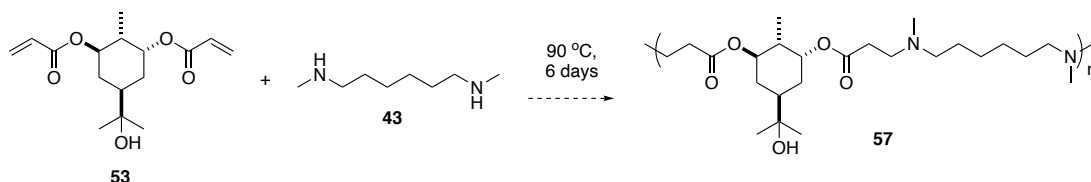
#### 4.3.4 Synthesis of terpene-derived poly $\beta$ -(amino ester)s via the aza-Michael polymerisation

With the four terpene-diacrylate monomers in hand, 1,6-hexane diamine (**43**) was chosen as a suitable diamine co-monomer with which to form polymers by the aza-Michael polymerisation. This is a di-secondary diamine, which is predicted to form linear polymers in the reaction with the diacrylates. In Chapter 3 of this thesis, this amine was found to have suitable nucleophilicity to enable the ring-opening of epoxides in a polyaddition mechanism, to form oligo-( $\beta$ -amino alcohol)s. These oligomers were then found to have suitable properties to allow their solubility in water and were found to exhibit synergistic, antifungal activity.<sup>107</sup> It was anticipated that in this instance, the reaction with diacrylates would lead to the formation of linear poly-( $\beta$ -amino ester)s, which would also be polycationic in physiologic pH,<sup>248</sup> and it was anticipated the aliphatic hexyl linker of the amine monomer might again be useful in modulating the amphiphilicity of the polymer. With these properties, it was hypothesised that the resulting polymers that form may also have applications in antifungal or antimicrobial formulations or coatings. The biodegradability of the ester linkages may also render the polymers useful for biomedical formulations (so as to avoid accumulation *in vivo*) and open up the possibility of studying the recyclability and circularity of the polymers.

##### 4.3.4.1 Initial investigations

Due to the nature of the usual applications for these polymers being employed in gene delivery and nanomedicine,<sup>251,252,255,264</sup> often water-soluble (and biocompatible) monomers are used, and as a result, the polymerisations are often conducted in hydrophilic solvents such as water and ethanol, and often mixtures of these.<sup>251,254</sup> However, there is also evidence which suggests that the aza-Michael polymerisation can take place in the absence of solvent (or any additional components such as catalysts).<sup>251,265</sup> Given that the reaction is 100% atom efficient and usually

undergoes high conversions, almost all the criteria of the 12 principles of green chemistry can be met in this polymerisation.<sup>265</sup> With this in mind, investigations began in the absence of solvent or catalyst, with diacrylate **53** heating to 90 °C (**Scheme 45**).



**Scheme 45.** Proposed reaction of diacrylate **53** with diamine **43** in the synthesis of poly-(β-amino ester) **57**.

As such, the two monomers were measured into a vial and heated to 90 °C in an oil bath. The BHT which was added to the sample in the synthesis of the diacrylate monomers was not removed, so as to avoid radical polymerisation, especially at the elevated temperature. The two monomers were stirred together for 7 days, at which point the vial was removed from heat and allowed to cool in air. The resulting material was insoluble in THF so was analysed by GPC using a chloroform eluent with 1 % v/v Et<sub>3</sub>N. By GPC, this was found to contain polymers of 3200 g·mol<sup>-1</sup>, corresponding to 14 repeat units, with a dispersity of 2.04 (**Table 13, entry 1**). Similarly, <sup>1</sup>H NMR analysis showed that the acrylate peaks had completely diminished, and the α-ester protons had shifted (**Figure 101**).



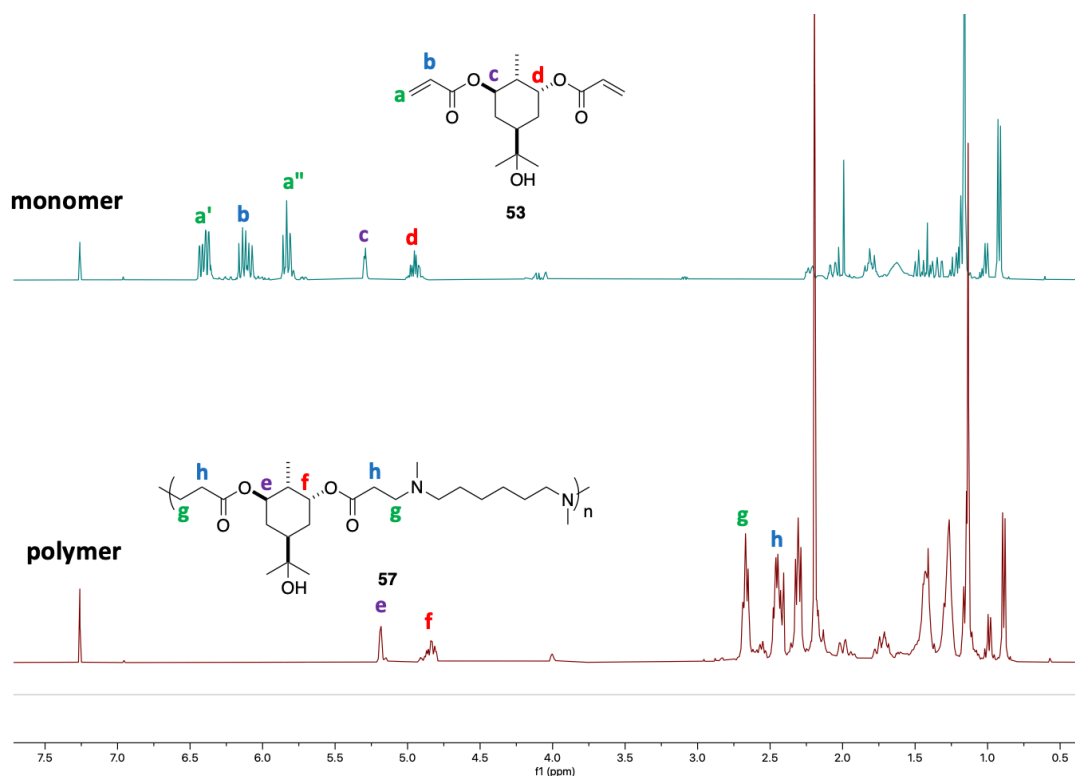


**Figure 101.** Stacked <sup>1</sup>H NMR spectra of monomer **53** (top) and its conversion to polymer **57** (bottom).

While the results from this polymerisation were generally positive, it was investigated whether or not the addition of a solvent would aid the polymerisation in reaching higher molecular weights. As such, the reaction was conducted for a second time, this time employing acetonitrile as a solvent. As the boiling point of acetonitrile is 82 °C, the reaction was conducted at 70 °C rather than 90 °C, as before. The result was polymers of 2900 g·mol<sup>-1</sup>, corresponding to a DP of 13 and Đ = 1.96 (**Table 13, entry 2**). These results are very similar to the reaction conducted in the absence of solvent and so it was concluded that the addition of the solvent was not beneficial to the reaction. However, Blakney *et al.* recently reported that when triethylamine was added, the resulting polymers were double the length of those made without the amine catalyst.<sup>253</sup> As such, a third reaction was conducted with the two monomers at 70 °C over 7 days, with both acetonitrile as a solvent and Et<sub>3</sub>N. In this case however, no

doubling of the molecular weight was observed; the resulting polymers actually decreased in chain length, having a  $M_n$  of  $1800 \text{ g}\cdot\text{mol}^{-1}$  with a DP of just 8. The dispersity in this case was 1.98 (**Table 13, entry 3**). It is hypothesised that this lower molecular weight was a result of the dilution of the sample.<sup>253</sup>

While the reaction in the absence of solvent or catalyst produced polymers of quite favourable length and dispersity, a reaction time of six days is quite long, and it is quite costly in terms of energy to heat a sample at  $90 \text{ }^\circ\text{C}$  for this length of time. Additionally, these conditions render the scale up and industrial use of this synthesis difficult. However, in 2010 Kall *et al.* investigated the microwave-induced aza-Michael addition reaction in water and found that the reaction proceeded very efficiently in excellent yields.<sup>266</sup> More recently, Gurnani *et al.* reported that microwave heating improved the synthesis of poly(amido amine)s by the same aza-Michael type reaction, cutting reaction times from two weeks to 4 hours.<sup>254</sup> As such, microwave heating of these terpene-based samples was investigated to see if reaction times could be reduced.

As a comparison to the results of the conventional heating reaction, the two components were added to the microwave vial in the absence of solvent or catalyst and heated to  $90 \text{ }^\circ\text{C}$  for just 12 hours. The resulting polymer was analysed by  $^1\text{H}$  NMR and found to be identical to the those synthesised by conventional heating (**Figure 102**).

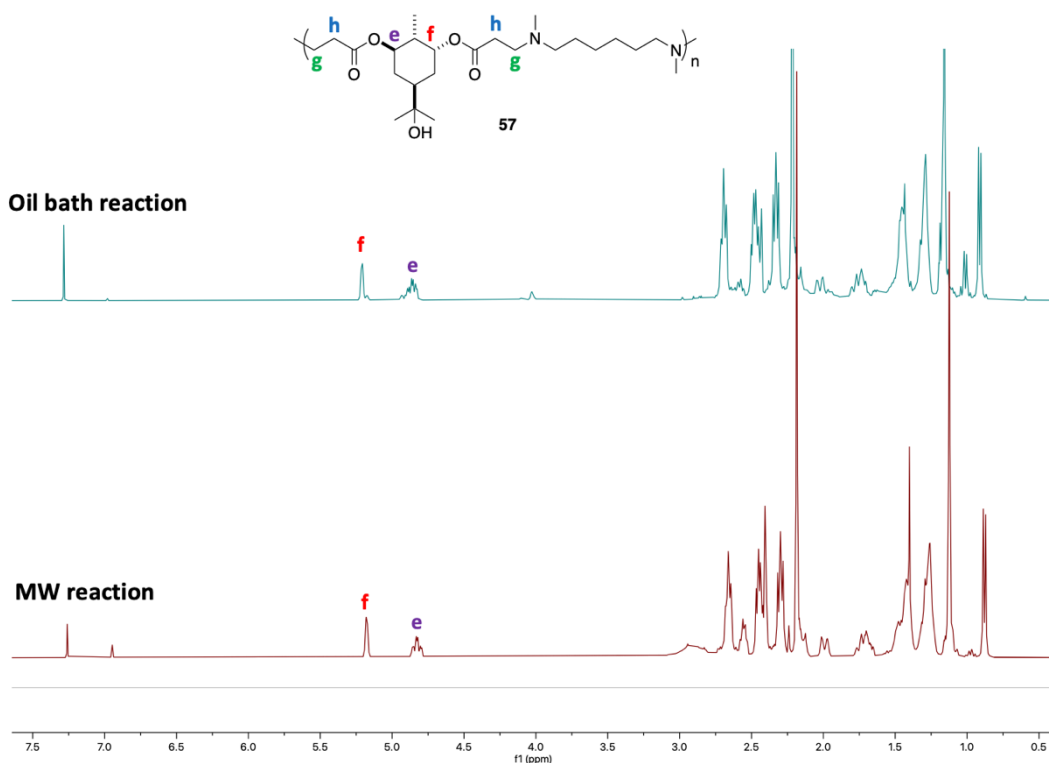


**Figure 102.** Stacked  $^1\text{H}$  NMR spectra of the aza-Michael polymerisation conducted using conventional methods in an oil bath over 7 days (top) and same reaction conducted in the microwave over 12 hours (bottom).

When analysed by GPC, the polymer was found to be of similar molecular weight to the one synthesised by conventional methods: the  $M_n$  was found to be  $2600 \text{ g}\cdot\text{mol}^{-1}$ , corresponding to a DP of 12, with  $\mathcal{D} = 1.52$  (**Table 13, entry 4**). Two more comparisons were then conducted using microwave heating, to see if the addition of solvent and/or the  $\text{Et}_3\text{N}$  catalyst would help synthesise higher molecular weight polymers. The use of the microwave involves the components being heated in a pressurised, sealed vessel, and this gives the extra advantage of allowing the reaction to be conducted at temperatures above the boiling points of the solvents. Therefore, the final reactions were conducted in the microwave over 12 hours with acetonitrile at  $90 \text{ }^\circ\text{C}$  and  $120 \text{ }^\circ\text{C}$ . The latter also contained  $\text{Et}_3\text{N}$  to investigate if this would help form longer polymer chains. The result was polymers of  $2200 \text{ g}\cdot\text{mol}^{-1}$  and  $2700 \text{ g}\cdot\text{mol}^{-1}$  for the  $90 \text{ }^\circ\text{C}$  and  $120 \text{ }^\circ\text{C}$  reactions, respectively (**Table 13, entries 5 and 6**). This corresponds to

DPs of 10 and 12, and the two polymers were also relatively monodisperse, with  $\mathcal{D} = 1.55$  and 1.35.

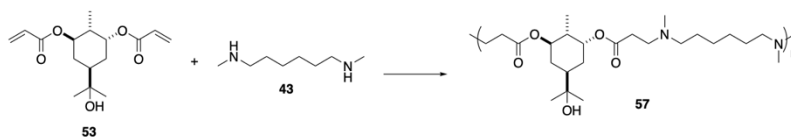


**Table 13**

Entry	Heat source	time	Conditions	$M_n$ ( $\text{g mol}^{-1}$ )	$\mathcal{D}$	DP
1	Oil bath	7 days	90 °C, neat	3200	2.04	14
2	Oil bath	7 days	70 °C, MeCN	2900	1.96	13
3	Oil bath	7 days	70 °C, Et <sub>3</sub> N, MeCN	1800	1.98	8
4	Microwave	12 hours	90 °C, neat	2600	1.52	12
5	Microwave	12 hours	90 °C, MeCN	2200	1.55	10
6	Microwave	12 hours	120 °C, Et <sub>3</sub> N, MeCN	2700	1.35	12

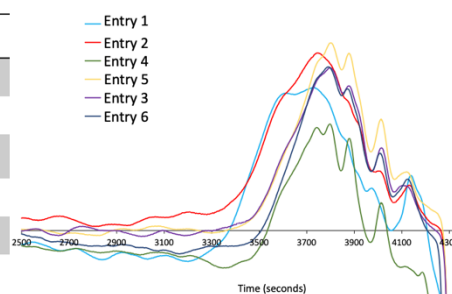


**Table 13.** The series of aza-Michael polymerisations conducted with monomers **53** and **43** to generate poly-( $\beta$ -amino ester) **57**, using both conventional and microwave heating, and the corresponding GPC data. The GPC chromatogram is also shown (right), indicating the similar results from each sample.

Given that each reaction indicated that polymers of relatively similar length and dispersities were forming in each case, it was concluded that the use of the microwave was more favourable than generic heating in an oil bath, as the cost in terms of energy was far reduced by heating for only 12 hours as opposed to 7 days.

#### 4.3.4.2 Solvent Screen

The use of microwave heating allows higher temperatures to be accessed compared to conventional heating in an oil bath, including temperatures above the boiling point of the solvent.<sup>267</sup> This is considered the factor that ultimately aids in significantly reducing reaction times through kinetic acceleration of the reaction, which is not only more convenient, but also much greener in term of the energy cost of synthesising these polymers.<sup>268</sup>

Microwave heating occurs when the microwave irradiation excites polar molecules due to their dipolar character. The oscillating magnetic field then causes these dipoles to align with the electric field, and heat is generated as a result of friction of movement of the molecules as they rotate and collide. A rapid internal heating of the molecules in the reaction therefore takes place.<sup>267</sup> It follows that the polarity of the solvent should also have an effect on the heating of the molecules, and it has been shown that polar solvents can cause an acceleration of reaction components that are low-absorbing.<sup>267</sup> The parameter of concern in this case relates to the dielectric coefficient: highly dielectric materials lead to a strong absorption of microwave radiation, and consequently a rapid heating of the medium is observed.<sup>268</sup> There is much evidence in the literature to suggest that polar solvents are optimal for the aza-Michael reaction,<sup>252-255,269</sup> including work by Kall *et al.* which demonstrated that the high dielectric constant of water (when used as a solvent) allows for the microwave-induced activation of both the amine and ketone moieties, which greatly facilitates the reaction.<sup>266</sup> As a result, a solvent screen was conducted with the terpene diacrylate **53** and the diamine **43**, to investigate the effects that polar solvents might have on the overall polymerisation products, and whether or not higher molecular weight species could be obtained. Five solvents were screened using the same reaction conditions: the monomers were added in a 1:1 molar ratio (1.69 mmol) in 1 M solvent (1.7 mL) with Et<sub>3</sub>N (1.5 mL). The screening began with 2-MeTHF, a non-polar solvent which is bio-renewable and would result in a high sustainability for the reaction, given a promising result. Methanol, ethanol and water were also screened, as polar, bio-renewable solvents.

The results indicated that either 2-MeTHF or acetonitrile gave the best results, producing polymers of 2300 g·mol<sup>-1</sup> or 2700 g·mol<sup>-1</sup>, respectively. The sample conducted in 2-MeTHF had a dispersity of 1.56, and a DP of 10 (**Table 14, entry 2**). Both methanol and ethanol gave significantly poorer results, with molecular weights of 800 and 1400 g·mol<sup>-1</sup>, respectively (**Table 14, entries 3 and 4**). The terpene diacrylate was found to be insoluble in water, resulting in two phases for this reaction. The resulting material resulted completely insoluble in chloroform, THF and DMF and as a result it was not possible to retrieve

any data on this sample. It is possible that this sample may have undergone crosslinking *via* a radical mechanism, though this remained unconfirmed (**Table 14, entry 5**).

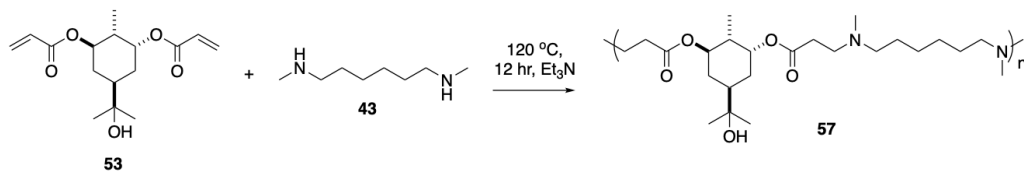


**Table 14**

Entry	Solvent	$M_n$ ( $\text{g mol}^{-1}$ )	$\mathcal{D}$	DP
1	MeCN	2700	1.35	12
2	2-MeTHF	2300	1.56	10
3	MeOH	800	1.24	4
4	EtOH	1400	1.54	6
5	H <sub>2</sub> O	n/a	n/a	n/a

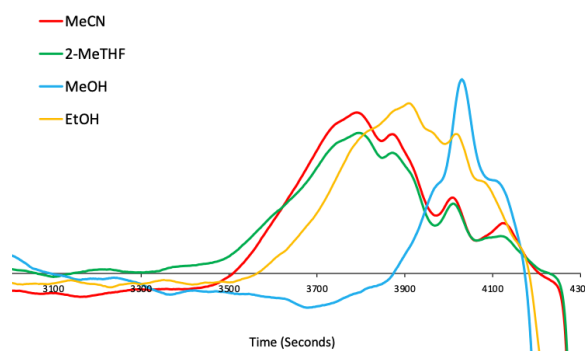
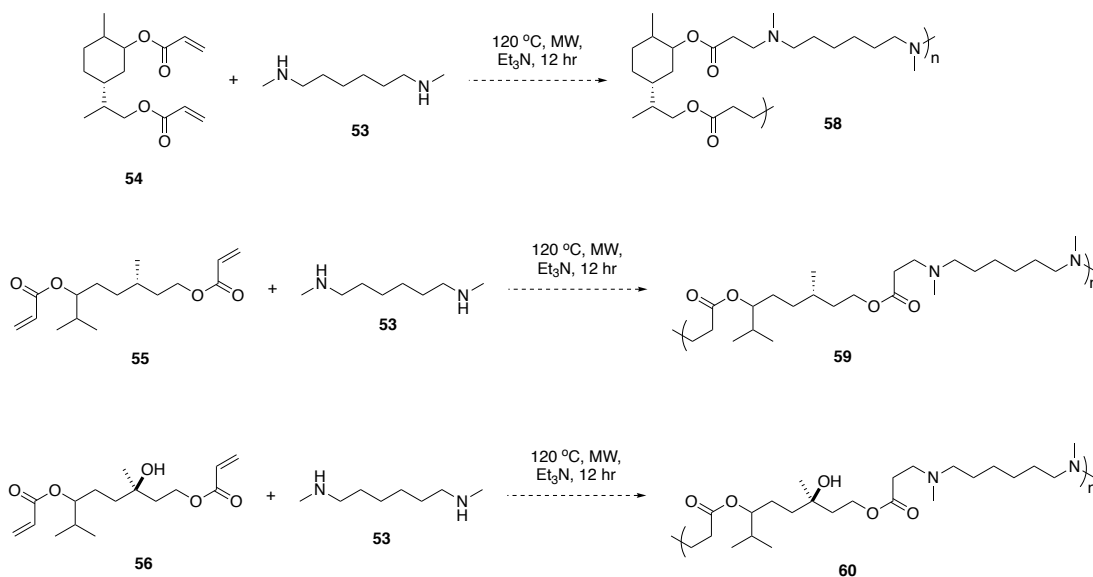


**Table 14.** The GPC data resulting from the solvent screen of the aza-Michael polymerisation reaction between **53** and **43**, to produce polymer **57**. GPC chromatogram is also shown (right).

As a result of this small solvent screen, it was concluded that acetonitrile was the most optimal solvent for dissolving this non-polar terpene diacrylate monomer, which allowed for formation of the highest molecular weight polymers with narrowest dispersities ( $\mathcal{D} < 1.6$ ), followed closely by the bio-based solvent 2-MeTHF ( $\mathcal{D} < 2$ ). As a result, these conditions were carried forward and extended to the three other terpene-based diacrylates.

#### 4.3.4.3 Full terpene-diacrylate aza-Michael polymerisations

The conditions used in the solvent screen reaction with acetonitrile (**table 14, entry 1**) with **53** and **43** were extended to the other terpene diacrylates **54**, **55** and **56**. The same diamine, **43** was employed as a co-monomer in these reactions to synthesise polymers **58**, **59\*** and **60** (**Scheme 46**).



**Scheme 46.** The proposed syntheses of poly( $\beta$ -amino ester)s **58**, **59\*** and **60**, with monomers **54**, **55** and **56**, using the conditions optimised for the microwave-accelerated synthesis of polymer **57**.

In each case, the results indicated that the reaction proceeded even better with these other terpene-diacrylates than it had done for **53**, based on the molecular weight of the samples. Using these conditions with **54**, polymers of up to 4000 g·mol<sup>-1</sup> (by M<sub>n</sub>) with dispersities of 1.52 were formed, corresponding to a DP of 19 (**Table 15, entry 2**). Monomer **55** also successfully underwent the polymerisation, forming polymers of 3200 g·mol<sup>-1</sup>, with DP = 15 and  $\bar{D}$  = 1.51 (**Table 15, entry 3**).\* The linalool-based diacrylate **56** formed the longest polymer chains of any of the monomers, with a DP of 22, corresponding to an M<sub>n</sub> of 4900 g·mol<sup>-1</sup>, with  $\bar{D}$  = 1.62 (**Table 15, entry 4**).

\*See Missing Data Caveat section 4.4 relating to this work

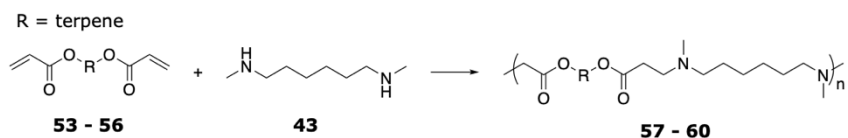


**Table 15**

Entry	monomer	polymer	$M_n$ ( $\text{g mol}^{-1}$ )	$\bar{D}$	DP
1	53	57	2700	1.35	12
2	54	58	4000	1.52	19
3	55	59	3200	1.51	15
4	56	60	4900	1.62	22

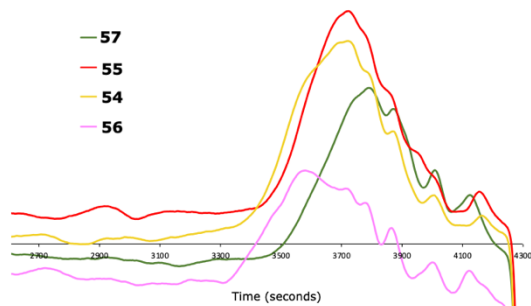


**Table 15.** GPC data relating to the polymerisations of monomers **53**, **54**, **55\*** and **56** with diamine **43**, producing polymers **57**, **58**, **59\*** and **60**, respectively. The GPC chromatogram is also shown.

Unfortunately for this project the COVID-19 pandemic meant that a full investigation into these polymers, including both the optimisation of their synthesis and any potential applications, could not be realised. As such, there now remain many avenues of investigation for this research. Nonetheless, these reactions have detailed for the first time a facile and green synthesis of terpene-based poly( $\beta$ -amino ester)s (both monomers and polymers), and have substantially improved the sustainability and scalability of this polymerisation through the use of microwave heating.<sup>254</sup>

\*See Missing Data Caveat section 4.4 relating to this work



#### 4.4 Missing Data Caveat

The linear terpene citronellol (**13**) was employed in the hydroboration/oxidation reaction in the formation of diol **48**, as described in the aims section 4.2. However, the data for this compound has since been lost and so it was not possible to report its formation formally in the experimental section of this chapter. Nevertheless, a discussion of the synthesis of **48** is included in section 4.3.1, alongside the other terpene-diols. As the is incomplete to back up these results, this discussion should be interpreted as the most likely outcomes of the reaction if they were conducted in the future.

The data for the subsequent reaction of **48** in the formation of diacrylate **55** was retained. Therefore, for the reactions employing **48** as a starting reagent, the thesis can be read as though the compound was obtained commercially from other sources.

Similarly, while data was retained for diacrylate **55**, unfortunately the full, formal data relating to the corresponding polymer **59** was also lost, and so the results relating to this polymer must also be read as the most likely outcomes if the reactions were to be repeated. For these reasons, the compounds are not reported in full in the experimental section which follows this chapter.

## 4.5 Conclusions

A series of diol and triol compounds were synthesised from terpene-based biomass using a robust and facile protocol, which allows for the anti-Markovnikov product to be accessed, resulting in six compounds each with two nucleophilic alcohol groups (**Figure 103**).

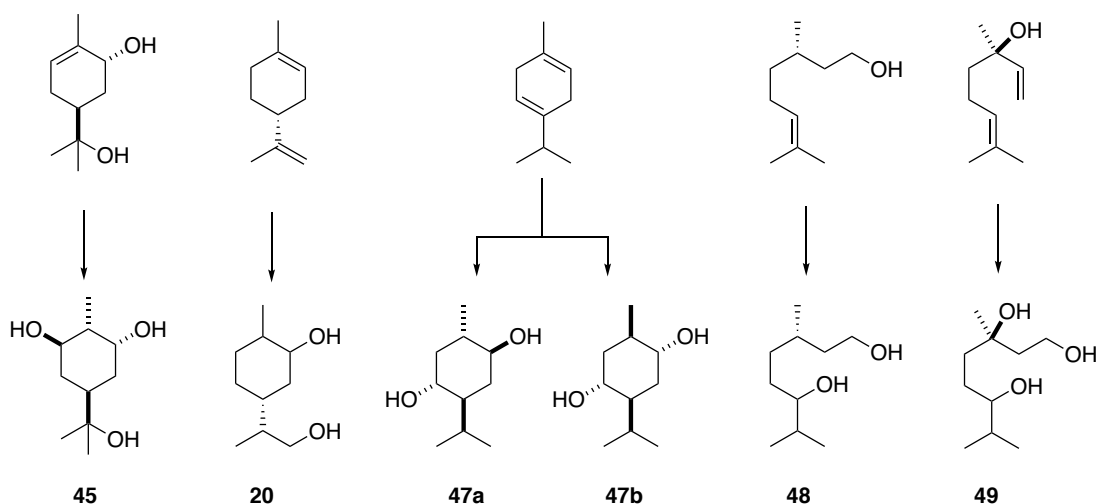


**Figure 103.** The six poly-ols (**45**, **20**, **47a**, **47b**, **48** and **49**) synthesised via Brown's hydroboration/ oxidation mechanism from bio-based, commercially available terpenes. Each poly-ol contains two nucleophilic alcohol groups.

The six poly-ol compounds were synthesised *via* Brown's hydroboration/oxidation conditions.<sup>256</sup> While this protocol does not score particularly well in terms of green or sustainable chemistry, there are many examples of green methodologies which are increasingly being investigated with terpene biomass to generate similar poly-ol products.<sup>47,58,245,270</sup> In this work, for practicality and time reasons, the poly-ols were synthesised *via* the hydroboration/oxidation, however it is envisaged that future research would look to synthesising these compounds from more green and sustainable routes.

The use of these poly-ols as monomers in polycondensation polymerisations were then investigated. Initially, camphoric acid was

employed as a co-monomer, with the aim of synthesising fully terpene-based polyesters. However, it was found that the steric bulk of camphoric acid was such that the nucleophilic addition of secondary alcohols to the terpene-based diacid was inhibited. It is envisaged that polyesterification would instead be possible with these terpene poly-ols and other bio-based diacids such as azelaic acid or sebacic acid. Unfortunately, time restraints (in particular relating to the COVID-19 pandemic) meant that it was not possible to fully investigate these alternative polymers, however, initial results with **45** and sebacic acid found that polymers of approximately  $2700 \text{ g}\cdot\text{mol}^{-1}$  (corresponding to a DP of 7) with a dispersity of 2.0 were formed. Lanteri *et al.* recently reported a method for the synthesis of two diols from citronellol *via* regioselective photooxidation followed by reduction, and demonstrated that monomers of this nature could be used to generate co-polyesters by polycondensation.<sup>271</sup> It is envisioned that the diol **48** could also be used to form similar polymers.

To further exploit these terpenes for polymerisations, four of the six poly-ols were then converted to their corresponding di-acrylate compounds (**Figure 104**). Unfortunately, due to time restraints, compounds **47a** and **47b** were not carried forward for these investigations.

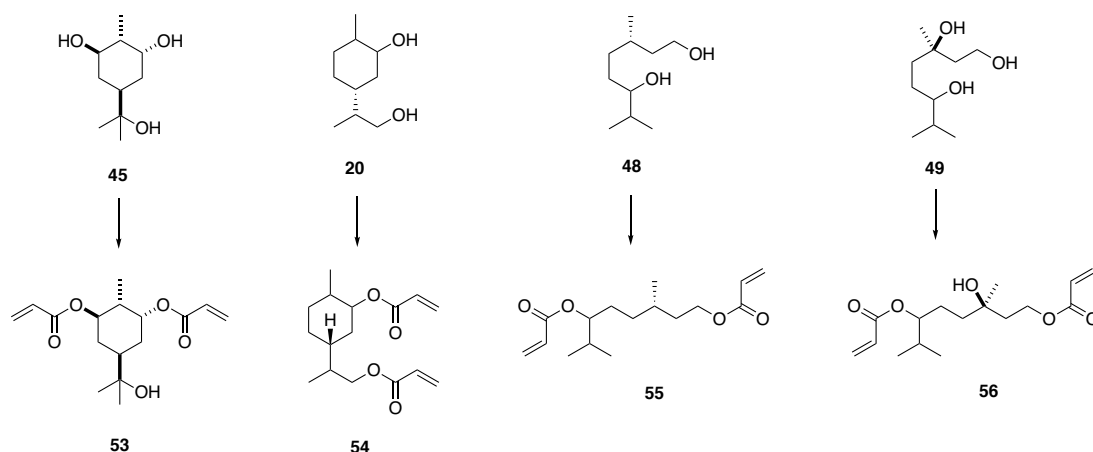


**Figure 104.** The conversion of poly-ols **45**, **20**, **48** and **49** to the corresponding di-acrylate compounds **53**, **54**, **55** and **56**.

The di-acrylates were synthesised from the pol-ols *via* a sustainable route employing acrylic acid and the coupling agent T3P<sup>®</sup>, avoiding the use of chlorinated and toxic solvents and reagents.<sup>45</sup> These were synthesised in very good to excellent yields (72% - 92%).

These di-acrylates were then employed in aza-Michael polymerisations with the di-secondary diamine 1,6-dimethyl hexane diamine (**43**) (**Figure 105**). Initially, the quality of the reaction was investigated with **53**, with which it was found that the reaction proceeded best in acetonitrile with Et<sub>3</sub>N as a catalyst. Additionally, the use of microwave heating found that reaction times could be reduced from 7 days at 70 °C to just 12 hours at 120 °C. These conditions formed poly-(β-amino ester)s of 2700 g·mol<sup>-1</sup> (i.e. DP = 12) with Đ = 1.35. When these conditions were applied to the remaining terpene diacrylates, even better results were observed, with polymers up to 4900 g·mol<sup>-1</sup>, corresponding to DPs of 22 and Đ = 1.62 being formed.

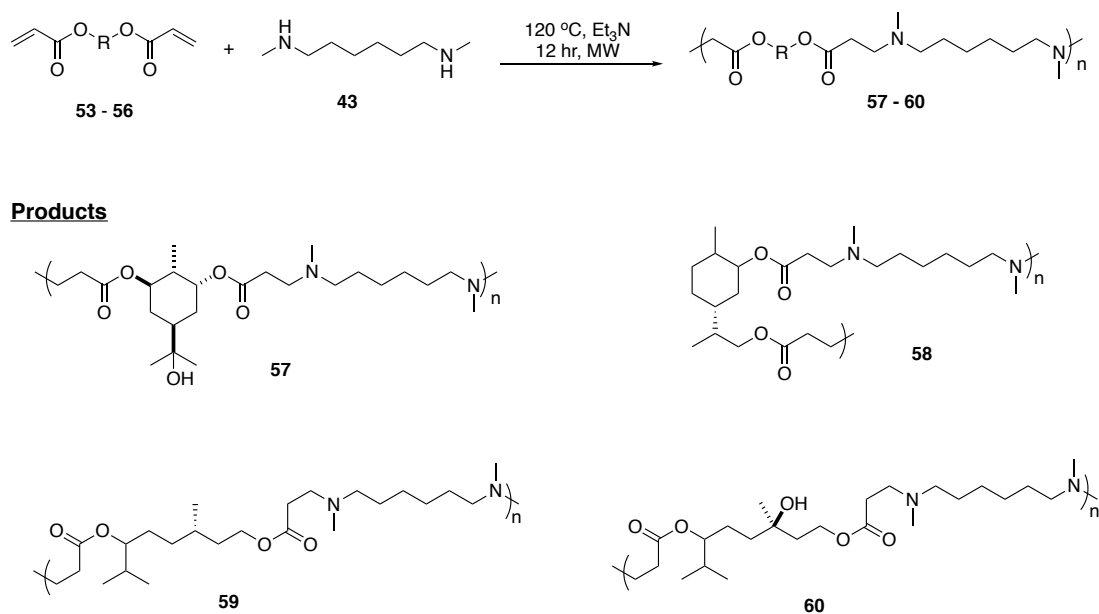


**Figure 105.** The general polymerisation of diacrylates **53** – **56** with **43** and their corresponding polymer products **57** – **60**.

Unfortunately, time restraints relating to the COVID-19 pandemic prevented any further investigations into this project and as such, there are many avenues of research left to explore.

In the first instance, it would be useful to expand upon the synthesis of bio-based polyesters using the terpene poly-ols. It is hypothesised that each poly-ol would form polyesters in a condensation mechanism with sebacic acid, as the preliminary investigations with **45** indicated. Furthermore, it would be interesting to investigate what sustainable syntheses might be available for these reactions so as to move away from the 'melt' polymerisation mechanism which typically employs high temperatures and often problematic catalysts.

Next, it would be interesting to investigate the synthesis of the terpene-based diacrylates that could form from diols **47a** and **47b**, and to employ them in the polymerisation of poly( $\beta$ -amino ester)s in the same way as the other terpene-diacrylates were. In this remit, further optimisation of these polymerisations might be useful. A full investigation into each of these poly( $\beta$ -amino ester)s, including thermal properties such as the glass transition temperatures would then be useful in helping to determine potential applications for these polymers. Given that at physiological pH the amine moieties should become protonated,<sup>248</sup> thus forming polycations, the anti-microbial properties of these polymers could then be investigated.

In future projects, it would be interesting to synthesise a terpene-based amine which could be used as a co-monomer with these diacrylates so as to form fully terpene-based polymers. Alternatively, a diamine with specific properties for a targeted application, such as a di-thiol linker for nucleic acid delivery, for example, could be investigated.

## 4.6 Experimental

### 4.6.1 *General Materials and Methods*

#### Materials

All reagents were purchased from a chemical supplier and used without further purification. Water was deionised before use. Dry solvents were obtained from solvent drying towers and contained <17 ppm of water. TLCs were performed on silica gel mounted on aluminium and visualised using potassium permanganate with gentle heating. Experiments carried out using inert conditions employed nitrogen by means of a Schlenk line, or an argon balloon.

#### Analytical Techniques

**<sup>1</sup>H NMR spectra** were recorded in deuterated chloroform (CDCl<sub>3</sub>) at 25°C, with Bruker 400 MHz spectrometers. <sup>1</sup>H NMR chemical shifts ( $\delta$ ) were recorded in parts per million (ppm), with the shift of CHCl<sub>3</sub> ( $\delta$  = 7.26 ppm) as the internal standard when CDCl<sub>3</sub> was used. The following abbreviations are used to designate the multiplicity of each signal; s, singlet; d, doublet; dd, doublet of doublets; dddd, doublet of doublet of doublet of doublets; t, triplet; dt, doublet of triplets; ddt, doublet of doublet of triplets; q, quartet; m, multiplet; app, apparent; br, broad. Couplings (*J*) are given in Hertz (Hz). **<sup>13</sup>C NMR spectra** were recorded in CDCl<sub>3</sub> on 100 MHz spectrometers. <sup>13</sup>C NMR chemical shifts ( $\delta$ ) were reported using the central line of CHCl<sub>3</sub> ( $\delta$  = 77.0 ppm) when CDCl<sub>3</sub> was used as the internal standard.

**Infra-Red spectra** were carried out using a Bruker Tensor 27 using an ATR attachment and peaks are quoted as  $\nu_{\max}$  in cm<sup>-1</sup>.

**High Resolution Mass Spectrometry** was conducted using a Bruker MicroTOF spectrometer operating in electrospray ionisation (ESI) mode.

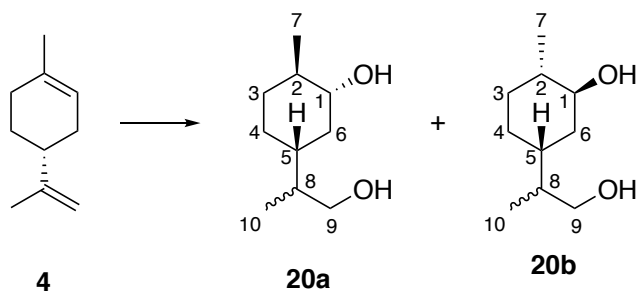
**Gel Permeation Chromatography (GPC)** was performed in CHCl<sub>3</sub> (HPLC grade, Fisher Scientific) with 1% v/v Et<sub>3</sub>N as the eluent at room temperature using two Agilent PL-gel mixed-D columns in series with a flow rate of 1 mLmin<sup>-1</sup>. A differential refractometer (DRI), was used for

sample detection. The system was calibrated using polycaprolactone standards.

#### 4.6.2 Synthesis of terpene-derived poly-ols

##### Synthesis of (5*R*)-5-(1-hydroxypropan-2-yl)-2-methylcyclohexan-1-ol

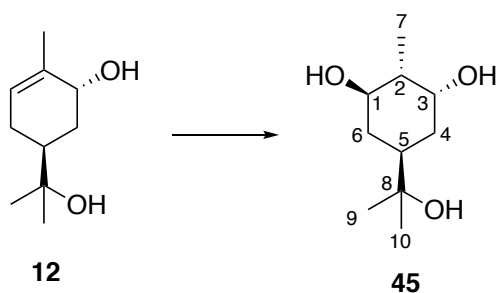
##### (20)



To a solution of (*R*)-limonene (5.9 mL, 36.77 mmol) in dry THF (40 mL) under argon was added borane solution (1 M solution in THF; 73.53 mmol, 74 mL), dropwise at 0 °C. The solution was stirred for 2 hours before 2M sodium hydroxide solution was added (74 mL, 147.06 mmol) at 0 °C, followed by hydrogen peroxide solution (30% v/v, 15 mL, 147.06 mmol). The solution was stirred at room temperature for a further 2 hours before extracting the water layer with diethyl ether (2x 150 mL). The organic extract was subsequently washed with sodium carbonate solution (2x 100 mL) and brine (2x 100 mL) before being dried over Na<sub>2</sub>SO<sub>4</sub>. The solvent was removed under reduced pressure to yield the crude material as a yellow oil. Purification by silica gel chromatography (40% Ethyl acetate in Petroleum ether) afforded the title compound **20** as a mixture of diastereomers **20a** and **20b** (3:1) as a pale, yellow oil (5.629 g; 32.73 mmol; 89%). **FTIR** (ATR)  $\nu_{\max}/\text{cm}^{-1}$  = 3316 (OH), 3307, 2954, 2923, 2872, 1036 (C-O), **<sup>1</sup>H NMR:** (400 MHz, CDCl<sub>3</sub>)  $\delta_{\text{H}}$  = 3.65 – 3.56 (m, 2H, H-9a' and H-9b'), 3.53 – 3.43 (m, 2H, H-9a'' and H-9b''), 3.21 – 3.08 (m, 2H, H-1a and H-1b), 1.96 – 1.85 (m, 2H, H-6a' and H-6b'), 1.79 – 1.68 (m, 2H, H-4a' and H-4b'), 1.62 – 1.43 (m, 6H, CH<sub>2</sub>, CH and C-2a and C-2b), 1.28 – 1.17 (m, 2H, CH and CH), 1.15 – 1.06 (m, 2H, H-6a'' and H-6b''), 1.04 – 0.94 (m, 10H, H-7a and H-7b, CH<sub>2</sub>), 0.93 – 0.85 (m, 6H, H-10a and H-10b). **<sup>13</sup>C NMR** (100 MHz, MeOD)  $\delta_{\text{C}}$  = 76.6 (C-1a or C-1b),

76.5 (C-1a or C-1b) 66.1 (C-9a and C-9b), 40.3 (CH), 40.2k (CH), 39.9 (CH<sub>2</sub>), 38.2 (CH), 33.3 (CH<sub>2</sub>), 27.8 (CH<sub>2</sub>), 18.4 (C-7a and C-7b), 13.5 (C-10a or C-10b), 13.3 (C-10a or C-10b). **HRMS** (ESI<sup>+</sup>) *m/z* [M+Na<sup>+</sup>] calculated for [C<sub>10</sub>H<sub>20</sub>O<sub>2</sub>Na]<sup>+</sup> 195.1361 found 195.1363 (M + Na<sup>+</sup>).

Synthesis of (1*R*,3*S*,5*s*)-5-(2-hydroxypropan-2-yl)-2-methylcyclohexane-1,3-diol (**45**)



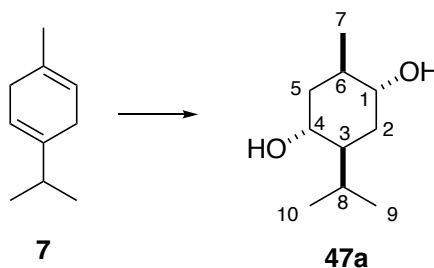
To a pre-dried flask of *trans*-sobrerol under argon was added dry THF (60 mL). The mixture was stirred on ice and borane solution (1 M in THF; 117.7 mmol; 118 mL) was added dropwise *via* syringe. This was then stirred at room temperature for 3 hours before 2 M sodium hydroxide solution was added (88 mL, 176.5 mmol) at 0 °C, followed by hydrogen peroxide solution (30% v/v, 18 mL, 176.5 mmol). The mixture was further stirred for 16 hours before sat. aq. Na<sub>2</sub>SO<sub>3</sub> was added (50 mL) and following further stirring for 10 minutes, the volatiles and water were removed by reduced pressure. The remaining material was re-dissolved in hot MeCN (80 °C) and undissolved solids were filtered while keeping the glassware hot. The filtrate was then kept at -20 °C for four hours before the recrystallised title compound was formed as a white, solid precipitate and collected by Büchner filtration (6.19 g, 32.94 mmol 56% yield by <sup>1</sup>H NMR). **FTIR** (ATR)  $\nu_{\max}/\text{cm}^{-1}$  = 3329 (OH), 2975, 2928, 2003, 1686, 1461, 1437, 1380 (C-OH), 1363, 1324, 1266, 1239, 1214, 1178, 1149, 1081, 1049, 1034. **<sup>1</sup>H NMR:** (400 MHz, CDCl<sub>3</sub>)  $\delta_{\text{H}}$  = 3.95 – 3.89 (m, 1H, H-3), 3.50 (td, *J* = 10.8, 4.3 Hz, 1H, H-1), 2.13 – 2.00 (m, 1H, H-4'), 1.94 – 1.78 (m, 2H, H-6' and H-3), 1.36 – 1.28 (m, 1H, H-2), 1.28 – 1.20 (m, 1H, H-6''), 1.16 (d, *J* = 4.2 Hz, 6H, H-9 and H-10) 1.09 (d, *J* = 6.8 Hz, 3H,



H-7), 1.07 – 0.98 (m, 1H, H-4''). **<sup>13</sup>C NMR** (100 MHz, MeOD)  $\delta_c$  = 72.7 (C-8), 72.6 (C-3), 72.2 (C-1), 45.1 (C-2), 42.4 (C-5), 37.7 (C-4), 35.6 (C-6), 27.4 (C-9 or C-10), 26.8 (C-9 or C-10), 14.9 (C-7). **HRMS** (ESI<sup>+</sup>)  $m/z$  [M+Na<sup>+</sup>] calculated for [C<sub>10</sub>H<sub>20</sub>O<sub>3</sub>Na]<sup>+</sup> 211.1310 found 211.1308 (M + Na<sup>+</sup>).

Synthesis of (1*R*,2*S*,4*R*,5*R*)-2-isopropyl-5-methylcyclohexane-1,4-diol

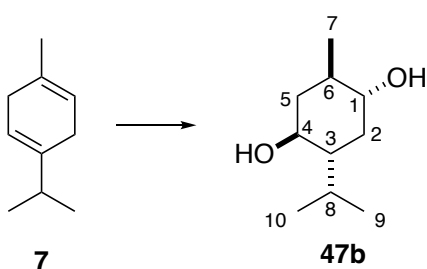
**(47a)**



To a solution of  $\gamma$ -terpinene (5.9 mL, 36.77 mmol) in dry THF (40 mL) under argon was added borane solution (1 M solution in THF; 73.53 mmol, 75 mL), dropwise at 0 °C. The solution was stirred for 2 hours before 2M sodium hydroxide solution was added (74 mL, 147.05 mmol) at 0 °C, followed by hydrogen peroxide solution (30% v/v, 15 mL, 147.05 mmol). The solution was stirred at room temperature for a further 2 hours before extracting the water layer with diethyl ether (2x 100 mL). The organic extract was subsequently washed with sodium carbonate solution (2x 100 mL) and brine (2x 100 mL) before being dried over Na<sub>2</sub>SO<sub>4</sub>. The solvent was removed under reduced pressure to yield the crude material as a yellow oil. Purification by silica gel chromatography (40% EtOAc in Petroleum ether) afforded the diastereomer **47a** as a white solid (1.698 g; 9.87 mmol; 27%). **FTIR** (ATR)  $\nu_{\max}/\text{cm}^{-1}$  = 3247 (OH), 2956 (C-H), 2872 (C-H), 1721, 1635, 1619, 1453, 1406, 1385, 1370, 1341, 1296, 1270, 1193, 1148 (C-O), 1096 (C-O), 1041, 1023, 1000; **<sup>1</sup>H NMR**: (400 MHz, MeOD)  $\delta_H$  = 3.37 (td,  $J$  = 10.6, 4.3 Hz, 1H, H-1), 3.06 (ddd,  $J$  = 10.9, 9.7, 4.2 Hz, 1H, H-4), 2.19 (heptd,  $J$  = 7.0, 2.8 Hz, 1H, H-8), 1.91 (dt,  $J$  = 12.7, 4.0 Hz, 1H, H-5'), 1.79 (dt,  $J$  = 12.6, 3.7 Hz, 1H, H-3), 1.41 – 1.31 (m, 1H, H-6), 1.31 – 1.25 (m, 1H, H-2''), 1.09 – 1.04 (m, 1H, H-5''), 1.00

(d,  $J = 6.4$  Hz, 3H, H-7), 0.93 (d,  $J = 7.1$  Hz, 3H, H-9 or H-10), 0.82 (d,  $J = 6.9$  Hz, 3H, H-9 or H-10);  **$^{13}\text{C}$  NMR** (100 MHz, MeOD)  $\delta_{\text{C}} = 76.7$  (C-4), 71.3 (C-1), 49.7 (C-6), 43.7 (C-2), 39.5 (C-3), 33.4 (C-5), 26.7 (C-8), 21.5 (C-9 or C-10), 18.8 (C-7), 16.18 (C-9 or C-10); **HRMS** (ESI<sup>+</sup>)  $m/z$  [M+Na<sup>+</sup>] calculated for [C<sub>10</sub>H<sub>20</sub>O<sub>2</sub>Na]<sup>+</sup> 195.1361 found 195.1361 (M + Na<sup>+</sup>).

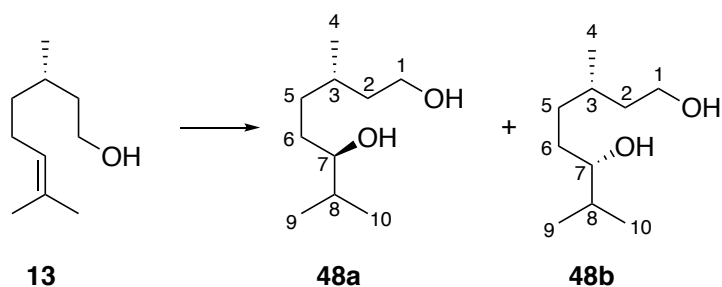
Synthesis of (1*S*,2*R*,4*R*,5*R*)-2-isopropyl-5-methylcyclohexane-1,4-diol  
**(47b)**



To a solution of  $\gamma$ -terpinene (5.9 mL, 36.77 mmol) in dry THF (40 mL) under argon was added borane solution (1 M solution in THF; 73.53 mmol, 75 mL), dropwise at 0 °C. The solution was stirred for 2 hours before 2M sodium hydroxide solution was added (74 mL, 147.05 mmol) at 0 °C, followed by hydrogen peroxide solution (30% v/v, 15 mL, 147.05 mmol). The solution was stirred at room temperature for a further 2 hours before extracting the water layer with diethyl ether (2x 100 mL). The organic extract was subsequently washed with sodium carbonate solution (2x 100 mL) and brine (2x 100 mL) before being dried over Na<sub>2</sub>SO<sub>4</sub>. The solvent was removed under reduced pressure to yield the crude material as a yellow oil. Purification by silica gel chromatography (40% EtOAc in Petroleum ether) afforded the diastereomer **47b** as a white solid (1.7962 g, 10.44 mmol, 28%). **FTIR** (ATR)  $\nu_{\text{max}}/\text{cm}^{-1} = 3279$  (OH), 2950 (C-H), 2915 (C-H), 2867 (C-H), 1711, 1505, 1463, 1439, 1385, 1377, 1368, 1334, 1310, 1293, 1249, 1201, 1164, 1152, 1096 (C-O), 1074, 1002;  **$^1\text{H}$  NMR** (400 MHz, MeOD)  $\delta_{\text{H}} = 3.75$  (td,  $J = 6.8, 3.5$  Hz, 1H, H-1), 3.42 (td,  $J = 6.8, 3.6$  Hz, 1H, H-4), 1.93 – 1.80 (m, 2H, H-3 and H-8), 1.80 – 1.71 (m, 1H, H-2'), 1.71 – 1.55 (m, 2H, H-4' and H-4''), 1.55 –

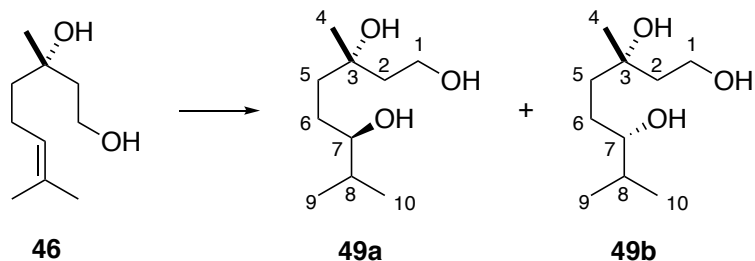
1.39 (m, 2H, H-2" and H-6), 0.97 (d,  $J = 7.0$  Hz, 3H, H-7), 0.91 (dd,  $J = 9.3, 6.8$  Hz, 6H, H-9 and H-10).  **$^{13}\text{C}$  NMR** (100 MHz, MeOD)  $\delta_{\text{C}} = 72.2$  (C-4), 67.9 (C-1), 47.5 (C-6), 36.9 (C 2), 35.8 (C-3), 29.4 (C-5), 27.5 (C-8), 21.6 (C-9 and C-10), 18.5 (C-7); **HRMS** (ESI<sup>+</sup>)  $m/z$  [M+Na<sup>+</sup>] calculated for [C<sub>10</sub>H<sub>20</sub>O<sub>2</sub>Na]<sup>+</sup> 195.1361 found 195.1361 (M + Na<sup>+</sup>).

Synthesis of (3*S*,6*R*)-3,7-dimethyloctane-1,6-diol (**48a**) and (3*S*,6*S*)-3,7-dimethyloctane-1,6-diol (**48b**)\*



To a solution of (*S*)-citronellol (5.8 mL, 32.05 mmol) in dry THF (30 mL) under argon was added borane solution (1 M solution in THF; 38.46 mmol, 38.5 mL), dropwise at 0 °C. The solution was stirred for 2 hours before 2M sodium hydroxide solution was added (64 mL, 128.21 mmol) at 0 °C, followed by hydrogen peroxide solution (30% v/v, 13.1 mL, 128.21 mmol). The solution was stirred at room temperature for a further 2 hours before removing the solid precipitate by Büchner filtration. The filtrate was then collected and the water layer was extracted with diethyl ether (2x 150 mL). The organic extract was subsequently washed with sodium carbonate solution (2x 100 mL) and brine (2x 100 mL) before being dried over Na<sub>2</sub>SO<sub>4</sub>. The solvent was removed under reduced pressure to yield the crude material as a yellow oil. Purification by silica gel chromatography (60% EtOAc in Petroleum ether) afforded the title compound as a pale yellow oil in a 1:1 mixture of diastereomers (**48a**: **48b**) (3.941 g; 22.65 mmol; 71%). \*Data is incomplete and has been lost; the compound **48** should be considered the most probably outcome if the reaction were to be repeated.

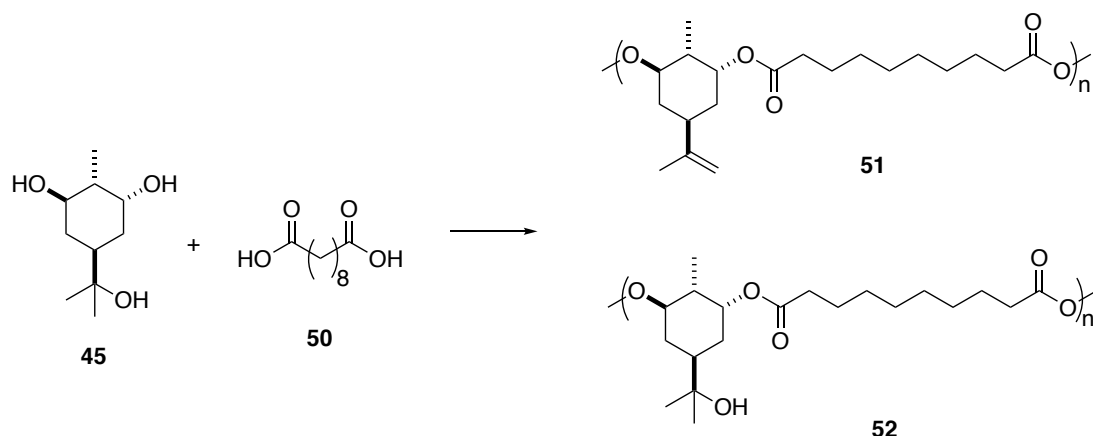
Synthesis of (3*S*,6*R*)-3,7-dimethyloctane-1,3,6-triol (**49a**) and (3*S*,6*S*)-3,7-dimethyloctane-1,3,6-triol (**49b**)



To a solution of linalool (5.8 mL, 32.47 mmol) in dry THF (30 mL) under argon was added borane solution (1 M solution in THF; 64.94 mmol, 65 mL), dropwise at 0 °C. The solution was stirred for 2 hours before 2M sodium hydroxide solution was added (65 mL, 129.87 mmol) at 0 °C, followed by hydrogen peroxide solution (30% v/v, 13.3 mL, 129.87 mmol). The solution was stirred at room temperature for a further 2 hours before extracting the water layer with diethyl ether (2x 150 mL). The organic extract was subsequently washed with sodium carbonate solution (2x 100 mL) and brine (2x 100 mL) before being dried over Na<sub>2</sub>SO<sub>4</sub>. The solvent was removed under reduced pressure to yield the crude material as a yellow oil. Purification by silica gel chromatography (60% EtOAc in Petroleum ether) afforded the title compound as a pale yellow oil in a 1:1 mixture of diastereomers (**49a**:**49b**) (1.56 g; 8.21 mmol; 25%). **FTIR** (ATR)  $\nu_{\text{max}}/\text{cm}^{-1}$  = 3328 (OH), 2956 (C-H), 2874 (C-H), 1725, 1463, 1419, 1373, 1255, 1124 (C-O); **<sup>1</sup>H NMR** (400 MHz, MeOD)  $\delta_{\text{H}}$  = 3.97 – 3.79 (m, 4H, H-1a and H-1b), 3.34 (td,  $J$  = 5.8, 2.6 Hz, 2H, H-6a and H-6b), 1.92 – 1.53 (m, 12H, H-7a, H-7b, H-5a', H5b', H-4a, H-4b, H-2a and H-2b), 1.53 – 1.36 (m, 2H, H-5a'' and H-5b''), 1.26 – 1.20 (m, 6H, H-10a and H-10b), 0.91 (ddd,  $J$  = 6.8, 3.2, 1.7 Hz, 12H, H-9a, H-9b, H-10a and H-10b); **<sup>13</sup>C NMR** (100 MHz, MeOD)  $\delta_{\text{C}}$  = 77.3 (C-6a and C-6b), 73.5 (C-3a or C-3b), 73.4 (C-3a or C-3b), 59.9 (C-1a or C-1b), 59.8 (C-1a or C-1b), 42.4 (C-2a or C-2b), 41.5 (C-2a or C-2b), 39.3 (C-4a or C-4b), 39.2 (C-4a or C-4b), 33.9 (C-7a or C-7b), 33.8 (C-7a or C-7b), 28.2 (C-5a or C-5b), 28.0 (C-5a or C-5b), 27.0 (C-10a or C-10b), 26.6 (C10a or C-10b), 19.0 (C-8a or C-8b or C-9a or C-9b), 18.9 (C-8a or C-8b or C-9a or C-9b),

17.7 (C-8a or C-8b or C-9a or C-9b), 17.6 (C-8a or C-8b or C-9a or C-9b); **HRMS** (ESI<sup>+</sup>)  $m/z$  [M+H<sup>+</sup>] calculated for [C<sub>10</sub>H<sub>21</sub>O<sub>2</sub>]<sup>+</sup> 191.1647 found 191.1638 (M + H<sup>+</sup>).

#### 4.6.3 Synthesis of polyester **50** and **51**

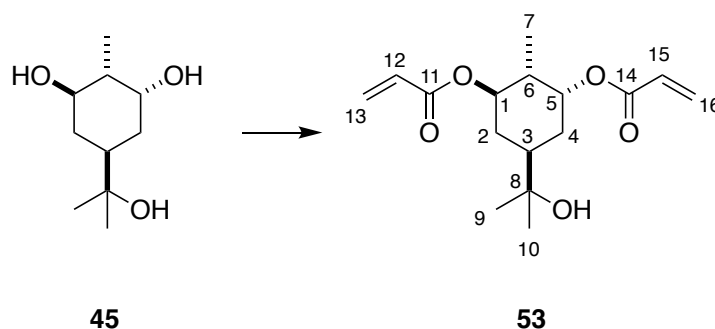


All reagents and glassware were dried at 100 °C for 24 hours prior to use. A dry glass vial was charged with **45** (0.519 g, 2.66 mmol) and **50** (0.545 g, 2.66 mmol) and the mixture was heated to 190 °C under Argon. After approximately 20 minutes when the reagents had visibly melted, SnOct<sub>2</sub> was added (11 mg, 0.026 mmol) and the reaction was heated to 190 °C under vacuum for 24 hours. After this time, the sample was removed from the heat and vacuum and allowed to cool in air. The polymer was isolated as a brown solid, as a mixture of products **51** and **52**.  $M_n$  from **GPC**: 3200 g·mol<sup>-1</sup> and  $\bar{D}$  2.0. **FTIR** (ATR)  $\nu_{\max}/\text{cm}^{-1}$  = 2976, 2936, 1726 (C=O), 1645, 1375, 1154 (C-O), 1066 (C-O); **<sup>1</sup>H NMR** (400 MHz, CDCl<sub>3</sub>)  $\delta_H$  = 5.19 (s, 1H, CH), 4.91 – 4.78 (m, 1H, CH), 4.71 (s, 0.23H, CH<sub>2</sub>), 4.67 (s, 0.27 H, CH<sub>2</sub>), 2.38 – 2.23 (m, 5H, CH<sub>2</sub>), 2.19 – 2.07 (m, 1H, CH<sub>2</sub>), 2.03 – 1.89 (m, 1H, CH<sub>2</sub>), 1.77 – 1.67 (m, 2H, CH), 1.66 – 1.54 (m, 6H, CH<sub>2</sub>), 1.30 (s, 10H, CH<sub>2</sub>), 1.15 (d,  $J$  = 3.6 Hz, 6H, CH<sub>3</sub>), 0.98 – 0.80 (m, 3H, CH<sub>3</sub>). **<sup>13</sup>C NMR** (100 MHz, CDCl<sub>3</sub>)  $\delta_C$  = 173.6 (C=O), 173.5 (C=O), 147.9 (CR<sub>4</sub>), 109.6 (CH<sub>2</sub>), 74.3 (C-O), 74.0 (CR<sub>4</sub>) 73.7 (C-O), 71.9 (CR<sub>4</sub>), 41.5

(CH), 39.9 (CH), 34.8 (CH<sub>2</sub>), 34.7 (CH<sub>2</sub>), 32.7 (CH<sub>2</sub>), 31.3 (CH<sub>2</sub>), 29.2 (CH<sub>2</sub>), 27.6 (CH<sub>3</sub>), 27.1 (CH<sub>3</sub>), 20.9 (CH), 14.0 (CH).

#### 4.6.4 Syntheses of terpene-derived di-acrylates

##### Synthesis of (1R,2R,3R,5R)-5-(2-hydroxypropan-2-yl)-2-methylcyclohexane-1,3-diyl diacrylate (**53**)

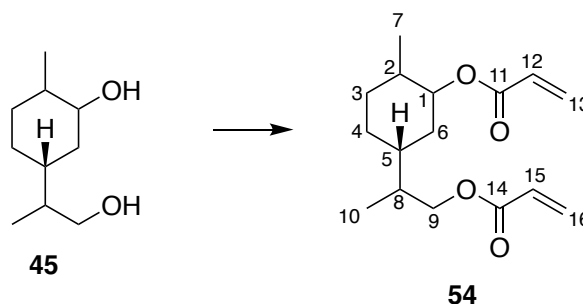


To a round bottom flask charged with **45** (7.23 g, 38.46 mmol) was added acetonitrile (80 mL), Et<sub>3</sub>N (32 mL, 230.7 mmol), acrylic acid (6 mL, 84.61 mmol) and butylated hydroxy toluene (BHT) (84 mg, 0.385 mmol). Then T3P® (45 mL, 75.64 mmol) was added dropwise on ice. The mixture was stirred, exposed to air, for 16 hours. After this time Et<sub>2</sub>O (2x 75 mL) was added and the mixture was washed with 1M HCl (2x 50 mL), then sat. aq. NaHCO<sub>3</sub> (2x 50 mL) and brine (100 mL), before the organic extracts were collected and dried over MgSO<sub>4</sub>. The volatiles were then removed with a flow of air to afford the title compound as a viscous, orange oil. (8.89 g, 30.03 mmol, 78%). **FTIR** (ATR)  $\nu_{\text{max}}/\text{cm}^{-1}$  = 3504 (OH), 2969, 2881, 1717 (C=O), 1635 (C=C), 1618 (C=C), 1457, 1405, 1369, 1295, 1269, 1187, 1122 (C-O), 1046; **<sup>1</sup>H NMR**: (400 MHz, CDCl<sub>3</sub>)  $\delta_{\text{H}}$  = 6.50 – 6.30 (m, 2H, H-13' and H-16'), 6.19 – 6.04 (m, 2H, H-12 and H-15), 5.89 – 5.76 (m, 2H, H-13'' and H-16''), 5.29 (q,  $J$  = 3.0 Hz, 1H, H-5), 5.05 – 4.85 (m, 1H, H-1), 2.27 – 2.12 (m, 1H, H-2'), 2.11 – 2.02 (m, 1H, H-4'), 1.88 – 1.74 (m, 1H, H-3 and H-6), 1.41 – 1.30 (m, 1H, H-4''), 1.25 – 1.18 (m, 1H, H-2''), 1.16 (s, 6H, H-9 and H-10), 0.92 (d,  $J$  = 6.7 Hz, 3H, H-7); **<sup>13</sup>C NMR** (100 MHz, CDCl<sub>3</sub>)  $\delta_{\text{C}}$  = 166.0 (C-11 or C-14), 165.7 (C-11 or C-14), 131.1 (C-13 or C-16), 130.8 (C-13 or C-16), 128.8 (C-12 or C-15), 128.6 (C-12 or C-15), 74.7 (C-1), 74.1 (C-5), 71.9 (C-8), 41.5 (C-3), 40.1 (C-6), 32.7 (C-2) 31.2 (C-4), 27.4 (C-9 or C-10), 27.3 (C-9 or C-10);

**HRMS** (ESI<sup>+</sup>)  $m/z$  [M+Na<sup>+</sup>] calculated for [C<sub>16</sub>H<sub>24</sub>O<sub>5</sub>Na]<sup>+</sup> 319.1521 found 319.1519 (M + Na<sup>+</sup>).

Synthesis of 2-((1R)-3-(acryloyloxy)-4-methylcyclohexyl)propyl acrylate

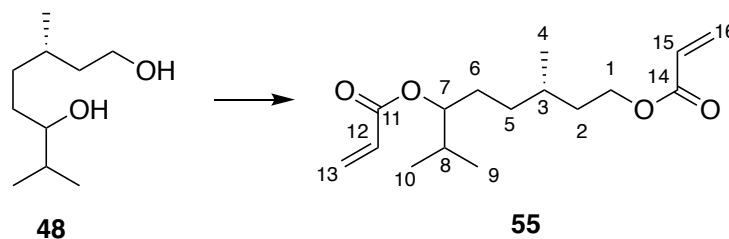
**(54)**



To a round bottom flask charged with **20** (5.629 g, 32.73 mmol) was added acetonitrile (66 mL), BHT (109 mg, 0.49 mmol), Et<sub>3</sub>N (27 mL, 196.39 mmol) and acrylic acid (5 mL, 72.00 mmol). Then T3P® (45 mL, 72.00 mmol) was added dropwise on ice. The mixture was stirred, exposed to air, for 16 hours. After this time Et<sub>2</sub>O (2x 75 mL) was added and the mixture was washed with 1M HCl (2x 50 mL), then sat. aq. NaHCO<sub>3</sub> (2x 50 mL) and brine (100 mL), before the organic extracts were collected and dried over MgSO<sub>4</sub>. The volatiles were then removed with a flow of air to afford the title compound as an orange oil. (6.42 g, 22.91 mmol, 72%).

**FTIR** (ATR)  $\nu_{\text{max}}/ \text{cm}^{-1}$  = 2930, 2875, 1719 (C=O), 1635 (C=C), 1619, 1457, 1406, 1294, 1269, 1188 (C-O), 1049; **<sup>1</sup>H NMR:** (400 MHz, CDCl<sub>3</sub>)  $\delta_{\text{H}}$  = 6.42 – 6.34 (m, 2H, H-16' and H-13'), 6.17 – 6.05 (m, 2H, H-12 and H-15), 5.85 – 5.76 (m, 2H, H-13 and H-16), 4.90 – 4.71 (m, 0.25H, H-1a), 4.51 (tdd,  $J$  = 10.8, 4.4, 2.4 Hz, 0.75H, H-1b), 4.27 – 3.82 (m, 2H, H-9), 2.06 – 1.90 (m, 1H, CH<sub>2</sub>), 1.89 – 1.01 (m, 8H, CH<sub>2</sub> and CH), 1.01 – 0.84 (m, 6H, H-10 and H-7). **<sup>13</sup>C NMR** (100 MHz, CDCl<sub>3</sub>)  $\delta_{\text{C}}$  = 166.4 (C-14 or C-11), 166.1 (C-14 or C-11), 130.7 (C-13 or C-16), 130.5 (C-13 or C-16), 129.0 (C-12 or C-15), 128.7 (C-12 or C-15), 78.5 (C-1a), 74.9 (C-1b), 67.8 (C-9a), 67.5 (C-9b), 38.3 (CH), 37.5 (CH), 37.1 (CH<sub>2</sub>), 35.9 (CH<sub>2</sub>), 33.3 (CH<sub>2</sub>), 29.5 (CH<sub>2</sub>), 27.6 (CH<sub>2</sub>), 18.3 (C-7), 13.6 (C-10). **HRMS** (ESI<sup>+</sup>)  $m/z$  [M+Na<sup>+</sup>] calculated for [C<sub>16</sub>H<sub>24</sub>O<sub>4</sub>Na]<sup>+</sup> 303.1572 found 303.1572 (M + Na<sup>+</sup>).

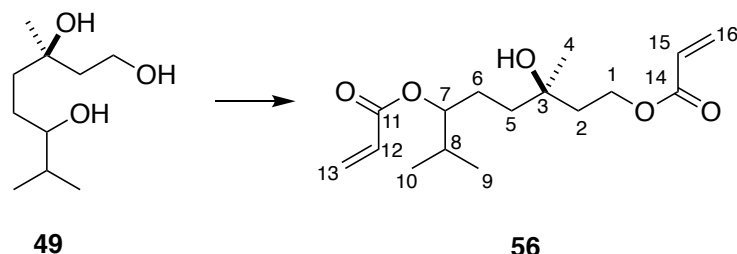
### Synthesis of (3S)-3,7-dimethyloctane-1,6-diyl diacrylate (**55**)



To a round bottom flask charged with **48** (5.57 g, 32.02 mmol) was added acetonitrile (64 mL), BHT (112 mg, 0.48 mmol), Et<sub>3</sub>N (27 mL, 192.1 mmol) and acrylic acid (4.8 mL, 70.43 mmol). Then T3P® (42 mL, 74.43 mmol) was added dropwise on ice. The mixture was stirred, exposed to air, for 16 hours. After this time Et<sub>2</sub>O (2x 75 mL) was added and the mixture was washed with 1M HCl (2x 50 mL), then sat. aq. NaHCO<sub>3</sub> (2x 50 mL) and brine (100 mL), before the organic extracts were collected and dried over MgSO<sub>4</sub>. The volatiles were then removed with a flow of air to afford the title compound as a yellow oil (7.94 g, 28.16 mmol, 88%). **FTIR** (ATR)  $\nu_{\text{max}}/\text{cm}^{-1}$  = 2961, 2875, 1718 (C=O), 1635 (C=C), 1620, 1462, 1406, 1389, 1295, 1269, 1186 (C-O), 1131, 1046; **<sup>1</sup>H NMR**: (400 MHz, CDCl<sub>3</sub>)  $\delta_{\text{H}}$  = 6.36 (dt,  $J$  = 17.4, 1.4 Hz, 2H, H-13' and H-16'), 6.15 – 6.03 (m, 2H, H-12 and H-15), 5.79 (dt,  $J$  = 10.4, 1.6 Hz, 2H, H-13'' and H-15''), 4.78 (dt,  $J$  = 8.1, 4.9 Hz, 1H, H-7), 4.28 – 4.00 (m, 2H, H-1), 1.84 (app. pd,  $J$  = 6.9, 5.4 Hz, 1H, H-8), 1.71 – 1.60 (m, 1H, H-2'), 1.54 (m, 2H, H-6), 1.50 – 1.42 (m, 1H, H-2''), 1.41 – 1.35 (m, 1H, H-3), 1.35 – 1.24 (m, 1H, H-5'), 1.20 – 1.02 (m, 1H, H-1''), 0.95 – 0.84 (m, 9H, H-9, H-10 and H-4). **<sup>13</sup>C NMR** (100 MHz, CDCl<sub>3</sub>)  $\delta_{\text{C}}$  = 166.4 (C-12 or C-14), 166.3 (C-12 or C-14), 130.6 (C-13 or C-16), 130.4 (C-13 or C-16), 129.0 (C-12 or C-15), 128.7 (C-12 or C-15), 78.9 (C-7), 63.0 (C-1), 35.5 (C-2), 32.7 (C-5), 31.6 (C-8), 30.0 (C-3), 28.6 (C-6), 19.6 (C-9 or C-10), 19.4 (C-9 or C-10), 18.7 (C-4); **HRMS** (ESI<sup>+</sup>)  $m/z$  [M+Na<sup>+</sup>] calculated for [C<sub>16</sub>H<sub>26</sub>O<sub>4</sub>Na]<sup>+</sup> 305.1729 found 305.1736 (M + Na<sup>+</sup>).



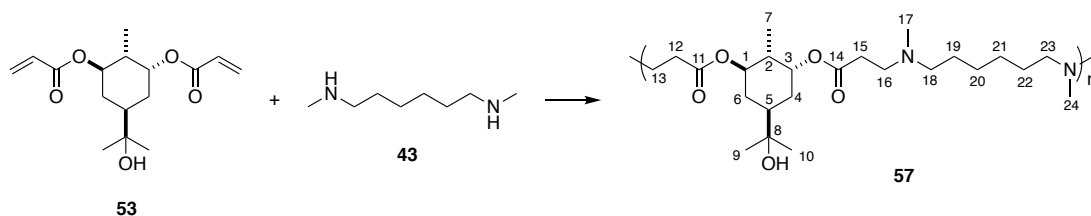
Synthesis of (3R)-3-hydroxy-3,7-dimethyloctane-1,6-diyl diacrylate (**56**)



To a round bottom flask charged with **49** (2.38 g, 11.54 mmol) was added acetonitrile (23 mL), BHT (39 mg, 0.16 mmol), Et<sub>3</sub>N (9 mL, 64.42 mmol) and acrylic acid (1.62 mL, 23.62 mmol). Then T3P® (7 mL, 23.62 mmol) was added dropwise on ice. The mixture was stirred, exposed to air, for 16 hours. After this time Et<sub>2</sub>O (2x 50 mL) was added and the mixture was washed with 1M HCl (2x 30 mL), then sat. aq. NaHCO<sub>3</sub> (2x 30 mL) and brine (75 mL), before the organic extracts were collected and dried over MgSO<sub>4</sub>. The volatiles were then removed with a flow of air to afford the title compound as a yellow oil (3.38 g, 11.34 mmol, 92%). **FTIR** (ATR)  $\nu_{\text{max}}/\text{cm}^{-1}$  = 3499 (OH), 2965, 2877, 1718 (C=O), 1636 (C=C), 1618, 1465, 1406, 1295, 1271, 1191 (C-O), 1047; **<sup>1</sup>H NMR**: (400 MHz, CDCl<sub>3</sub>)  $\delta_{\text{H}}$  = 6.37 (dt,  $J$  = 17.4, 1.6 Hz, 2H, H-13' and H-16'), 6.09 (ddd,  $J$  = 17.4, 10.4, 5.1 Hz, 2H, H-12 and H-15), 5.80 (dt,  $J$  = 10.4, 1.7 Hz, 2H, H-13'' and H-16''), 4.85 – 4.73 (m, 1H, H-7), 4.29 (td,  $J$  = 6.9, 2.1 Hz, 2H, H-1), 1.92 – 1.74 (m, 1H, H-8), 1.72 – 1.54 (m, 2H, H-6), 1.53 – 1.42 (m, 2H, H-5), 1.20 (d,  $J$  = 2.5 Hz, 3H, H-4), 0.89 (d,  $J$  = 6.8 Hz, 6H, H-9 and H-10). **<sup>13</sup>C NMR** (100 MHz, CDCl<sub>3</sub>)  $\delta_{\text{C}}$  = 166.3 (C-11 or C-14), 166.2 (C-11 or C-14), 130.9 (C-13 or C-16), 130.6 (C-13 or C-16), 128.9 (C-12 or C-15), 128.5 (C-12 or C-15), 78.9 (C-7), 71.6 (C-3), 61.3 (C-1), 40.1 (C-2), 38.3 (C-5), 31.7 (C-8), 27.2 (C-4), 25.7 (C-6), 18.69 (C-9 or C-10), 17.7 (C-9 or C-10). **HRMS** (ESI<sup>+</sup>)  $m/z$  [M+Na<sup>+</sup>] calculated for [C<sub>16</sub>H<sub>26</sub>O<sub>5</sub>Na]<sup>+</sup> 321.1678 found 321.1685 (M + Na<sup>+</sup>).

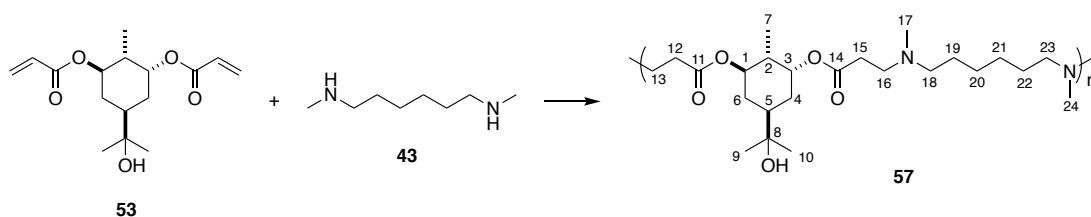
#### 4.6.5 Synthesis of terpene-based $\beta$ -(amino ester)s via the aza-Michael polymerisation

##### Synthesis of polymer **57** by conventional heating (oil bath)



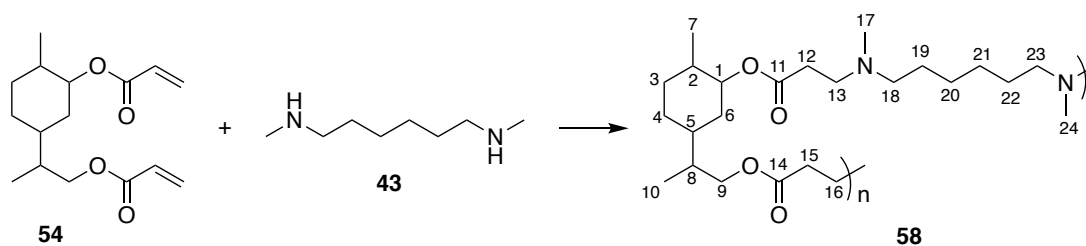
Diacrylate **53** (1.06 g, 3.47 mmol) and diamine **43** (0.62 mL, 3.472 mmol) were measured into an 8-dram vial which was heated in an oil bath to 90 °C. The monomers were stirred together for 7 days, after which time the polymer **57** was isolated without further purification as a viscous, orange oil.  $M_n$  from **GPC**: 3200 g·mol<sup>-1</sup> and  $\bar{D}$  2.0. **FTIR** (ATR)  $\nu_{\text{max}}$ / cm<sup>-1</sup> = 3326 (OH), 2932, 2855, 2793, 1726 (C=O), 1457, 1362, 1307, 1177 (C-O), 1123 (C-O), 1033; **<sup>1</sup>H NMR** (400 MHz, CDCl<sub>3</sub>)  $\delta_{\text{H}}$  = 5.19 (d,  $J$  = 3.0 Hz, 1H, H-3), 4.89 – 4.74 (m, 1H, H-1), 2.71 – 2.62 (m, 4H, H-13 and H-16), 2.50 – 2.39 (m, 4H, H-12 or H-15), 2.35 – 2.25 (m, 4H, H-18 and H-23), 2.19 (s, 6H, H-17 and H-24), 2.18 – 2.16 (m, 1H, H-5), 2.05 – 1.96 (m, 1H, H-4 or H-6), 1.77 – 1.66 (m, 1H, H-2), 1.47 – 1.39 (m, 4H, H-19 and H-22), 1.29 – 1.23 (m, 4H, H-20 and H-21), 1.13 (s, 6H, H-9 and H-10), 0.89 (d,  $J$  = 6.6 Hz, 3H, H-7). **<sup>13</sup>C NMR** (100 MHz, CDCl<sub>3</sub>)  $\delta_{\text{C}}$  = 172.4 (C-11 or C-14), 172.3 (C-11 or C-14), 74.5 (C-1), 74.0 (C-3), 71.7 (C-8), 57.6 (C-18 or C-23), 57.5 (C-18 or C-23), 53.1 (C-13 or C-16), 53.0 (C-13 or C-16), 42.0 (C-17 and C-24), 41.5 (C-5), 39.9 (C-2), 32.8 (C-12 or C-15), 32.7 (C-12 or C-15), 31.2 (C-4 and C-6), 27.6 (C-19, C-20 and C-22), 27.4 (C-28), 27.3 (C-9 and C-10), 13.9 (C-7).

### Synthesis of polymer **57** by microwave heating



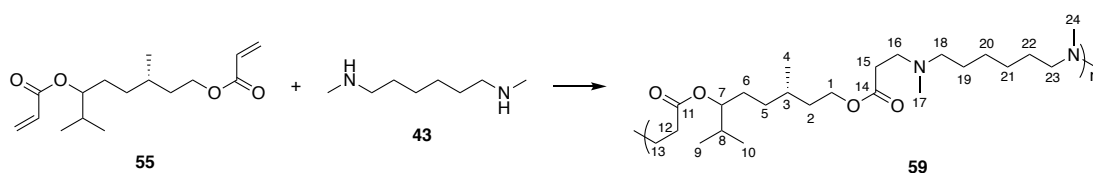
To a microwave vial charged with acetonitrile (1.7 mL, 1 M) and Et<sub>3</sub>N (1.2 mL, 8.44 mmol) was added diacrylate **52** (0.51 g, 1.69 mmol) and diamine **43** (0.32 mL, 1.69 mmol). The vial was sealed and the sample was heated under microwave radiation to 120 °C for 12 hours. After this time the mixture was precipitated into cold petroleum ether and this sample was stored at -20 °C for 2 hours, before centrifugation at 4500 g for 5 minutes. The organic layer was decanted to yield the polymer **57** as an orange, viscous oil.  $M_n$  from **GPC**: 2700 g·mol<sup>-1</sup> and  $\bar{D}$  1.37. **FTIR** (ATR)  $\nu_{\max}/\text{cm}^{-1}$  = 3326 (OH), 2931, 2855, 2792, 1726 (C=O), 1457, 1363, 1307, 1177 (C-O), 1122 (C-O), 1033; **<sup>1</sup>H NMR** (400 MHz, CDCl<sub>3</sub>)  $\delta_{\text{H}}$  = 5.18 (d,  $J$  = 3.0 Hz, 1H, H-3), 4.83 (td,  $J$  = 11.0, 4.3 Hz, 1H, H-1), 2.72 – 2.61 (m, 4H, H-13 and H-16), 2.60 – 2.52 (m, 2H, H-4' or H-6''), 2.48 – 2.42 (m, 4H, H-12 and H-15), 2.42 – 2.38 (m, 1H, H-5), 2.30 (t,  $J$  = 7.6 Hz, 4H, H-18 and H-23), 2.19 (s, 6H, H-17 and H-24), 2.07 – 1.92 (m, 1H, H-4'' or H-6''), 1.81 – 1.62 (m, 1H, H-2), 1.46 – 1.35 (m, 4H, H-19 and H-22), 1.33 – 1.21 (m, 4H, H-20 and H-21), 1.12 (s, 6H, H-9 and H-10), 0.88 (d,  $J$  = 6.7 Hz, 3H, H-7). **<sup>13</sup>C NMR** (100 MHz, CDCl<sub>3</sub>)  $\delta_{\text{C}}$  = 172.4 (C-11 or C-14), 172.3 (C-11 or C-14), 74.5 (C-1), 73.9 (C-3), 71.7 (C-8), 57.6 (C-18 or C-23), 57.5 (C-18 or C-23), 53.1 (C-13 or C-16), 53.0 (C-13 or C-16), 42.0 (C-17 and C-24), 41.5 (C-5), 39.9 (C-2), 32.9 (C-12 or C-15), 32.7 (C-12 or C-15), 31.2 (C-4 and C-6), 27.6 (C-19, C-20 and C-22), 27.4 (C-28), 27.3 (C-9 and C-10), 13.9 (C-7).

### Synthesis of polymer **58**



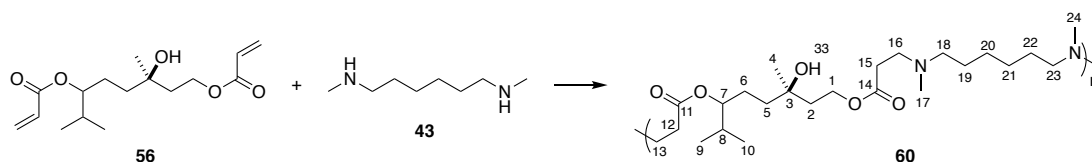
To a microwave vial charged with acetonitrile (1.7 mL, 1 M) was added **54** (0.51 g, 1.79 mmol), **43** (0.32 mL, 1.79 mmol) and Et<sub>3</sub>N (1.2 mL, 8.92 mmol). The vial was sealed, and the sample was heated under microwave radiation to 120 °C for 12 hours. After this time the mixture was precipitated into cold petroleum ether and this sample was stored at -20 °C for 2 hours, before centrifugation at 4500 g for 5 minutes. The organic layer was decanted to yield the polymer **58** as an yellow, viscous oil.  $M_n$  from **GPC**: 4030 g·mol<sup>-1</sup> and  $\bar{D}$  1.52. **FTIR** (ATR)  $\nu_{\max}/\text{cm}^{-1}$  = 2929, 2954, 2791, 1730 (C=O), 1646, 1457, 1374, 1306, 1172 (C-O), 1036; **<sup>1</sup>H NMR** (400 MHz, CDCl<sub>3</sub>)  $\delta_H$  = 4.80 – 4.62 (m, 0.3H, H-1b), 4.52 – 4.35 (m, 0.7H, H-1a), 4.15 – 3.96 (m, 1H, H-9'), 3.95 – 3.75 (m, 1H, H-9''), 2.73 – 2.61 (m, 4H, H-13 and H-16), 2.58 – 2.52 (m, 2H, H-4 or H-6), 2.51 – 2.39 (m, 4H, H-12 and H-15), 2.35 – 2.27 (m, 4H, H-18 and H-23), 2.20 (s, 6H, H-17 and H-24), 1.95 – 1.84 (m, 1H, H-4' or H-6'), 1.84 – 1.55 (m, 5H, H-5, H-2, H-3' and H-4' or H-6'), 1.51 – 1.37 (m, 4H, H-19 and H-22), 1.34 – 1.22 (m, 4H, H-20 and H-21), 1.17 – 0.98 (m, 3H, H-4'' or H-6'', H-3, H-2), 0.97 – 0.79 (m, 6H, H-7 and H-10). **<sup>13</sup>C NMR** (100 MHz, CDCl<sub>3</sub>)  $\delta_C$  = 172.9 (C-11 or C-14), 172.5 (C-11 or C-14), 78.3 (C-1), 67.8 (C-9), 57.7 (C-18 and C-23), 53.2 (C-13 or C-16), 53.0 (C-13 or C-16), 42.1 (C-17 and C-24), 38.5 (C-2 or C-5 or C-8), 38.2 (C-2 or C-5 or C-8), 37.5 (C-2 or C-5 or C-8), 35.9 (C-3 or C-4 or C-6), 34.7 (C-3 or C-4 or C-6), 32.9 (C-3 or C-4 or C-6), 32.6 (C-12 or C-15), 27.6 (C-19 and C-22, or, C-20 and C-21), 18.4 (C-7 and C-10).

### Synthesis of polymer **59**



To a microwave vial charged with acetonitrile (1.7 mL, 1 M) was added **55** (0.52 g, 1.77 mmol), **43** (0.32 mL, 1.77 mmol) and Et<sub>3</sub>N (1.2 mL, 8.86 mmol). The vial was sealed, and the sample was heated under microwave radiation to 120 °C for 12 hours. After this time the mixture was precipitated into cold petroleum ether and this sample was stored at -20 °C for 2 hours, before centrifugation at 4500 g for 5 minutes. The organic layer was decanted to yield the polymer **59** as a yellow, viscous oil.  $M_n$  from **GPC**: 3170 g·mol<sup>-1</sup> and Đ 1.51. *\*Data is incomplete and has been lost; the compound **48** should be considered the most probable outcome if the reaction were to be repeated.*

### Synthesis of polymer **60**



To a microwave vial charged with acetonitrile (1.7 mL, 1 M) was added **56** (0.54g, 1.69 mmol), **43** (0.32 mL, 1.69 mmol) and Et<sub>3</sub>N (1.2 mL, 8.39 mmol). The vial was sealed, and the sample was heated under microwave radiation to 120 °C for 12 hours. After this time the mixture was precipitated into cold petroleum ether and this sample was stored at -20 °C for 2 hours, before centrifugation at 4500 g for 5 minutes. The organic layer was decanted to yield the polymer **60** as a yellow, viscous oil.  $M_n$  from **GPC**: 3170 g·mol<sup>-1</sup> and Đ 1.51. **FTIR** (ATR)  $\nu_{\text{max}}/\text{cm}^{-1}$  = 3431 (OH), 2932, 2856, 2794, 1728 (C=O), 1460, 1419, 1365, 1174 (C-O), 1125 (C-O), 1060; **<sup>1</sup>H NMR** (400 MHz, CDCl<sub>3</sub>)  $\delta_{\text{H}}$  = 4.74 (dd,  $J$  = 8.2, 4.8 Hz, 1H, H-7), 4.22 (td,  $J$  = 6.9, 2.1 Hz, 2H, H-1), 2.73 – 2.61 (m, 4H, H-13

and H-16), 2.50 – 2.42 (m, 4H, H-12 and H-15), 2.35 – 2.27 (m, 4H, H-18 and H-23), 2.19 (d,  $J = 3.7$  Hz, 6H, H-17 and H-24), 1.88 – 1.70 (m, 3H, H-6 and H-8), 1.66 – 1.54 (m, 2H, H-5), 1.52 – 1.37 (m, 8H, H-2, H-19 and H-22), 1.35 – 1.23 (m, 4H, H-20 and H-21), 1.17 (d,  $J = 3.1$  Hz, 3H, H-4), 0.89 (d,  $J = 6.8$  Hz, 6H, H-9 and H-10).  **$^{13}\text{C}$  NMR** (100 MHz,  $\text{CDCl}_3$ )  $\delta_{\text{C}} = 172.7$  (C-11 and C-14), 78.7 (C-7), 71.3 (C-3), 61.3 (C-1), 57.5 (C-19 and C-23), 53.2 (C-13 and C-16), 42.0 (C-17 and C-24), 40.1 (C-6), 38.3 (C-2), 32.9 (C-12 and C-15), 31.5 (C-8), 27.6 (C-19 and C-22), 27.2 (C-20 and C-21), 25.5 (C-5), 18.7 (C-9 or C-10), 17.8 (C-9 or C-10).

## 5 Conclusions and future outlook

Between the three experimental chapters of this thesis, the versatility and diversity of monoterpenes in both small molecule and polymer chemistry has been demonstrated. As a source of renewable carbon that does not compete directly with food sources,<sup>35,68</sup> which is inexpensive (often a waste-stream of already-established industries<sup>9</sup>), and which features an assortment of functionalities, terpenes can be considered a model feedstock from which to synthesise a wealth of compounds, including polymers. By employing terpenes in polymer chemistry and formulations, it can also be possible to capitalise upon some of their well-known, natural properties, for example their anti-microbial<sup>78,199</sup> or medicinal<sup>80,81,272,273</sup> benefits, and to incorporate these into novel materials.

The first experimental chapter of this thesis detailed a project in which the high functionality of terpenes can lend itself useful in ring-opening polymerisations. It was demonstrated that primary and secondary alcohol groups of a range of terpenoids have suitable nucleophilicity to act as initiators for lactide and also the cyclic carbonate monomer, TMC. This was achieved using a fully green synthesis, employing only bio-based reagents, catalysts and solvents. The result was a small library of PDLLA oligomers, each featuring the terpenoid initiator as a head group. In each case, the structural integrity of the initiator was maintained (of course with the exception of the alcohol which initiated the polymerisation), allowing for the possibility of post-polymerisation modifications *via* the alkene moieties. Although a thiol-click reaction was attempted in this work as a post-polymerisation conjugation, the reaction did not go to completion, and as such, future work for this project would involve the optimisation of this, or other, post-polymerisation modifications. Thiol-click reactions with terpene double bonds are widely reported in the literature,<sup>37,66,274</sup> indicating the potential, once the reaction is optimised, to conjugate molecules tailored for a specific applications, such as drugs or dyes, to the polymers. Alternatively, the terpene head groups could be used simply as a docking point for the production of highly functionalisable, degradable polymeric platforms.

Possibly the most significant finding from this work, however, was not in the potential application of the polymers after the functionalisation of the alkene groups, but of the properties of the oligomers themselves, which was bestowed by the terpene initiators. Each of the terpene-initiated PDLLA oligomers were found to self-assemble in water to produce well-defined nanoparticles. This is something which a homopolymer of PDLLA is unable to do. In particular, the sample made from the terpenoid *trans*-sobrerol (**12**) produced nanoparticles that were particularly stable over a 48 hour period. This highlights another advantage of the switch from DCM to 2-MeTHF: not only does it allow for the generation of these oligomers through a more green and sustainable process, but also enables the solubility of **12** (insoluble in DCM), giving access to these unique terpenoid-based nanoparticles.

A comparison between the **12**-PDLLA oligomers with 10 and 20 lactide repeat units found that by modifying the hydrophobic/ hydrophilic balance through extension of the hydrophobic oligomer chain in this way, the CAC of the nanoparticles could be tuned. PDLLA<sub>20</sub> was found to form smaller nanoparticles (103 nm rather than 176 nm of PDLLA<sub>10</sub>), and was found to have a smaller CAC of just 70  $\mu\text{g mL}^{-1}$ . Given that these nanoparticles were found to be devoid of any major cytotoxicity, there may be potential applications for these bio-based, renewable surfactants in biomaterial applications. Furthermore, the research suggests that monoterpenoids bearing a nucleophilic alcohol group can be considered a toolbox of renewable and highly functionalisable small molecules for a new generation of ROP initiators. Coupled with the sustainable solvent 2-MeTHF and bio-based catalyst DBU, this ROP process employing terpenes has introduced a method of synthesising natural and bio-renewable surfactants, embracing the concept of the circular economy and 12 principles of green chemistry.

In addition to their use as initiators for ROP, the second chapter of the thesis detailed a way in which a terpenoid compound could be functionalised to produce a bis-epoxide monomer. The ene-one functionality of (*R*)-carvone was found to undergo epoxidation when reacted with alkaline hydrogen peroxide, in well-known, green and sustainable synthesis. Then it was shown that the exocyclic alkene could



also undergo epoxidation using a well-documented reaction with *m*CPBA. However, this second step is not atom-economic, and produces a by-product, chlorobenzoic acid, as stoichiometric waste. The reaction is also very exothermic, a particular issue when working at a large scale, and includes DCM as a solvent, which is a suspected carcinogen and extremely toxic.<sup>107,214</sup> To avoid the use of this reagent, an alternative synthesis was designed, featuring dimethyl dioxirane as the oxidant. This was made *in situ* from the reaction of acetone and Oxone<sup>®</sup>, the commercial name for potassium peroxymonosulfate, an inexpensive, stable salt.<sup>209</sup> As a result, this method was found to efficiently and cheaply bring about the epoxidation of the exocyclic alkene, avoiding the use of metal catalysts, and the organic monomer product was easily isolated without the use of chlorinated solvents, or the need for further purification. It is envisaged that this procedure could be employed as a method in which to produce bis-epoxide monomers from a wealth of terpenes, producing a toolbox of analogous monomers. The protocol has already been reported with limonene, carveol,  $\alpha$ -pinene and farnesol.<sup>209,275</sup>

Following the synthesis of this carvone-based bis-epoxide, its polymerisation with two diamines were investigated, the di-primary diamine 1,6-hexane diamine (**41**) and the di-secondary 1,6-dimethyl hexane diamine (**43**). The reactions of these diamines with the bis-epoxide can be viewed as models for the reactions of (theoretically) any aliphatic di-primary or di-secondary diamine, respectively. Therefore, future work for this research might look to investigating the polymerisation of terpene bis-epoxides with other, more functional diamines, for specific applications. For example, to enhance the hydrophilicity of the polymers or oligomers, a diamine with an ethylene glycol linker could be used. It would also be interesting to investigate the swelling and any potential hydrogel properties of these (or other) networks of polymers.

In this work, the carvone bis-epoxide was polymerised with the diamine co-monomer in the absence of catalysts or solvents, resulting in networks of  $\beta$ -amino amine oligomers when the **41** was used, and linear ones when **43** was used. The networks of polymers made with **41** were found to be very poorly soluble in a range of solvents, particularly water and DMSO, which precluded their ability to be tested for antimicrobial

effects. However, the linear oligomers made from the carvone bis-epoxide and the di-secondary diamine **43** were found to have suitable hydrophilicity to facilitate their use in synergistic, anti-fungal investigations.

It was determined that these linear,  $\beta$ -amino amine oligomers were found to act in synergy with the known fungicide IPBC and the antifungal drug amphotericin B, against *Trichoderma virens* and *Candida albicans*, respectively. The synergy was demonstrated using growth inhibition assays, checkerboard assays and disk diffusion assays in both cases. These quantitative analysis showed that the presence of the terpene-based oligomers decreased the minimum inhibitory concentration (MIC) of IPBC by up to 64-fold, and of amphotericin B by 8-fold.<sup>107</sup> Significantly, at the supplied concentrations, both the oligomers alone and the antifungals were inactive against the respective fungi, highlighting the advantage of the combination therapy: with lesser amounts of each agent required, a therapy is likely cheaper, and less susceptible to developing resistance. Additionally, the re-purposing of known antifungals can help alleviate the burden of discovering new anti-microbials, and circumvents the requirement for new clinical approval.

It is hypothesised that the synergistic anti-fungal relationship that is observed with these oligo-( $\beta$ -amino amine)s is the result of a combination of membrane disruption and conventional antifungal activity between the combined components. Time restrains in relation to the recent COVID-19 pandemic meant that it was not possible to explore these mechanism studies, and as such this remains an area of interest to investigate as future work on this project. In relation to this, it is hypothesised that a fluorophore could be conjugated to the ketone moiety of the oligomer backbone, which might allow for visualisation of where this component is acting on the cell. Additionally, there are examples in the literature of fluorophores being conjugated to amphotericin B,<sup>276,277</sup> which may allow for the visualisation of whether or not the components are acting on the same, or different, parts of the cell. Understanding this would help to shed light on the possible mechanisms of action of the synergistic components, which may in turn aid in the development of new antimicrobial formulations of bio-based oligomers such as these.

The functionalisation of terpenes has proved to have a wealth of potential for polymer chemistry,<sup>46</sup> and increasingly, methods are being developed which can allow for these functionalisations to take place using sustainable protocols and even on-scale.<sup>47,48,245</sup> In seeking to expand upon the potential for terpenes to be employed as monomers in sustainable polymerisations, the third and final experimental chapter saw the synthesis of five terpene-based poly-ols which were employed both as monomers and as monomer precursors for known and novel polymerisations, respectively.

These five terpenes were selected from some of the most abundant terpene-based biomass, and those which are commercially available and produced on an industrial scale.<sup>34</sup> The five that were selected were also identified as those which were predicted to form poly-ols with only two nucleophilic alcohols. This was important for their further syntheses, as it minimises the likelihood of branching reactions; the goal in this work was to form linear polymers. The hydroboration/oxidation was used to synthesise these poly-ols, with each of the terpenes undergoing the reaction as predicted. In most cases, purification of these compounds was achieved by silica gel chromatography, and this also allowed for the separation of diastereomers of the  $\gamma$ -terpinene derived diol, **47a** and **47b**.

In future work, it would be interesting to investigate more sustainable routes to these poly-ol monomers, and to improve the yields in some cases. Furthermore, a wider variety of terpene monomers could be synthesised, as well as those with more than two nucleophilic alcohol groups. In particular, alcohol-bearing monomers derived from geraniol, nerol, carveol and carvone would all be interesting options to investigate, the synthesis of which proved to be beyond the scope of this thesis.

Given a successful synthesis of these monomers, it follows that their potential for polymerisation would be of interest. In this work, the polycondensation of the five poly-ols with camphoric acid was investigated. Unfortunately, using melt conditions, the reactions were not found to proceed and so an alternative di-acid was investigated instead. This gave promising preliminary results for the reaction of the triol **45** and the 10-carbon sebacic acid. However, this work is very much at an early stage of investigation, with much room left to explore. To begin expanding this

research, it could of course involve extending the polymerisation to all of the terpene-based poly-ols. In addition, the optimisation of the reaction could be investigated, including some investigations into more sustainable polymerisation methods, such as the use of enzymatic catalysts. The di-acid co-monomer could also be substituted for alternatives with specific applications in mind, or those which may allow for post-polymerisation modifications. Additionally, it may be worth investigating the use of these terpene-based poly-ols for alternative polymerisation types, for example as initiators in branched ROP. Evidently, much potential remains for these compounds as both monomers and precursors in polymer chemistry.

In this work, the poly-ols were subsequently converted to their corresponding di-acrylate compounds for the purpose of investigating their use as monomers in aza-Michael polymerisations. Of the four terpenoids that were investigated, each one easily underwent the esterification, which followed a sustainable synthetic route, producing four terpene-diacrylate monomers in good to excellent yields and without the need for further purification. Unfortunately, a lack of material and time (as a result of the COVID-19 pandemic) meant that it was not possible to investigate the synthesis of the two potential  $\gamma$ -terpinene derived di-acrylate monomers, and as such, this remains an obvious piece of potential future research.

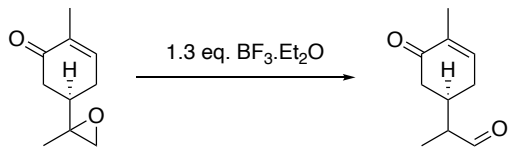
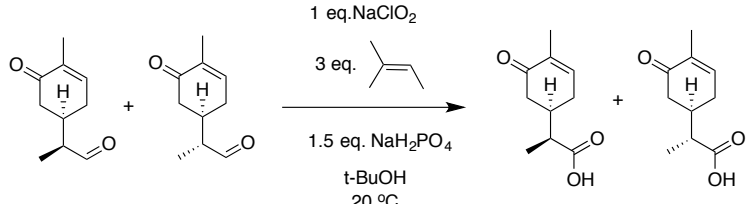
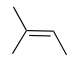
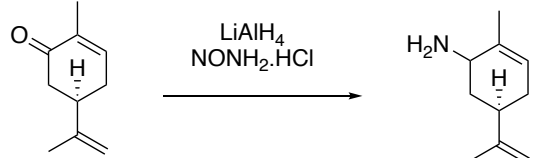
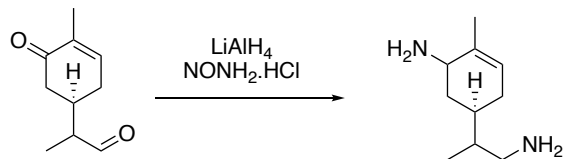
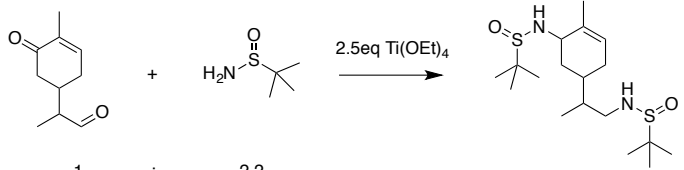
Owing to the previous success with the di-secondary diamine **43** in the generation of  $\beta$ -amino alcohol oligomers for anti-fungal purposes<sup>107</sup> (Chapter 3 of this thesis), this compound was employed again as a co-monomer with the diacrylates, in the synthesis of poly( $\beta$ -amino ester)s. It is hypothesised that this amine would again impart suitable amphiphilic character to the polymer, which may result in biocidal or anti-microbial activity.<sup>146</sup> As such, this could be a potential area of investigation into the applications of these polymer materials in future works. Alternatively, future investigations might involve the substitution of the diamine **43** with one tailored for a specific application or for post-polymerisation modifications. Another option might be to investigate the synthesis of a terpene-based amine which could be employed as a co-monomer. This would allow for a fully 'plant-based' polymer to be synthesised, with the two monomers derived from terpene biomass.

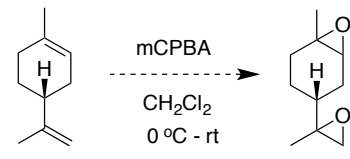
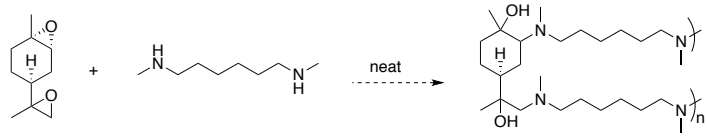
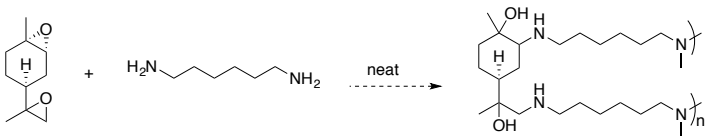
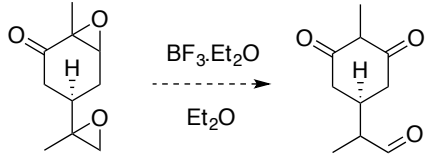
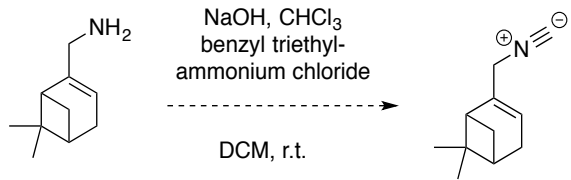
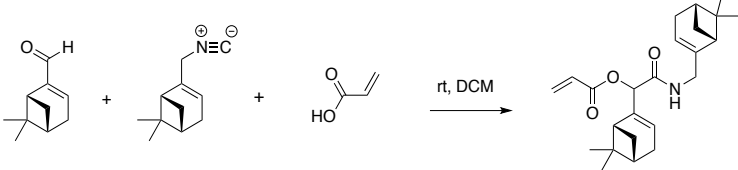
In this research, a brief study was conducted into the optimisation of the polymerisation reactions. It was concluded that the best polymerisation conditions in this instance employed acetonitrile as a solvent with Et<sub>3</sub>N as a catalyst. Additionally, the use of microwave heating found that reaction times could be reduced from 7 days at 70 °C to just 12 hours at 120 °C. However, even with these results in hand, there is much left to investigate in relation to this reaction, including the quantities and concentrations of solvent and catalyst used, and the reaction times and temperatures in the microwave. This project introduces for the first time the use of terpenes in the aza-Michael polymerisation, which in itself is relatively new and slowly becoming popularised in the field of polymer chemistry. The use of the microwave heating is also a relatively new area of investigation for these polymerisation types. As such, this project presents a new and exciting area of sustainable polymer research, with much potential and plenty of opportunities for a variety of applications.

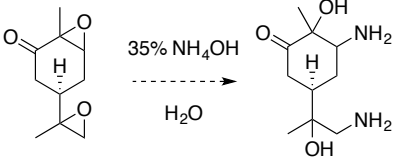
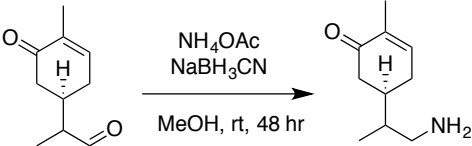
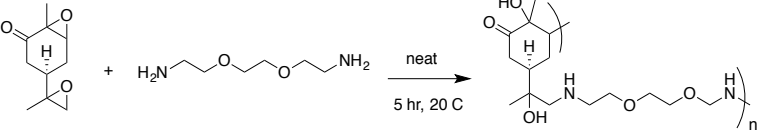
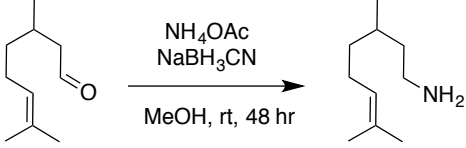
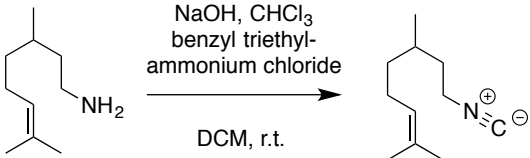
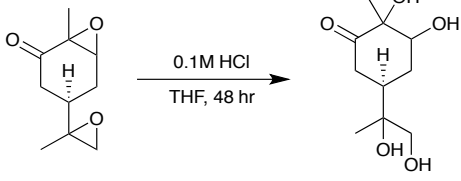
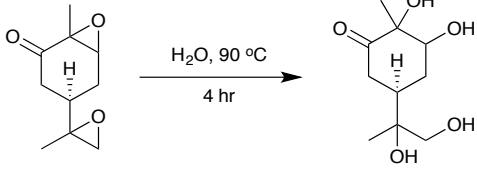
Terpenes are a diverse family of small molecules known for their anti-microbial properties and are employed industrially for their fragrances and flavours. Throughout this thesis it has been demonstrated that by incorporating them as feedstocks for polymerisations, it may be possible to capitalise upon these properties for a variety of applications, in addition to improving the sustainability and circularity of polymer materials. The future of terpenes in polymer-therapeutic fields remains one with much potential and opportunity.

## 6 Appendix

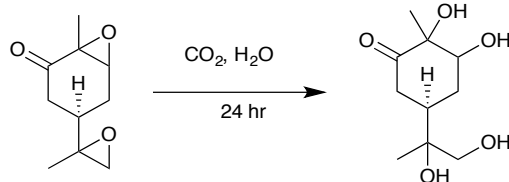
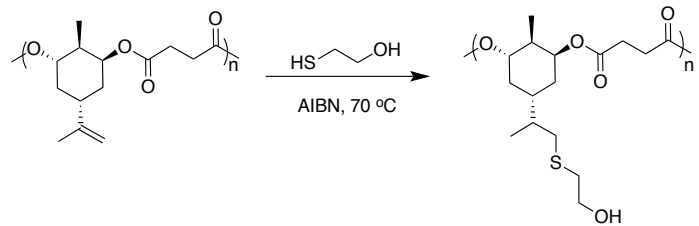
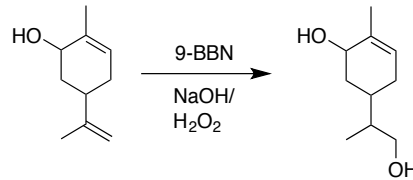
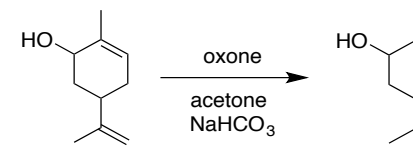
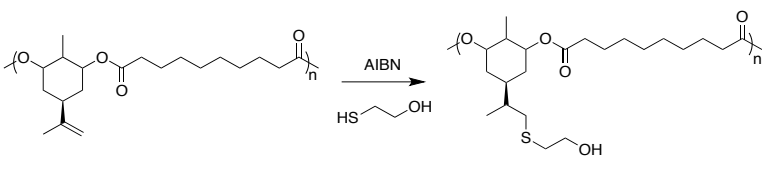
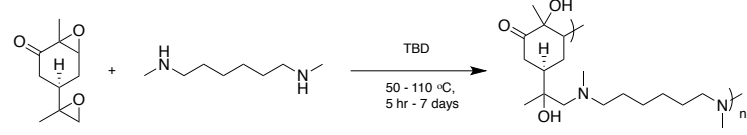
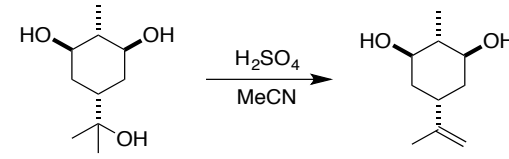
Although a variety of reactions are discussed within this thesis, which feature varying degrees of success, there were many more reactions which were attempted that were not successful, or didn't warrant inclusion in the main work. To aid future students, however, it might be helpful to see details on some of these additional reactions attempted, and so a variety of the most significant are included herein. For a more complete account on the results, the reader is directed to the relevant laboratory notebooks.

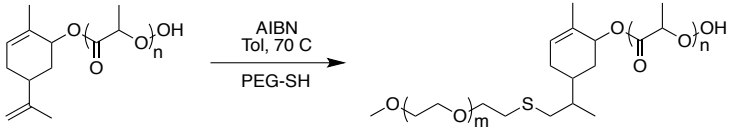
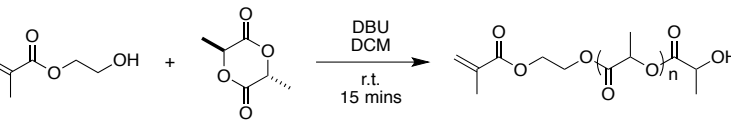
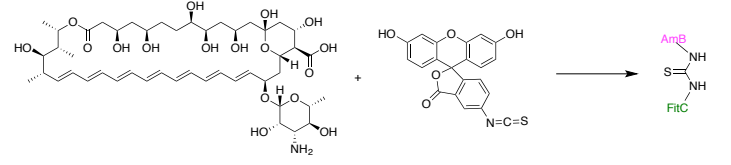
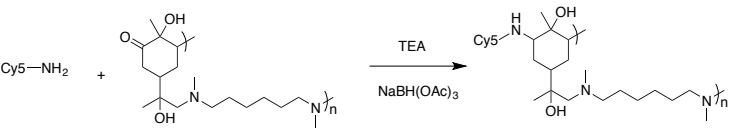
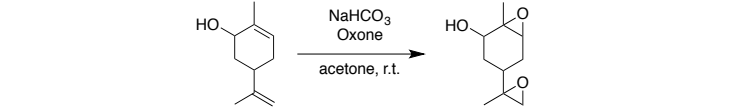
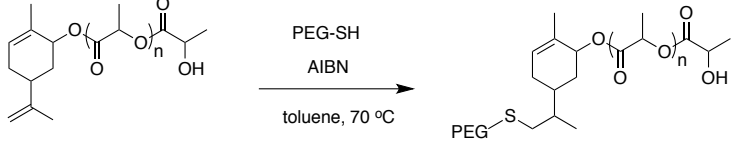
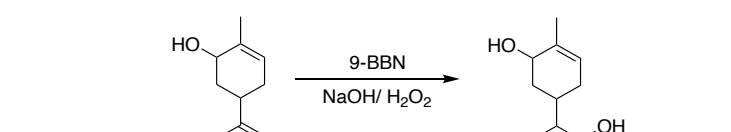
Reaction	Results & Comments
 <p>1.3 eq. <math>\text{BF}_3 \cdot \text{Et}_2\text{O}</math></p>	<ul style="list-style-type: none"> <li>Went to completion</li> <li>HF gas eluted</li> <li>Not a green synthesis</li> </ul>
 <p>1 eq. <math>\text{NaClO}_2</math> 3 eq.  1.5 eq. <math>\text{NaH}_2\text{PO}_4</math> t-BuOH 20 °C</p>	<ul style="list-style-type: none"> <li>didn't work</li> <li>Acetic acid formed as only product</li> </ul>
 <p><math>\text{LiAlH}_4</math> <math>\text{NONH}_2 \cdot \text{HCl}</math></p>	<ul style="list-style-type: none"> <li>No reaction</li> </ul>
 <p><math>\text{LiAlH}_4</math> <math>\text{NONH}_2 \cdot \text{HCl}</math></p>	<ul style="list-style-type: none"> <li>No reaction</li> </ul>
 <p>1 : 2.2</p> <p>2.5eq <math>\text{Ti}(\text{OEt})_4</math></p>	<ul style="list-style-type: none"> <li>Went to completion</li> </ul>

Reaction	Results & Comments
 <p> <chem>C=C1C2CC(C1)CC2</chem> <math>\xrightarrow[\text{CH}_2\text{Cl}_2, 0^\circ\text{C} - \text{rt}]{\text{mCPBA}}</math> <chem>C12OC1C(C2)C</chem> </p>	<ul style="list-style-type: none"> <li>Went to completion</li> <li>Complex mixture of 4 diastereomers</li> </ul>
 <p> <chem>C12OC1C(C2)C</chem> + <chem>CN(C)CCN(C)CCN(C)CCN(C)CC</chem> <math>\xrightarrow{\text{neat}}</math> <chem>C12OC1C(C2)C(O)N(C)CCN(C)CCN(C)CCN(C)CC(O)N(C)CCN(C)CC</chem> </p>	<ul style="list-style-type: none"> <li>Successful</li> <li>Similar results to carvone analogue</li> </ul>
 <p> <chem>C12OC1C(C2)C</chem> + <chem>NCCCCCN</chem> <math>\xrightarrow{\text{neat}}</math> <chem>C12OC1C(C2)C(O)NCCCCCN(O)NCCCCCN</chem> </p>	<ul style="list-style-type: none"> <li>Successful</li> <li>Similar results to carvone analogue</li> </ul>
 <p> <chem>C12OC1C(C2)C</chem> <math>\xrightarrow[\text{Et}_2\text{O}]{\text{BF}_3 \cdot \text{Et}_2\text{O}}</math> <chem>CC(=O)C12C(C)CC1C2</chem> </p>	<ul style="list-style-type: none"> <li>No product isolated</li> </ul>
 <p> <chem>C12C(C)CC1C2N</chem> <math>\xrightarrow[\text{DCM, r.t.}]{\text{NaOH, CHCl}_3, \text{benzyl triethylammonium chloride}}</math> <chem>C12C(C)CC1C2[N+]#N</chem> </p>	<ul style="list-style-type: none"> <li>Successful</li> <li>Not a green synthesis</li> <li>Rhona Savin made amine reagent</li> </ul>
 <p> <chem>C12C(C)CC1C2C=O</chem> + <chem>C12C(C)CC1C2[N+]#N</chem> + <chem>C=CC(=O)O</chem> <math>\xrightarrow{\text{rt, DCM}}</math> <chem>C12C(C)CC1C2C(=O)OC(=O)C=CNC12</chem> </p>	<ul style="list-style-type: none"> <li>No product isolated, complex mixture</li> </ul>

Reaction	Results & Comments
 <p>35% NH<sub>4</sub>OH H<sub>2</sub>O</p>	<ul style="list-style-type: none"> <li>No product isolated</li> </ul>
 <p>NH<sub>4</sub>OAc NaBH<sub>3</sub>CN MeOH, rt, 48 hr</p>	<ul style="list-style-type: none"> <li>Inconclusive</li> <li>complex mixture.</li> </ul>
 <p>neat 5 hr, 20 C</p>	<ul style="list-style-type: none"> <li>Inconclusive</li> </ul>
 <p>NH<sub>4</sub>OAc NaBH<sub>3</sub>CN MeOH, rt, 48 hr</p>	<ul style="list-style-type: none"> <li>Successful</li> </ul>
 <p>NaOH, CHCl<sub>3</sub> benzyl triethyl- ammonium chloride DCM, r.t.</p>	<ul style="list-style-type: none"> <li>Successful</li> <li>Not a green synthesis</li> </ul>
 <p>0.1 M HCl THF, 48 hr</p>	<ul style="list-style-type: none"> <li>No product isolated</li> </ul>
 <p>H<sub>2</sub>O, 90 °C 4 hr</p>	<ul style="list-style-type: none"> <li>No product isolated</li> </ul>



Reaction	Results & Comments
 <p>Reaction of a bicyclic acetal-protected diene with <math>\text{CO}_2</math> and <math>\text{H}_2\text{O}</math> for 24 hr to form a bicyclic diol.</p>	<ul style="list-style-type: none"> <li>No product isolated</li> </ul>
 <p>Reaction of a polymer with a bicyclic acetal-protected diene and a thiol using AIBN at 70 °C.</p>	<ul style="list-style-type: none"> <li>No product isolated</li> </ul>
 <p>Reaction of a diene with 9-BBN, NaOH, and <math>\text{H}_2\text{O}_2</math> to form a diol.</p>	<ul style="list-style-type: none"> <li>Didn't go to completion; requires column chromatography</li> </ul>
 <p>Reaction of a diene with oxone in acetone and <math>\text{NaHCO}_3</math> to form a bicyclic acetal-protected diol.</p>	<ul style="list-style-type: none"> <li>No product isolated; complex mixture</li> </ul>
 <p>Reaction of a polymer with a bicyclic acetal-protected diene and a thiol using AIBN.</p>	<ul style="list-style-type: none"> <li>No product isolated</li> </ul>
 <p>Reaction of a bicyclic acetal-protected diene with a tertiary amine using TBD at 50 - 110 °C, 5 hr - 7 days.</p>	<ul style="list-style-type: none"> <li>No difference to no-catalyst version</li> </ul>
 <p>Reaction of a diol with <math>\text{H}_2\text{SO}_4</math> in MeCN to form a diene.</p>	<ul style="list-style-type: none"> <li>Inconclusive</li> </ul>

Reaction	Results & Comments
	<ul style="list-style-type: none"> <li>No product isolated</li> </ul>
	<ul style="list-style-type: none"> <li>Successful</li> </ul>
	<ul style="list-style-type: none"> <li>Successful</li> <li>Attachment of Amphotericin B to Fit-C (green) fluorophore</li> </ul>
	<ul style="list-style-type: none"> <li>Successful</li> <li>Attachment of polymer-44 to Cy-5 (red) fluorophore</li> </ul>
	<ul style="list-style-type: none"> <li>No product isolated</li> <li>inconclusive</li> </ul>
	<ul style="list-style-type: none"> <li>No product isolated</li> </ul>
	<ul style="list-style-type: none"> <li>Didn't go to completion</li> <li>complex mixture, requires column chromatography</li> </ul>

## 7 References

- 1 H. Staudinger, *Ber. Dtsch. Chem. Ges.*, 1920, **53**, 1073–1085.
- 2 M. Peplow, *Nature*, 2016, **536**, 266–268.
- 3 Ellen MacArthur Foundation, *The New Plastics Economy: Rethinking the future of plastics*, 2016.
- 4 M. Okada, *Prog. Polym. Sci.*, 2002, **27**, 87–133.
- 5 Y. Zhu, C. Romain and C. K. Williams, *Nature*, 2016, **540**, 354–362.
- 6 A. Llevot, P. K. Dannecker, M. von Czapiewski, L. C. Over, Z. Soyler and M. A. R. Meier, *Chem. - A Eur. J.*, 2016, **22**, 11510–11521.
- 7 A. Gandini, T. M. Lacerda, A. J. F. Carvalho and E. Trovatti, *Chem. Rev.*, 2016, **116**, 1637–1669.
- 8 C. Williams and M. Hillmyer, *Polym. Rev.*, 2008, **48**, 1–10.
- 9 M. R. Thomsett, T. E. Storr, O. R. Monaghan, R. A. Stockman and S. M. Howdle, *Green Mater.*, 2016, **4**, 115–134.
- 10 Y. Zhong, P. Godwin, Y. Jin and H. Xiao, *Adv. Ind. Eng. Polym. Res.*, 2020, **3**, 27–35.
- 11 M. A. Hillmyer and W. B. Tolman, *Acc. Chem. Res.*, 2014, **47**, 2390–2396.
- 12 S. Kabasci, in *Plastic Waste and Recycling*, Elsevier Inc., Oberhausen, North Rhine-Westphalia, 2020, pp. 67–96.
- 13 P. Anastas and N. Eghbali, *Chem. Soc. Rev.*, 2010, **39**, 301.
- 14 A. K. Mohanty, M. Misra and L. T. Drzal, *J. Polym. Environ.*, 2002, **10**, 19–26.
- 15 K. Yao and C. Tang, *Macromolecules*, 2013, **46**, 1689–1712.
- 16 Z. Wang, M. S. Ganewatta and C. Tang, *Prog. Polym. Sci.*, 2020, **101**, 101197.
- 17 K. Parker, J. P. Garancher, S. Shah and A. Fernyhough, *J. Cell. Plast.*, 2011, **47**, 233–243.
- 18 K. Madhavan Nampoothiri, N. R. Nair and R. P. John, *Bioresour. Technol.*, 2010, **101**, 8493–8501.
- 19 S. Inkinen, M. Hakkarainen, A. C. Albertsson and A. Södergård, *Biomacromolecules*, 2011, **12**, 523–532.
- 20 M. R. Yates and C. Y. Barlow, *Resour. Conserv. Recycl.*, 2013, **78**, 54–66.

- 21 A. Mahapatro and D. K. Singh, *J. Nanobiotechnology*, 2011, **9**, 55.
- 22 K. K. Bawa and J. K. Oh, *Mol. Pharm.*, 2017, **14**, 2460–2474.
- 23 L. Montero De Espinosa and M. A. R. Meier, *Eur. Polym. J.*, 2011, **47**, 837–852.
- 24 A. Gandini, *Macromolecules*, 2008, **41**, 9491–9504.
- 25 A. Naseem, S. Tabasum, K. M. Zia, M. Zuber, M. Ali and A. Noreen, *Int. J. Biol. Macromol.*, 2016, **93**, 296–313.
- 26 F. José Borges Gomes, R. E. de Souza, E. O. Brito and R. C. Costa Lelis, *J. Appl. Biotechnol. Bioeng.*, 2020, **7**, 100–105.
- 27 N. Mandleker, A. Cayla, F. Rault, S. Giraud, F. Salaün, G. Malucelli and J.-P. Guan, in *Lignin - Trends and Applications*, InTech Open, 2018, pp. 207–231.
- 28 C. M. Byrne, S. D. Allen, E. B. Lobkovsky and G. W. Coates, *J Am Chem Soc*, 2004, **126**, 11404–11405.
- 29 M. Mascal and E. B. Nikitin, *Angew. Chemie - Int. Ed.*, 2008, **47**, 7924–7926.
- 30 A. Gandini, *Prog. Polym. Sci.*, 1997, **22**, 1203–1379.
- 31 M. Belgacem and A. Gandini, in *Monomers, Polymers and Composites from Renewable Resources*, eds. M. Naceur Belgacem and A. Gandini, Elsevier Ltd., Oxford, 1st edn., 2008, pp. 17–38.
- 32 M. Winnacker, *Angew. Chemie - Int. Ed.*, 2018, **57**, 14362–14371.
- 33 S. L. Kristufek, K. T. Wacker, Y.-Y. T. Tsao, L. Su and K. L. Wooley, *Nat. Prod. Rep.*, 2017, **34**, 433–459.
- 34 K.-G. Fahlbusch, F.-J. Hammerschmidt, J. Panten, W. Pickenhagen, D. Schatkowski, K. Bauer, D. Garbe and H. Surburg, in *Ullmann's Encyclopedia of Industrial Chemistry*, Wiley-VCH, Holzminden, 2012, vol. 15, pp. 74–198.
- 35 M. Thomsett, J. C. Moore, A. Buchard, R. Stockman and S. M. Howdle, *Green Chem.*, 2019, **21**, 149–156.
- 36 A. L. Holmberg, K. H. Reno, R. P. Wool and T. H. Epps, III, *Soft Matter*, 2014, **10**, 7405–7424.
- 37 A. C. Weems, K. R. Delle Chiaie, J. C. Worch, C. J. Stubbs and A. P. Dove, *Polym. Chem.*, 2019, **10**, 5959–5966.
- 38 B. P. Mooney, *Biochem J*, 2009, **418**, 219–232.
- 39 E. Manaila, M. D. Stelescu and G. Craciun, *Aspects Regarding*

*Radiation Crosslinking of Elastomers*, InTech, 2012.

- 40 P. A. Wilbon, F. Chu and C. Tang, *Macromol. Rapid Commun.*, 2013, **34**, 32–43.
- 41 W. J. Roberts and A. R. Day, *J. Am. Chem. Soc.*, 1950, **72**, 1226–1230.
- 42 J. A. A. M. Castro and R. P. F. Guine, *J. Appl. Polym. Sci.*, 2001, **82**, 2558–2565.
- 43 M. Winnacker and B. Rieger, *ChemSusChem*, 2015, **8**, 2455–2471.
- 44 S. Kobayashi, C. Lu, T. R. Hoye and M. A. Hillmyer, *J. Am. Chem. Soc.*, 2009, **131**, 7960–7961.
- 45 M. F. Sainz, J. A. Souto, D. Regentova, M. K. G. G. Johansson, S. T. Timhagen, D. J. Irvine, P. Buijsen, C. E. Koning, R. A. Stockman and S. M. Howdle, *Polym. Chem.*, 2016, **7**, 2882–2887.
- 46 P. Sahu, P. Sarkar and A. K. Bhowmick, *ACS Sustain. Chem. Eng.*, 2017, **5**, 7659–7669.
- 47 P. S. Löser, P. Rauthe, M. A. R. Meier and A. Llevot, *Philos. Trans. R. Soc. A*, 2020, **378**, 20190267.
- 48 M. A. Droesbeke and F. E. Du Prez, *ACS Sustain. Chem. Eng.*, 2019, **7**, 11633–11639.
- 49 M. Taherimehr and P. P. Pescarmona, *J. Appl. Polym. Sci.*, 2014, **131**, 1–17.
- 50 C. Martín and A. W. Kleij, *Macromolecules*, 2016, **49**, 6285–6295.
- 51 F. Parrino, A. Fidalgo, L. Palmisano, L. M. Ilharco, M. Pagliaro and R. Ciriminna, *ACS Omega*, 2018, **3**, 4884–4890.
- 52 M. Bähr, A. Bitto and R. Mülhaupt, *Green Chem.*, 2012, **14**, 1447.
- 53 V. Schimpf, B. S. Ritter, P. Weis, K. Parison and R. Mülhaupt, *Macromolecules*, 2017, **50**, 944–955.
- 54 H. J. Park, C. Y. Ryu and J. V. Crivello, *J. Polym. Sci. Part A Polym. Chem.*, 2013, **51**, 109–117.
- 55 B. Kheira, H. Aicha and Y. Ahmed, *J. Chem. Pharm. Res.*, 2015, **7**, 988–993.
- 56 H. Morinaga, N. Ogawa, M. Sakamoto and H. Morikawa, *J. Polym. Sci.*, 2019, **57**, 1–8.
- 57 R. M. Carman and K. D. Klika, *Aust. J. Chem.*, 1991, **44**, 1803–1808.
- 58 W. B. Cunningham, J. D. Tibbetts, M. Hutchby, K. A. Maltby, M. G.

- Davidson, U. Hintermair, P. Plucinski and S. D. Bull, *Green Chem.*, 2020, **22**, 513–524.
- 59 L. P. Carrodeguas, F. Castro-gómez, J. González-fabra, C. Bo and A. W. Kleij, *Chem. Eur. J.*, 2015, **21**, 6115.
- 60 F. Della Monica and A. W. Kleij, *Polym. Chem.*, 2020, **11**, 5109–5127.
- 61 J. A. Garden, P. K. Saini and C. K. Williams, *J. Am. Chem. Soc.*, 2015, **137**, 15078–15081.
- 62 G. Trott, J. A. Garden and C. K. Williams, *Chem. Sci.*, 2019, **10**, 4618–4627.
- 63 CN103333329, 2013.
- 64 O. Hauenstein, M. Reiter, S. Agarwal, B. Rieger and A. Greiner, *Green Chem.*, 2016, **18**, 760–770.
- 65 M. Firdaus and M. A. R. Meier, *Green Chem.*, 2013, **15**, 370.
- 66 M. Firdaus, L. Montero De Espinosa and M. A. R. Meier, *Macromolecules*, 2011, **44**, 7253–7262.
- 67 D. Zhang, M. A. Hillmyer and W. B. Tolman, *Biomacromolecules*, 2005, **6**, 2091–2095.
- 68 J. R. Lowe, W. B. Tolman and M. A. Hillmyer, *Biomacromolecules*, 2009, **50**, 2003–2008.
- 69 J. R. Lowe, M. T. Martello, W. B. Tolman and M. A. Hillmyer, *Polym. Chem.*, 2011, **2**, 702–708.
- 70 K. K. W. Mak, Y. M. Lai and Y.-H. Siu, *J. Chem. Educ.*, 2006, **83**, 1058.
- 71 P. N. Stockmann, D. Van Opdenbosch, A. Poethig, D. L. Pastoetter, M. Hoehenberger, S. Lessig, J. Raab, M. Woelbing, C. Falcke, M. Winnacker, C. Zollfrank, H. Strittmatter and V. Sieber, *Nat. Commun.*, 2020, **11**, 509.
- 72 P. N. Stockmann, D. L. Pastoetter, M. Woelbing, C. Falcke, M. Winnacker, H. Strittmatter and V. Sieber, *Macromol. Rapid Commun.*, 2019, **40**, 1–7.
- 73 M. Winnacker, S. Vagin, V. Auer and B. Rieger, *Macromol. Chem. Phys.*, 2014, **215**, 1654–1660.
- 74 N. Komatsu, S. Simizu and T. Sugita, *Synth. Commun.*, 1992, **22**, 277–279.

- 75 M. Imoto, H. Sakurai and T. Kono, *J. Polym. Sci.*, 1961, **L**, 467–473.
- 76 M. Winnacker, A. Tischner, M. Neumeier and B. Rieger, *RSC Adv.*, 2015, **5**, 77699–77705.
- 77 F. L. Hatton, *Polym. Chem.*, 2020, **11**, 220–229.
- 78 A. Stamm, M. Tengdelius, B. Schmidt, J. Engström, P. O. Syrén, L. Fogelström and E. Malmström, *Green Chem.*, 2019, **21**, 2720–2731.
- 79 A. Yuta and J. N. Baraniuk, *Curr. Allergy Asthma Rep.*, 2005, **5**, 243–251.
- 80 P. L. Crowell, *Breast Cancer Res. Treat.*, 1997, 46, 191–197.
- 81 M. R. V. Santos, F. V. Moreira, B. P. Fraga, D. P. de Sousa, L. R. Bonjardim and L. J. Quintans, *Brazilian J. Pharmacogn.*, 2011, **21**, 764–771.
- 82 I. A. Saeedi, T. Andritsch and A. S. Vaughan, *Polymers (Basel)*, , DOI:10.3390/polym11081271.
- 83 G. D. Considine and P. H. Kulik, in *Van Nostrand's Scientific Encyclopedia*, JohnWiley & Sons, Inc., 2006, pp. 1–9.
- 84 E. A. Baroncini, S. Kumar Yadav, G. R. Palmese and J. F. Stanzione, *J. Appl. Polym. Sci.*, 2016, **133**, 1–19.
- 85 Grand View Research, *Epoxy Resin Market Analysis By Application (Paints & Coatings, Wind Turbine, Composites, Construction, Electrical & Electronics, Adhesives) And Segment Forecasts To 2024*, 2016.
- 86 I. Faye, M. Decostanzi, Y. Ecochard and S. Caillol, *Green Chem.*, 2017, **19**, 5236–5242.
- 87 F. L. Jin, X. Li and S. J. Park, *J. Ind. Eng. Chem.*, 2015, **29**, 1–11.
- 88 W. R. Ashcroft, *Three Bond Tech. News*, 1990, **32**, 1–10.
- 89 F. Gonzalez Garcia, M. E. Leyva and A. Antonio Alencar de Queiroz, 2009.
- 90 I. N. Hadjinikolaou, J. P. Bell and L. Spangberg, *MRS Proc.*, 1987, **110**, 451–454.
- 91 A. Matsumoto, Y. Kaneda and H. Aota, *J. Polym. Sci. Part A Polym. Chem.*, 2011, **49**, 3997–4004.
- 92 K. Dušek, M. Ilavsky and S. Luňák, *J. Polym. Sci.*, 1975, **53**, 29–44.
- 93 L. Matejka, *Macromolecules*, 2000, **33**, 3611–3619.
- 94 J. Clayden, N. Greeves and S. Warren, in *Organic Chemistry*, Oxford

- University Press, Oxford, 2nd edn., 2012, pp. 438–439.
- 95 C. François, S. Pourchet, G. Boni, S. Rautiainen, J. Samec, L. Fournier, C. Robert, C. M. Thomas, S. Fontaine, Y. Gaillard, V. Placet and L. Plasseraud, *Comptes Rendus Chim.*, 2017, **20**, 1006–1016.
- 96 E. D. Gmbh and C. Technologies, *Polymer (Guildf.)*, 2010, **48**, 1973–1978.
- 97 C. Negrell, A. Cornille, P. de Andrade Nascimento, J.-J. J. Robin, S. Caillol, P. de A. Nascimento, J.-J. J. Robin and S. Caillol, *Eur. J. Lipid Sci. Technol.*, 2017, **119**, 1–13.
- 98 S. Kumar, S. K. Samal, S. Mohanty and S. K. Nayak, *Polym. - Plast. Technol. Eng.*, 2018, **57**, 133–155.
- 99 T. Shimokawaji and A. Sudo, *J. Polym. Sci.*, 2020, 1–7.
- 100 F. Ferdosian, Z. Yuan, M. Anderson and C. Xu, *Thermochim. Acta*, 2015, **618**, 48–55.
- 101 Y. Li, F. Xiao and C. P. Wong, *J. Polym. Sci. Part A Polym. Chem.*, 2007, **45**, 181–190.
- 102 V. Froidevaux, C. Negrell, S. Caillol, J. P. Pascault and B. Boutevin, *Chem. Rev.*, 2016, **116**, 14181–14224.
- 103 H. Baumann, M. Bühler, H. Fochem, F. Hirsinger, H. Zoblein and J. Falbe, *Angew. Chemie*, 1988, **27**, 41–62.
- 104 A. K. Handa, T. Fatima and A. K. Mattoo, *Front. Chem.*, 2018, **6**, 1–18.
- 105 H. Q. Pham and M. J. Marks, in *Ullmann's Encyclopedia of Industrial Chemistry*, Wiley-VCH, Texas, 2012, pp. 155–244.
- 106 Z. A. A. Hamid, A. Blencowe, G. Qiao and G. Stevens, *Adv. Mater. Res.*, 2013, **626**, 681–685.
- 107 D. M. O'Brien, C. Vallieres, C. Alexander, S. M. Howdle, R. A. Stockman and S. V. Avery, *J. Mater. Chem. B*, 2019, **7**, 5222–5229.
- 108 F. Siedenbiedel and J. C. Tiller, *Polymers (Basel)*, 2012, **4**, 46–71.
- 109 N. A. Peppas and A. Khademhosseini, *Nature*, 2016, **540**, 335–336.
- 110 D. G. Anderson, J. A. Burdick and R. Langer, *Sci. Perspect.*, 2004, **305**, 1923–1924.
- 111 A. S. Kulshrestha and A. Mahapatro, in *Polymers for Biomedical Applications*, American Chemical Society, Washington DC, 2008, pp. 1–7.



- 112 A. Teo, A. Mishra, I. Park, Y.-J. Kim, W.-T. Park and Y. J. Yoon, *ACS Biomater. Sci. Eng.*, 2016, **2**, 454–472.
- 113 E. T. Baran and R. L. Reis, in *Natural Based Polymers for Biomedical Application*, Woodhead Publishing, 2008, pp. 597–623.
- 114 C. de las H. Alarcón, S. Pennadam and C. Alexander, *Chem. Soc. Rev.*, 2005, **34**, 276–285.
- 115 T. Hyeon and V. Rotello, *Chem. Soc.*, 2012, **41**, 2545–2561.
- 116 B. L. Banik, P. Fattahi and J. L. Brown, *Wiley Interdiscip. Rev. Nanomedicine Nanobiotechnology*, 2016, **8**, 271–299.
- 117 Y. Shi, *Adv. Ther.*, 2020, **3**, 1900215.
- 118 J. Shi, P. W. Kantoff, R. Wooster and O. C. Farokhzad, *Nat. Rev. Cancer*, 2017, **17**, 20–37.
- 119 T. Sun, Y. S. Zhang, B. Pang, D. C. Hyun, M. Yang and Y. Xia, *Angew. Chemie - Int. Ed.*, 2014, **53**, 12320–12364.
- 120 F. Danhier, E. Ansorena, J. M. Silva, R. Coco, A. Le Breton and V. Préat, *J. Control. Release*, 2012, **161**, 505–522.
- 121 S. Tran, P.-J. DeGiovanni, B. Piel and P. Rai, *Clin. Transl. Med.*, 2017, **6**, 44.
- 122 Y. Xiao, X. Tan, Z. Li and K. Zhang, *J. Mater. Chem. B*, 2020, 6697–6709.
- 123 K. E. Washington, R. N. Kularatne, V. Karmegam, M. C. Biewer and M. C. Stefan, *Wiley Interdiscip. Rev. Nanomedicine Nanobiotechnology*, 2017, **9**, e1446.
- 124 C. Vallieres, A. L. Hook, Y. He, V. C. Crucitti, G. Figueredo, C. R. Davies, L. Burroughs, D. A. Winkler, R. D. Wildman, D. J. Irvine, M. R. Alexander and S. V Avery, *Sci. Adv.*, 2020, **6**, eaba6574.
- 125 B. Pelaz, C. Alexiou, R. A. Alvarez-Puebla, F. Alves, A. M. Andrews, S. Ashraf, L. P. Balogh, L. Ballerini, A. Bestetti, C. Brendel, S. Bosi, M. Carril, W. C. W. Chan, C. Chen, X. Chen, X. Chen, Z. Cheng, D. Cui, J. Du, C. Dullin, A. Escudero, N. Feliu, M. Gao, M. George, Y. Gogotsi, A. Grünweller, Z. Gu, N. J. Halas, N. Hampp, R. K. Hartmann, M. C. Hersam, P. Hunziker, J. Jian, X. Jiang, P. Jungebluth, P. Kadhiresan, K. Kataoka, A. Khademhosseini, J. Kopeček, N. A. Kotov, H. F. Krug, D. S. Lee, C. M. Lehr, K. W. Leong, X. J. Liang, M. Ling Lim, L. M. Liz-Marzán, X. Ma, P. Macchiarini, H.

- Meng, H. Möhwald, P. Mulvaney, A. E. Nel, S. Nie, P. Nordlander, T. Okano, J. Oliveira, T. H. Park, R. M. Penner, M. Prato, V. Puentes, V. M. Rotello, A. Samarakoon, R. E. Schaak, Y. Shen, S. Sjöqvist, A. G. Skirtach, M. G. Soliman, M. M. Stevens, H. W. Sung, B. Z. Tang, R. Tietze, B. N. Udugama, J. S. VanEpps, T. Weil, P. S. Weiss, I. Willner, Y. Wu, L. Yang, Z. Yue, Q. Zhang, Q. Zhang, X. E. Zhang, Y. Zhao, X. Zhou and W. J. Parak, *ACS Nano*, 2017, **11**, 2313–2381.
- 126 A. Arora and A. Mishra, *Mater. Today Proc.*, 2018, **5**, 17156–17161.
- 127 A. A. Dundas, O. Sanni, J. F. Dubern, G. Dimitrakis, A. L. Hook, D. J. Irvine, P. Williams and M. R. Alexander, *Adv. Mater.*, 2019, **31**, 1–6.
- 128 A. A. Dundas, V. Cuzzucoli Crucitti, S. Haas, J. F. Dubern, A. Latif, M. Romero, O. Sanni, A. M. Ghaemmaghami, P. Williams, M. R. Alexander, R. Wildman and D. J. Irvine, *Adv. Funct. Mater.*, 2020, **30**, 2001821.
- 129 M. S. Shoichet, *Macromolecules*, 2010, **43**, 581–591.
- 130 M. A. Ghalia and Y. Dahman, *J. Polym. Res.*, , DOI:10.1007/s10965-017-1227-2.
- 131 M. Jamshidian, E. A. Tehrany, M. Imran, M. Jacquot and S. Desobry, *Compr. Rev. Food Sci. Food Saf.*, 2010, **9**, 552–571.
- 132 J. K. Oh, *Soft Matter*, 2011, **7**, 5096–5108.
- 133 C. P. Rivero, Y. Hu, T. H. Kwan, C. Webb, C. Theodoropoulos, W. Daoud and C. S. K. Lin, in *Current Developments in Biotechnology and Bioengineering: Solid Waste Management*, eds. J. W.-C. Wong, R. D. Tyagi and A. Pandey, Elsevier B.V., Amsterdam, 2017, pp. 1–26.
- 134 O. Dechy-Cabaret, B. Martin-Vaca and D. Bourissou, *Chem. Rev.*, 2004, **104**, 6147–6176.
- 135 N. Yuntawattana, T. M. Mcguire, C. B. Durr, A. Buchard and C. K. Williams, *Catal. Sci. Technol.*, 2020, **10**, 7226–7239.
- 136 A. P. Dove, *ACS Macro Lett.*, 2012, **1**, 1409–1412.
- 137 B. G. G. Lohmeijer, R. C. Pratt, F. Leibfarth, J. W. Logan, D. A. Long, A. P. Dove, F. Nederberg, J. Choi, C. Wade, R. M. Waymouth and J. L. Hedrick, *Macromolecules*, 2006, **39**, 8574–8583.
- 138 H. Phan, R. I. Minut, P. McCrorie, C. Vasey, R. R. Larder, E. Krumins, M. Marlow, R. Rahman, C. Alexander, V. Taresco and A. K. Pearce, *J.*

- Polym. Sci. Part A Polym. Chem.*, 2019, **57**, 1801–1810.
- 139 C. E. Vasey, A. K. Pearce, F. Sodano, R. Cavanagh, T. Abelha, V. Cuzzucoli Crucitti, A. B. Anane-Adjei, M. Ashford, P. Gellert, V. Taresco and C. Alexander, *Biomater. Sci.*, 2019, **7**, 3832–3845.
- 140 T. Casalini, F. Rossi, A. Castrovinci and G. Perale, *Front. Bioeng. Biotechnol.*, 2019, **7**, 1–16.
- 141 J. Zhang, in *Encyclopedia of Membranes*, 2014, pp. 1–4.
- 142 Y. Nakama, in *Cosmetic Science and Technology: Theoretical Principles and Applications*, Elsevier Inc., Kanagawa, Japan, 2017, pp. 231–244.
- 143 N. Dave and T. Joshi, *Int. J. Appl. Chem.*, 2017, **13**, 663–672.
- 144 D. G. Hayes and G. A. Smith, in *Biobased Surfactants (second edition) synthesis, properties and applications*, Elsevier Inc., Second Edi., 2019, pp. 3–38.
- 145 S. De, S. Malik, A. Ghosh, R. Saha and B. Saha, *RSC Adv.*, 2015, **5**, 65757–65767.
- 146 A. Chen, H. Peng, I. Blakey and A. K. Whittaker, *Polym. Rev.*, 2017, **57**, 276–310.
- 147 C. Pulce and J. Descotes, *Hum. Toxicol.*, 1996, 683–702.
- 148 N. Jalilzadeh, N. Samadi, R. Salehi, G. Dehghan, M. Iranshahi, M. R. Dadpour and H. Hamishehkar, *Sci. Rep.*, 2020, **10**, 1606.
- 149 L. Q. Yang, B. He, S. Meng, J. Z. Zhang, M. Li, J. Guo, Y. M. Guan, J. X. Li and Z. W. Gu, *Polymer (Guildf.)*, 2013, **54**, 2668–2675.
- 150 H. S. Azevedo, T. C. Santos and R. L. Reis, in *Natural-Based Polymers for Biomedical Applications*, 2008, pp. 106–128.
- 151 M. A. Velazco-Medel, L. A. Camacho-Cruz, J. C. Lugo-González and E. Bucio, *Med. Devices Sensors*, 2021, **4**, 1–23.
- 152 S. L. Percival, L. Suleman, C. Vuotto and G. Donelli, *J. Med. Microbiol.*, 2015, **64**, 323–334.
- 153 C. Vallières, R. Raulo, M. Dickinson and S. V. Avery, *Front. Microbiol.*, 2018, **9**, 1–15.
- 154 A. H. Fairlamb, N. A. R. Gow, K. R. Matthews and A. P. Waters, *Nat Microbiol*, 2017, **1**, 16092.
- 155 E. Moreno-Martinez, C. Vallieres, S. L. Holland and S. V. Avery, *Sci. Rep.*, 2015, **5**, 1–11.

- 156 T. J. Gintjee, M. A. Donnelley and G. R. Thompson, *J. Fungi*, 2020, **6**, 28.
- 157 I. Sovadinova, E. F. Palermo, M. Urban, P. Mpiga, G. A. Caputo and K. Kuroda, *Polymers (Basel)*., 2011, **3**, 1512–1532.
- 158 Y. Xue, H. Xiao and Y. Zhang, *Int. J. Mol. Sci.*, 2015, **16**, 3626–3655.
- 159 M. C. Jennings, K. P. C. Minbiole and W. M. Wuest, *ACS Infect. Dis.*, 2016, **1**, 288–303.
- 160 D. B. Vieira and A. M. Carmona-Ribeiro, *J. Antimicrob. Chemother.*, 2006, **58**, 760–767.
- 161 L. A. Rank, N. M. Walsh, R. Liu, F. Y. Lim, J. W. Bok, M. Huang, N. P. Keller, S. H. Gellman and C. M. Hull, *Antimicrob. Agents Chemother.*, 2017, **61**, 1–15.
- 162 H. Mortazavian, L. L. Foster, R. Bhat, S. Patel and K. Kuroda, *Biomacromolecules*, 2018, **19**, 4370–4378.
- 163 L. H. Yin, B. Ran, T. J. Hu, C. Yang, J. J. Fei and Y. H. Li, *RSC Adv.*, 2017, **7**, 6006–6012.
- 164 C. Vallières, N. Singh, C. Alexander and S. V. Avery, *ACS Infect. Dis.*, 2020, **6**, 2950–2958.
- 165 M. Spitzer, N. Robbins and G. D. Wright, *Virulence*, 2017, **8**, 169–185.
- 166 W. Liu, L. P. Li, J. D. Zhang, Q. Li, H. Shen, S. M. Chen, L. J. He, L. Yan, G. T. Xu, M. M. An and Y. Y. Jiang, *PLoS One*, 2014, **9**, e103442.
- 167 C. A. Weems, K. R. Delle Chiaie, J. C. Worch, C. J. Stubbs and A. P. Dove, *Polym. Chem.*, 2019, **10**, 5959–5966.
- 168 A. K. Pearce, C. E. Vasey, A. B. Anane-Adjei, F. Sodano, V. C. Crucitti, D. J. Irvine, S. M. Howdle, C. Alexander and V. Taresco, *Macromol. Chem. Phys.*, 2019, **220**, 1900270.
- 169 W. F. Hölderich, J. Röseler, G. Heitmann and A. T. Liebens, *Catal. Today*, 1997, **37**, 353–366.
- 170 D. B. Bleier and M. J. Elrod, *J. Phys. Chem. A*, 2013, **117**, 4223–4232.
- 171 M. R. Thomsett, University of Nottingham, 2018.
- 172 K. A. Da Silva Rocha, J. L. Hoehne and E. V. Gusevskaya, *Chem. - A Eur. J.*, 2008, **14**, 6166–6172.
- 173 J. Kaminska, M. A. Schwegler, A. J. Hoefnagel and H. van Bekkum,

- Recl. des Trav. Chim. des Pays-Bas*, 1992, **111**, 432–437.
- 174 A. D. Jenkins, R. F. T. Stepto, P. Kratochvíl and U. W. Suter, *Pure Appl. Chem.*, 1996, **68**, 2287–2311.
- 175 G. Englezou, K. Kortsen, A. A. C. Pacheco, R. Cavanagh, J. C. Lentz, E. Krumins, C. Sanders-Velez, S. M. Howdle, A. J. Nedoma and V. Taresco, *J. Polym. Sci.*, 2020, 1571–1581.
- 176 D. M. O'Brien, R. L. Atkinson, R. Cavanagh, A. A. C. C. Pacheco, R. Larder, K. Kortsen, E. Krumins, A. J. Haddleton, C. Alexander, R. A. Stockman, S. M. Howdle and V. Taresco, *Eur. Polym. J.*, 2020, **125**, 109516.
- 177 P. G. Laye, S. B. Warrington, G. R. Heal, D. M. Price, R. Wilson and P. Haines, *Principles of Thermal Analysis and Calorimetry*, The Royal Society of Chemistry, 2002.
- 178 K. Y. Law, *J. Phys. Chem. Lett.*, 2014, **5**, 686–688.
- 179 V. Taresco, J. Suksiriworapong, R. Creasey, J. C. Burley, G. Mantovani, C. Alexander, K. Treacher, J. Booth and M. C. Garnett, *J. Polym. Sci. Part A Polym. Chem.*, 2016, **54**, 3267–3278.
- 180 H. Matsuno, R. Matsuyama, A. Yamamoto and K. Tanaka, *Polym. J.*, 2015, **47**, 505–512.
- 181 A. M. Pinto, S. Moreira, I. C. Gonçalves, F. M. Gama, A. M. Mendes and F. D. Magalhães, *Colloids Surfaces B Biointerfaces*, 2013, **104**, 229–238.
- 182 I. Yildirim, T. Yildirim, D. Kalden, G. Festag, N. Fritz, C. Weber, S. Schubert, M. Westerhausen and U. S. Schubert, *Polym. Chem.*, 2017, **8**, 4378–4387.
- 183 A. J. Shnoudeh, I. Hamad, R. W. Abdo, L. Qadumii, A. Y. Jaber, H. S. Surchi and S. Z. Alkelany, in *Biomaterials and Bionanotechnology*, Elsevier Inc., 2019, pp. 561–562.
- 184 Sigma-Aldrich, *Tween 20 Technical Sheet*, Saint Louis, 1993.
- 185 Sigma-Aldrich, *TRITON X-100 Technical Sheet*, Saint Louis, 1999.
- 186 A. Sharma, S. V. Madhunapantula and G. P. Robertson, *Expert Opin Drug Metab Toxicol.*, 2012, **8**, 47–69.
- 187 N. Hoshyar, S. Gray, H. Han and G. Bao, *Nanomedicine (Lond)*, 2016, **11**, 673–692.
- 188 H. F. Wang, H. Z. Jia, Y. F. Chu, J. Feng, X. Z. Zhang and R. X. Zhuo,

- Macromol. Biosci.*, 2014, **14**, 526–536.
- 189 Thermo Fisher Scientific, *CyQUANT™ LDH Cytotoxicity Assay*, 2019.
- 190 M. Nazari, M. Kurdi and H. Heerklotz, *Biophys. J.*, 2012, **102**, 498–506.
- 191 R. J. Cavanagh, P. A. Smith and S. Stolnik, *Mol. Pharm.*, 2019, **16**, 618–631.
- 192 J. J. Arnold, F. Ahsan, E. Meezan and D. J. Pillion, *J. Pharm. Sci.*, 2004, **93**, 2205–2213.
- 193 R. D. Groot and K. L. Rabone, *Biophys. J.*, 2001, **81**, 725–736.
- 194 A. R. Goddard, S. Pérez-nieto, T. M. Passos, B. Quilty, K. Carmichael, D. J. Irvine and S. M. Howdle, *Green Chem.*, 2016, **18**, 4772–4786.
- 195 K. Fukushima, *Biomater. Sci.*, 2016, **4**, 9–24.
- 196 P. Mckeown, M. Kamran, M. G. Davidson, M. D. Jones, L. A. Románramírez and J. Wood, *Green Chem.*, 2020, **22**, 3721.
- 197 Z. Zhang, R. Kuijter, S. K. Bulstra, D. W. Grijpma and J. Feijen, *Biomaterials*, 2006, **27**, 1741–1748.
- 198 C. E. Vasey, A. K. Pearce, F. Sodano, R. Cavanagh, T. Abelha, V. Cuzzucoli Crucitti, A. B. Anane-Adjei, M. Ashford, P. Gellert, V. Taresco and C. Alexander, *Biomater. Sci.*, 2019, **7**, 3832–3845.
- 199 K. K. Aggarwal, S. P. S. Khanuja, A. Ahmad, V. K. Gupta and S. Kumar, *Flavour Fragr. J.*, 2002, **17**, 59–63.
- 200 Z. A. A. Hamid, A. Blencowe, B. Ozcelik, J. A. Palmer, G. W. Stevens, K. M. Abberton, W. A. Morrison, A. J. Penington and G. G. Qiao, *Biomaterials*, 2010, **31**, 6454–6467.
- 201 U. M. Vakil and G. C. Martin, *J. Appl. Polym. Sci.*, 1992, **46**, 2089–2099.
- 202 M. Danial, C. My-Nhi Tran, P. G. Young, S. Perrier and K. A. Jolliffe, *Nat. Commun.*, 2013, **4**, 2780.
- 203 M. Fernández de Ullivarri, S. Arbulu, E. Garcia-Gutierrez and P. D. Cotter, *Front. Cell. Infect. Microbiol.*, 2020, **10**, 105.
- 204 Y. Yuan, F. Zhou, H. Su and Y. Zhang, *Sci. Rep.*, 2019, **9**, 1–11.
- 205 L. E. Prevette, D. M. Mullen and M. M. Banaszak Holl, *Mol. Pharm.*, 2010, **7**, 870–883.
- 206 R. H. Borgwardt, *Ind. Eng. Chem. Res.*, 1998, **37**, 3760–3767.
- 207 J. Clayden, N. Greeves and S. Warren, in *Organic Chemistry*, Oxford

- University Press, Oxford, 2nd edn., 2012, pp. 825–832.
- 208 F. P. Byrne, S. Jin, G. Paggiola, T. H. M. Petchey, J. H. Clark, T. J. Farmer, A. J. Hunt, C. Robert McElroy and J. Sherwood, *Sustain. Chem. Process.*, 2016, **4:7**, 1–24.
- 209 L. Charbonneau, X. Foster and S. Kaliaguine, *ACS Sustain. Chem. Eng.*, 2018, **6**, 12224–12231.
- 210 K. P. Zeller, M. Kowallik and P. Haiss, *Org. Biomol. Chem.*, 2005, **3**, 2310–2318.
- 211 R. A. Johnson and K. Barry Sharpless, *Compr. Org. Synth.*, 1991, 389–436.
- 212 R. Curci, M. Florentino, L. Troisi, J. O. Edwards and R. H. Pater, *J. Org. Chem.*, 1980, **45**, 4758–4760.
- 213 H. M. C. Ferraz, R. M. Muzzi, T. De O. Vieira and H. Viertler, *Tetrahedron Lett.*, 2000, **41**, 5021–5023.
- 214 S. Vidal, *ACS Cent. Sci.*, 2020, **6**, 83–86.
- 215 A. K. Saini, C. M. Carlin and H. H. Patterson, *J. Polym. Sci. Part A Polym. Chem.*, 1993, **31**, 2751–2758.
- 216 B. R. Donovan and D. L. Patton, in *Encyclopedia of Polymeric Nanomaterials*, eds. S. Kobayashi and K. Müllen, Springer, Berlin, Heidelberg, Berlin, 2015, pp. 2268–2273.
- 217 T. Yokozawa and A. Yokoyama, *Polym. J.*, 2004, **36**, 65–83.
- 218 S. Kéki, M. Zsuga and Á. Kuki, *J. Phys. Chem. B*, 2013, **117**, 4151–4155.
- 219 J. Clayden, N. Greeves and S. Warren, in *Organic Chemistry*, Oxford University Press, Oxford, 2nd edn., 2012.
- 220 Agilent Technologies Inc., 2017, Publication 5991-2720EN.
- 221 P. J. Flory, *J. Am. Chem. Soc.*, 1936, **58**, 1877–1885.
- 222 W. H. Carothers, *Trans. Faraday Soc.*, 1936, **32**, 39–49.
- 223 Y. Wu, M. Ding, J. Wang, B. Zhao, Z. Wu, P. Zhao, D. Tian, Y. Ding and A. Hu, *CCS Chem.*, 2020, **2**, 64–70.
- 224 C. Capello, U. Fischer and K. Hungerbühler, *Green Chem.*, 2007, **9**, 927–93.
- 225 H. A. Contreras-Cornejo, L. Macias-Rodriguez, C. Cortes-Penagos and J. Lopez-Bucio, *Plant Physiol.*, 2009, **149**, 1579–1592.
- 226 C. D. Jensen, J. Thormann and K. E. Andersen, *Contact Dermatitis*,

- 2003, **48**, 155–157.
- 227 Canadian Council of Ministers of the Environment 1999, *Canadian Water Quality Guidelines for the Protection of Aquatic Life: IPBC*. In: *Canadian environmental quality guidelines*, Winnipeg, 1999.
- 228 A. Gitchaiwat, A. Kositchaiyong, K. Sombatsompop, B. Prapagdee, K. Isarangkura, N. Sombatsompop and A. Kositchaiyong, *J. Appl. Polym. Sci.*, 2012, **128**, 371–379.
- 229 M. C. Arendrup, J. Meletiadis, J. W. Mouton, K. Lagrou, P. Hamal and J. Guinea, 2017, **7.3**, 1–21.
- 230 M. H. Hsieh, C. M. Yu, V. L. Yu and J. W. Chow, *Diagn. Microbiol. Infect. Dis.*, 1993, **16**, 343–349.
- 231 F. C. Odds, *J. Antimicrob. Chemother.*, 2003, **52**, 1.
- 232 D. S. Palacios, I. Dailey, D. M. Siebert, B. C. Wilcock and M. D. Burke, *Proc. Natl. Acad. Sci. U. S. A.*, 2011, **108**, 6733–6738.
- 233 T. M. Anderson, M. C. Clay, A. G. Cioffi, K. A. Diaz, G. S. Hisao, M. D. Tuttle, A. J. Nieuwkoop, G. Comellas, N. Maryum, S. Wang, B. E. Uno, E. L. Wildeman, T. Gonen, C. M. Rienstra and M. D. Burke, *Nat. Chem. Biol.*, 2014, **10**, 400–406.
- 234 A. Erdogan and S. S. C. Rao, *Curr. Gastroenterol. Rep.*, 2015, **17**, 1–7.
- 235 K. Johansen Helle and C. Gøtzsche Peter, *Cochrane Database Syst. Rev.*, 2014, CD000969.
- 236 L. M. Douglas and J. B. Konopka, *PLoS Genet.*, 2019, **15**, 1–26.
- 237 M. Cokol-Cakmak, F. Bakan, S. Cetiner and M. Cokol, *J. Vis. Exp.*, 2018, **2018**, e57713.
- 238 M. Belinsky and A. K. Jaiswal, *Cancer Metastasis Rev.*, 1993, **12**, 103–117.
- 239 A. A. Zalata, N. Lammer Tijn, A. Christophe and F. H. Comhaire, *Int. J. Androl.*, 1998, **21**, 289–294.
- 240 J. O'Brien, I. Wilson, T. Orton and F. Pognan, *Eur. J. Biochem.*, 2000, **267**, 5421–5426.
- 241 R. D. de Castro, T. M. P. A. de Souza, L. M. D. Bezerra, G. L. S. Ferreira, E. M. M. de Brito Costa and A. L. Cavalcanti, *BMC Complement. Altern. Med.*, 2015, **15**, 1–7.
- 242 M. Ponec, M. Haverkort, Y. L. Soei, J. Kempenaar and H. Bodde, *J.*



- Pharm. Sci.*, 1990, **79**, 312–316.
- 243 G. Faria, C. R. B. Cardoso, R. E. Larson, J. S. Silva and M. A. Rossi, *Toxicol. Appl. Pharmacol.*, 2009, **234**, 256–265.
- 244 M. D. Johnson, C. MacDougall, L. Ostrosky-zeichner, J. R. Perfect and J. H. Rex, *Antimicrob. Agents Chemother.*, 2004, **48**, 693–715.
- 245 A. Hernandez-Ortega, M. Vinaixa, Z. Zebec, E. Takano and N. S. Scrutton, *Sci. Rep.*, 2018, **8**, 14396.
- 246 W. H. Carothers, *J. Am. Chem. Soc.*, 1929, **51**, 2548–2559.
- 247 P. J. Flory, *Chem. Rev.*, 1946, **39**, 137–197.
- 248 D. M. Lynn and R. Langer, *J. Am. Chem. Soc.*, 2000, **122**, 10761–10768.
- 249 F. Danusso and P. Ferruti, *Polymer (Guildf.)*, 1970, **11**, 88–113.
- 250 P. J. Flory, *J. Am. Chem. Soc.*, 1939, **61**, 3334–3340.
- 251 B. D. Mather, K. Viswanathan, K. M. Miller and T. E. Long, *Prog. Polym. Sci.*, 2006, **31**, 487–531.
- 252 A. Y. Rulev, *Russ. Chem. Rev.*, 2011, **80**, 197–218.
- 253 A. K. Blakney, Y. Zhu, P. F. McKay, C. R. Bouton, J. Yeow, J. Tang, K. Hu, K. Samnuan, C. L. Grigsby, R. J. Shattock and M. M. Stevens, *ACS Nano*, 2020, **14**, 5711–5727.
- 254 P. Gurnani, A. K. Blakney, J. Yeow, C. R. Bouton, R. J. Shattock, M. M. Stevens and C. Alexander, *Polym. Chem.*, 2020, **11**, 5861–5869.
- 255 W. Cheng, D. Wu and Y. Liu, *Biomacromolecules*, 2016, **17**, 3115–3126.
- 256 H. C. Brown and C. D. Pfaffenberger, *Tetrahedron*, 1975, **31**, 925–928.
- 257 O. Nsengiyumva and S. A. Miller, *Green Chem.*, 2019, **21**, 973–978.
- 258 M. von Czapiewski, K. Gugau, L. Todorovic and M. A. R. Meier, *Eur. Polym. J.*, 2016, **83**, 359–366.
- 259 M. S. Lima, C. S. M. F. Costa, J. F. J. Coelho, A. C. Fonseca and A. C. Serra, *Green Chem.*, 2018, **20**, 4880–4890.
- 260 E. F. Palermo, D.-K. Lee, A. Ramamoorthy and K. Kuroda, *J Phys Chem B*, 2011, **115**, 366–375.
- 261 J. Clayden, N. Greeves and S. Warren, in *Organic Chemistry*, Oxford University Press, Oxford, 2nd edn., 2012, p. 570.
- 262 D. C. Harrowven, D. D. Pascoe, D. Demurtas and H. O. Bourne,

- Angew. Chemie - Int. Ed.*, 2005, **44**, 1221–1222.
- 263 P. Ferruti, *J. Polym. Sci. Part A Polym. Chem.*, 2013, **51**, 2319–2353.
- 264 F. Saviano, T. Lovato, A. Russo, G. Russo, C. R. Bouton, R. J. Shattock, C. Alexander, F. Quaglia, A. K. Blakney, P. Gurnani and C. Conte, *J. Mater. Chem. B*, 2020, 4940–4949.
- 265 A. Genest, D. Portinha, E. Fleury and F. Ganachaud, *Prog. Polym. Sci.*, 2017, **72**, 61–110.
- 266 A. Kall, D. Bandyopadhyay and B. K. Banik, *Synth. Commun.*, 2010, **40**, 1730–1735.
- 267 K. Kempe, C. R. Becer and U. S. Schubert, *Macromolecules*, 2011, **44**, 5825–5842.
- 268 M. Nüchter, B. Ondruschka, W. Bonrath and A. Gum, *Green Chem.*, 2004, **6**, 128–141.
- 269 F. Matloubi Moghaddam, M. Mohammadi and A. Hosseinnia, *Synth. Commun.*, 2000, **30**, 643–650.
- 270 B. O. Burek, S. Bormann, F. Hollmann, J. Z. Bloh and D. Holtmann, *Green Chem.*, 2019, **21**, 3232–3249.
- 271 D. Lanteri, S. Quattrosoldi, M. Soccio, A. Basso, D. Cavallo, A. Munari, R. Riva, N. Lotti and L. Moni, *Front. Chem.*, 2020, **8**, 85.
- 272 J. Sun, *Altern. Med. Rev.*, 2007, **12**, 259–264.
- 273 V. R. Sinha and M. Pal Kaur, *Drug Dev. Ind. Pharm.*, 2000, **26**, 1131–1140.
- 274 M. Firdaus, *Asian J. Org. Chem.*, 2017, **6**, 1702–1714.
- 275 L. Charbonneau, X. Foster, D. Zhao and S. Kaliaguine, *ACS Sustain. Chem. Eng.*, 2018, **6**, 5115–5121.
- 276 P. K. Gupta, A. K. Jaiswal, S. Asthana, A. Dube and P. R. Mishra, *Biomacromolecules*, 2015, **16**, 1073–1087.
- 277 L. Zhang, D. Hu, M. Salmain, B. Liedberg and S. Boujday, *Talanta*, 2019, **204**, 875–881.